

**DESIGN OF A NEUTRON SPECTROMETER AND
SIMULATIONS OF NEUTRON MULTIPLICITY
EXPERIMENTS WITH NUCLEAR DATA
PERTURBATIONS**

by

SIMON R. BOLDING

B.S., Kansas State University, 2011

A THESIS

submitted in partial fulfillment of the
requirements for the degree

MASTER OF SCIENCE

Department of Mechanical and Nuclear Engineering
College of Engineering

KANSAS STATE UNIVERSITY

Manhattan, Kansas

2013

Approved by:

Major Professor

J. Kenneth Shultis

Abstract

Simulations were performed using MCNP5 to optimize the geometry of a neutron spectrometer. The cylindrical device utilizes micro-structured neutron detectors encased in polyethylene moderator to identify sources based on energy spectrum. Sources are identified by comparison of measured detector responses to predetermined detector response templates that are unique to each neutron source. The design of a shadow shield to account for room scattered neutrons was investigated as well. For sufficient source strength in a void, the optimal geometric design was able to detect all sources in 1000 trials, where each trial consists of simulated detector responses from 11 unique sources. When room scatter from a concrete floor was considered, the shadow shield corrected responses were capable of correctly identifying 96.4% of the simulated sources in 1000 trials using the same templates.

In addition to spectrometer simulations, a set of neutron multiplicity experiments from a plutonium sphere with various reflector thicknesses were simulated. Perturbations to nuclear data were made to correct a known discrepancy between multiplicity distributions generated from MCNP simulations and experimental data. *Energy-dependent* perturbations to the *total* number of mean neutrons per fission $\bar{\nu}$ of ^{239}Pu ENDF/B-VII.1 data were analyzed. Perturbations were made using random samples, correlated with corresponding covariance data. Out of 500 unique samples, the best-case $\bar{\nu}$ data reduced the average deviation in the mean of multiplicity distributions between simulation and experiment to 4.32% from 6.73% for the original data; the average deviation in the second moment was reduced from 13.87% to 8.74%. The best-case $\bar{\nu}$ data preserved k_{eff} with a root-mean-square deviation (RMSD) of 0.51% for the 36 Pu cases in the MCNP validation suite, which is comparable to the 0.49% RMSD produced using the original nuclear data. Fractional shifts to microscopic cross sections were performed and multiplicity and criticality results compared. A 1.5% decrease in fission cross section was able to correct the discrepancy in multiplicity distributions greater than the $\bar{\nu}$ perturbations but without preserving k_{eff} .

Table of Contents

Table of Contents	iii
List of Figures	vi
List of Tables	ix
Acknowledgements	xi
1 Introduction	1
1.1 A Neutron Source Identification Spectrometer	1
1.2 Simulations of Multiplicity Distributions	4
2 Theory	6
2.1 Relevant Probability and Statistics	6
2.1.1 Random Variables and Probability Distribution Functions	6
2.1.2 Expectation Values and Moments	7
2.1.3 Covariance and Correlation Matrices	8
2.1.4 Sample Mean and Variance	8
2.1.5 Useful Distributions	9
2.1.6 Generating Random Samples from a Distribution	11
2.1.7 Generating a Set of Correlated Random Samples	12
2.1.8 Error Propagation Formula	13
2.1.9 χ^2 Goodness-of-Fit Statistic	15
2.2 Nuclear Data and Radiation Interactions	16
2.2.1 Attenuation of Neutral Particles	16
2.2.2 Microscopic Cross Section	17
2.2.3 Neutron Flux Density	18
2.2.4 Effective Neutron Multiplication Factor	19
2.2.5 Neutrons Released per Fission ν	20
2.3 Monte Carlo Transport Code	21
2.3.1 The Monte Carlo Method and MCNP	21
2.3.2 Non-Analog Variance Reduction in MCNP	21

3	Review of Neutron Spectrometry	24
3.1	The Unfolding Problem	24
3.1.1	The Unfolding Equation	24
3.1.2	Regularizing the Set of Algebraic Equations	26
3.2	Solution Methods	27
3.3	Neutron Spectrometer Designs	28
3.3.1	Single Detector Response Systems	28
3.3.2	Multiple Detector Response Systems	28
4	Simulations of a Neutron Source Identification Spectrometer	31
4.1	Methodology	31
4.1.1	Overview	31
4.1.2	Source Identification Based on a FOM	32
4.2	MCNP5 Model	36
4.2.1	Geometry and Neutron Sources	36
4.2.2	Simplified Model of Perforated Neutron Detectors	37
4.2.3	Detector Response in MCNP5	39
4.2.4	Boron in Circuit Boards	40
4.2.5	Variance Reduction and MCNP5 Parameters	40
4.2.6	Verifying Artificial Detector Model Using MCNP6	41
4.3	Geometric Optimization	46
4.3.1	Motivation	46
4.3.2	Development of Objective Function	50
4.3.3	Simulated Responses	52
4.4	Automation of Simulations and Data analysis	54
4.5	Corrections to the FOM for MCNP Simulations	55
4.6	Optimization Results	56
4.6.1	Optimal Detector Spacing for a Fixed Radius	57
4.6.2	Determination of Threshold Source Strength and Θ for Correct Source Identification	63
4.6.3	Radius of the Moderator	69
4.6.4	Optimal Moderator Aspect Ratio with a Fixed Weight	70
4.7	Detecting WGPu versus ^{240}Pu	72
4.8	Shadow Shield Design and Optimization	74
4.8.1	Motivation	74
4.8.2	Source Identification with Shadow Shield Measurements	77
4.8.3	Comparison of Shield Designs	78
4.8.4	MCNP Model	78
4.8.5	Shadow Shield Thickness	82
4.8.6	Optimal Shield Location	83
4.8.7	Results with Optimal Shield Design	87
4.9	Conclusions, Recommendations, and Future Work	91

5	Simulations of Neutron Multiplicity Measurements with Perturbations to Nuclear Data	93
5.1	Motivation	93
5.2	Background	94
	5.2.1 Neutron Multiplicity Distributions	94
	5.2.2 Application of Multiplicity Distributions	95
5.3	Pu Experiments and Multiplicity Measurements	97
	5.3.1 Overview of Experimental Setup	97
	5.3.2 Previous Modeling Work	98
5.4	Methodology	99
	5.4.1 Modifying Nuclear Data Files	99
	5.4.2 Correlated Random Sampling of $\bar{\nu}$ in ACE Files	100
	5.4.3 Energy-Averaged Perturbations of Capture Cross Section	102
	5.4.4 Energy-Averaged Perturbations of Fission Cross Section	103
	5.4.5 Quantifying Shifts in Cross Sections	104
5.5	Data Generation, Simulations, and Comparison to Experimental Data	104
5.6	Results for $\bar{\nu}$ Perturbations	106
5.7	Results of Cross Section Perturbations	115
	5.7.1 Results of Capture Cross Section Perturbations	115
	5.7.2 Results of Fission Cross Section Perturbations	120
	5.7.3 Results of Altering both Fission and Capture	121
5.8	Conclusions	126
5.9	Summary and Suggestions for Future Work	127
	Bibliography	128
	A Changes in Probabilities of Interaction Events	133
	B Spectrometer Scripts and Codes	135
	C Spectrometer MCNP Files	175
	D Example Tabulated Data for Spectrometer Simulations	186
	E Multiplicity Scripts and Codes	197
	F Multiplicity and Criticality MCNP Input Files	247

List of Figures

1.1	Cylindrical neutron spectrometer with illustration of materials and possible neutron paths	3
2.1	Neutrons incident upon an infinite slab of thickness T	17
4.1	Simulated spectrometer responses from various sources, followed by the normalized spectra, where the counts in each detector is divided by the counts in the second detector. The relative standard error for all data points is $< 0.5\%$.	33
4.2	Illustration of section of double-stacked straight-trenched detector concept, not to scale.	37
4.3	Dimensions of a unit cell of a perforated, straight-trenched detector	42
4.4	Comparison of detector responses for AmBe, PuBe, and 14.1 MeV fusion sources. All responses are normalized to second detector. All relative errors are less that 0.7%. The dashed line indicates the artificial detectors, and the solid line indicates an explicit MCNP6 model.	48
4.5	Comparison of detector responses for ^{252}Cf and ^{240}Pu sources. All responses are normalized to second detector. All relative errors are less that 0.7%. The dashed line indicates the artificial detectors, and the solid line indicates an explicit MCNP6 model.	49
4.6	Illustration of dimensions for axial cross section of spectrometer with $N_{det} = 6$ detectors.	57
4.7	Comparison of various values of uniform detector spacing t for various numbers of detectors and fixed $r=10\text{cm}$	59
4.8	Comparison of Θ for different values of N_{det} with optimal values of t	60
4.9	Comparison of spectrometer intrinsic efficiency (ϵ_{spec}) and Θ for various t and 11 detectors.	61
4.10	Comparison of normalized spectrometer intrinsic efficiencies (ϵ_{spec}) and Θ s for various t and 10 and 11 detectors	62
4.11	Comparison of Θ and p_{succ} , the probability of correctly identifying all sources in a trial, for various source strengths.	67
4.12	Comparison of Θ for various source strengths and N_{det}	68
4.13	Comparison of Θ and radius of moderator r	70
4.14	Comparison of Θ for different geometries with a fixed value of w of 4.84 kg. .	71
4.15	Comparison of neutron source energy spectra for WGPu, ^{240}Pu , and ^{252}Cf . .	73
4.16	Comparison of detector spectra from different fission neutron sources.	74

4.17	Illustration of the two shadow shield measurements. Several possible neutron paths are illustrated: (A) neutrons deflected or absorbed in the shield, (B) neutrons scattered off of the environment entering the front of the spectrometer without interacting in the shield, (C) line-of-site neutrons, and (D) neutrons scattered off of the environment entering the front of the device.	76
4.18	Geometry for room shine scenario.	79
4.19	Dimensions for room shine scenario.	80
4.20	Comparison of room-scatter spectra with no correction and void spectra.	84
4.21	Axial slice of shadow shield with dimension labels.	84
4.22	Comparison of net detector spectra for various shadow shield thicknesses.	85
4.23	Comparison of net detector spectra at last few detector positions.	86
4.24	Comparison of net detector spectra with void spectra for a 20-cm thick shadow shield at a location of $z = 0.5$	88
4.25	Comparison of net spectra with room scatter included and void for various z , using a 20-cm thick shadow shield.	89
4.26	Comparison of the effect of room type on detector spectra.	91
5.1	Illustration of construction of a multiplicity distribution from a neutron pulse train. Multiplicity is the number of neutrons detected in one gate width; frequency is the number of gates with a certain multiplicity in counting time T	95
5.2	Illustration of multiplicity experiments (not to scale).	97
5.3	Semi-log plot of $\bar{\nu}$ versus energy for trial 303 and ENDF/B-VII.1.	110
5.4	Plot of $\bar{\nu}$ versus energy for trial 303 and ENDF/B-VII.1 for energies 85 to 150 eV.	111
5.5	Plot of number of standard deviations that trial 303 shifted $\bar{\nu}$ from original ENDF/B-VII.1 data by energy bin.	112
5.6	Plot of percent deviation of $\bar{\nu}$ for trial 303 from the original ENDF/B-VII.1 data at each evaluated energy.	112
5.7	Comparison of multiplicity distributions using original ENDF/B-VII.1 data and experimental multiplicity distributions. Distributions are for (A) bare Pu sphere, (B) 0.5-cm reflector, (C) 1.0-cm reflector, (D) 1.5-cm reflector, and (E) 3.0-cm reflector.	113
5.8	Comparison of multiplicity distributions using trial 303 (modified ENDF/B-VII.1 $\bar{\nu}$ data) and experimental multiplicity distributions. Distributions are for (A) bare Pu sphere, (B) 0.5-cm reflector, (C) 1.0-cm reflector, (D) 1.5-cm reflector, and (E) 3.0-cm reflector.	114
5.9	Comparison of multiplicity distributions for the 3.0-cm polyethylene reflected sphere of Pu.	117
5.10	Comparison of multiplicity distributions for -1.14% reduced energy averaged $\bar{\nu}$ and experimental multiplicity distributions. Distributions are for (A) bare Pu sphere, (B) 0.5-cm reflector, (C) 1.0-cm reflector, (D) 1.5-cm reflector, and (E) 3.0-cm reflector.	123

5.11 Comparison of multiplicity distributions for 16% increased σ_c from case 1 and experimental multiplicity distributions. Distributions are for (A) bare Pu sphere, (B) 0.5-cm reflector, (C) 1.0-cm reflector, (D) 1.5-cm reflector, and (E) 3.0-cm reflector.	124
5.12 A comparison of multiplicity distributions for σ_f reduced 1.5% and experimental multiplicity distributions; σ_s was increased to compensate for changes in σ_f , as described in case 4 of Section 5.4.3. Distributions are for (A) bare Pu sphere, (B) 0.5-cm reflector, (C) 1.0-cm reflector, (D) 1.5-cm reflector, and (E) 3.0-cm reflector.	125

List of Tables

4.1	Neutron sources used for spectrometer simulations.	36
4.2	Geometric specifications for unit cell of a perforated, straight-trenched device.	43
4.3	Crystalline LiF ($\rho = 2.635\text{g cm}^{-3}$) material composition for MCNP6 model.	44
4.4	Natural Si ($\rho = 2.3290\text{g cm}^{-3}$) material composition for MCNP6 model.	44
4.5	FR4 printed circuit board ($\rho = 2.635\text{g cm}^{-3}$) material composition for MCNP6 model.	44
4.6	Comparison of detector responses generated using artificial MCNP5 and explicit MCNP6 detector models. The detector indexing is $i = \text{Position} / (3.0 \text{ cm})$. Errors are reported as absolute.	47
4.7	Comparison of optimal value of Θ with respect to t for the values of N_{det} from Fig. 4.7.	58
4.8	Comparison of Θ and p_{succ} , the probability of correctly identifying all sources in a trial, for various source values of total incident neutrons S_0	65
4.9	Comparison of $\sigma(\Delta_{min}^{(n)})$, Θ , and S_0 for a spectrometer with 11 detectors, $r = 10$ cm, and $t = 3.5$ cm. Note, $\sigma(\Delta_{min}^{(n)})$ here is the sample standard deviation for $\Delta_{min}^{(n)}$, not the standard error in the mean of the $\{\Delta_{min}^{(n)}\}$ $\sigma(\Theta)$. The relation is $\sigma(\Delta_{min}^{(n)}) = \sqrt{N_{corr}}\sigma(\Theta)$	66
4.10	Comparison of aspect ratios and Θ for a variety of N_{det} and a fixed weight of w at 4.84 kg.	72
4.11	Concrete ($\rho = 2.70 \text{ g cm}^{-3}$) material composition for room scatter simulations.	80
4.12	Comparison of χ_{red}^2 values for different shadow shield thicknesses.	85
4.13	Comparison of χ_{red}^2 for different locations of a 20-cm thick shadow shield.	87
4.14	Source identification data with room scatter from an enclosed room.	90
4.15	Source identification data with room scatter from a concrete floor.	91
5.1	FOM and χ^2 values for ten trials with lowest FOM values, and original and shifted ENDF/B-VII.1 data.	107
5.2	Comparison of k_{eff} for different data with the MCNP criticality validation benchmark suite.	108
5.3	Comparison of first and second multiplicity moments for different thicknesses of polyethylene reflector.	109
5.4	A comparison of results for case 1 where σ_c was increased and σ_t was increased to compensate for the change, at each energy.	117

5.5	A comparison of results for case 2 in which σ_c was increased and σ_s was increased to keep the ratio of scattering to σ_t the same as in the original data; σ_t was increased to compensate for the changes in σ_c and σ_s	118
5.6	A comparison of results for case 3 in which σ_c was increased and σ_s was increased to keep the ratio of σ_c to σ_s the same as in the original data; σ_t was increased to compensate for the change in σ_c and σ_s	118
5.7	A comparison of results for case 4 in which σ_c was increased and σ_s was decreased to keep σ_t the same as in the original data, for neutron energies greater than 1 keV.	119
5.8	A comparison of results for case 1 in which σ_c was increased and σ_s was decreased to keep σ_t the same. Changes were made to cross sections for neutron energies above E_{cut}	119
5.9	A comparison of results for reduced σ_f with σ_t reduced to compensate for the changes, as described in case 1.	120
5.10	A comparison of results for σ_f alterations of case 4. Cross sections were altered for neutron energies greater than 1 keV.	121
5.11	A comparison of the results for case 5 in which σ_c was increased and σ_f was decreased to keep σ_t the same as in the original data, for energies above E_{cut}	121
D.1	Simulation data for spectrometer with geometry parameters $N_{det} = 11$, $r = 10.00$ cm, and $t = 2.00$ cm.	187
D.2	Simulation data for spectrometer with geometry parameters $N_{det} = 11$, $r = 10.00$ cm, and $t = 3.00$ cm.	188
D.3	Simulation data for spectrometer with geometry parameters $N_{det} = 11$, $r = 10.00$ cm, and $t = 3.50$ cm.	189
D.4	Simulation data for spectrometer with geometry parameters $N_{det} = 11$, $r = 10.00$ cm, and $t = 4.00$ cm.	190
D.5	Simulation data for spectrometer with geometry parameters $N_{det} = 11$, $r = 10.00$ cm, and $t = 4.50$ cm.	191
D.6	Simulation data for spectrometer with geometry parameters $N_{det} = 11$, $r = 10.00$ cm, and $t = 5.00$ cm.	192
D.7	Simulated counting data from point sources of strength $s_0 = 10^9$ n cm ⁻² above a concrete floor; FOM^{\min} and $FOM^{\min+}$ represent the lowest and second lowest FOM values, respectively, and C_i^{net} is the room shine net spectra, i.e., $C_i^{net} = C_i^{ns} - C_i^s$. Values in the table of "Correct" and "Inorrect" indicate whether the source was correctly identified.	193

Acknowledgments

First and foremost, I would like to thank Dr. Shultis for taking me back as a graduate student. His constant wisdom, patience, and easy-going personality made this a relatively painless process. I would like to acknowledge Dr. C.J. Solomon at LANL for his mentorship and assistance while producing this work. In addition, I would like to thank my parents for 20 some odd years of guidance and support, as well as for embracing my choice to depart the farmstead to pursue academic ventures. Finally, I would like to thank Madeline Miller for accepting two years of long distance, albeit they were great years, without professing a single complaint on the matter.

This research was performed using funding received from the DOE Office of Nuclear Energy's Nuclear Energy University Programs. The spectrometer design work was supported in part by the Defense Threat Reduction Agency (DTRA) contracts DTRA-12-C-0004, DTRA-01-03-C-0051, and DTRA-01-02-0-0067-003.

Chapter 1

Introduction

This thesis discusses results of simulations related to two unique applications of neutron measurements: neutron spectrometry and multiplicity counting. Chapter 2 provides the necessary statistics and theory of radiation to understand the computations and modeling for the spectrometer and nuclear data studies. A summary of previous methods and designs in neutron spectrometry are given in Chapter 3. Chapter 4 focuses on the spectrometer design methodology for this work, as well as presenting optimization results. Finally, nuclear data perturbations and simulated multiplicity distribution results are discussed in Chapter 5.

1.1 A Neutron Source Identification Spectrometer

As nuclear safeguards become increasingly important, a method for quickly discriminating among different types of neutron sources is vital. The measurement and rapid identification of the distribution of the kinetic energy of neutrons has seen broad study and application since the 1960s with the invention of portable neutron spectrometers. The primary utility of neutron spectrometry has been the ability to estimate the dose experienced by radiation workers. Neutron spectrometry has seen recent resurgence in the field of nuclear safeguards. The control and identification of special nuclear material is important for global security, and the ability to quantify fissionable materials is crucial for fuel reprocessing and modern reactor designs to be viable. Research in design of spectrometers for dosimetry has provided a framework of methods for determining neutron energy spectra based on the theory of unfolding the original spectra from a set of energy-dependant measurements. However, unfolding is a complex, subjective, and generally unstable numerical process. A spectrometer that does not depend on unfolding neutron spectra has been developed at Kansas State University. The device and methodology has been demonstrated to be effective at identifying neutron sources based on direct analysis of energy-dependent measurements [Cooper et al.,

2011]. This neutron source identification spectrometer is optimized and evaluated via Monte Carlo simulations in this work.

The neutron source identification spectrometer design in this thesis uses micro-structured semiconductor neutron detectors (MSNDs) described by Shultis and McGregor [2009]. These MSNDs are efficient at detecting thermal-energy neutrons (with kinetic energy near 0.025 eV) and are capable of 43% efficiency through summation of the output from two stacked, offset detection volumes [Bellinger et al., 2010]. The thickness of the detection volume (parallel to the direction of irradiation) for a double-stacked device is around 0.1 cm deep, a desirable feature for creating a compact spectrometer. The cross sectional area of the devices can be increased to the necessary areas by placing multiple MSNDs together and summing their outputs. In addition to the small thickness and high efficiency, the semiconductor detectors are made primarily of silicon, which has a relatively low neutron interaction cross section. This results in detectors that cause minimal perturbation of the neutron field at non-thermal energies. The low perturbation allows multiple detectors to be placed within the same moderator and provide multiple energy-dependent data points from a single geometric configuration and measurement. Not needing multiple time-consuming measurements significantly improves the overall speed of source identification.

The geometry of the spectrometer consists of an array of MSNDs placed along the axis of a cylinder of high density polyethylene (HDPE) moderator. A sheet of Cd is placed behind each detector to prevent backscattered thermal neutrons from being detected. Figure 1.1 depicts the basic geometric features of a spectrometer consisting of 11 thermal neutron detectors; Detail View A provides an illustration of materials and possible neutron trajectories through the spectrometer. As neutrons travel through the moderator, they lose kinetic energy through scattering collisions. If a neutron slows to thermal energies within a detection volume, the probability of absorption and identification at position is extremely high. For neutrons with higher initial energies, more scattering collisions are required to reach thermal energy, on average. This leads to higher energy neutrons having a higher probability of being absorbed at deeper positions in the spectrometer. Thus, each detector position has a particular energy of incident neutrons on the spectrometer that it is most likely to detect. It is noted that because of the stochastic behavior of neutron scattering, each detector is sensitive to a range of energies, i.e., a fast, mono-energetic source would produce counts in multiple detectors. The sheets of Cd help to limit the range of energies each detector is sensitive to by preventing backscattered thermal neutrons from entering detector volumes from the back.

Because each detector position is sensitive to a particular energy, with some distribution about that energy, the set of detector responses are unique for a particular energy distribution of incident neutrons. Because all bare neutron sources have a particular energy distribution,

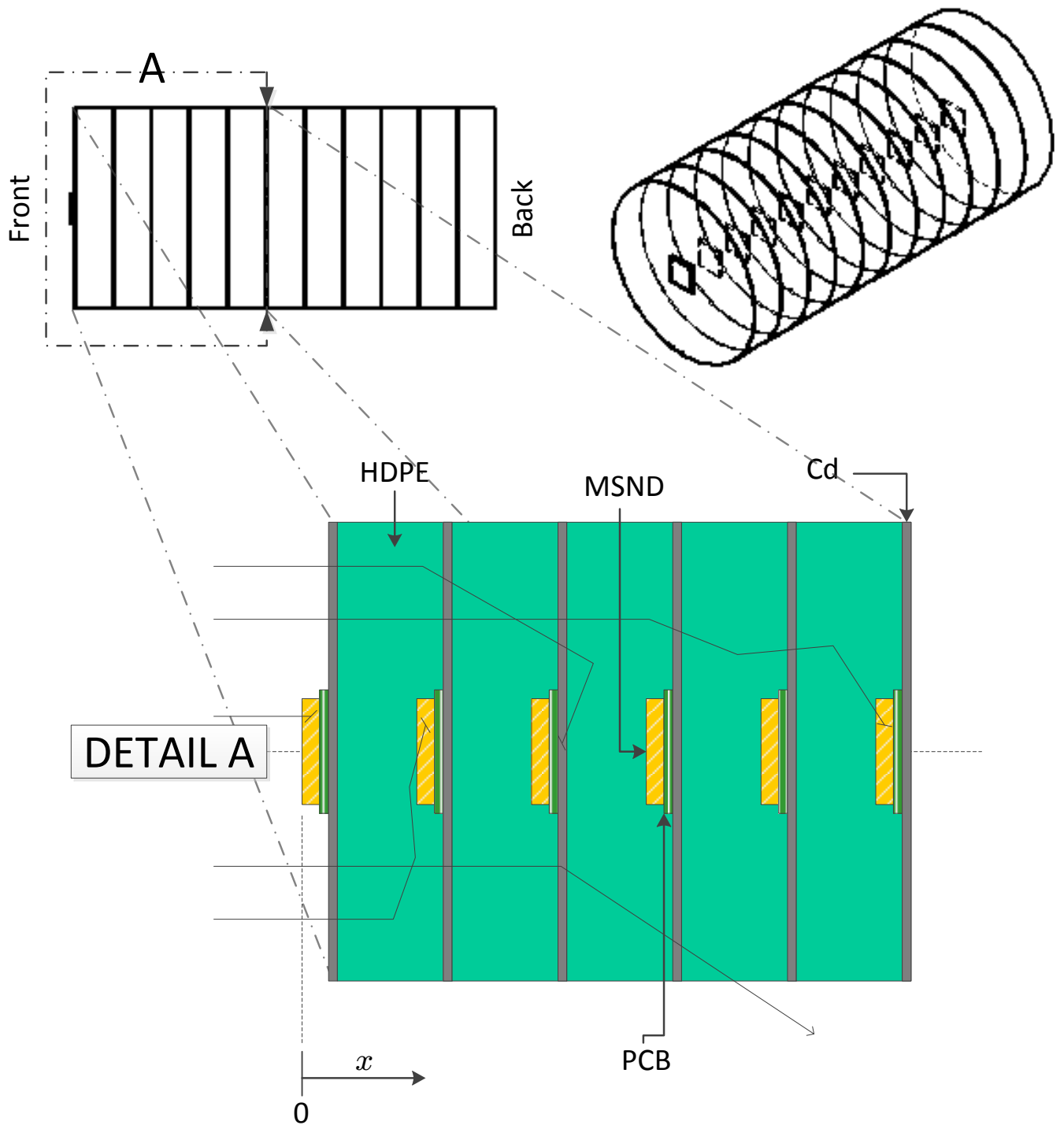


Fig. 1.1: Cylindrical neutron spectrometer with illustration of materials and possible neutron paths

the expected response in each detector per incident neutron is unique to a source. By normalizing the responses in all of the responses to one detector position, the dependence on source strength can be removed. Thus, if room scatter can be accounted for, a library of normalized responses for different sources can be created. An experimental measured response is then compared to the different responses in the library to identify the most likely source. The source library can be created from either experimental measurements or accurate simulations. Comparison of a measured response to the library templates is computationally very efficient and simple, which leads to rapid source identification by a low-power on-board microprocessor; post-processing of measured data and user input required for unfolding is not needed with this template matching method.

First, this work develops a method to quantify the quality of a neutron spectrometer via an objective function based on the statistical confidence of neutron source identifications. This objective function is then applied to the spectrometer through many Monte Carlo simulations to optimize the geometry of the device. The Monte Carlo N-Particle (MCNP5) code was used for these simulations. Simulation studies are also performed to determine the design and effect of location of a shadow shield to account for roomshine. The shadow shield is a known method for calibrating neutron spectrometry experiments that attempts to remove the effect of room-scattered neutrons. Remarks and considerations for future work for the source identification spectrometer are then discussed.

1.2 Simulations of Multiplicity Distributions

The second main focus of this work applies MCNP simulations to a different field of neutron measurements. In particular, use of time dependent data from neutron measurements to construct multiplicity distributions is investigated. A neutron multiplicity distribution depicts the probability of a particular number of neutrons created within a multiplying system being measured over some fixed short amount of time, and is discussed more thoroughly in Chapter 5. Multiplicity distributions are based on coincident events, and they are used to quantify neutron multiplication parameters in a system. Multiplicity distributions have seen their main application in the passive assay of subcritical multiplying systems, specifically quantifying the fissionable material in a device. The validation of simulation tools for modeling such measurements is of great importance to nuclear safeguards and control of special nuclear materials. Monte Carlo modeling is known to inaccurately recreate a particular set of relatively simple multiplicity experiments of reflected plutonium spheres, consisting mostly of the isotope ^{239}Pu [Mattingly, 2009]. The cause of this discrepancy has been narrowed down to the nuclear data [Miller et al., 2010].

Investigation of these experiments has an arguably more important auxiliary benefit. When nuclear data are tabulated for use in simulation codes, there are adjustments performed to the original experimental data with the interest of matching the results of benchmark criticality experiments. The data are not well validated against subcritical experiments. The results in this work demonstrate that subcritical results need to be considered when nuclear data evaluations are performed to create simulation tools that can correctly model such systems. The framework for the work herein can be applied to develop a set of data for a specific task, in this case highly multiplying, fast, subcritical systems.

For this work, perturbations are made to nuclear data to correct the discrepancy between experimental and simulated multiplicity experiments. The focus of perturbations is correctly preserving statistical correlations and uncertainties from experimental measurements of the nuclear data. The primary nuclear data type of interest is the average number of neutrons produced per fission $\bar{\nu}$. Energy-dependent perturbations are made to help conserve the overall balance of neutrons in the system, as increases at one energy may be compensated by decreases at another energy. Additionally, energy-averaged shifts to cross sections are analyzed to determine the sensitivity of the system to $\bar{\nu}$, relative to cross section alterations.

In Chapter 5, a brief overview of neutron multiplicity distributions is given. Then, the experiments to be analyzed and previous simulation work are described. The methods for generating correlated, perturbed nuclear data and comparing the results of multiplicity simulations for the perturbed data sets are discussed. Perturbations were made to nuclear data for ^{239}Pu and simulations of multiplicity distributions performed to determine the effect and correction caused by the individual perturbations. Simulations were performed using the sets of perturbed data as the input for the MCNP5 code with special subroutines for studying subcritical systems. The reflected plutonium spheres are modeled explicitly and neutron multiplicity distributions are generated using a post-processing script. Results are discussed and compared.

Chapter 2

Theory

2.1 Relevant Probability and Statistics

2.1.1 Random Variables and Probability Distribution Functions

A continuous random variable is a variable that maps the occurrence of a particular event onto a set of real numbers, in a one-to-one manner [Hogg et al., 2013]. The value of the random variable is in general unknown until a realization (i.e., an observation or sampling) of the variable occurs. Typically upper-case characters are used to indicate a random variable, whereas lower-case is used to indicate the value of a sample on the variable. It is noted that samples are a random variable themselves until realization occurs [Hogg et al., 2013], but in this work samples refer to the value of realizations on a random variable. The probability of the random variable taking on a particular value can be known in advance and is defined using probability distribution functions. The cumulative distribution function (CDF) is a non-decreasing, positive function $F(x)$ whose values lie between 0 and 1. For a random variable X with CDF $F(x)$, the value of $F(x)$ represents the probability that X will have a value less than or equal to x (in standard notation $F(x) = P(X \leq x)$). Related to the CDF, is the probability density function (PDF). The PDF $f(x)$ is defined as

$$f(x) = \frac{dF(X)}{dx}. \quad (2.1)$$

Explicitly, the value $f(x) dx$ represents the probability of finding X in dx about x . Therefore, normalization requires

$$\int_{-\infty}^{\infty} f(x) dx = 1. \quad (2.2)$$

From the above definitions, it is straightforward that the PDF can be used to compute the probability of finding X between a and b , where $a < b$ and $a, b \in S_X$, as

$$P(a < x < b) = \int_a^b f(x) dx. \quad (2.3)$$

It is noted that the PDF and CDF are defined for all real numbers by definition, even though the random variable may be defined for some subset of all real numbers. The support (S_X above) of a random variable is defined as the points in the domain of a random variable for which the probability is positive; in this work the supports of random variables are given to identify their domain; it is assumed the PDF is zero elsewhere. The discussion in this section is for continuous random variables but can be easily extended to discrete random variables, as discussed in literature [Hogg et al., 2013; Shultis and Dunn, 2011].

2.1.2 Expectation Values and Moments

An expectation value for a function $g(x)$ is defined as

$$E[g(x)] = \int_{-\infty}^{\infty} g(x)f(x) dx, \quad (2.4)$$

where $f(x)$ is the PDF for the random variable X . The expected value of a function represents the mean, or average, value of the function that would be calculated using repeated observed values of x . Some special expectations are useful to define the shape and behavior of a distributions, in particular the moments and their combinations. The n -th moment of a PDF is defined as

$$M_n = E(x^n) = \int_{-\infty}^{\infty} x^n, f(x) dx. \quad (2.5)$$

The first moment is the mean value of the random variable X , notated as μ . A particularly useful combination of moments is defined as the variance, σ^2 , which can be shown to be [Hogg et al., 2013]

$$\sigma^2 = \int_{-\infty}^{\infty} (x - \mu)^2 f(x) dx = M_2 - (M_1)^2. \quad (2.6)$$

The square root of the variance is defined as the standard deviation. The standard deviation is useful in defining statistical confidence intervals about the mean.

2.1.3 Covariance and Correlation Matrices

Consider a set of N *dependent* random variables $X_i : i = 1, 2, \dots, N$. The covariance between two of any variables in this set, X_i and X_j , is

$$\text{Cov}(X_i, X_j) = E(X_i X_j) - E(X_i)E(X_j). \quad (2.7)$$

From the above definition of variance, $\text{Cov}(X_i, X_i) = \sigma^2(i)$. From the covariance between each all pairs of terms, a covariance matrix Σ is formed as

$$\Sigma_{ij} = \text{Cov}(X_i, X_j) : i = 1, 2, \dots, N; j = 1, 2, \dots, N. \quad (2.8)$$

The syntax here is Σ_{ij} is the matrix element of the i -th row and j -th column of a matrix Σ . Directly related to a covariance matrix Σ is its correlation matrix, \mathbf{C} , with elements, known as correlation coefficients,

$$C_{ij} = \frac{\Sigma_{ij}}{\sqrt{\Sigma_{ii}\Sigma_{jj}}} : i = 1, 2, \dots, N; j = 1, 2, \dots, N. \quad (2.9)$$

The correlation matrix provides a measure of the interdependence between the i -th and j -th variable, i.e., on average if the value of one variable is observed, the correlation coefficient provides the expected behavior of the second. All values of the correlation matrix are between -1 and 1. A negative value indicates that if the probability of observing large values of the i -th variable is high, then the second variable is expected to be small, on average; the converse is also true. Positive correlation coefficients indicate that if the probability of observing a large value of a variable is high, then the probability of observing large values of the second variable is also high; again, the converse is also true. The magnitudes of the values indicate the strength of the correlation, with the diagonal terms being the strongest at 1 (the correlation of a variable with itself is perfect). A set of independent variables would have zero for all off-diagonal terms of \mathbf{C} .

2.1.4 Sample Mean and Variance

Often, the exact moments of a distribution (population moments) are unknown because the CDF and PDF can be complicated or unknown; population moments can also be undefined if the integrals in the previous section diverge. However, samples from a distribution can be used to estimate the population moments. Here, a set of samples is formally a set of independent, random observations of a random variable with some distribution. The sample mean \bar{X} is simply the average of a set of N discrete samples $\{x_i : i = 1, 2, \dots, N\}$ on the

random variable X with PDF $f(x)$, i.e.,

$$\bar{x} = \frac{1}{N} \sum_{i=1}^N x_i. \quad (2.10)$$

Similarly, the sample variance s^2 is given by

$$s^2 = \frac{1}{N-1} \sum_{i=1}^N (x_i - \bar{x})^2. \quad (2.11)$$

The subtraction of one from N in the above equation comes as a result of a loss of a degree of freedom by approximating the population mean with the sample mean [Shultis and Dunn, 2011]. The sample mean and variance can be shown to be unbiased estimates of the population mean and variance, respectively [Hogg et al., 2013]. An estimator T is an unbiased estimator of Y if $E(T) = Y$; an estimate is just the realization of an estimator T . It can also be shown that as $N \rightarrow \infty$, the sample mean and variance converge in probability to the population mean and variance [Hogg et al., 2013]. It is noted that the notation for sample and population statistics is poor (particularly for the variance), where population statistics are discussed and notated, where sample statistics are actually applied.

2.1.5 Useful Distributions

Several distributions are used throughout this work. The PDFs for these distributions are stated here with justification for application. In all cases, the random variable of interest is X with PDF $f(x; \theta)$, where θ is one or more distribution parameters required to fully define the distribution. Derivations, sampling methods, and other relations for these distributions can be found in literature [Shultis and Dunn, 2011; Press et al., 1992].

Binomial Distribution

The binomial distribution has application for a sequence of discrete, independent random trials which have a binomial outcome, i.e., either the outcome occurs or does not occur, with the same probability of success p for each trial. Radiation counting measurements have a binary outcome, i.e., either a count was made or not, so the number of counts observed in a detector can be modeled as a binomial distributed variable. The number of successes X in N independent trials, with probability of success in each trial p , is described as

$$f(x; p, N) = \frac{N!}{(N-x)!x!} p^x (1-p)^{N-x} \quad x = 0, 1, \dots, N. \quad (2.12)$$

Poisson Distribution

The Poisson distribution is a discrete distribution that is useful for describing independent, identical trials that have a low probability of success in each trial, where the number of trials is large (usually the number of trials occurs over some relatively large, fixed time interval). For a binomial distributed variable, if the value of N is very large with a small value of p , then the Poisson distribution is a good approximation for the binomial distribution; the approximation is applicable for $N \gtrsim 20$, provided that $Np < 5$ [Shultis and Dunn, 2011]. Radiation counting measurements can be appropriately modeled as a Poisson process [Tsoulfanidis, 1995]. The distribution is fully-defined by the mean, μ , of the distribution, which is also the rate of successful trials occurring. The number of successful trials X has the distribution:

$$f(x; \mu) = \frac{\mu^x e^{-\mu}}{x!} \quad x = 0, 1, \dots \quad (2.13)$$

Unit Uniform Distribution

The unit uniform distribution is for a continuous random variable X between 0 and 1 exclusive, with equal probability of occurrence at each X . The unit uniform distribution has utility in sampling pseudo-random numbers from other distributions. The unit uniform distribution has no distribution parameters and PDF

$$f(x) = 1 \quad x \in (0, 1). \quad (2.14)$$

Chi-squared Distribution

The χ^2 distribution is for continuous random variables X defined over $(0, \infty)$. The distribution has application in optimization schemes and hypothesis testing. The degrees of freedom, r , is the mean of X and used to fully define the distribution as

$$f(x; r) = \frac{1}{\Gamma(r/2)2^{r/2}} x^{r/2-1} e^{-x/2} \quad x \in (0, \infty), \quad (2.15)$$

where Γ is the standard gamma function [Hogg et al., 2013]; for integers α , $\Gamma(\alpha) = (\alpha - 1)!$.

Gaussian (Normal) Distribution

The Gaussian (normal) distribution is for continuous random variables $X \in (-\infty, \infty)$. Although it has many applications, its primary use in this work is for confidence intervals based on the central limit theorem, as discussed in Hogg et al. [2013]. It can also be used to approximate binomial and Poisson distributions accurately in some cases. The distribution

is fully-defined by its mean μ and variance σ^2 , notated as $N(\mu, \sigma^2)$, with PDF

$$f(x; \mu, \sigma^2) = \frac{1}{\sqrt{2\pi\sigma}} e^{-(\mu-x)^2/(2\sigma^2)} \quad x \in (-\infty, \infty). \quad (2.16)$$

The multivariate normal distribution is more complicated, but can be used to fully described the distribution of multiple variables which have normal distributions with different means, variances, and correlation between variables; the mean of each variable and the correlation matrix fully defines the multivariate normal distribution.

2.1.6 Generating Random Samples from a Distribution

In any Monte Carlo simulation, it is necessary to sample random numbers from various distributions. There have been many algorithms developed for efficiently sampling pseudo-random numbers from a unit uniform distribution [Shultis and Dunn, 2011; Press et al., 1992]. The unit uniform distribution for a random variable U has a PDF defined as $f_U(u) = 1, u \in [0, 1]$. The CDF of this distribution is given by $F_U(u) = u, u \in [0, 1]$. Since numbers can efficiently be sampled from this distribution, it is useful to know the transformation between random variables that allows for a variable with a uniform distribution to take on any other distribution.

To determine the transformation, consider a continuous random variable X defined to be the transformation $X = F^{-1}(U)$, where $F^{-1}(y)$ is the solution to the equation $F(x) = y$, for any continuous CDF $F(x)$. The goal is to determine the distribution of X , i.e. $F_X(x)$, and if it is $F(X)$, then the transformation performs the desired goal. Because F is a CDF, it is a monotonically non-decreasing function between 0 and 1, therefore the relation between X and U is one-to-one. Transformations between variables without a one-to-one relation require regions of the support to be analyzed individually, as demonstrated in [Hogg et al., 2013]. Since the transformation is one-to-one, the distribution of X is given by

$$F_X(x) = P(X \leq x) = P(F^{-1}(U) \leq x). \quad (2.17)$$

Applying F to both sides of the inequality in the right most term yields

$$F_X(x) = P(F[F^{-1}(U)] \leq F(x)) = P(U \leq F(x)). \quad (2.18)$$

But the probability of U being less than some value is simply the CDF of U . The CDF of U is $F_U(u) = u$, therefore:

$$F_X(x) = P(U \leq F(x)) = F_U[F(x)] = F(x). \quad (2.19)$$

Hence, the distribution of X is the CDF of interest F , which had no constraints other than continuity. Since samples from a distribution are distributed with that distribution, samples from the unit uniform distribution can be transformed to create samples from another distribution by simply applying the inverse CDF. There are many efficient sampling techniques developed for when the inverse does not exist [Hogg et al., 2013; Shultis and Dunn, 2011].

2.1.7 Generating a Set of Correlated Random Samples

Normally-distributed, independent random variables, and samples of them, can be correlated using data from a corresponding covariance matrix (with corresponding correlation matrix). In general, to correlate a vector of normally distributed random variables using a $N \times N$ correlation matrix \mathbf{C} , a decomposition of the form [Rousseuw and Molenberghs, 1993]

$$\mathbf{V}\mathbf{V}^T = \mathbf{C}. \quad (2.20)$$

is needed. Here \mathbf{V} , with transpose \mathbf{V}^T , is any matrix that obeys the above equation, and \mathbf{C} is the correlation matrix associated with the set of data that is being sampled.

Once a matrix \mathbf{V} is found, a vector \mathbf{R} of n independent, normally-distributed random numbers is correlated via [Rousseuw and Molenberghs, 1993]

$$\tilde{\mathbf{R}} = \mathbf{V}\mathbf{R}. \quad (2.21)$$

where $\tilde{\mathbf{R}}$ is the vector of correlated random numbers. The vector \mathbf{R} is sampled from the standard normal distribution, i.e., $N(0, 1)$, and then modified to match the desired mean and variance after correlation [Rousseuw and Molenberghs, 1993].

There are multiple types of decomposition that produce a \mathbf{V} that is valid for Eq. (2.20). Two common decompositions for correlated sampling are Cholesky and eigenvalue decompositions; the latter is more robust. For the Cholesky decomposition of a matrix \mathbf{C} , \mathbf{V} in Eq. (2.21) is a lower-triangular (or symmetric upper-triangular) matrix. In an eigenvalue decomposition of a matrix \mathbf{C} , \mathbf{V} of Eq. (2.21) takes the form

$$\mathbf{V} = \mathbf{Q}\mathbf{D}. \quad (2.22)$$

Here, \mathbf{Q} is a matrix where the j -th column vector represents the orthonormal eigenvector corresponding to the j -th eigenvalue, λ_j , of the matrix \mathbf{C} . The matrix \mathbf{D} is a diagonal matrix with the j -th diagonal element $D_{jj} = \sqrt{\lambda_j}$. The eigenvalue decomposition may require orthogonalization after decomposition if \mathbf{C} contains degenerate (repeated) eigenval-

ues [Rousseuw and Molenberghs, 1993]. For an intuitive understanding of how these methods sample from the correlation matrix, consider that the matrix \mathbf{Q} is an orthonormal basis for \mathbf{C} . Thus, the multiplication \mathbf{VR} is transforming the vector \mathbf{R} into the basis of \mathbf{Q} , such that the distribution of variables in $\tilde{\mathbf{R}}$ is now the multivariate normal distribution with correlation matrix \mathbf{C} .

Cholesky decomposition is only valid for symmetric, positive-definite (PD) matrices, but the eigenvalue decomposition described above is valid for (at least) positive-semidefinite (PSD) matrices [Rousseuw and Molenberghs, 1993]. A matrix \mathbf{A} is PD if $\mathbf{X}^T \mathbf{A} \mathbf{X} > 0$, for all real vectors \mathbf{X} ; the matrix A is PSD if $\mathbf{X}^T \mathbf{A} \mathbf{X} \geq 0$. For the eigenvalue decomposition, if \mathbf{C} is non-PSD the eigenvalues will be negative, resulting in non-real elements of \mathbf{D} . A true covariance matrix is PD, but the statistical techniques used to estimate covariance matrices from observed data can lead to PSD and non-PSD matrices [Rousseuw and Molenberghs, 1993]. A fix-up method can be applied to correct non-PSD matrices using the eigenvalue decomposition method. The fix-up method generates a modified \mathbf{C} that is PSD given by

$$\mathbf{C}' = (\mathbf{QD}')(\mathbf{QD}')^T. \quad (2.23)$$

In the above equation, \mathbf{D}' is a diagonal matrix with matrix elements: $D'_{jj} = \sqrt{|\lambda_j|}$. \mathbf{Q} is the same orthonormal eigenvector matrix from the initial decomposition in Eq. (2.22).¹

The now PSD matrix \mathbf{C}' is then transformed into a correlation matrix such that the diagonal elements are all unity, i.e.,

$$\tilde{C}_{ij} = \frac{C'_{ij}}{\sqrt{C'_{ii} C'_{jj}}} \quad (2.24)$$

The new correlation matrix, $\tilde{\mathbf{C}}$, has different off-diagonal (co-relation) values than the original correlation matrix. However, for a \mathbf{C} with negative eigenvalues relatively small in magnitude, the new off-diagonal elements change minimally from the original values. The new matrix $\tilde{\mathbf{C}}$ can then be decomposed to find a \mathbf{V} for sampling.

2.1.8 Error Propagation Formula

It is often of interest to determine the uncertainty, stochastic or systematic, in a computed result. The uncertainty in a computed result comes directly from the uncertainty in the

¹Although the elements of \mathbf{D} in the original decomposition are complex, numerical eigenvalue decomposition methods (e.g. those in Press et al. [1992]) determine the eigenvalues (i.e., $\lambda_i = (D^T D)_{ii}$) and eigenvectors of a matrix, rather than the decomposition given in Eq. (2.22). Thus, the matrix of eigenvectors \mathbf{Q} and eigenvalues can be obtained from a non-PSD matrix.

observed values of the variables used to calculate it. If a functional relation between the observed variables and the final result is known, then the error propagation equation provides a method of approximating the uncertainties in the result, based on the independent variables the result depends on [Dunn, 2005].

The following derivation of the general error propagation equation is for independent distributed statistical errors, but the result can be directly applied to independent systematic errors; the requirement in both cases is that the observed variables are generally distributed near the observed values (e.g., normally distributed) [Dunn, 2005].

Consider a result f that is a function of a vector of n independent random variables $\mathbf{X} = \{X_i : i = 1, 2, \dots, n\}$, i.e., $f = f(\mathbf{X})$. A random variable is simply a variable whose value is unknown before observation and follows some distribution. Although there are some special cases [Dunn, 2005], in general the exact relation between uncertainties of independent observed variables and a functional result is unknown. An approximation is introduced by expanding f as a first order Taylor polynomial [Dunn, 2005], i.e.,

$$f(\mathbf{X}) \approx f(\mathbf{X}_{obs}) + \sum_{i=1}^n \frac{\partial f}{\partial X_i} (X_i - X_{i,obs}). \quad (2.25)$$

In the above equation, the vector \mathbf{X}_{obs} represents the observed values of each variable X_i used to compute the result f . For a linear combination of independent random variables, $T = \sum_{i=1}^n a_i Y_i$, with combination coefficients $\{a_i\}$, the variance can be shown to be [Hogg et al., 2013]

$$\sigma^2(T) = \sum_{i=1}^n a_i^2 \sigma^2(Y_i) \quad (2.26)$$

With the assumption all variances are defined.

In Eq. (2.25), $f(\mathbf{X})$ is written as a linear combination with $a_i = \partial f / \partial X_i$ and a constant term $f(\mathbf{X}_{obs})$. The constant term does not contribute to the variance $\sigma^2[f(\mathbf{X})]$. Combining these results with Eq. (2.26) yields the result for any \mathbf{X} near \mathbf{X}_{obs} (to first order):

$$\sigma(f) = \sqrt{\left(\frac{\partial f}{\partial X_1} \sigma(X_1)\right)^2 + \left(\frac{\partial f}{\partial X_2} \sigma(X_2)\right)^2 + \dots + \left(\frac{\partial f}{\partial X_n} \sigma(X_n)\right)^2}, \quad (2.27)$$

where the square root has been taken to yield the standard deviation of f , $\sigma(f)$, about the observed value \mathbf{X}_{obs} . The above equation is referred to as the general formula for error propagation and can be applied to determine the uncertainty about any observed value; lower case variables have been used to indicate that this result applies to any observed variables, not exclusively to stochastic errors. The truncation error introduced by the first order Taylor

approximation is relatively small because the uncertainties are generally assumed to be small. This approximation may be very poor, depending on the functional form of f [Taylor, 1997].

2.1.9 χ^2 Goodness-of-Fit Statistic

A chi-squared goodness-of-fit statistic can be used to compare the accuracy of a set of statistical observed data to some reference set of data (e.g. an exact solution or experimental data). A statistic is simply a function of a set of random samples on random variables that provides information about those random variables [Hogg et al., 2013]. Consider the random variable Y specified as

$$Y = \sum_{i=1}^N \left(\frac{X_i - \mu_i}{\sigma_i} \right)^2, \quad (2.28)$$

where μ_i and σ_i are respectively the mean and variance of the i -th random variable X_i . Random samples of the random variable Y are defined as the χ^2 goodness-of-fit statistic. If the set of n random variables $\{X_i : i = 1, 2, \dots, N\}$ are normally distributed, i.e., $X_i \sim N(\mu_i, \sigma_i^2)$, then Y has a χ^2 distribution with n degrees of freedom (labeled as $\chi^2(n)$) [Hogg et al., 2013]. The set of random variables $\{X_i\}$ will take on a χ^2 distribution for various other distributions of X_i as well.

An approximate chi-squared goodness-of-fit statistic can be used to compare the accuracy of a set of statistical observed data to some reference set of data (e.g. an analytical solution, expected value, or experimental data). The true mean and variance of the distribution may not be known and there may be statistical uncertainty in the estimated mean that needs to be accounted for as well. To account for these statistical uncertainties one uses the chi-squared statistic

$$\chi^2 = \sum_{i=1}^N \frac{(R_i - S_i)^2}{\sigma^2(R_i) + \sigma^2(S_i)}, \quad (2.29)$$

where R_i and S_i are the observed and reference value of the i -th of N measurements, with their respective sample variances $\sigma^2(R_i)$ and $\sigma^2(S_i)$. The two sample variances may be approximated as the square of the standard errors of R_i and S_i , respectively. The value of χ^2 gives a measure of the accuracy of each observed data point as compared to the corresponding reference data point, weighted by the uncertainty in each. For comparing the quality of unique sets of observed data (or multiple sets of reference data), the set with the lowest χ^2 value produces a result that is closest to the reference measurements.

Application of the standard error propagation formula and ignoring the variance of the

variances, the standard error for χ^2 , $\sigma(\chi^2)$, is given by

$$\sigma(\chi^2) = 2\sqrt{\chi^2}. \quad (2.30)$$

The above equation is used to determine if sets of observed data whose chi-squared values are near each other produce distinguishable results. It is of note that this is not the true variance of the statistic, but an approximation which can be very poor depending on the functional behavior of the values of R_i and S_i .

A reduced chi squared value can also be used for goodness of fit tests. The reduced chi-squared value, χ_{red}^2 , is given as

$$\chi_{red}^2 = \frac{\chi^2}{\eta}. \quad (2.31)$$

Here η is the number of degrees of freedom and the remaining variables are as before. The approximate uncertainty in χ_{red}^2 is similar for χ^2 , i.e.,

$$\sigma(\chi_{red}^2) = 2\sqrt{\frac{\chi_{red}^2}{\eta}}. \quad (2.32)$$

The utility of the reduced chi-squared value is that it normalizes for the number of data points. The normalization allows for a comparison to multiple sets of data, allowing for each set of data to carry equal weight in the comparison. It is noted that a χ_{red}^2 statistic is not distributed as $\chi^2(1)$, as might be expected [Hogg et al., 2013].

2.2 Nuclear Data and Radiation Interactions

2.2.1 Attenuation of Neutral Particles

Consider a uniform beam of neutrons I_0 (n cm^{-2}) incident upon an infinite slab of an *isotropic* medium, as depicted in Fig. 2.1. The total probability of interaction per unit differential length is defined as the macroscopic cross section, Σ_t (cm^{-1}). The probability of a neutron interacting in a differential pathlength dx is $\Sigma_t dx$ [Shultis and Dunn, 2011]. Defining x to be the coordinate along the transverse axis of the slab, the intensity of uncollided neutrons $I^0(x)$ at a distance x into the slab is of interest. The rate of change of $I^0(x)$ with respect to x at some value of x is proportional to the amount of uncollided particles at x , therefore

$$\frac{dI^0(x)}{dx} = -P(\text{Interaction in } dx) * I^0(x) = -\Sigma_t I^0(x). \quad (2.33)$$

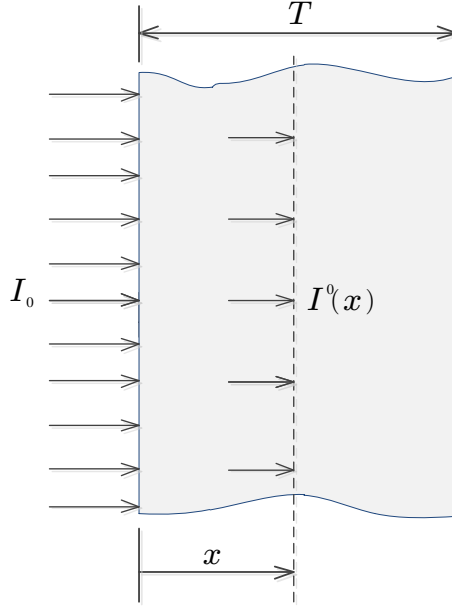


Fig. 2.1: Neutrons incident upon an infinite slab of thickness T .

The solution to the above differential equation yields

$$I^0(x) = I_0 e^{-\Sigma_t x}. \quad (2.34)$$

Therefore, the intensity of uncollided neutrons is attenuated exponentially. The PDF for the probability of interacting at x is easily shown to be $f(x) = \Sigma_t e^{-\Sigma_t x}$ [Shultis and Dunn, 2011]. The probability of a neutron interacting in the slab is thus

$$P(\text{Interaction}) = 1 - e^{-\Sigma_t T}. \quad (2.35)$$

2.2.2 Microscopic Cross Section

The primary form of interaction for neutrons is with the nucleus of atoms in the medium. The rate of interaction per differential length, Σ_t above, is proportional to the density of atoms. The density of atoms per unit volume (or number density) N for a medium composed of a single elemental isotope is given by

$$N = \frac{\rho N_a}{\mathcal{A}}, \quad (2.36)$$

where N_a is Avogadro's number, ρ is the mass density, and \mathcal{A} is the atomic weight of the

element. With the above definition, the definition of Σ_t becomes

$$\Sigma_t \propto N = \sigma_t N. \quad (2.37)$$

The proportionality constant σ_t (cm^2) is defined as the microscopic cross section and independent of N . The value of σ_t represents the total probability of interaction per unit differential path length, normalized to a single target atom [Shultis and Faw, 2000]. Because the values of σ are very small, the unit of barns is typically used, defined as $1\text{b} = 10^{-24}\text{cm}^2$. For an isotropic medium, the microscopic cross section is typically a function of the energy of neutron and the particular isotope of nuclei present. In general, cross sections are relatively larger at lower energies.

Cross sections are typically tabulated for each fundamental type of interaction, and the occurrence of types of interactions are mutually exclusive events, therefore

$$\sigma_t = \sum_{i=1}^n \sigma_i, \quad (2.38)$$

where σ_i is the cross section for the i -th of n types of interactions. The main interactions for neutrons are absorption, fission, and elastic and inelastic scattering, which are discussed thoroughly in [Shultis and Faw, 2000]. The terminology of absorption and capture can vary in literature. Often absorption includes the fission and capture cross section, whereas capture usually refers to (n, γ) reaction; the notation is *target nucleus(incident particle, outgoing particle)resulting nucleus*, where the two nuclei are often omitted in a general case. For clarity, herein neutron capture cross section is used to refer to any interaction in which a neutron is absorbed without reemission of any neutrons (sometimes called a removal cross section), i.e. $\sigma_c = \sigma_{n,\gamma} + \sigma_{n,p} + \sigma_{n,\alpha} + \dots$.

For a composite medium of isotopes, the total macroscopic cross section is given by

$$\Sigma_t = \sum_{j=1}^{n_{iso}} N_j \sigma_t, j, \quad (2.39)$$

where the subscript j represents the j -th of n_{iso} isotopes.

2.2.3 Neutron Flux Density

An important property used to quantify a field of neutrons in a medium is the neutron fluence. Consider a hypothetical sphere of volume ΔV with a field of neutrons traversing the volume in any direction over some time t . The neutron fluence is defined as [Shultis and

Faw, 2000]

$$\Phi = \lim_{\Delta V \rightarrow \infty} \left[\frac{\sum_i s_i}{\Delta V} \right], \quad (2.40)$$

where s_i is the path length traversed through the volume by the i -th neutron track. In an alternative definition, the neutron fluence (units of cm^{-2}) is the number of particles that have traversed a sphere of differential cross-sectional area, at a point. The neutron flux density (abbreviated as flux) is the time-derivative of the fluence, i.e.,

$$\phi = \frac{d\Phi(t)}{dt} \quad (2.41)$$

which is constant in time for steady-state applications. In general, the steady-state flux is a function of neutron energy, direction, and position; respectively, $\phi = \phi(E, \mathbf{\Omega}, \vec{r})$. The scalar flux is the angular integrated flux, i.e., $\phi(E, \vec{r})$, and in many detection application cases the energy dependence is also integrated out. The flux can be defined alternatively as the product of the neutron density per volume and the neutron speed. The flux is referring to the scalar flux throughout this work.

The utility of the neutron flux is to directly calculate the reaction rate density using the macroscopic cross section. The reaction rate density is the average number of interactions occurring per unit volume, per unit time. Using the definition of flux as the differential total path length traversed by all neutrons at a point, per unit time, and the macroscopic cross section Σ_t as the differential probability of interaction per unit length, the reaction rate density is

$$R(\vec{r}) = \Sigma_t(\vec{r})\phi(\vec{r}). \quad (2.42)$$

Another useful parameter is the neutron current. The neutron current is the first angular moment of the directionally dependent neutron flux. The current is useful because it provides a measure of the net number of particles per unit area entering a surface.

2.2.4 Effective Neutron Multiplication Factor

In a system in which fission is present, the criticality of the system can be quantified by the effective neutron multiplication factor, k_{eff} . Here, fission is referring to the process of an unstable nucleus decomposing into two or more fragments. Fission can occur spontaneously from unstable isotopes (e.g. ^{240}Pu), or it can be induced by an incident neutron. When fission occurs, multiple neutrons can be released. Thus, induced fission allowing for a self-sustaining chains of neutron reactions to occur. Such a system is said to be critical. Quantifying the sustainability of the population neutrons in a system is the value of k_{eff} defined as [Shultis

and Faw, 2008]

$$k_{eff} = \frac{\# \text{ neutrons produced from fission in one generation}}{\# \text{ of neutrons removed from the system in preceding generation}}. \quad (2.43)$$

The value of k_{eff} is a product of the material properties and geometry of the system. A system which produces a value of k_{eff} of unity is critical. In a critical system, the fission process allows for the population of neutrons to remain constant in time. If $k_{eff} > 1$, then the system is said to be supercritical. If $k_{eff} < 1$, the system is subcritical.

2.2.5 Neutrons Released per Fission ν

Typically, when fission occurs, one or more neutrons of varying energy are released from the excessively energetic fission products, effectively instantaneously. The number of free neutrons produced per fission, ν , is a vital parameter in modeling systems in which fission occurs. In this work, ν is used to refer to the mean number of neutrons produced from *induced* fission only, as it is the main interest. It is also noted that typically ν is divided into prompt (induced fission) and delayed (fission fragments releasing neutrons through radioactive decay at a later time) components. For this work, ν is referring to the sum of the prompt and delayed neutrons, i.e., the *total* number of neutrons released per fission.

The parameter ν is formally a discrete random variable. The distribution of ν is dependent upon the energy of incident neutron (i.e., $\nu = \nu(E)$) and the isotope of the target nucleus. The distribution of $\nu(E)$ at an energy E is in general binomial, but it is known to be well-approximated by shifted Gaussian distributions [X-5 Monte Carlo Team, 2003]. Typically, the mean of the distribution, $\bar{\nu}$, and variance σ^2 are used to quantify unique distributions for each energy and isotope. Typical values of $\bar{\nu}$ range from 1-4 for fissile isotopes, generally increasing with the energy of incident neutron.

For Monte Carlo simulations that investigate criticality, only sampling of $\bar{\nu}(E)$ is needed to properly recreate average macroscopic quantities (such as tallies or the neutron multiplication factor k_{eff}) [X-5 Monte Carlo Team, 2003]. This is due to the large number of neutrons present in the system. To sample $\bar{\nu}$, such criticality simulations typically sample the integer values that bracket $\bar{\nu}(E)$, such that the mean of the sampled values is $\bar{\nu}(E)$. For subcritical simulations, the distribution of $\nu(E)$ must be more accurately sampled. The typical sampling method is to sample integer values of $\nu(E)$ based on a Gaussian distribution that properly identifies the distribution of $\nu(E)$ for a particular isotope and energy. The Gaussian distribution has $\bar{\nu}(E)$ as a mean at each energy E , but the value of the variance is typically a constant for each isotope.

2.3 Monte Carlo Transport Code

2.3.1 The Monte Carlo Method and MCNP

The Monte Carlo method is a stochastic method, which can be used to estimate average values of physical parameters by simulating realistic behavior of the system of interest. In short, the Monte Carlo method is to generate a large number of simulated trials (known as histories), and then look at the average behavior of the histories. For radiation transport, a history consists of creating and tracking a particle through a medium, using appropriate radiation physics, until the particle terminates through leakage or absorption. The simulation uses appropriate probability distributions (based on nuclear data) to simulate interactions and trajectories of particles. Tallies are used to estimate some aspect of the radiation field. Tallies are an estimate of the mean of some random variable (e.g. the neutron fluence). A tally is estimated by taking the average of the contributions to some physical feature of the neutron field of all particle histories. The statistical error associated with tallies is also estimated, typically using the sample standard deviation of the tally of interest. The theory behind the Monte Carlo method is discussed in detail in literature [Shultis and Dunn, 2011].

The majority of raw data in this work are generated from the Monte Carlo N-Particle (MCNP) code (primarily version 5.1.51). The MCNP code is a general-purpose, fully 3-dimensional transport code that allows for simulations of coupled neutron, photon, and charge particle phenomena [X-5 Monte Carlo Team, 2003]. The code contains tabulated nuclear data for all isotopes of interest. MCNP performs simulations by interpreting user-created text input files which specify geometry, material properties, and physics and simulation parameters. MCNP uses a Monte Carlo method that is continuous in phase space, i.e., particle tracks are continuous in energy, direction, and location. Tallies allow estimates of the neutron flux, current, and reaction rate densities, as well as their respective statistical uncertainties. MCNP6 is capable of accurate estimation of charge deposition by charge particles in a radiation detector. Along with the uncertainty in tallies, MCNP performs a series of ten statistical tests to determine the statistical validity and convergence of tally scores and uncertainties. A full description of specific features of the code, as well as an overview of Monte Carlo modeling of radiation physics, can be found in the manual [X-5 Monte Carlo Team, 2003].

2.3.2 Non-Analog Variance Reduction in MCNP

Various non-analog simulation techniques are available to reduce the uncertainty in tallies and to help pass the ten statistical tests without increasing the number of particle histories.

Several of these techniques used in design of the spectrometer to improve the efficiency of simulations are discussed here. There are other analog truncation methods (such as particle energy cut-offs) implemented implicitly, which are straight forward and discussed in Shultis and Faw [2004].

The basic goal of variance reduction techniques is to decrease the uncertainty in a tally, without increasing the number of histories. Additionally, variance reduction helps to improve convergence of the problem and pass the ten statistical tests provided by MCNP. Passing these tests provides assurance that the central limit theorem (see Shultis and Dunn [2011]) is valid for the tally of interest. When the central theorem is valid, the tally has a Gaussian distribution with a mean and standard deviation given by the tally's reported value and sample standard deviation. To ensure that variance reduction techniques do not introduce bias into the mean, the techniques must also operate on the so-called weight, or importance, of the particle history. When tallies sum a property of a particle during a history, the particular properties are multiplied by the corresponding weight of the particle in the summation. This prevents biasing of results [X-5 Monte Carlo Team, 2003].

Implicit Capture

Implicit capture is a feature that is turned on by default in MCNP5. When a particle undergoes an absorption event, rather than terminating the history, the history is continued with the particle's weight reduced by a factor equal to the conditional probability of non-absorption ($1 - \sigma_c/\sigma_t$). This feature cannot be used in charge deposition simulations, where the exact location of absorption is of importance [X-5 Monte Carlo Team, 2003].

Cell-Based Splitting

MCNP geometry is divided into contiguous geometric regions known as cells, which have an importance assigned to them. Non-void cells that are closer to a tally are generally considered more important to the problem. The importance in these cells can be increased as the position gets closer to tallies of interest as a form of variance reduction.

If a particle crosses from one cell to another with higher importance, the particle is divided into n particles with the same velocity as the original particle; the weight of each new particle is the original particle weight reduced by a factor of $1/n$. The factor n is the ratio of the importance of the cell the particle is entering to the importance of the cell the particle is exiting. A form of uniform random sampling is performed to produce an integer number of new histories. If a particle enters a cell with lower importance than its current cell, then the history is either terminated with a probability proportional to the ratio of the

importances, or it is continued with the weight increased by a factor equal to the inverse of the ratio. It is noted that the ratio is independent of the weight of the particle traversing the surface; it is only dependent upon the two cell importances.

Cell splitting can cause a bias in results by truncating the model if the splitting being performed is too extreme. As a good rule of thumb, it is ideal to have the number of particles in each cell to be approximately equal [X-5 Monte Carlo Team, 2003]. It is also important that adjacent cells should not increase or decrease in importance by more than a factor of 4.

Russian Roulette

Similar to splitting is the Russian roulette technique. Russian roulette is performed to terminate histories that are very unlikely to contribute to a tally, based on the weight of the particle. When the weight of a particle drops below a certain threshold value during a history (the weight is reduced by other variance reduction techniques), the history is either terminated or continued. The probability of terminating the history is inversely proportional to weight of the particle. If the history continues, then it is continued with a weight increased by a factor equal to the inverse of the weight.

Directional Source Biasing

Biasing the emission direction of created source particles can produce very effective results in MCNP. This is typically useful for isotropic point sources. To illustrate the technique, consider a point source and a detector in a void. Then, only neutrons traveling directly at the detector volume would be detected. The remaining histories would terminate without interacting or contributing to the tally. To improve efficiency, the simulation should only sample source particles with directions that will contribute to the tally. Assuming some reference direction is specified, source biasing is typically performed based on the cosine of the polar angle between the reference and particle emission directions. Emission over the azimuthal angle as measured from the reference direction is assumed to be isotropic. To prevent biasing, the weight of each emitted source particle is reduced by the fractional subtended solid angle. If particles are only emitted between polar angles with cosines between μ_{min} and μ_{max} , the weights are given by (assuming all particles would otherwise start with a weight of 1) $(\mu_{max} - \mu_{min})/2$. In other cases, source particles in a particular direction may be required to back-scatter from a distant wall before reaching the tally. Performing source biasing in this case introduces modeling truncation error, essentially replacing that region of the problem with a void. This truncation error may be negligible in many cases to the mean, but the loss of those rare events will significantly improve the convergence of the problem.

Chapter 3

Review of Neutron Spectrometry

This chapter reviews current and previous methods for neutron spectrometry. Only portable, relatively quick discriminating spectrometer designs are of interest, so methods (e.g. time of flight) used for discerning neutron energies for precise needs are not discussed, but can be found in the literature [Tsoulfanidis, 1995; Brooks and Klein, 2002]. The general unfolding problem and solution methods are developed, then designs utilizing this method, as well as others, are discussed.

3.1 The Unfolding Problem

3.1.1 The Unfolding Equation

The general approach of spectrum unfolding is to identify a source spectrum from a series of measured responses that represent different unique energy ranges. The general relation for an unfolding problem for an energy spectrum can be stated as [Tsoulfanidis, 1995]

$$M(E) = \int_0^{\infty} R(E, E')S(E') dE', \quad (3.1)$$

where $M(E)$ is the measured distribution function with respect to energy E , $S(E')$ is the distribution of the number of source particles emitted as a function of E' , and $R(E, E')$ is a kernel that represents the probability an emitted source neutron at energy E' is measured at energy E and is known as the response function. Often response functions are adjusted to account for dose. The general term dose refers to some measure of the correlation between biological effect and an observed response based on deposited energy and type of radiation, as a function of incident particle energy. Although the focus of this work is in identifying the type of neutron sources based on energy spectrum, most spectrometry designs and research

focus on estimating radiation dose. The primary difference between unfolding a dose and an energy spectrum is in the definition of the response functions.

Eq. (3.1) is a Fredholm integral equation of the first kind [Twomey, 1963]. The general method is to solve for $S(E')$, assuming the response function is known via measurement or simulations, by inverting the measured responses $M(E)$. The function $M(E)$ is generally not continuous. Rather, discrete values are measured which represent the energy-integrated response over a certain energy range, i.e.,

$$M(E) \approx M_i, \quad E_i < E < E_{i+1}, \quad (3.2)$$

where

$$M_i = \int_{E_i}^{E_{i+1}} M(E) dE, \quad i = 1, 2, \dots, N_{det}. \quad (3.3)$$

Here N_{det} is the number of unique energy-dependent detector measurements. The response function $R(E, E')$ can be determined by experiment or simulation.

The inverse problem of Eq. (3.1) can be discretized by application of some appropriate numerical quadrature scheme, i.e.,

$$\int_0^{\infty} f(E') dE' \simeq \sum_{j=1}^{N_{erg}} w_j f(E'_j), \quad (3.4)$$

where $f(E')$ is any continuous function of E' , and N_{erg} is the number of discrete energy groups of the solution. Application of this numerical quadrature to the right hand side of Eq. (3.1), with the substitution of Eq. (3.3) for $M(E)$, yields the set of linear algebra equations

$$M_i = \sum_{j=1}^{N_{erg}} R_{ij} S_j, \quad i = 1, 2, \dots, N_{det}, \quad (3.5)$$

where $R(E, E')$ has been discretized to form a response matrix with elements

$$R_{ij} = w_j \int_{E_i}^{E_{i+1}} R(E, E_j) dE, \quad j = 1, 2, \dots, N_{erg} \text{ and } i = 1, 2, \dots, N_{det}. \quad (3.6)$$

The desired solution is the discretized source energy spectrum, i.e., $S_j = S(E_j)$ for $j = 1, 2, \dots, N_{erg}$. Typically in neutron detection measurements, primarily only thermal neutrons are detected directly because of higher absorption probabilities in detection materials at lower energies. Higher energy neutrons are lowered to thermal energies for detection by adding moderator to the system. Therefore, a unique detector-moderator arrangement is needed for

each value M_i , so generally the number of measurements is limited.

3.1.2 Regularizing the Set of Algebraic Equations

As neutron energies are typically continuous, inferring a neutron energy spectrum from a limited number of detector measurements is a difficult problem. For continuous energy sources, unfolding the discrete measured spectrum usually leads to an underdetermined system of linear equations (i.e., $N_{erg} > N_{det}$). An underdetermined problem is one in which there are more unknowns than equations, which leads to an infinite number of solutions or no solution. An underdetermined set of equations is an ill-posed problem mathematically. In the case of unfolding, there are typically an infinite number of solutions so that some a priori information must be input into the solution method. The additional information is applied to achieve a unique and realistic (e.g., non-negative) solution.

The general approach of solving an underdetermined system is to regularize the set of equations. Regularization is a process that introduces assumptions about the solution that provide additional equations. After regularization, the total number of equations equals the number of variables, leading to a solvable set of linear equations. The general approach of regularization is to minimize the expression [Press et al., 1992]

$$\mathcal{A}[\mathbf{S}] + \lambda\mathcal{B}[\mathbf{S}], \quad (3.7)$$

where \mathbf{S} is a column vector containing the desired solution spectrum $\{S_j : j = 1, 2, \dots, N_{erg}\}$, $\mathcal{A}[\mathbf{S}]$ is a positive functional that measures how well the solution \mathbf{S} satisfies Eq. (3.5), and $\mathcal{B}[\mathbf{S}]$ is a positive functional that measures how well \mathbf{S} satisfies some a priori information applied to regularize the system. Here, the weighting factor λ is a parameter of the solution. For increasing values of λ , between 0 and ∞ , the solution $\mathbf{S}(\lambda)$ provides a trade-off of the minimization of \mathcal{A} and \mathcal{B} . The choice of λ is determined by the user. Although the choice of λ is subjective, a common choice is to determine λ such that $\mathcal{A}[\mathbf{S}]$ ensures \mathbf{S} agrees with the values of M_i within one standard deviation, for all i [Press et al., 1992].

The forms of \mathcal{A} and \mathcal{B} vary with solution method, in some cases leading to non-linear equations [Press et al., 1992]. A common choice for \mathcal{A} is a χ^2 goodness-of-fit statistic. The functional \mathcal{B} provides a numerical measure of the smoothness of each of the $S_j(E)$ or their derivatives. For linear regularization, $\mathcal{B} = \mathbf{S}^T\mathbf{H}\mathbf{S}$, where \mathbf{H} is a smoothing matrix. The smoothing matrix is chosen such that the functional form of the S_j is assumed (e.g., quadratic or cubic). The matrix \mathbf{H} applies finite differencing to the derivatives of the S_j such that the minimization of \mathcal{B} produces the desired shape of the solution. The specific form of smoothing matrices, as well as higher-order and non-linear regularization methods,

can be found in [Press et al., 1992].

3.2 Solution Methods

Many methods and computer codes have been developed to regularize equations and unfold the source energy spectrum. Often the methods of constraining the solution are semi-empirical and subjective, requiring the user to have substantial experience. Smoothing of data after unfolding is often applied [Tsoufanidis, 1995]. Historically, a constrained linear-least-squares method was utilized, but suffered from numerical instability [Twomey, 1963]. The linear-least-squares method is a zeroth-order regularization method, i.e., there is no constraint on the smoothness of the derivatives of the solution [Press et al., 1992]. Iterative solution methods are far more common and have been used and studied extensively. The class of iterative solution methods involved in underdetermined problems are often numerically unstable and computationally demanding (relative to an on-board processor for real time spectrometry). Also, an estimated solution from the user is typically required, so the user must have a good estimate of what the source is to begin with. Two of the more common commercial codes which modern codes have adapted and improved upon are SPUNIT [Brackenbush, 1983] and BUNKI [Miller, 1993]. Neural-networking and genetic based algorithm codes have been developed more recently to unfold spectra that have the potential to be more efficient and portable [Fayegh, 1993; Mukherjee, 2002]. To simplify the process of unfolding, recently a more user-friendly rendition of SPUNIT has been developed by Vega-Carrillo et al. [2012], as well as a user interface compilation of unfolding codes by Sweezy et al. [2002].

Although smoothing of calculated data is generally not desired, it has been shown in application to improve unfolding results [Tsoufanidis, 1995]. Data smoothing attempts to make the spectrum more continuous and physically realistic based on an expected solution and behavior of the data curve. The general approach to smoothing is to estimate the expected average behavior of the true spectrum, at some point in the unfolded spectrum, based on the behavior of surrounding energy points and fitting some form of a polynomial between those points. This is repeated in a pointwise manner, essentially removing distortion from statistical noise. A brief overview of smoothing methods can be found in [Grissom and Koehler, 1971].

3.3 Neutron Spectrometer Designs

In this section, neutron spectrometer designs are divided into two categories. The first set of designs are those that use a single energy-averaged measurement to estimate the response or dose from a multiple-energy neutron field. The second are those which use multiple energy-dependent observations to calculate the response or dose, typically through unfolding. The latter are more comparable in application to the design in this work, while the former is discussed briefly because it is the most commonplace use of neutron spectrometry in study and application [Thomas and Alevra, 2002].

3.3.1 Single Detector Response Systems

Detection systems used for estimating a dose from a variable energy neutron field via a single detector response are the most commonplace application of energy-dependent neutron data Brooks and Klein [2002]. The Bonner sphere [ICRU, 2001] is the most commonly used device to estimate neutron dose. The basic design of a Bonner sphere is a thermal neutron detector surrounded by a sphere of polyethylene moderator. The encapsulated detector demonstrates a similar energy-dependent response function to that of a human phantom [ICRU, 2001]. Thus, a single measurement from a Bonner sphere is directly comparable to the expected dose experienced by a human in the same neutron field. Many models of spherical and cylindrical designs have been implemented since Bonner sphere was introduced in 1960, as discussed by Thomas and Alevra [2002]. Modifications to the design over the last decade have focused on reducing weight (e.g. the WENDI design [Olsher, 2000] and [Yoshida et al., 2011]). For neutron dose measurements near high-energy particle accelerators, several recent designs [Biju et al., 2012; McLean and Justus, 2012; Yoshida et al., 2011] utilize a heavy metal, e.g. tungsten or zirconium, to convert very high energy neutrons (10 MeV–1 GeV) into multiple neutrons at lower energies via (n, xn) reactions.

3.3.2 Multiple Detector Response Systems

The historical method of gathering energy dependent information about a neutron field is through measurements from multiple Bonner spheres of differing diameters, first proposed in Bramblett [1960]. The Bonner sphere spectrometry (BSS) system is based on taking individual measurements with a thermal neutron detector surrounded by spheres of varying radius of polyethylene. The measurements are typically unfolded to estimate either the energy spectrum or an energy-dependent dose. The number of measurements needed to identify an energy spectrum correctly may vary, but usually a minimum of around six

measurements is needed [Thomas and Alevra, 2002]. Additionally, although each sphere is primarily sensitive to a single range of neutron energies, there is overlap of response functions in different energy ranges (i.e., multiple spheres demonstrate a measurable response from a monoenergetic source) [Brooks and Klein, 2002]. This is the fundamental difficulty in unfolding energy spectra from a BSS system. Overall, BSS systems are able to cover a wider range of energies with a higher efficiency than most other systems, but the unfolded spectrum has poor energy resolution [Thomas and Alevra, 2002]. A BSS system is not ideal for identification of special nuclear material because of the requirement of individual device measurements, large moderator weight, and poor resolution.

An alternative design that has been studied extensively is proton recoil spectrometers. Proton recoil spectrometers are based on interactions of a neutron with a proton (in the form of hydrogen within the detection volume), and the measurement of the kinetic energy of the resulting recoil proton after the collision. As the proton is of similar mass as the neutron, it can potentially absorb all of the kinetic energy of an interacting neutron. All the data to determine the spectra can be obtained from a single measurement using a multichannel analyzer [Flaska and Pozzi, 2007*a*], rather than the multiple individual measurements needed with a BSS system. Organic scintillators are favorable for recoil spectrometers because they allow discrimination of gamma and neutron signal through pulse-shape analysis of the time-dependent detector output voltage [Brooks and Klein, 2002].

The application of recoil spectrometers for quick source identification is limited by their relatively small energy range and low efficiency. Proton recoil spectrometers are typically only effective within the range of 50 keV – 4 MeV [Brooks and Klein, 2002]. PRESCILA is a current mixed detector design that is capable of unfolding dose estimates over a much wider energy range [Olsher, 2004]. PRESCILA utilizes a proton recoil and cadmium coated thermal neutron detector to measure fast, epithermal, and thermal neutrons simultaneously. The device provides wide-range dose in a single measurement, but demonstrates large inaccuracies in some energy ranges (as high as 300%) [Caruso et al., 2011].

For the specific application of source identification, a neutron scatter camera using recoil spectrometers and time of flight measurements has been used to distinguish among different neutron sources [Brennan et al., 2011]. The device utilizes 32 liquid scintillator sections where proton recoils are measured and time of flight is coupled to scattering events to determine the angle and energy of incident neutrons; the resulting spectra are then unfolded. The device has been shown to identify individual sources correctly, but is not portable and the required neutron population for identification is not discussed in the article.

A different method utilizing proton recoil which does not depend on energy unfolding has been studied previously by Flaska and Pozzi [2007*b*]. The method utilizes a well-developed

method for discriminating gamma rays from neutrons based on the difference in the magnitude and shape of detector output pulse heights, relative to the pulse tails. In addition to no unfolding, another favorable attribute of the method is the potential ability to identify sources in the presence of shielding, as the pulse height shapes showed minimal change [Flaska and Pozzi, 2007a]. Another advantage of this method is that it potentially will require far fewer neutron counts than other methods. Experiments and simulations have been performed, demonstrating proof of concept. The robustness and applicability of the method have not been studied beyond identification of ^{252}Cf , americium-beryllium, and americium-lithium sources.

Some recent spectrometer designs have used multiple detectors encased in a single large moderator. The appeal of this design is to obtain the efficient, wide-range energy measurements of a BSS system in a single measurement. Having all the detectors in the moderator and making the measurements simultaneously requires detectors that provide high efficiency for minimal volume and perturb the neutron flux minimally. A design using three ^3He position sensitive thermal neutron detectors in a sphere of polyethylene was built and tested by Toyokawa et al. [1997]. The device was able to estimate dose over a wide energy range, but it was not as accurate as BSS systems (typically underestimating at most energies), and dose estimates were directionally dependent. A design similar in construction to that of this work has been implemented which utilizes an array of pixelated detectors embedded in a cylinder of HDPE by Caruso et al. [2011]. The pixelated detectors consist of a hexagonal array of high-efficiency perforated neutron detectors [Shultis and McGregor, 2009]. The pixelated detectors allow radial information about the neutron field to be measured, making spectrum unfolding more accurate and efficient. Unfolded dose estimates were able to match dose curves to within 15% for several sources over a large energy range; these dose estimates are more accurate than designs currently available utilizing a single detection measurement.

Chapter 4

Simulations of a Neutron Source Identification Spectrometer

The focus of this chapter is the optimization and design of a new type of neutron spectrometer [Cooper et al., 2011]. Although it is referred to as a spectrometer, the device discussed herein identifies the type of a neutron source based on measurements which implicitly depend on the neutron energy spectrum. The actual energy spectrum of a source is never explicitly determined from the detector measurements. However, any unfolding techniques used by other spectrometers could, in principle, be applied to measurements made with this spectrometer.

First, the methodology for the source identification technique used by the spectrometer being studied is presented. Then, the geometry and the MCNP model is discussed. After that, methodology and results for optimizing the geometry of the system are given. A method utilizing a neutron shadow shield to correct measurements for room-scattered neutrons is also investigated. Finally, closing remarks and suggestions for future design work are given.

4.1 Methodology

4.1.1 Overview

As discussed in Chapter 1, the spectrometer consists of cylindrical sections of HDPE with high efficiency thermal neutron detectors contained within. A sheet of Cd is placed behind each detector to reduce the effect of backscattered neutrons. A large library of unique spectrometer responses, known as templates, is pre-generated. On page 33, Fig. 4.1 plots several example spectrometer responses for different types of bare neutron sources that were simulated with the MCNP5 model discussed later in Section 4.2.1; the detector responses

are given as counts per neutron incident upon the front of the spectrometer. The detector responses are then normalized by dividing the response at each detector position by the response in the second detector position, as demonstrated in the figure. The normalization removes dependence of the detector responses on the intensity of incident neutrons. Each set of normalized detector responses forms a template. As discussed in Chapter 1, each template is unique to an incident neutron energy spectra. Ideally, templates are generated for all possible neutron sources for the particular spectrometry application. To identify a neutron source, a measured spectrum of detector counts (normalized to the second detector position) is compared against each template in the library. The template which is most similar to the measured spectra identifies the most likely neutron source.

Although there are relatively few neutron sources (e.g., AmBe, PuBe, and spontaneous fission sources) compared to the number of different radioisotopes, the neutron spectra emitted by these sources can be many as a consequence of inert material surrounding the source material perturbing the original source spectrum. The effect of shielding materials must be accounted for in application by including templates for different source and shielding combinations. The required robustness of templates to account for the effect of shielding on spectrometer responses is not considered in this work.

4.1.2 Source Identification Based on a FOM

To determine the most likely source for a set of observed detector measurements (herein referred to as a detector spectrum), the individual measurements at each detector position are compared to corresponding reference values for different sources. Comparisons are made using an approximate χ^2 statistic as a figure of merit (FOM). As discussed above, the reference spectra are unique to each neutron source¹. For a particular measured spectrum, a FOM is calculated for each template. The template that produces the lowest FOM is identified as the most likely source.

For a spectrometer with N_{det} detectors irradiated by neutrons with some unknown energy distribution, a set of measurements $\{C_i : i = 1, 2, \dots, N_{det}\}$ is observed. Here, C_i is the counts recorded by the detector in the i -th position (position indices are indexed with 1 being nearest the source, and N_{det} being farthest from the source). To remove dependence in these values on the strength of the neutron source under investigation, the set of counts is normalized such that one of the detector's counts is unity. Then, the logarithm of each normalized value is taken to simplify error propagation calculations later on. The set of

¹Although only bare neutron sources are considered in this work, templates could account for factors such as shielding. Thus, a particular energy distribution of incident neutrons is all that is specified by a unique "neutron source" in this chapter.

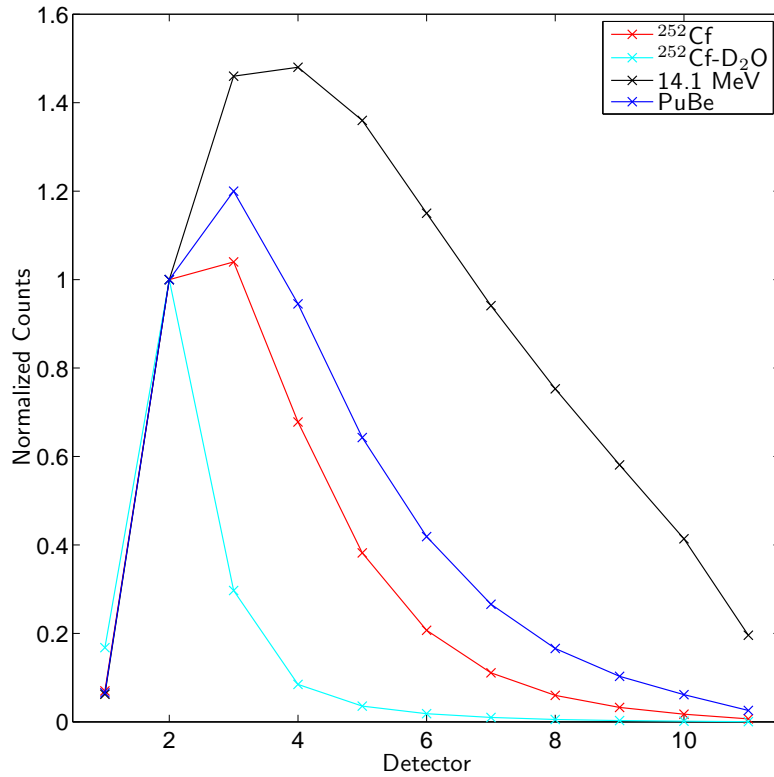
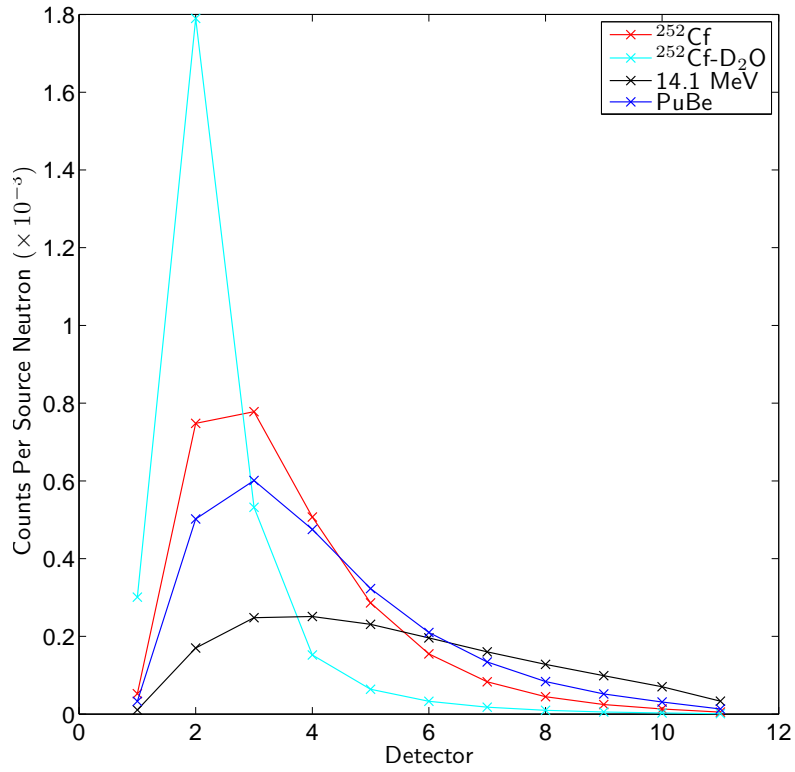


Fig. 4.1: Simulated spectrometer responses from various sources, followed by the normalized spectra, where the counts in each detector is divided by the counts in the second detector. The relative standard error for all data points is $< 0.5\%$.

observed, normalized detector counts is $\{R_i : i = 1, 2, \dots, N_{det}\}$, where the response R_i from the i -th detector is given as

$$R_i = \ln \left(\frac{C_i}{C_{norm}} \right). \quad (4.1)$$

The value C_{norm} is the counts in the chosen normalization position in the spectrometer. The normalization position used in this work is the *second* detector location. This position was chosen because it typically yields the highest count rate.

A set of reference spectra (templates) for each neutron source must be pre-generated for source identification. A unique template is needed for each of N_{src} neutron sources to be identified. The set of template responses is

$$\{S_i^j : i = 1, 2, \dots, N_{det}; j = 1, 2, \dots, N_{src}\}. \quad (4.2)$$

Here, S_i^j is the response from the i -th detector that is expected from the j -th reference neutron source, given by

$$S_i^j = \ln \left(\frac{r_i^j}{r_{norm}^j} \right), \quad (4.3)$$

where r_i^j is the reference detector measurement for the i -th detector, from the j -th neutron source. Because these detector measurements are normalized, they can be taken as tallies from a simulation which are normalized to per source neutron. Restated for clarity: the j -th template contains the spectrum of normalized N_{det} responses $\{S_i^j : i = 1, 2, \dots, N_{det}\}$, for the j -th source.

The approximate χ^2 goodness of fit statistic, given by Eq. (2.29), is used to determine the most likely neutron source for an experimentally observed spectrum. The approximate χ^2 statistic is used as a FOM to determine which template matches the observed responses most accurately. The FOM for the j -th template is defined as

$$FOM^j = \sum_{i=1}^{N_{det}} \frac{(R_i - S_i^j)^2}{\sigma^2(R_i) + \sigma^2(S_i^j)}. \quad (4.4)$$

Application of the standard error propagation formula, given in Eq. (2.27), to R_i and S_i and yields the approximate variances

$$\begin{aligned} \sigma^2(R_i) &= \frac{\sigma^2(C_i)}{C_i^2} + \frac{\sigma^2(C_{norm})}{C_{norm}^2} \\ \sigma^2(S_i^j) &= \frac{\sigma^2(r_i^j)}{(r_i^j)^2} + \frac{\sigma^2(r_{norm}^j)}{(r_{norm}^j)^2}. \end{aligned} \quad (4.5)$$

Because the distribution of observed counts in a detector usually follows a Poisson distribution, as described in Section 2.1.5, the observed counts is used as the mean of the Poisson distribution, and the uncertainty for a particular observed measurement is taken as $\sigma^2(C_i) = C_i$. When this result is substituted into Eq. (4.5), the uncertainties above reduce to

$$\begin{aligned}\sigma^2(R_i) &= \frac{1}{C_i} + \frac{1}{C_{norm}} \\ \sigma^2(S_i^j) &= \frac{\sigma^2(r_i^j)}{(r_i^j)^2} + \frac{\sigma^2(r_{norm}^j)}{(r_{norm}^j)^2}.\end{aligned}\tag{4.6}$$

The lower the value of FOM^j , relative to the FOM of other sources, the more accurately the j -th template spectrum matches the observed spectrum. Thus, the FOM corresponding to the template which is most likely the source is given by

$$FOM^{min} = \min \{FOM^j : j = 1, 2, \dots, N_{temp}\},\tag{4.7}$$

where N_{temp} is the number of templates and FOM^{min} is the minimum of the set of FOM values. It is noted that typically a system is optimized by increasing the FOM, unlike here, where lower values are preferred. The FOM nomenclature was chosen to prevent confusion with χ^2 hypothesis testing (as well as other χ^2 values in this work) and to emphasize that the FOM statistic is approximate and not necessarily sampled from a χ^2 distribution.

The random variables, from which the values $\{FOM^j\}$ are sampled, follow distributions that are generally unknown. As a result, the source corresponding to $FOM_{(0)}$ is not necessarily the correct source (particularly when there are insufficient counts in the detectors). To give a measure of how uncertain a source identification is, an approximate standard deviation of the FOM values is used. From Eq. (2.30), the standard deviation in a FOM value is approximated as

$$\sigma(FOM) = 2\sqrt{FOM}.\tag{4.8}$$

It is of note that Eq. (4.8) is not the true standard deviation; it is an approximation based on the standard error propagation formula, which predicts the behavior of FOM values from uncertainty in the counting and template measurements. The error propagation formula uses a first order Taylor series approximation, which can be very inaccurate for some functions. It is also noted that because $FOM \in [0, \infty)$, the confidence intervals are asymmetrical. In general, standard Gaussian confidence intervals are not applicable here.

The degrees of freedom of the FOM value is $N_{det} - 1$. The reduction by one degree is because the detector spectra are normalized to the counts in one detector; the values R_{norm} and S_{norm} will always be 1, and thus that detector never contributes to the FOM .

4.2 MCNP5 Model

4.2.1 Geometry and Neutron Sources

An MCNP model of the spectrometer described in this chapter was developed to optimize design parameters. In the base model, the spectrometer is placed in a void. A disk source of the same radius as the spectrometer irradiates the front of the device. The intensity of the source is uniform over the frontal area, and all source neutrons are created with direction equal to the inward normal of the front surface of the spectrometer.

The energy spectrum of the source is dependent on the simulation. The input file used by automation scripts, labeled *source_list.txt*, containing all of the MCNP format source energy spectra and can be found in Appendix B on page 144. The spectra are tabulated in different formats which are described in the MCNP5 manual [X-5 Monte Carlo Team, 2003]. A description of the neutron sources and the nomenclature used to identify the sources in *source_list.txt* is given in Table 4.1. The literature reference for each of the distributed-energy neutron sources is also given in Table 4.1.

Table 4.1: Neutron sources used for spectrometer simulations.

Identifier	Reference	Description
cfd2O	Ryan [1998]	A ^{252}Cf spontaneous fission source, moderated by a 30-cm diameter sphere of D_2O .
pube	Ryan [1998]	A ^{238}Pu -Be coupled (α, n) neutron source.
ambe	IAEA Report 403 [2001]	An Am-Be couple (α, n) neutron source.
cf252mcnp	X-5 Monte Carlo Team [2003]	A bare ^{252}Cf spontaneous fission source. Energy spectrum follows a Watt's distribution [X-5 Monte Carlo Team, 2003], which is a predefined distribution in MCNP.
pubers	IAEA Report 403 [2001]	A ^{238}Pu -Be coupled (α, n) neutron source, with room scattered neutrons included, softening the energy spectrum.
triga	Ryan [1998]	A measured spectrum from a TRIGA reactor.
puo2	Ryan [1998]	A measured spectrum from a PuO_2 source.
fusion	X-5 Monte Carlo Team [2003]	A monoenergetic 14.1 MeV source from a $^2\text{H} + ^3\text{H}$ reaction fusion neutron source.
50kev	—	A 50 keV monoenergetic neutron source.
1mev	—	A 1 MeV monoenergetic neutron source.
100ev	—	A 100 eV monoenergetic neutron source.

The geometry of the spectrometer is created in contiguous cylindrical sections, as depicted in Fig. 1.1. Each section contains a MSND with printed circuit board (PCB), backed by a 0.1 cm thick cylinder of Cd and a section of HDPE. With the exception of the first detector, the front and side faces of each MSND is surrounded by HDPE of the previous detector section. The MSND has a cross sectional area of $2 \text{ cm} \times 2 \text{ cm}$ square and a 0.1 cm depth. The PCB is a slightly larger in area at $2.1 \times 2.1 \text{ cm}^2$, with a depth of 0.157 cm. The number of sections, the cross-sectional area of the spectrometer, and the thickness of HDPE in each section is a variable, dependent on the particular simulation. An example input file can be found in Appendix C on page 176.

4.2.2 Simplified Model of Perforated Neutron Detectors

The neutron spectrometer design being studied uses an array of double-stacked, perforated Si semiconductor detectors backfilled with LiF. The concept of the double-stacked, straight-trenched devices is shown in Fig. 4.2. Thermal neutrons are absorbed by ${}^6\text{Li}$ through ${}^6\text{Li}(n, t)\alpha$ interactions. The semiconductor volume collects charge from the triton and alpha ions to create a detection pulse. Modeling the complex structure and charge collection of the devices would require considerable effort and loss of calculation efficiency. A simplified, artificial model of the perforated neutron detectors was used that preserves the thermal neutron absorption detection efficiency of the devices. The model was verified, as detailed in Section 4.2.6.

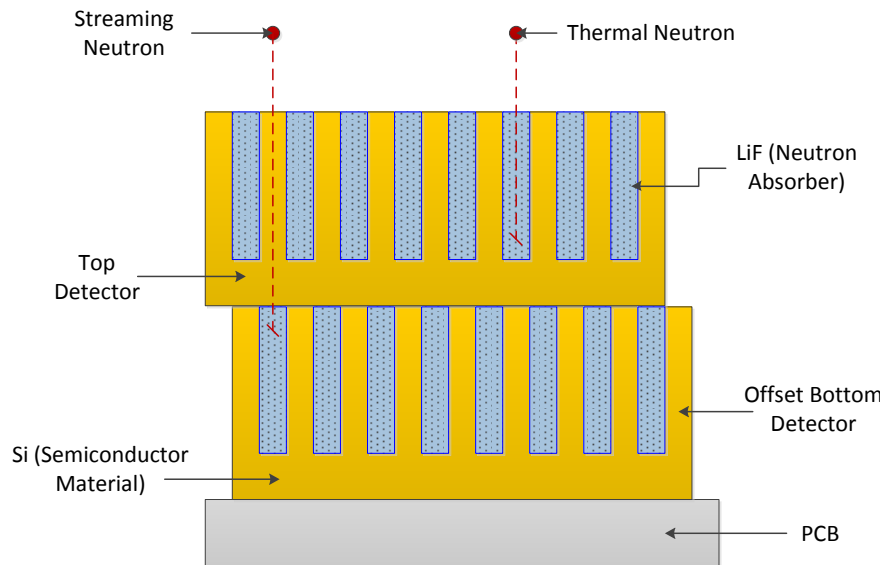


Fig. 4.2: Illustration of section of double-stacked straight-trenched detector concept, not to scale.

In the artificial model, the total volume of the double-stacked detector is unchanged. The

detector volume is modeled in MCNP as ${}^6\text{Li}$ at a reduced density that produces the same probability of absorbing a thermal neutron as the thermal neutron absorption detection efficiency of the device. Here, detection efficiency is defined as the probability of an absorption event depositing enough charge to be an observable event. In the artificial model, the Si and F are ignored as they have minimal effect on thermal neutron interactions relative to the high absorption in ${}^6\text{Li}$. Although Si and F have larger interaction coefficients at higher energies, relative to the moderator they have a minimal effect.

Because interactions besides absorption are negligible in ${}^6\text{Li}$ at thermal energies, exponential attenuation of neutrons via the absorption cross section can be assumed. For a normally-incident beam of thermal neutrons, the probability of neutron absorption in a slab of thickness T of ${}^6\text{Li}$ is

$$\epsilon_{thermal} = 1 - \exp \left[-\frac{\rho({}^6\text{Li})N_a}{\mathcal{A}({}^6\text{Li})}\bar{\sigma}_{n,t}({}^6\text{Li})T \right], \quad (4.9)$$

where N_a is Avagadro's constant, $\bar{\sigma}_{n,t}({}^6\text{Li})$ is the thermal-averaged cross section, $\rho({}^6\text{Li})$ is the effective density, and $\mathcal{A}({}^6\text{Li})$ is the atomic weight of ${}^6\text{Li}$. Solving for $\rho({}^6\text{Li})$ required to achieve a given efficiency ϵ produces

$$\rho({}^6\text{Li}) = -\frac{\ln(1 - \epsilon)\mathcal{A}({}^6\text{Li})}{N_a\bar{\sigma}_{n,t}({}^6\text{Li})T}. \quad (4.10)$$

The thermal (2200 m s^{-1}) cross section $\sigma_{n,t}({}^6\text{Li})$ is 940 b [Chart of the Nuclides, 16th Ed.]. The (n, t) cross section is assumed to have a $1/\sqrt{E}$ behavior with respect to incident neutron energy E over the thermal energy range. With this assumption, and the assumption that the thermal neutrons are in equilibrium at room temperature, the thermal-averaged cross section becomes [Stacey, 2007]

$$\bar{\sigma}_{n,t}({}^6\text{Li}) = \frac{\sqrt{\pi}}{2}\sigma_{n,t}({}^6\text{Li}) = 833 \text{ b}. \quad (4.11)$$

The detection region for each module of the spectrometer consists of a 2×2 array of 1 cm^2 devices, with a total detector thickness of 0.1 cm. The region was modeled in MCNP as a 2 cm \times 2 cm, 0.1 cm thick rectangular box (a detector volume, V_d , of 0.4 cm^3). The intrinsic detection efficiency of the devices was taken as 50%; this is an achievable detection efficiency of a dual-stacked device with this thickness [Shultis and McGregor, 2009]. Although this may not be the actual efficiency of the devices, it will not affect the optimization results of the spectrometer. As long as the efficiency of the devices is uniform, the results will not be affected because a different detection efficiency can be compensated for by increasing the

total count time. The effective density of ${}^6\text{Li}$ given by Eq. (4.10) for a rectangular box that is 0.1 cm thick with a 4 cm² face was found to be $\rho({}^6\text{Li}) = 0.08353 \text{ g cm}^{-3}$.

4.2.3 Detector Response in MCNP5

The FM card (text input parameters in MCNP are referred to as cards) in MCNP5 was used to convert the F4 cell-volume averaged flux tally to counts per source neutron [X-5 Monte Carlo Team, 2003]. The FM card was used with 2 options: the reaction id, *rid*, for the interaction of interest and the constant multiplier C . The FM card with these options modifies an F4 response to be

$$R \text{ (counts per source neut.)} = C \int_0^\infty \sigma_{n,t}(E)\Phi(E) dx, \quad (4.12)$$

where R is the simulated detector response and $\Phi(E)$ is the average fluence over the detector volume V_d per source particle (the result of the F4 tally). For the detection volume discussed in Section 4.2.2, C is given by

$$C = V_d \frac{\rho({}^6\text{Li})N_a}{\mathcal{A}({}^6\text{Li})} \times 10^{-24}. \quad (4.13)$$

The *rid* for the (n, t) reaction is 105, and for $\epsilon = 50\%$, Eq. (4.13) reduces to $C = 0.0083216V_d$. For the particular case of the detectors modeled here with $V_d = 0.4 \text{ cm}^3$ for each artificial double-stacked detector volume, the value is $C = 0.0033286$. It should be noted that the FM card in this case is specific to a material card, but also specific to the volume of the cells of the F4 tally. The use of the FM card in this manner determines the expectation value of a particular reaction rate in a volume by integrating the product of the energy-dependent neutron flux and cross section of the reaction over all neutron energies. Thus, the result of this tally is approximating the number of neutrons, per source particle, that would deposit at least 300 keV of energy in an explicit model of a detector.

The tallies for the response from each detectors are grouped into a single input tally card. MCNP then multiplies the individual responses for the F4 tallies by the necessary multiplier. The detector volume cells in the model begin at cell 10, increasing by 10 with increasing detector depth. For example, the tally specification for a spectrometer with 5 detectors would be

```
F4:N    10 20 30 40 50
FM4    0.0033286  2 105
```

where 2 is the detection material number and 105 is the *rid*. The TF input parameter was then

used to modify how MCNP checks statistical convergence. The deepest detector position for any particular spectrometer is the most likely tally to have poor statistics because particle histories are less likely to reach it. As an example input, to get the statistical tests for the last cell for the above F4 tally, the TF4 input would be

```
TF4 5 7j
```

where 5 indicates to use the fifth entry on the tally card F4 for statistical convergence tests, and 7j simply skips the remaining optional inputs for the card.

4.2.4 Boron in Circuit Boards

The PCBs on the back of perforated semiconductor detectors used in the spectrometer are placed on contain neutron absorbers, namely B and Br used for flame retardant purposes, as well as other materials such as Cu and C. The thermal neutron absorption cross section of ^{10}B is large (3,840 b [Chart of the Nuclides, 16th Ed.]). The concentration of these materials in PCBs is proprietary to manufacturers, and thus generally unknown.

To include the amount of ^{10}B in the models, an equivalent atom density of ^{10}B over the volume of the PCB board was modeled. The amount of ^{10}B in the device was determined based on thermal neutron absorption efficiency of the board, as measured by experiments performed at Kansas State University. The determined atom density is 5.3×10^{20} ^{10}B atoms cm^{-3} . Although other materials may be accounting for thermal absorption, this should result in the thermal absorption of the board being modeled accurately. Other materials were not included. With the exception of Br, the other materials should have minimal effect on the non-thermal energy spectrum. Because the PCB is so thin, scattering interactions at higher energies are minimal, relative to the HDPE moderator. Although Br has absorption resonances at epithermal energies, it is not included because it can not be estimated easily through absorption efficiency experiments. The added B in PCBs had negligible effect on results because the Cd sheets prevent thermal neutrons backscattering into detectors anyway.

4.2.5 Variance Reduction and MCNP5 Parameters

Several variance reduction techniques, discussed in Section 2.3.2, were employed for all the MCNP simulations of the spectrometer in this chapter. Implicit capture (a default setting in MCNP) was used. Also, cell splitting was performed over the region of the spectrometer. The goal of splitting in the spectrometer simulation is to increase the likelihood of particles reaching the detectors deeper in the spectrometer. Cell splitting was automated with a script because the ideal cell importances will vary depending on the source and geometry.

Cell splitting is performed with the intent of uniform population in the individual cells representing sections of the spectrometer (including particles created from the process of splitting). Rather than performing this balancing on all cells within the spectrometer, the HDPE sections of the spectrometer were analyzed. The Cd, PCB, and detection volume cells were then adjusted to the importance that the corresponding HDPE section was increased to. This is because the volume of the detectors is so small that the importance increase, based on particle balance, would be excessively large. The importance in the front detector is not adjusted.

A short simulation was performed for each file using 30,000 particle histories. The number of particle tracks entering each HDPE section is then tallied. Each cell’s importance is then adjusted in the actual input file to be

$$\text{IMP}_j = \frac{T_{max}}{T_j} \quad (4.14)$$

where T_j is the number of tracks entering the j -th HDPE section, IMP_j is the new importance of all cells in the j -th detector section, and T_{max} is the largest number of tracks entering any of the HDPE sections in the spectrometer; the original importance of all cells is 1. This process could be repeated multiple times, but one iteration was sufficient for these simulations.

For the base model described above, MCNP simulations were performed for 2×10^8 particle histories (denoted by “NPS” in MCNP). The default neutron physics parameters were used. The script which handles running simulations of MCNP input files, `hydra_run.py`, had a built in automation routine to ensure that all 10 statistical tests were passed. If the tests were failed, then the simulation is continued for 20% more particle histories. This process is repeated for up to five repetitions.

4.2.6 Verifying Artificial Detector Model Using MCNP6

The method of modeling the double-stacked, perforated semiconductor devices discussed in Section 4.2.2 was verified using MCNP6. Previous work has demonstrated responses that are comparable to experimental data as well [Cooper et al., 2011]. MCNP6 allows coupled neutron and charged particle transport modeling. The code was used to model the explicit detector geometry and simulate a detector response. MCNP6 is only in Beta testing, but provides the most viable method for verifying the detector modeling. For brevity, an equivalent volume, reduced density ^6Li model of a detector as described in Section 4.2.2 is referred to as an artificial detector; an MCNP6 model is referred to as an explicit detector model.

Description of Geometry Modeling

In the MCNP6 model, the detailed geometry of a trenched perforated Si detector, backfilled with LiF, was modeled explicitly. A device was chosen that would yield a dual-stacked efficiency close to the 50% considered in Section 4.2.2. The definitions for the unit cell geometry that is repeated to form straight trenched devices are given in the section view in Fig. 4.3; the values for the specific device modeled are given in Table 4.2. The cross-sectional area is taken to be 4 cm^2 to simulate the 2×2 array of devices that is used at each location within the spectrometer model. The trenches of each single device were modeled by creating alternating cells of Si and LiF that fill the detection volume via the FILL command [X-5 Monte Carlo Team, 2003]. The bulk Si material was then created as a separate cell to fill the remainder of the detection volume. Two of such detector volumes were stacked with their absorbers offset to reduce streaming and form a double-stacked device. The second detector was offset by $25 \mu\text{m}$ to center the absorber in the second detector over the non-absorbing side walls of the first detector. An illustration of the double-stacked geometry is given in Fig. 4.2. To complete the detector model, the stacked regions were placed on the same volume of PCB as the artificial model, but with a more accurate modeling of the FR4 type PCB; the boron content is the same. To create a spectrometer, the above model of detector and PCB were duplicated at positions throughout the HDPE cylinder with sheets of Cd behind them, as in the original model. The material properties for the MCNP6 model are given in Tables 4.3

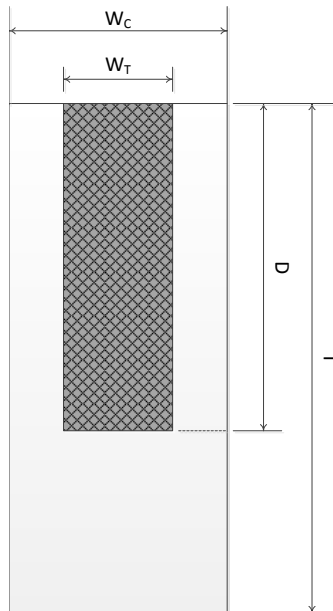


Fig. 4.3: Dimensions of a unit cell of a perforated, straight-trenched detector

and 4.4 beginning on page 44.

Table 4.2: Geometric specifications for unit cell of a perforated, straight-trenched device.

Dimension	Value (μm)
W_T	30
W_C	50
D	350
T	500

Creating a Pulse Height Energy Spectrum in MCNP6

MCNP6 allows the actual phenomena occurring in perforated detectors to be modeled and for a pulse height energy spectrum from charge deposition by reaction products to be simulated. The simulation tracks neutrons, with fully analog physics, from birth until they are absorbed or leaked from the system. If a ${}^6\text{Li}(n, t)\alpha$ reaction occurs, the created triton and alpha particle are tracked until they reach the cutoff energy or leave the detection volume. Charge deposited by the reaction products tracks is recorded. Here, an assumption is introduced that the charge collection efficiency of the device is 100%, i.e., any charge deposited in the semiconductor region of a detector contributes to the pulse height spectrum.

An F4 tally is used on the semiconductor in the detector volume to generate a simulated pulse height spectrum. The F4 tally with E4 card determines the probability distribution for a source particle depositing a certain amount of energy in a cell during its history. The F4 tally includes energy deposited via all tracks and secondary particles of any type in a history. It is worth noting that this is different than typical energy distributions for MCNP tallies which give the distribution of particle energies as they contribute to the tally. The FT card (special treatment for tallies) was also used. In particular, the FT card was used with the PHL option. For the PHL option, the FT card modifies an F4 tally to be an energy pulse height spectrum with anti-coincidence for multiple cells within the MCNP6 model [X-5 Monte Carlo Team, 2003]. This card is necessary because the Si sidewalls of the trenches are a separate cell from the bulk Si material. Thus, the PHL card is used to simulate a pulse height spectrum from energy deposited in either the side walls or bulk Si. To simulate the use of a low-level discriminator (LLD) and compensate for the assumption of a perfect charge collection efficiency, only histories which deposit greater than 300 keV of energy are considered a detected event. All neutron histories which contribute more than 300 keV of energy are then summed. Thus, this tally is used to determine the probability per source

Table 4.3: Crystalline LiF ($\rho = 2.635\text{g cm}^{-3}$) material composition for MCNP6 model.

MCNP Library	Mass Fraction
3006.70c	0.225502
3007.70c	0.016789
9019.70c	0.757709

Table 4.4: Natural Si ($\rho = 2.3290\text{g cm}^{-3}$) material composition for MCNP6 model.

MCNP Library	Atomic Fraction
14028.70c	0.92223
14029.70c	0.04685
14030.70c	0.03092

Table 4.5: FR4 printed circuit board ($\rho = 2.635\text{g cm}^{-3}$) material composition for MCNP6 model.

MCNP Library	Mass Fraction
1001.70c	0.010
5010.70c	0.0053
5011.70c	0.0147
6000.70c	0.040
8016.70c	0.390
13027.70c	0.010
14028.70c	0.230
29063.70c	0.140
29065.70c	0.060
35079.70c	0.050
35081.70c	0.050

neutron of at least 300 keV of energy being deposited within the semiconductor region of the detector.

Thermal Efficiency Verification

Efficiency simulation were performed in MCNP6 and MCNP5 to verify the artificial detector model described in Section 4.2.2. First, the dual-stacked device placed on a PCB described in Section 4.2.6 was modeled in MCNP6. The surface of the top detector was irradiated with a thermal, normal-incident neutron beam of the same cross sectional area as the top detector. The neutron beam was assumed to have a Maxwellian Energy distribution (see [X-5 Monte Carlo Team, 2003]) with a mode of 0.0254 eV. The pulse height spectrum tally described in Section 4.2.6 was used to determine the number of events that deposit greater than 300 keV per source neutron. The number of particle histories simulated was 10^7 .

The result of the thermal beam illuminating a double-stacked device produced 0.4728 ± 0.0001 counts per source neutron. All source neutrons entered the device, thus the thermal efficiency of this dual-stacked device was found to be $47.28 \pm 0.01\%$. This efficiency agrees with previous simulations [Shultis and McGregor, 2009]. Using $\epsilon = 0.4728$ in Eq. 4.10 yields an artificial ${}^6\text{Li}$ density of $0.07134 \text{ g cm}^{-3}$. This density substituted into Eq. 4.13 yields $C = 0.002857$. An MCNP5 input file was created using this C and $\rho({}^6\text{Li})$. The input file had the same geometry and source specification as the MCNP6 model except for the detection region of the explicit model was replaced with the artificial model. The tally method described in Section 4.2.3 was used. 10^8 neutron histories were simulated. The only variance reduction technique used in the artificial model is the default implicit capture method. The same ${}^6\text{Li}$ cross section library as the MCNP6 simulation was used, i.e., 3006.70c.

The MCNP5 simulation produced a thermal detector efficiency of $49.25 \pm 0.01\%$. This is in good agreement with the efficiency of the MCNP6 simulation that was used to produce the artificial model for the MCNP5 simulation. Accuracy is expected at thermal energies where the large (n, t) cross section of ${}^6\text{Li}$ dominates all interaction types.

Spectrometer Response Verification

A second scenario was simulated to verify the use of the artificial detector models. The main phenomena of interest is streaming of high energy neutrons through the spectrometer. Additionally, the accuracy of detector efficiency for the artificial model may be reduced when neutrons entering the MSNDs are not uniform in direction, traversing the device at all angles. Because only the relative responses are important in the *FOM* calculations, the detector responses are normalized to the second detector. A spectrometer was modeled with five

detector positions and a 6.0 cm radius of the cylindrical HDPE sections. The front faces of the detectors were 3.0 cm apart. The spectrometer model used the same detector and PCB dimensions as the above results, with 0.1 cm of natural Cd behind each PCB. The beam was of the same cross sectional area as the moderator. An MCNP6 and MCNP5 model of the spectrometer were made. The only difference was the explicit and artificial detector models for the MCNP6 and MCNP5 models, respectively. The number of histories for both simulations was 10^9 . The input file for the MCNP6 model is given on page 183.

Five different neutron sources were analyzed with both the MCNP5 and MCNP6 models: AmBe, PuBe, a monoenergetic fusion source (14.1 MeV), and spontaneous fission sources of ^{252}Cf and ^{240}Pu . The simulated detector spectrum from each source was normalized to the second detector. The counts per source neutron and normalized detector responses, as well as their associated errors, are given for each source simulation for the artificial and explicit detector models are given in Table 4.6. A plot of the results from the 14.1 MeV, AmBe, and PuBe sources is given in Fig. 4.4, and the results from spontaneous fission sources are depicted in Fig. 4.5.

The unnormalized responses are inaccurate, particularly in the first detector, even though the normalized responses appear to agree. The shape of the normalized curves, and how they compare to each other, is all that is of interest; differences in the responses are compensated for by increasing the number of neutrons. In all detector spectra, the artificial model slightly overpredicts the explicit model, but is in good agreement. The main emphasis of the difference in the two models is that the spectrum shows the same shape, and that for different sources the detector is higher. For ^{252}Cf and ^{240}Pu the simulated responses become very close, and for one detector location, the artificial ^{252}Cf response is higher than the ^{240}Pu response. This indicates that for this point, a ^{240}Pu source may be incorrectly identified. This simply suggests that care must be taken for sources that are close together, and that these artificial templates although good enough for the process of optimization, may not be able to be used as templates for identifying actual sources from experiment.

4.3 Geometric Optimization

4.3.1 Motivation

Simulations were performed to determine the optimal geometric configuration for the spectrometer. The optimal geometric configuration has the best ability to identify neutron sources without additional complexity or weight from the moderator. The parameters that were optimized for the spectrometer included the thickness of moderator between each de-

Table 4.6: Comparison of detector responses generated using artificial MCNP5 and explicit MCNP6 detector models. The detector indexing is $i = \text{Position} / (3.0 \text{ cm})$. Errors are reported as absolute.

Source	Position (cm)	Artificial Detector Model			Explicit Detector Model				
		r_i	$\sigma(r_i)$	r_i/r_2	$\sigma(r_i/r_2)$	r_i	$\sigma(r_i)$	r_i/r_2	$\sigma(r_i/r_2)$
AmBe	0	5.49E-04	9.00E-04	1.08E-01	1.89E-04	3.65E-04	5.20E-03	1.71E-01	9.28E-04
	3	5.07E-03	5.00E-04	1.00E+00	1.58E-03	2.13E-03	2.20E-03	1.00E+00	2.66E-03
	6	2.76E-03	7.00E-04	5.45E-01	9.02E-04	1.12E-03	3.00E-03	5.26E-01	1.76E-03
	9	1.22E-03	1.10E-03	2.40E-01	4.47E-04	5.14E-04	4.40E-03	2.41E-01	1.12E-03
	12	6.25E-04	1.60E-03	1.23E-01	2.70E-04	2.62E-04	6.20E-03	1.23E-01	7.87E-04
PuBe	0	1.85E-04	1.50E-03	8.09E-02	1.72E-04	1.28E-04	8.90E-03	1.29E-01	1.17E-03
	3	2.28E-03	8.00E-04	1.00E+00	1.70E-03	9.85E-04	3.20E-03	1.00E+00	3.53E-03
	6	2.41E-03	8.00E-04	1.06E+00	1.79E-03	1.00E-03	3.20E-03	1.02E+00	3.60E-03
	9	1.70E-03	9.00E-04	7.43E-01	1.30E-03	7.25E-04	3.70E-03	7.36E-01	2.94E-03
	12	1.01E-03	1.20E-03	4.41E-01	8.47E-04	4.27E-04	4.80E-03	4.34E-01	2.18E-03
²⁴⁰ Pu	0	3.39E-04	1.10E-03	8.67E-02	1.61E-04	2.22E-04	6.70E-03	1.33E-01	9.14E-04
	3	3.91E-03	6.00E-04	1.00E+00	1.62E-03	1.67E-03	2.40E-03	1.00E+00	2.83E-03
	6	3.46E-03	7.00E-04	8.86E-01	1.47E-03	1.43E-03	2.60E-03	8.55E-01	2.57E-03
	9	1.96E-03	9.00E-04	5.01E-01	8.77E-04	8.22E-04	3.50E-03	4.92E-01	1.87E-03
	12	9.40E-04	1.30E-03	2.40E-01	4.77E-04	3.92E-04	5.10E-03	2.35E-01	1.25E-03
²⁵² Cf	0	3.14E-04	1.20E-03	8.61E-02	1.65E-04	2.05E-04	7.00E-03	1.31E-01	9.39E-04
	3	3.64E-03	6.00E-04	1.00E+00	1.62E-03	1.56E-03	2.50E-03	1.00E+00	2.92E-03
	6	3.31E-03	7.00E-04	9.08E-01	1.50E-03	1.37E-03	2.70E-03	8.77E-01	2.71E-03
	9	1.93E-03	9.00E-04	5.29E-01	9.26E-04	8.09E-04	3.50E-03	5.18E-01	1.97E-03
	12	9.59E-04	1.30E-03	2.63E-01	5.22E-04	4.00E-04	5.00E-03	2.56E-01	1.34E-03
14.1 MeV	0	5.15E-05	2.80E-03	7.63E-02	2.42E-04	5.17E-05	1.39E-02	1.68E-01	2.35E-03
	3	6.75E-04	1.50E-03	1.00E+00	2.12E-03	3.08E-04	5.70E-03	1.00E+00	5.89E-03
	6	8.68E-04	1.30E-03	1.29E+00	2.55E-03	3.81E-04	5.10E-03	1.24E+00	6.58E-03
	9	8.07E-04	1.40E-03	1.20E+00	2.45E-03	3.57E-04	5.30E-03	1.16E+00	6.38E-03
	12	6.19E-04	1.50E-03	9.17E-01	1.95E-03	2.76E-04	6.00E-03	8.97E-01	5.55E-03

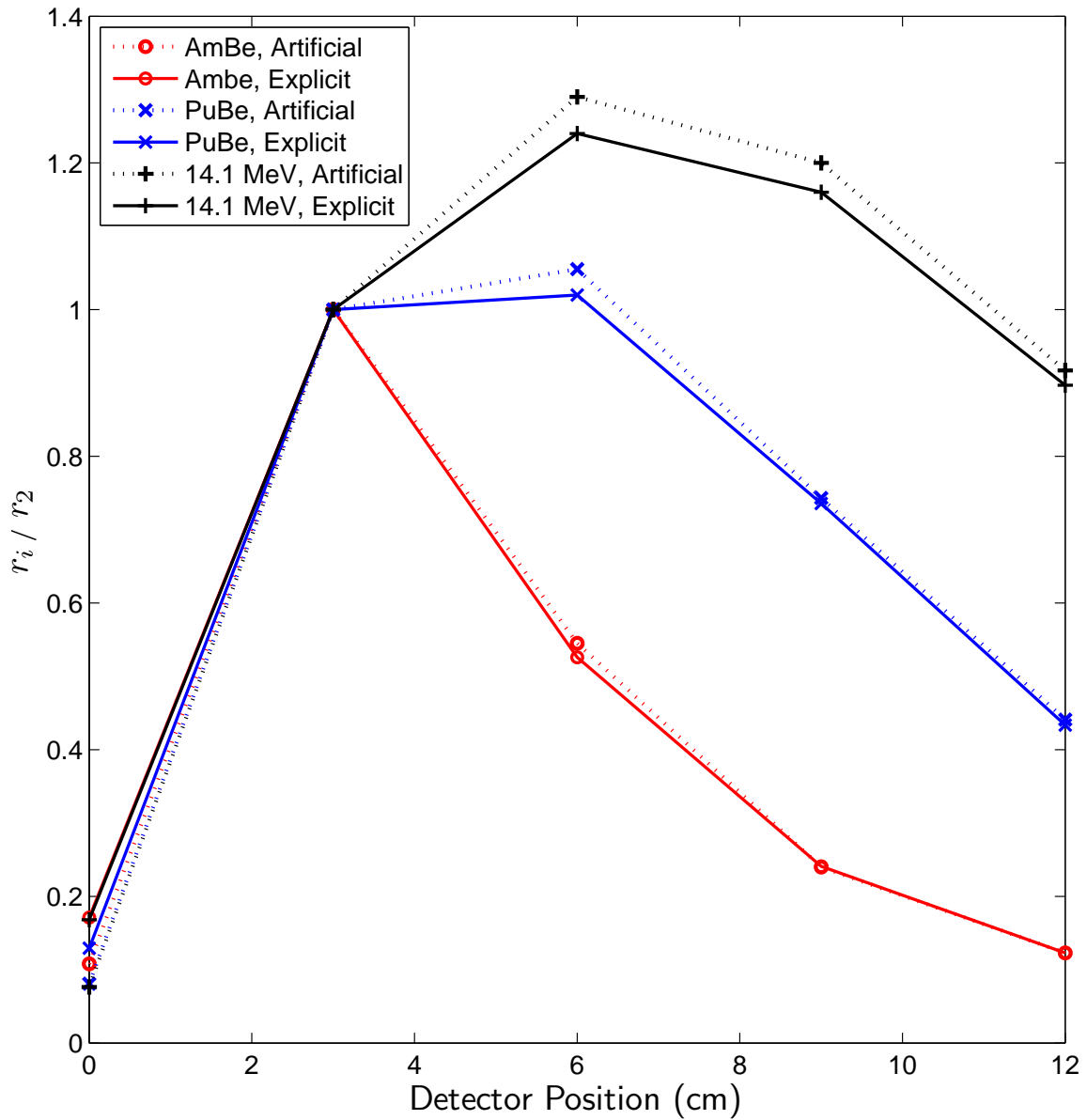


Fig. 4.4: Comparison of detector responses for AmBe, PuBe, and 14.1 MeV fusion sources. All responses are normalized to second detector. All relative errors are less than 0.7%. The dashed line indicates the artificial detectors, and the solid line indicates an explicit MCNP6 model.

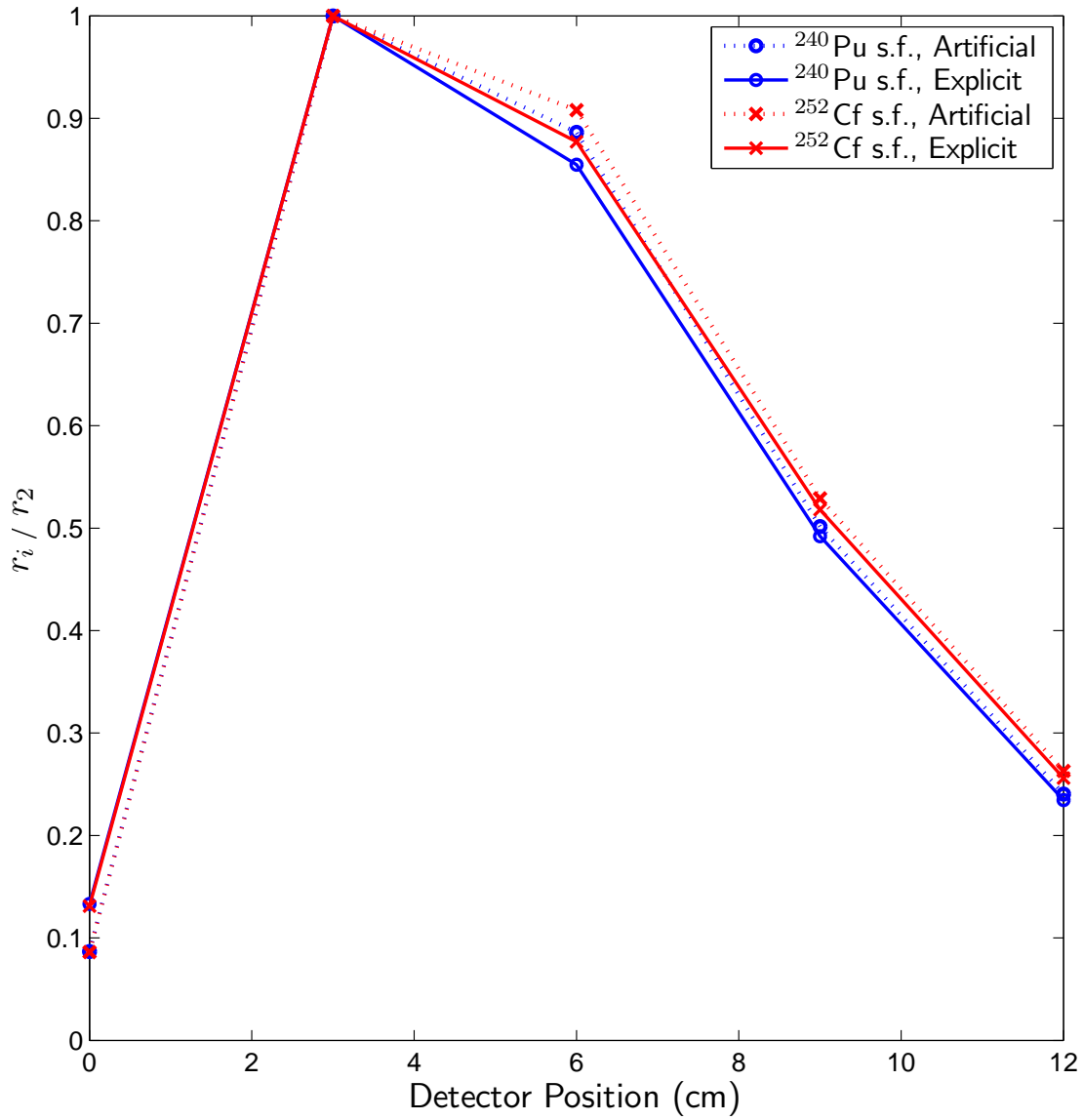


Fig. 4.5: Comparison of detector responses for ^{252}Cf and ^{240}Pu sources. All responses are normalized to second detector. All relative errors are less than 0.7%. The dashed line indicates the artificial detectors, and the solid line indicates an explicit MCNP6 model.

tector, the cross sectional area of the moderator, and the number of detectors in the spectrometer. The weight of the device was also considered, but a specific weight criteria was not specified other than usability as a hand-held device. The optimization was multidimensional and thus performed in several iterative steps. As there were minimal design criteria for the device, several constraints for the optimization were set based on initial simulation results. A general brute-force search was employed for optimization, as the tolerance on optimizations is sufficiently imprecise that more precise methods are not necessary.

4.3.2 Development of Objective Function

An objective function was developed to compare geometries based on their ability to identify sources via *FOM* values. An objective function provides a quantifiable measure of the quality of the results for a particular set of optimization parameters. Either the minimum or maximum of the objective function, depending on the definition of the function, provides the optimal set of parameters.

The goal of a spectrometer is to identify all sources accurately and with statistical confidence. For a particular experimentally measured spectrum, a *FOM* value is generated for each reference spectrum in the library. For correct identification of the neutron source, the lowest calculated *FOM* value should correspond to the reference spectrum associated with that source; the difference between the lowest value and the next closest must also be statistically significant for the source to have been identified with confidence. Thus, a deviation is formed for a particular source as the difference between the lowest and second lowest *FOM* values, relative to the larger uncertainty of the two values, i.e.,

$$\Delta = \frac{FOM^{min+} - FOM^{min}}{\sigma(FOM^{min+})}, \quad (4.15)$$

where FOM^{min} is the lowest FOM value, FOM^{min+} is the second lowest FOM value, and $\sigma(FOM^{min+})$ is the standard deviation of FOM^{min+} . The largest uncertainty of the two FOM values is $\sigma(FOM^{min+})$ rather than $\sigma(FOM^{min})$ because $\sigma(FOM) \propto \sqrt{FOM}$. Using the larger of the two uncertainties is more conservative. By dividing by the standard deviation, Eq. (4.15) removes any difference in *FOM* values caused by different numbers of detectors (increasing the degrees of freedom which proportionally increases the expected mean of *FOM* values). The spectrometer must be able to identify all neutron sources in a set of reference spectra in this manner. The case in which the spectrometer identifies the source with the lowest confidence is the minimum value of Δ for the set of all possible sources

$$\Delta_{\min} = \min \{ \Delta_i : i = 1, 2, \dots, N_{src} \}, \quad (4.16)$$

where N_{src} is the number of sources reference spectra are available for. The set of values $\{\Delta_i\}$ are stochastic, so Δ_{\min} is a random variable with some distribution. An expectation value for Δ_{\min} can be determined by averaging Δ_{\min} for many measured spectra that provides a measure of the ability of a particular geometry to discriminate between *FOM* values for various sources. Thus, the objective function Θ for the spectrometer is taken as the expectation value of Δ_{\min} , i.e.,

$$\Theta = \frac{1}{N_{corr}} \sum_{n=1}^{N_{corr}} \Delta_{\min}^{(n)}. \quad (4.17)$$

Here, $\Delta_{\min}^{(n)}$ is the n -th Δ_{\min} of N_{corr} trials in which all sources were correctly identified. Each trial contains a measured spectra for each of the N_{src} sources. It is noted that N_{trials} is the total number of trials simulated; however, N_{corr} in Eq. (4.17) only includes trials which identify all sources correctly. The sample standard deviation for Θ is computed as

$$\sigma(\Theta) = \frac{1}{\sqrt{N_{corr} - 1}} \sqrt{\overline{\Delta_{\min}^2} - \Theta^2}, \quad (4.18)$$

where

$$\overline{\Delta_{\min}^2} = \frac{1}{N_{corr}} \sum_{n=1}^{N_{corr}} (\Delta_{\min}^{(n)})^2, \quad (4.19)$$

is the expected value of the square of Δ_{\min} .

For a correctly identified source, a relatively high value of Θ indicates a large difference between the two lowest FOM values, relative to the statistical uncertainty in the values; this is considered to indicate a higher quality spectrometer. The confidence of identification is also dependent on the location of the lowest FOM value and its uncertainty. This is not considered because in general if Θ is high, then the separation is high, and the uncertainty in the lowest detector is proportional to the square root of that FOM.

The percentage of the N_{trials} that correctly identify a source is also tabulated as a statistic and considered a measure of quality. Here, frequentist statistics is assumed. Explicitly, $P(\text{correct identification of all Sources in a trial}) = p_{succ}$, where

$$p_{succ} = \frac{\# \text{ of trials where all sources were correctly identified}}{N_{trials}}. \quad (4.20)$$

4.3.3 Simulated Responses

The calculation of *FOM* requires the comparison of an observed detector spectrum to a reference spectrum. The reference spectra can be generated from the simulated detector responses of an MCNP simulation. For the purpose of optimization, it is not feasible to collect the many observed detector responses experimentally. As an alternative method, measured detector spectra can be generated by using counting statistics to sample from the reference spectra, as described in the remainder of this section. With artificially generated data, Monte Carlo sampling can be used to generate *FOM* values.

To generate an observed detector spectra, a response is sampled from an appropriate PDF for each detector in the spectrometer. The type and parameters of the PDF depend on the expected number of counts (i.e., the mean number of counts) present in the detector. The number of counts observed in a detector is a random variable which follows a Poisson distribution. A Poisson distribution for a random variable is fully defined by the mean of the random variable. Thus, if the mean number of counts observed in a detector is known, the observed number of counts is distributed as a Poisson distribution with that mean. Here, electronic noise and other phenomena in a detector that would distort the distribution are ignored.

The F4 MCNP tallies used to simulate detector responses discussed in Section 4.2.2 provide a normalized response function for each detector in the spectrometer. Each response function estimates the expected value of counts observed in a particular detector, per source neutron. The total number of source neutrons S_0 multiplied by the response function can be taken as the mean of the distribution that observed counts in such a detector would follow. Therefore, for a particular neutron source strength, the simulated observed number of counts in a detector would follow a Poisson distribution with a mean μ given by:

$$\mu_i = S_0 r_i. \quad (4.21)$$

Here, r_i is the MCNP response (tally) for the detector position of interest. For the MCNP model used for optimization, the number of neutrons incident upon the spectrometer is the same as S_0 because the beam is uniform and of the same size as the cross sectional area of the device. As a result, the nomenclature of neutron source strength is used throughout this chapter to refer to the total number of neutrons incident upon the spectrometer.

In application, the spectrometer will count for some fixed period of time, so for a uniform incident beam, the total incident neutrons would be given by

$$S_0 = s_0 AT, \quad (4.22)$$

where s_0 is the neutron source strength per unit time per unit area ($\text{n cm}^{-2} \text{s}^{-1}$), A is the cross-sectional area of the spectrometer, and T is the total count time. It should be remembered that this discussion is for a source beam of the same cross sectional area as the device.

For the purpose of comparing spectrometers with different cross sectional areas, it is more physically realistic to keep the source strength per unit area the same. Also, because T is a variable that can be linearly scaled in application to achieve a particular value of S_0 , it has no overall effect on optimizations. Thus, for a particular neutron field, the total number of incident neutrons per unit area over a certain time s_0 is kept constant when comparing different spectrometer geometries. The relation between S_0 and s_0 for a uniform, normal incident beam is $s_0 = S_0/A$. Although s_0 remains constant, S_0 is needed to determine detector responses, and is thus typically used to characterize the neutron source strength in this work.

A pseudo-random number generator is used to sample a random floating point number between 0 and 1. This random number is transformed to sample values from the appropriate Poisson PDF. For large values of μ , sampling from a Poisson distribution becomes computationally difficult and another method must be used. For a mean greater than 20, a particular Poisson distribution can be well approximated by a Gaussian distribution with the same mean as the Poisson distribution and a variance given by the square root of that mean [Tsoulfanidis, 1995]. Combining these results with the distributions defined in Section 2.1.5, the observed response in each detector is sampled from the PDF

$$f(N) = \begin{cases} \frac{1}{\sqrt{2\pi}\sigma} e^{-(\mu-N)^2/(2\sigma^2)} & \mu \geq 20 \\ \frac{\mu^N}{N!} e^{-\mu} & 0 \leq \mu < 20 \end{cases} \quad (4.23)$$

where $\sigma = \sqrt{\mu}$ is the standard deviation for the Gaussian PDF and N is rounded to be a discrete number after sampling for the Gaussian PDF. The pseudo-random number generator used was the Park and Miller Generator described in detail by Press et al. [1992]. The random variable with a uniform distribution was transformed to the appropriate distributions for N using methods and algorithms from Numerical Recipes by Press et al. [1992]. The Fortran90 code that performs the sampling is an executable generated from the **simul_resp.f90** source code, found on page 166. The random number seed for the random number generator is written to a file and passed between directories to ensure random numbers are not reused across trials.

It is noted that when comparing different cross-sectional areas of the spectrometer, the

input to the simulated response codes for the source strength can be confusing. As mentioned above, the source strength per unit area is kept constant, not the total number of neutrons incident upon the spectrometer. However, the input for source strength in the codes is given as the total number of incident neutrons. The source strength is scaled internally in the code by cross-sectional area to keep the source strength per unit area constant. Explicitly, the source strength that is input is scaled by the ratio of the cross-sectional area of the spectrometer of interest to that of a 10-cm radius spectrometer.

4.4 Automation of Simulations and Data analysis

To automate the procedure of performing the large number of simulations and processing data for optimization, a set of interconnected Python scripts (modules) was developed. Python is an efficient scripting language with many integrated pre-existing numerical analysis packages. In general, the Python modules created for the work described in this chapter are a mix of procedural and object-oriented programs. For the numerical analysis portion of the work, Fortran90 programs were written. These programs are executed using a Python wrapper script. Appendix B summarizes the function of each Python module and Fortran90 program on page 135. The actual source code and scripts are included in Appendix B as well, with the exception of straightforward modules. It is noted that the majority of the modules were not sufficiently robust enough to perform all simulations of interest, so modifications to the base code were made throughout.

The general procedure for performing simulations and data processing is as follows:

1. For each geometry and neutron source, create an MCNP input file.
2. Perform all MCNP simulations, ensuring that statistical tests are passed.
3. Organize output tallies from each file into individual tallies
4. For many trials:
 - (a) Simulate observed data from all sources
 - (b) Perform FOM calculations between all templates and simulated data
 - (c) Calculate Θ (and other parameters of interest) and add them to large data array
5. Average results from many trials

4.5 Corrections to the FOM for MCNP Simulations

Adjustments must be made to the *FOM* equations to correct for artificial biases in results introduced by MCNP simulations in the $\sigma(S_i^j)$ term. The corrections are artificial and are only necessary for optimization comparisons. The modified *FOM* statistic is given as

$$FOM^j = \sum_{i=1}^{N_{det}} \frac{(R_i - S_i^j)^2}{\sigma^2(R_i) + \beta_{rad}\beta_{NPS} \sigma^2(S_i^j)}, \quad (4.24)$$

where the factors β_{NPS} and β_{rad} are described below and all other factors are the same as before. This equation was used for comparing all optimization simulations.

Cross Sectional Area of Moderator

Adjusting the cross-sectional area of the spectrometer requires adjustment to the uncertainty $\sigma(S_i^j)$. The correction arises because tallies in MCNP are normalized to a response per source neutron, rather than per source per unit area. To explain this correction, consider the tally response of a particular detector in a spectrometer with some reference radius r_{ref} . In the MCNP simulations, the source is a uniform disk of the same orientation and radius as the spectrometer. In an analog sense, the tally gives the average response in the detector per neutron from a total source strength equal to the number of particle histories, NPS. The tally will have some sample standard deviation, $\sigma^{(0)}$. Now, consider a simulation with the same value of NPS but a smaller radius r . In this case, because the value of NPS is the same, the number of particle histories per source area has been increased, and thus particle histories are more likely to contribute to the tally, producing a smaller relative error (the tally is larger, but this is accounted for by how sampling is performed as discussed in Section 4.3.3).

The smaller uncertainty in the smaller radius case introduces a bias into the values of $\sigma(S_i^j)$. For comparison purposes, it is not reasonable for the geometry with a smaller radius to have a lower variance; in an experimentally collected template, a lower radius would not have a lower variance as the source strength per unit area is the same. To correct the bias in optimization simulations, a correction factor β_{rad} is applied to the uncertainties, rather than altering the value of NPS, to make all geometries have roughly equal relative errors. Scaling the relative errors by a ratio of the areas, and applying error propagation, the result is

$$\beta_{rad} = \frac{r_{ref}^2}{r^2}. \quad (4.25)$$

The value of r_{ref} is 10 cm for the optimization results in this chapter. The correction is performed in the executable with source code **fom.f90**.

Different Number of Particle Histories

A similar bias occurs when different values of NPS are used. The value of NPS is increased in some simulations to ensure that the 10 statistical tests in MCNP are passed. In general, for all tallies $\sigma \propto 1/\sqrt{NPS}$ [X-5 Monte Carlo Team, 2003]. Thus, the correction factor is

$$\beta_{NPS} = \sqrt{\frac{NPS}{NPS^{(0)}}}, \quad (4.26)$$

where NPS is the number of particle histories in the simulation which passes all statistical tests, and $NPS^{(0)}$ is the number of histories in the original simulation; all simulations are performed for the same number of histories initially. For the optimization simulations, $NPS^{(0)} = 2 \times 10^8$. The correction for this factor takes place in the code module `FOM_output.py`.

4.6 Optimization Results

For all of the optimization results in this section, Eq. (4.17) was used to determine Θ , a measure of the quality of a spectrometer. In all cases, $N_{trials} = 1000$ trials were performed. The number of trials that all sources were correctly identified was calculated as p_{succ} (Eq. (4.20)). For each trial, observed detector spectra were generated for each neutron source using the procedure described in Section 4.3.3. A uniform beam of incident neutrons was normally incident upon a spectrometer surrounded by a void, as described in Section 4.2.1. An illustration of a spectrometer with labeled dimensions can be seen in Fig. 4.6. The integer N_{det} refers to the number of detector positions in a spectrometer.

The only two sources simulated for the optimization studies were the spontaneous fission sources ^{240}Pu and ^{252}Cf . Only two sources were used for the optimization to limit the computational cost of simulations. Initial work determined that these two sources were consistently the most difficult to distinguish because of their similar Watt energy spectra. If these sources can be properly identified, all other sources should also be correctly identified. Additionally, these two sources have neutrons covering the spectrum of most neutron sources, with the exception of thermal neutrons. However, thermal neutrons are not a focus of optimization. Because there is no moderator between the source and the front detector, thermal neutrons are detected in the first detector, independent of the spectrometer geometry. It is of note that the ^{240}Pu source is exclusively fission neutrons from ^{240}Pu , and does not include neutrons from induced fission from ^{239}Pu that would be found in a mixture of ^{239}Pu and ^{240}Pu . The energy spectrum of neutrons leaving a sphere of Pu with a mix of ^{239}Pu and ^{240}Pu is

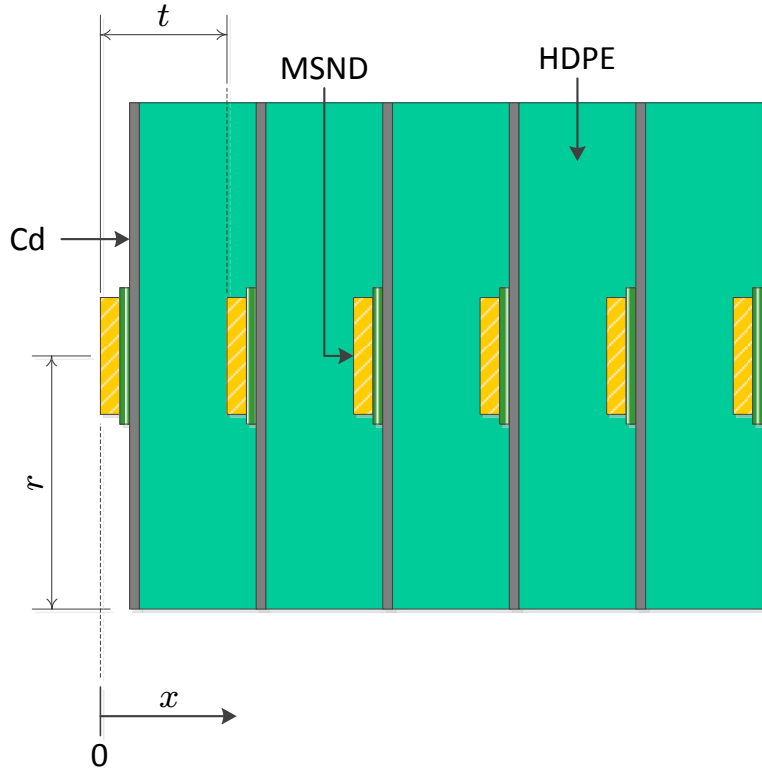


Fig. 4.6: Illustration of dimensions for axial cross section of spectrometer with $N_{det} = 6$ detectors.

known to have a slightly altered spectrum [Toraskar and Melkonian, 1971]. The ability to identify a mix of Pu isotopes is discussed in Section 4.7. The Python modules described previously were used to perform simulations of and generate the output data.

4.6.1 Optimal Detector Spacing for a Fixed Radius

Optimization was performed to determine the optimal spacing of detectors for spectrometers with various numbers of detectors. Only spectrometers utilizing between 3 and 11 detectors were considered. Simulations were performed with a relatively large fixed radius of HDPE moderator, $r = 10$ cm, and variable, uniform spacing t of detectors axially throughout the spectrometer. A large source strength was chosen to ensure all spectrometer geometries correctly identified all sources in all trials ($p_{succ} = 1$) for these initial simulations. The source strength of neutrons was taken to be 10^9 total incident neutrons (corresponding to an incident neutron flux per unit area of 3.18×10^6 n cm⁻²). Observations indicate the optimal detector spacing has some dependence on the source strength chosen, but it is negligible relative to the statistical uncertainties in the objective function and the increments of t .

A plot of Θ versus detector spacing t is given in Fig. 4.7 on page 59, for various numbers of detectors. The values of Θ represent the number of standard deviations of the second

lowest FOM value $\sigma[FOM^{min+}]$. A linear spline is connected between points for clarity. Error bars are depicted for $\sigma(\Theta)$, but are difficult to see in this plot because their length is smaller than the symbols used. For reference, an example set of data needed to compute Θ from the simulations for spectrometers with various t , $N_{det}=11$ detectors, and $r=10$ cm is given in Appendix D on page 187; the example data includes the MCNP5 tallies, simulated detector counts, and computed FOM values for the simulated spectra.

As Fig. 4.7 demonstrates, an optimal spacing t exists for each particular value of N_{det} . The specific values of t , Θ , and $\sigma(\Theta)$ for the optimal t are given for each value of N_{det} in Table 4.7. The performance is improved with increasing number of detectors, as would be expected because more data points allows for a better comparison and identification of a spectrum. Because there is no limit on the amount of moderator, increasing N_{det} will improve results, as long as neutrons can traverse the moderator to the back detectors.

Figure 4.8 is a plot of Θ versus the number of detectors for the peak values from Table 4.7. Even for 3 detectors, the spectrometer was able to correctly identify sources for a very large number of incident neutrons. However, for N_{det} below 6, the results are noticeably poorer. From 6 to 11 detectors, the results are roughly linear. The values of Θ begin to drop off nonlinearly below 6 detectors. This is because there just simply are not enough data points to distinguish between the very similar source spectra. Based on this result, and to limit the number of simulations, only detector geometries with N_{det} between 6 and 11 are explored for the remainder of this work. Also, at small values of N_{det} , the optimal value of t is large. At these large thicknesses of moderator, the spectrometer designs would perform very poorly when the source strength is low and room scatter is included to give more noise in the back detectors.

Table 4.7: Comparison of optimal value of Θ with respect to t for the values of N_{det} from Fig. 4.7.

N_{det}	t (cm)	Θ	$\sigma(\Theta)$
11	3.5	43.4131	0.013
10	4	41.2018	0.0135
9	4	39.8023	0.0131
8	5	37.4673	0.0127
7	5	34.9114	0.0126
6	5	30.7839	0.0123
5	7	26.5515	0.0119
4	7	19.0562	0.0102
3	10	12.8654	0.0085

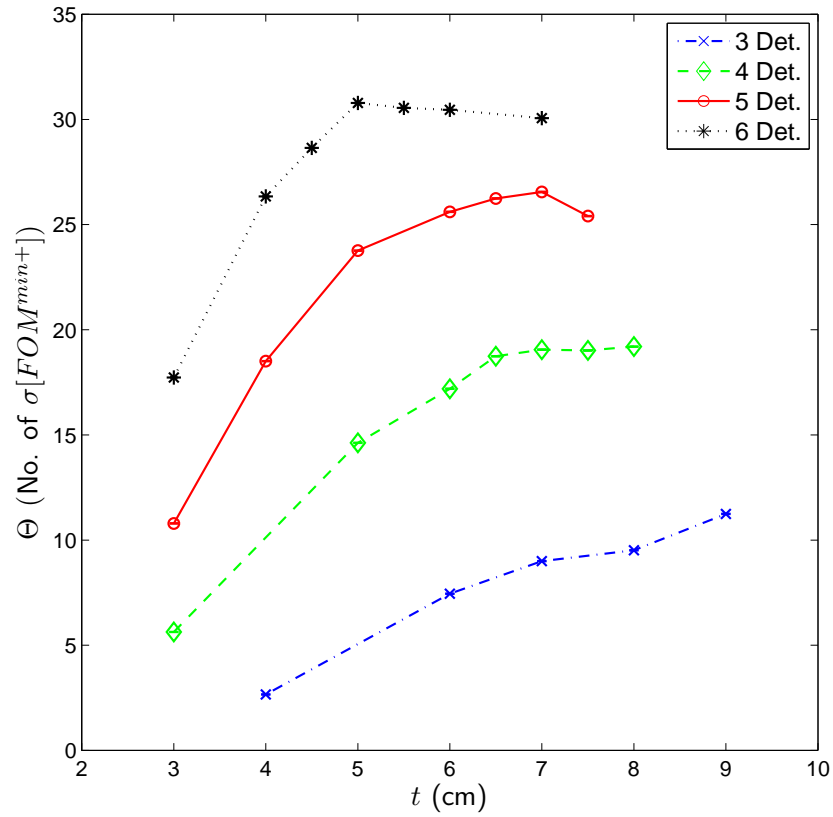
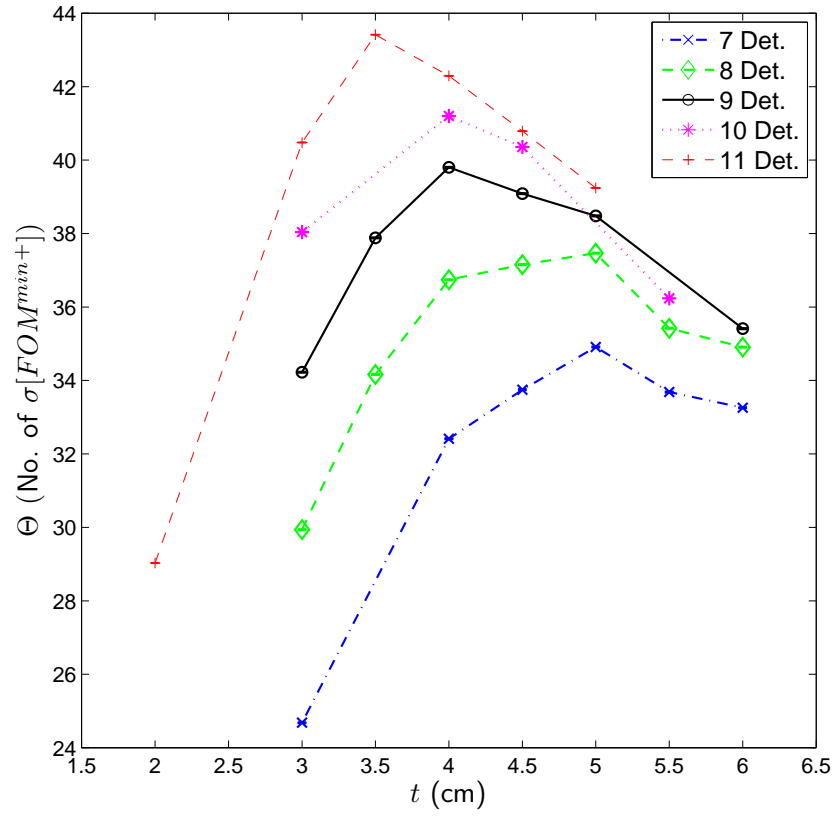


Fig. 4.7: Comparison of various values of uniform detector spacing t for various numbers of detectors and fixed $r=10\text{cm}$.

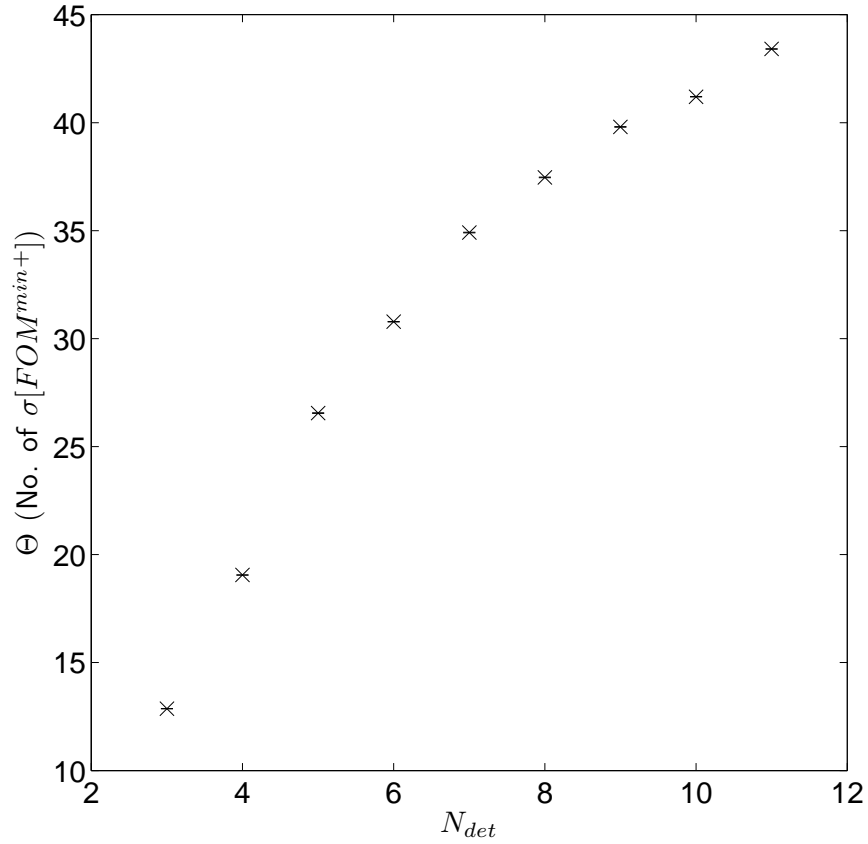


Fig. 4.8: Comparison of Θ for different values of N_{det} with optimal values of t .

In general, the optimal detector spacing is a balance between moderator thermalization and neutrons being absorbed in or leaking from the moderator. For the reference spectrum that is the correct source, with increasing source strength the value of FOM decreases; for templates that do not match the correct source, the value of FOM increases. Thus, it would be expected that the optimum value of Θ comes from the spectrometer geometry with the highest intrinsic efficiency. Interestingly, an increased efficiency of the device does not directly correspond to a higher Θ , as seen in Fig. 4.9. Here, the intrinsic efficiency of a spectrometer ϵ_{spec} is taken as the probability of an incident neutron being measured in any detector in the device; based on the $\{r_i\}$ detector tallies, which provide the expected counts in each detector per neutron incident on the front of the spectrometer, the spectrometer intrinsic efficiency is $\epsilon_{spec} = \sum_{i=1}^{N_{det}} r_i$. The values of ϵ_{spec} reported for each spectrometer geometry are taken as the average over those for ^{239}Pu and ^{252}Cf . A plot of ϵ_{spec} and Θ versus t is given for 10 and 11 detectors in Fig. 4.10; in this figure the values of ϵ_{spec} and Θ have been normalized to the maximum value for visual clarity. In both cases, the peak efficiency occurs at lower value of t than for the peak value of Θ . This result indicates that the quality of a spectrometer is not exclusively a function of efficiency, but also of the deviation of the detector responses r_i between adjacent templates.

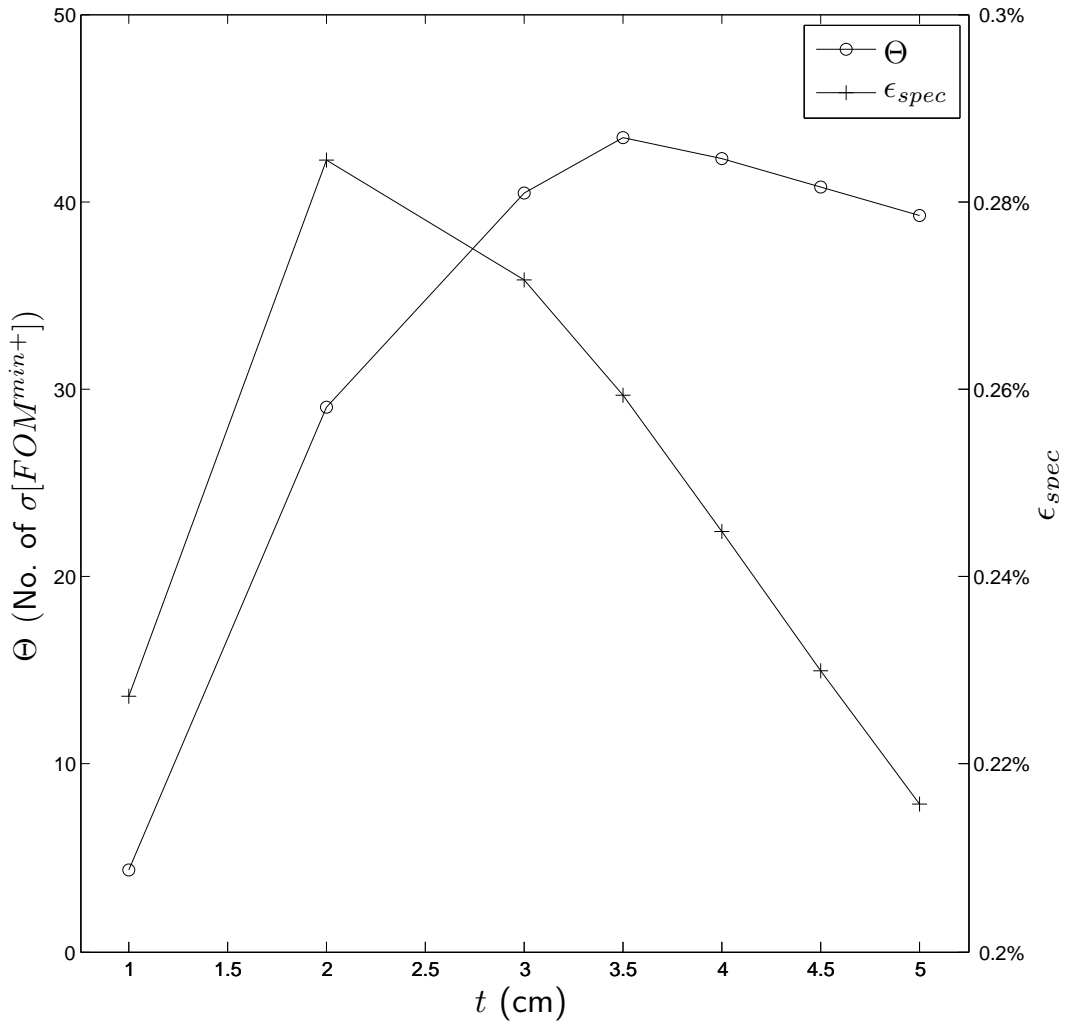


Fig. 4.9: Comparison of spectrometer intrinsic efficiency (ϵ_{spec}) and Θ for various t and 11 detectors.

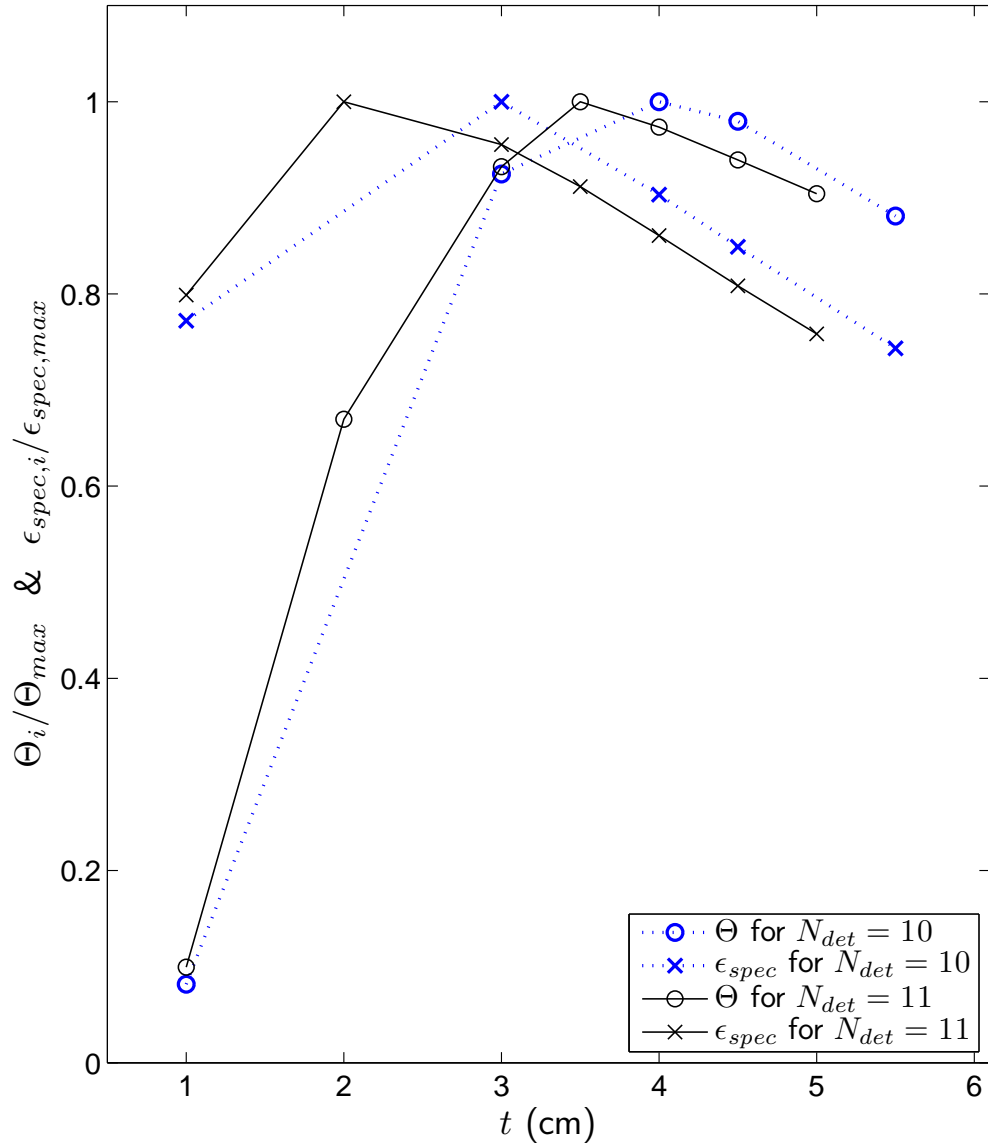


Fig. 4.10: Comparison of normalized spectrometer intrinsic efficiencies (ϵ_{spec}) and Θ s for various t and 10 and 11 detectors

4.6.2 Determination of Threshold Source Strength and Θ for Correct Source Identification

Motivation

Simulations were performed to determine the source strength used for the optimization of the weight and aspect ratio of the spectrometer, which are discussed in later sections. It is necessary to choose a particular source strength for all optimizations. With a sufficiently large number of incident neutrons, all sources in all trials are correctly identified for all spectrometer geometries, and Θ is large, so there is no particular geometry that is better at correctly identifying sources. Similarly, with too few source neutrons, the counts in each detector are too few, and the correct source is not identified, independent of spectrometer geometry. Additionally, the scenario in which fewer detectors may be preferable is when there are lower counts in the back detectors, so the spectrometer geometry should ideally be optimized near the threshold of identification. Because of these reasons, a source strength was determined for which all sources can be identified in the majority of trials, but Θ is small enough that the difference between unique geometries is significant.

An approximate value of how large Θ should be to correctly identify sources in the majority of trials is needed to determine the source strength for optimizations as well. Determining a threshold source strength for identification also helps to identify how many total counts would be necessary to correctly identify a source experimentally. Although Θ is an average quantity, the difference in the two lowest *FOM* values, relative to their uncertainty, can be calculated and used as an indicator of if counting time should be increased in an experiment. It is ideal to have some threshold value Θ_{\min} for which p_{succ} is greater than 0.95 if $\Theta > \Theta_{\min}$. Although the detector model is not ideal, and the actual detectors that are implemented may be of a slightly different efficiency and cross-sectional area, the results are dependent on the number of counts in each detector in the spectrometer. The results from this section could be scaled to determine how many counts are needed for a correct identification by multiplying the MCNP response functions by the threshold source strength.

Results

For fixed geometry, various source strengths were explored to determine a relation between Θ and p_{succ} , with the intent of determining Θ_{\min} . Fig. 4.11 compares Θ and p_{succ} for a range of total incident neutrons (S_0) from 10^5 to 10^7 and a geometry of $N_{det} = 11$, $r = 10$ cm, $t=3.5$ cm; values of S_0 were spaced equidistant logarithmically. Table 4.8 gives values of Θ , $\sigma(\Theta)$, and p_{succ} for various source strengths and three unique geometries. As demonstrated, for $\Theta < 1$ the value of p_{succ} is relatively low (less than 0.80). For $\Theta > 2$, the value of

p_{succ} is much higher (greater than 0.99 in all cases). Therefore, it is proposed that values of Θ greater than 2 have at least a 95% statistical confidence of correct source identification, and values of $\Theta < 1$ have no statistical significance of correct identification. It is noted that no general relation between confidence of identification and Θ is made here, other than these two proposed limits. The true distribution of Θ is unknown, and $\sigma(FOM)$ is a very approximate standard deviation. The values of Θ are formed with data randomly sampled from the precise means of distributions. In reality, because of neutrons scattering from the room, detector noise, and general differences between simulation and reality, the observed data points will be different than the means of the distributions. This will result in the values of FOM that correspond to the correct source being much larger than the ones found here. This may require the cutoff for theta to be higher, and that the relation between p_{succ} and Θ may demonstrate a different trend. Caution is advised in application of these results. However, for optimization purposes, a value of $\Theta_{min} = 2.0$ is more than sufficient.

Several sample statistics of $\Delta_{min}^{(n)}$ (described by Eq. (4.16)) were computed for the N_{corr} trials where sources were correctly identified; the sample statistics are compared for various source strengths. The sample standard deviation of $\Delta_{min}^{(n)}$ for $n = 1, 2, \dots, N_{corr}$, notated $\sigma(\Delta_{min}^{(n)})$, is given in Table 4.9. The average of the $\{\Delta_{min}^{(n)}\}$ is Θ . The minimum and maximum values of $\Delta_{min}^{(n)}$ from the N_{corr} trials¹ are also compared. For $\Theta > 2$, the values of $\Delta_{min}^{(n)}$ are fairly centralized around the mean, justifying the value of $\Theta_{min} = 2$ being used as a similar threshold of identification for $\Delta_{min}^{(n)}$ with individual measured spectra in application.

With a value of Θ_{min} set, various values of S_0 were explored for a variety of geometries to determine a source strength for the remainder of optimization simulations. Geometries that cover the spectrum of possible designs from 6 to 11 detectors were chosen for this set of simulations. The value of t for each value of N_{det} was based on the results for optimal spacing from Table 4.7. Fig. 4.12 gives a plot of Θ versus the number of detectors (with respective optimal thicknesses), for various values of S_0 . For 10^6 source neutrons, Θ was near 1 or slightly below for all 3 geometries, whereas for 10^7 , Θ was well above 3 in all cases. Thus, 10^7 is taken to be the value of S_0 for correct identification in the majority of trials, for all geometries, and used for the remainder of optimizations; this corresponds to a neutron source strength of 3.18×10^4 n cm⁻². The source strength is only determined to best order of magnitude because simulated detector efficiencies are not accurate necessarily with the real design, and the strength is primarily for optimization purposes. Also, the source strength chosen produces a Θ well above $\Theta_{min} = 2$ for all geometries, which is favorable because the amount of moderator is later decreased in Section 4.6.3.

¹It is noted for clarity that $\Delta_{min}^{(n)}$ is the minimum value of the $\{\Delta_i : i = 1, 2, \dots, N_{temp}\}$ for the n -th trial (in this case there are only two templates), and $\min\{\Delta_{min}^{(n)}\}$ is the minimum of that value from all trials.

Table 4.8: Comparison of Θ and p_{succ} , the probability of correctly identifying all sources in a trial, for various source values of total incident neutrons S_0 .

S_0	$N_{det} = 8$			$N_{det} = 10$			$N_{det} = 11$		
	Θ	$\sigma(\Theta)$	p_{succ}	Θ	$\sigma(\Theta)$	p_{succ}	Θ	$\sigma(\Theta)$	p_{succ}
1.0E+04	0.11	6.3E-03	0.001	0.11	6.8E-03	0.005	0.13	3.9E-03	0.188
1.3E+04	0.13	7.1E-03	0.008	0.12	7.4E-03	0.011	0.15	4.2E-03	0.206
1.8E+04	0.14	6.7E-03	0.011	0.12	6.0E-03	0.027	0.17	4.8E-03	0.211
2.4E+04	0.15	6.9E-03	0.020	0.14	6.4E-03	0.028	0.19	5.4E-03	0.266
3.2E+04	0.14	6.0E-03	0.056	0.15	6.0E-03	0.072	0.18	6.0E-03	0.266
4.2E+04	0.16	5.9E-03	0.079	0.17	6.1E-03	0.114	0.23	6.4E-03	0.273
5.6E+04	0.18	6.0E-03	0.145	0.20	6.6E-03	0.166	0.24	7.1E-03	0.341
7.5E+04	0.20	6.2E-03	0.191	0.23	7.0E-03	0.234	0.28	7.6E-03	0.339
1.0E+05	0.23	7.2E-03	0.292	0.27	8.0E-03	0.313	0.29	8.0E-03	0.409
1.3E+05	0.30	8.1E-03	0.364	0.29	8.6E-03	0.373	0.34	8.8E-03	0.449
1.8E+05	0.33	9.0E-03	0.413	0.35	9.8E-03	0.455	0.41	1.0E-02	0.496
2.4E+05	0.39	9.8E-03	0.506	0.41	1.0E-02	0.528	0.46	1.1E-02	0.560
3.2E+05	0.47	1.1E-02	0.589	0.50	1.2E-02	0.603	0.54	1.3E-02	0.582
4.2E+05	0.57	1.2E-02	0.646	0.58	1.3E-02	0.641	0.64	1.4E-02	0.649
5.6E+05	0.70	1.4E-02	0.720	0.73	1.4E-02	0.717	0.80	1.6E-02	0.715
7.5E+05	0.82	1.5E-02	0.776	0.87	1.5E-02	0.800	0.96	1.7E-02	0.823
1.0E+06	0.97	1.6E-02	0.850	1.09	1.7E-02	0.850	1.15	1.9E-02	0.854
1.3E+06	1.20	1.8E-02	0.905	1.29	1.9E-02	0.905	1.45	2.0E-02	0.919
1.8E+06	1.49	1.9E-02	0.933	1.61	2.0E-02	0.940	1.72	2.2E-02	0.953
2.4E+06	1.79	1.9E-02	0.966	1.96	2.1E-02	0.978	2.11	2.2E-02	0.975
3.2E+06	2.21	2.0E-02	0.988	2.39	2.2E-02	0.991	2.64	2.4E-02	0.996
4.2E+06	2.69	2.0E-02	0.993	2.93	2.1E-02	0.997	3.17	2.3E-02	0.997
5.6E+06	3.21	2.0E-02	0.994	3.52	2.0E-02	0.999	3.81	2.1E-02	1.000
7.5E+06	3.80	1.9E-02	0.996	4.16	1.9E-02	0.999	4.55	2.1E-02	1.000
1.0E+07	4.54	1.8E-02	0.996	4.96	1.9E-02	0.998	5.42	1.9E-02	1.000

Table 4.9: Comparison of $\sigma(\Delta_{\min}^{(n)})$, Θ , and S_0 for a spectrometer with 11 detectors, $r = 10$ cm, and $t = 3.5$ cm. Note, $\sigma(\Delta_{\min}^{(n)})$ here is the sample standard deviation for $\Delta_{\min}^{(n)}$, not the standard error in the mean of the $\{\Delta_{\min}^{(n)}\}$ $\sigma(\Theta)$. The relation is $\sigma(\Delta_{\min}^{(n)}) = \sqrt{N_{corr}}\sigma(\Theta)$.

S_0	Θ	$\sigma(\Delta_{\min}^{(n)})$	$\min\{\Delta_{\min}^{(n)}\}$	$\max\{\Delta_{\min}^{(n)}\}$
1.0e+04	0.13	0.09	2.25e-03	0.39
1.3e+04	0.14	0.10	1.90e-04	0.47
1.8e+04	0.16	0.11	9.12e-04	0.52
2.4e+04	0.19	0.13	2.19e-04	0.63
3.2e+04	0.20	0.13	4.13e-04	0.60
4.2e+04	0.22	0.15	1.61e-03	0.82
5.6e+04	0.23	0.16	1.96e-04	0.82
7.5e+04	0.27	0.18	3.33e-04	0.86
1.0e+05	0.30	0.19	2.96e-04	0.86
1.3e+05	0.35	0.22	3.95e-04	1.07
1.8e+05	0.40	0.25	7.64e-04	1.08
2.4e+05	0.48	0.29	7.34e-04	1.20
3.2e+05	0.55	0.33	6.74e-04	1.37
4.2e+05	0.66	0.37	3.07e-03	1.56
5.6e+05	0.81	0.44	2.10e-03	1.85
7.5e+05	0.96	0.50	7.10e-03	2.15
1.0e+06	1.15	0.56	1.04e-03	2.31
1.3e+06	1.41	0.61	1.43e-03	2.68
1.8e+06	1.74	0.66	4.23e-02	3.13
2.4e+06	2.13	0.71	3.60e-02	3.55
3.2e+06	2.60	0.69	4.49e-02	4.06
4.2e+06	3.17	0.71	8.52e-02	4.77
5.6e+06	3.84	0.68	5.85e-01	5.46
7.5e+06	4.53	0.67	1.53e+00	5.95
1.0e+07	5.38	0.64	2.39e+00	6.67

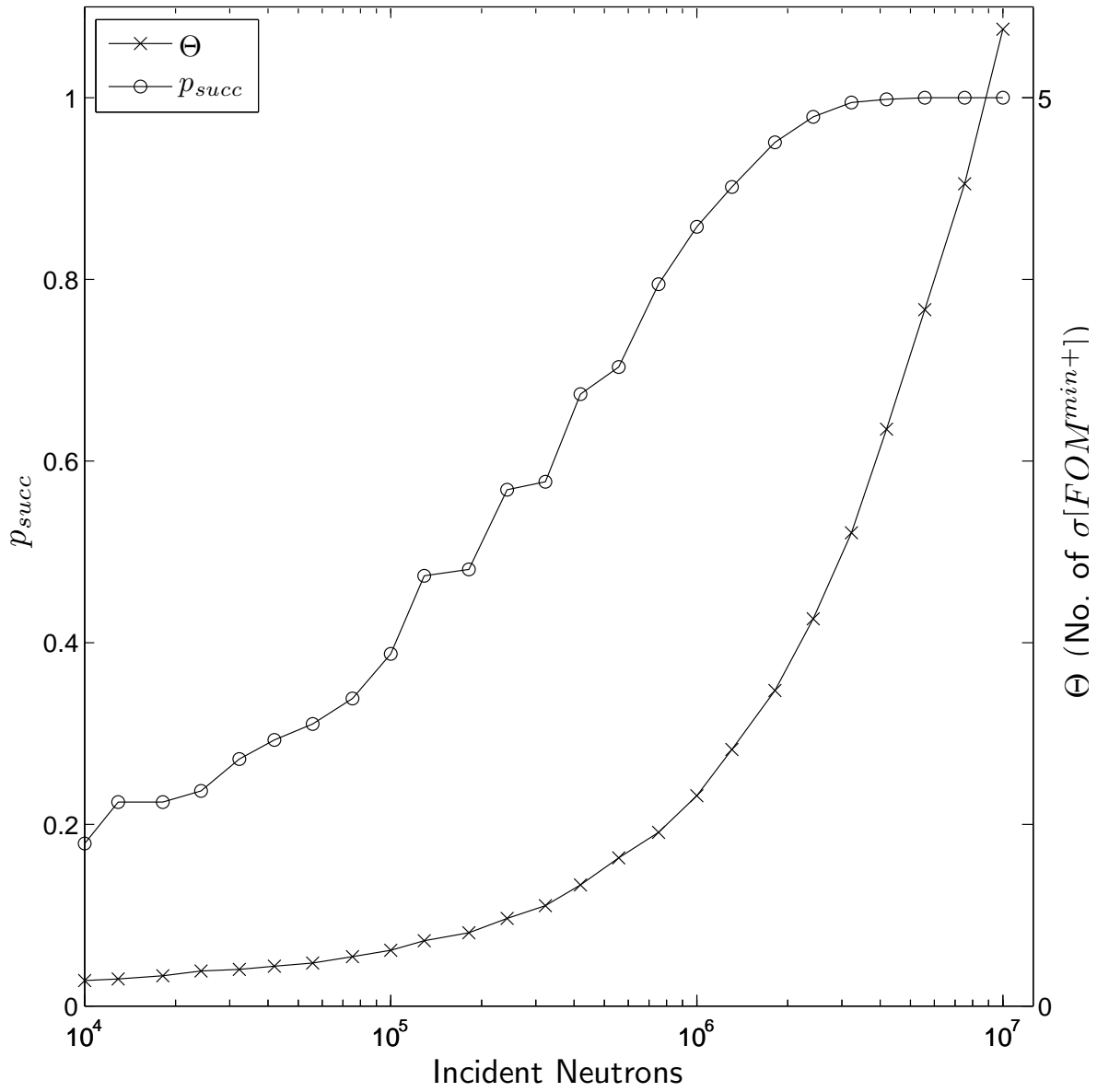


Fig. 4.11: Comparison of Θ and p_{succ} , the probability of correctly identifying all sources in a trial, for various source strengths.

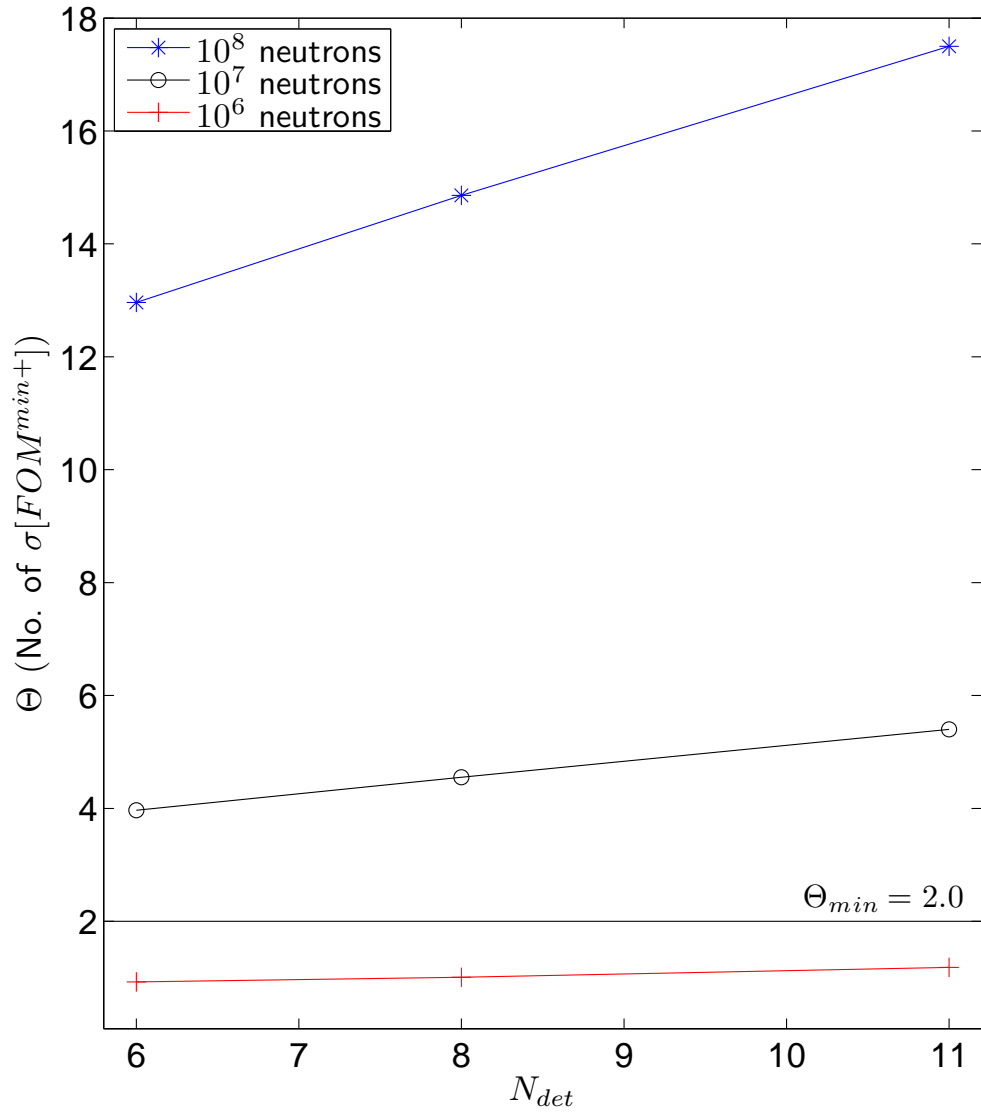


Fig. 4.12: Comparison of Θ for various source strengths and N_{det} .

4.6.3 Radius of the Moderator

Motivation

For a fixed source strength per unit area and a fixed value of t , increasing the moderator radius r improves the quality of the spectrometer by increasing the efficiency of the device. As the cross sectional area of moderator is increased, more neutrons are scattered towards the detectors, resulting in higher count rates. The increased counts, via improved spectrometer intrinsic efficiency, in each detector reduces the denominator error term for the observed responses in the FOM equation, improving the discrimination ability of the spectrometer. As the radius increases, the probability of scattered neutrons near the edge of the spectrometer reaching a detector *decreases* exponentially because of attenuation. Thus, with increasing values of r , the spectrometer efficiency (and consequently Θ) should have a diminishing rate of increase. Because the spectrometer is intended to be a portable hand-held device, the weight of the device should ideally be less than 15 lbs (6.8 kg). However, if r is reduced too much, an unacceptably long counting time would be required for source identification. Also, to fairly compare values of N_{det} , a specific weight of moderator must be chosen, or the largest value of N_{det} will always perform best, as demonstrated previously in Section 4.6.1.

Results

To determine a weight for optimization, spectrometers with different radii were analyzed with all other geometric parameters remaining constant. Fig. 4.13 plots Θ versus r . The geometric parameters were 6 and 4.0 cm for N_{det} and t , respectively. This geometry was chosen for conservatism because 6 is the minimum number of detectors being considered, and $t = 4.0$ cm is a non optimal value. If this geometry succeeds, than any geometry with more detectors and optimal t will also succeed. The neutron source strength $s_0 = 3.18 \times 10^4$ n cm⁻² determined in the previous section was used. Fig. 4.13 plots Θ versus r for this source strength and geometry. A sub-linear relation is demonstrated between Θ and r . The value of $r = 6.0$ cm is chosen to determine the weight w for optimization as it produces a $\Theta > \Theta_{min}$ in Fig. 4.13, with some conservatism for lower source strengths. For a spectrometer that has 11 detectors with optimal spacing $t = 3.5$ cm, a value of $r = 6$ cm yields a weight of 4.84 kg (10.67 lbs). This weight w accounts for the HDPE and the sheets of Cd in the spectrometer. The equation for determining the weight, w , is thus

$$w = \pi r^2 [\rho_{Cd} N_{det} t_{Cd} + t(N_{det} - 1)\rho_{HDPE}], \quad (4.27)$$

where the densities ρ_{Cd} and ρ_{HDPE} are 8.65 g cm^{-3} and 0.95 g cm^{-3} , respectively. The weight of 10.67 lbs is sufficient for a hand held device, and is thus used as the fixed weight for performing aspect ratio optimizations in the next section.

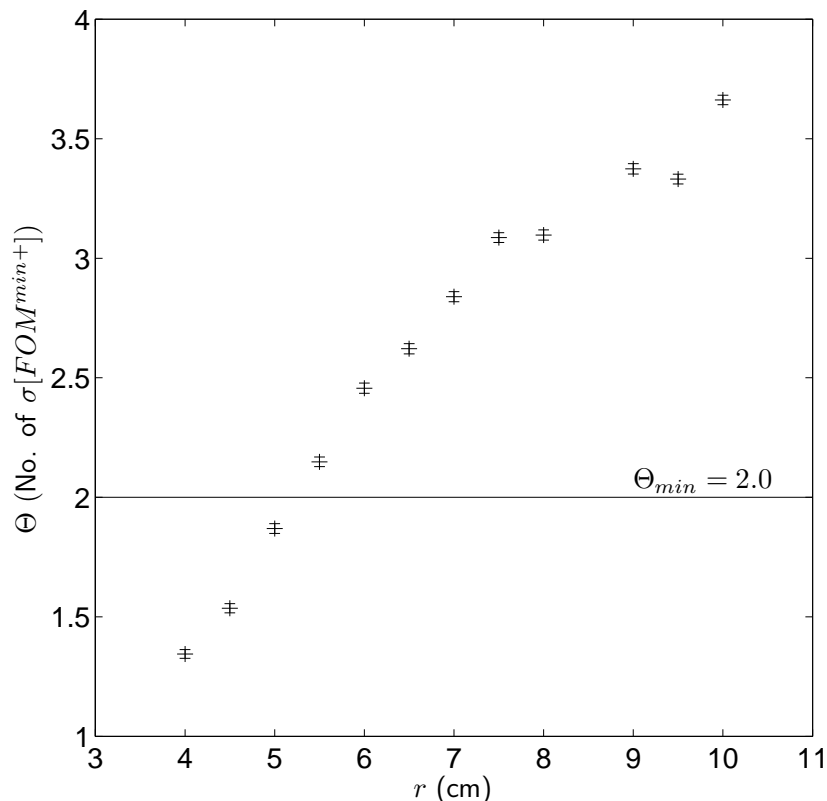


Fig. 4.13: Comparison of Θ and radius of moderator r .¹

4.6.4 Optimal Moderator Aspect Ratio with a Fixed Weight

Using the fixed weight of 10.67 lbs selected in the previous section, the aspect ratio, defined as $A_r = t/r$, was analyzed. The value of A_r was changed by adjusting the value of t , and then using the weight of the device to restrict the value of r . When Eq. (4.27) is solved for r , the equation becomes

$$r = \sqrt{\frac{w}{\pi [\rho_{Cd} N_{det} t_{Cd} + t(N_{det} - 1)\rho_{HDPE}]}} \quad (4.28)$$

Fig. 4.14 plots Θ as a function of t , for a weight of 10.67 lbs, with the value of r determined by the relation in Eq. (4.28). Table 4.10 provides values for Θ , as well as A_r . The maximum

¹Values of Θ vary unrealistically for $r > 7.5$ cm. The variations are caused by the statistical uncertainties in the MCNP tallies $\{r_i^j\}$ used to simulate measured data. Explicitly, Eq. (4.21) assumes that the μ_i are known exactly, which is inaccurate for simulates with larger r that converge slowly. The noise could be corrected for by using the Gaussian variance $\sigma^2(r_i)$ to sample a μ_i , before sampling C_i , for all i and sources.

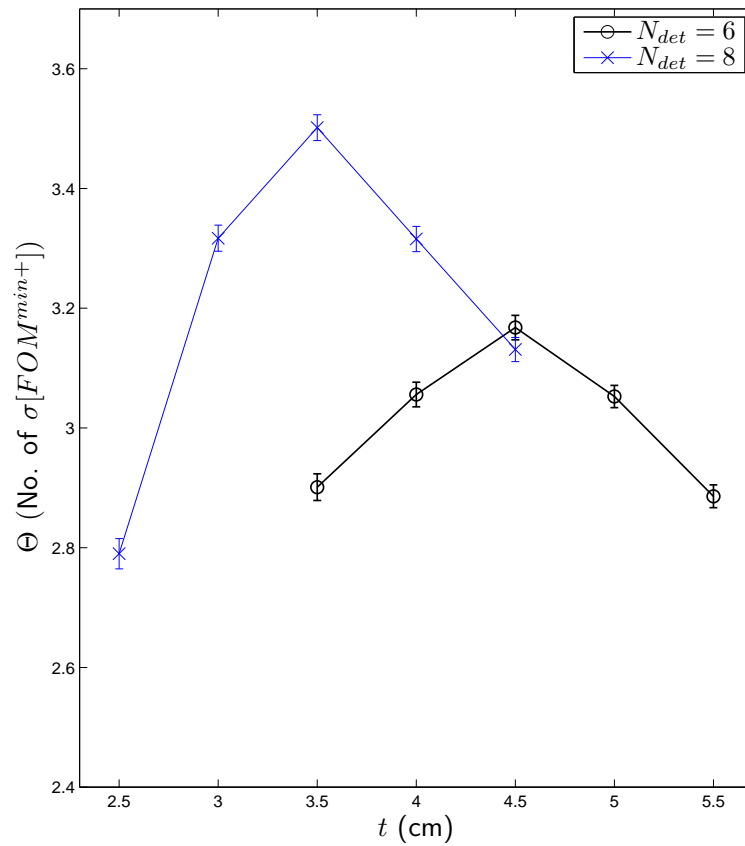
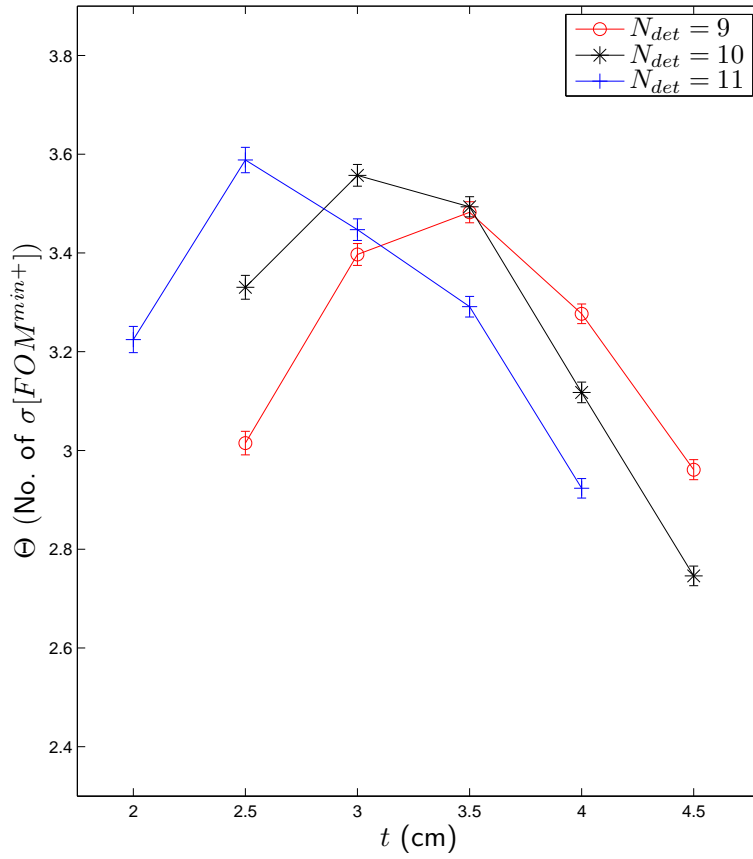


Fig. 4.14: Comparison of Θ for different geometries with a fixed value of w of 4.84 kg.

values are slightly different in this case as compared to the fixed radius results. It is of note that for a fixed weight, the 10 detector case performs very similarly to the 11 detectors case (the optima agree within one standard deviation). So, for the same weight (the main constraint on optimization), the number of detectors becomes relatively negligible at 10 detectors. With some conservatism, 11 detectors is a sufficient number of detector positions. To determine if the aspect ratio (a dimensionless parameter) is the key factor in the quality of the spectrometer, this process was repeated for different weights for the 9, 10, and 11 detector cases and found to produce optima at the same values of A_r , at least for the coarse spacing used here.

Table 4.10: Comparison of aspect ratios and Θ for a variety of N_{det} and a fixed weight of w at 4.84 kg.

N_{det}	r	t	A_r	Θ	$\sigma(\Theta)$
6	7.61	4.5	0.591	3.17	0.021
7	7.69	3.5	0.455	3.35	0.022
8	7.14	3.5	0.490	3.50	0.022
9	6.69	3.5	0.523	3.48	0.021
10	6.70	3.0	0.448	3.56	0.022
11	6.80	2.5	0.368	3.59	0.026

4.7 Detecting WGPu versus ^{240}Pu

The difference in energy spectra between ^{240}Pu and Weapons Grade Plutonium (WGPu) is due to the difference between energy of neutrons released from induced fission of ^{239}Pu and spontaneous fission of ^{240}Pu [Toraskar and Melkonian, 1971]. The optimization simulations were performed using the spontaneous fission energy spectrum of ^{240}Pu . To determine the ability of the spectrometer to identify a source of WGPu, simulations were performed and compared against that of the pure ^{240}Pu case.

The energy spectrum of WGPu is primarily a mix of neutrons from spontaneous fission of ^{240}Pu and induced fission of ^{239}Pu , some of which will be moderated to lower energies. The fractions of neutrons from induced and spontaneous fission will depend on the size and mixture of the WGPu. The larger the device is, the more readily induced fissions will occur, thus shifting the spectrum to consist more of energy of induced fission neutrons. The exact mixture and density of WGPu can vary, and in general is not known. For the simulations in this section, WGPu is taken to be a 4.0 kg sphere of a homogeneous mixture of 93%

^{239}Pu and 7% ^{240}Pu . The density is taken to be 19.84 g cm^{-3} , similar to the BeRP ball used in experiments discussed by Mattingly [2009]. It is noted that the energy of induced fission neutrons is relatively independent of incident neutron energy, and thus there is no coupling between incident and produced neutron energies. An MCNP5 simulation was used to determine the energy spectrum of the sphere of WGPu described above via an F1 tally on the edge of the sphere, which determines the total number of neutrons leaving the sphere. The sphere is in a void, and the source location of spontaneous fission neutrons from ^{240}Pu is uniform throughout the volume. The F1 tally is broken into 86 equal neutron energy intervals between 10^{-11} and 20 MeV. The resulting energy spectrum of neutrons leaving the sphere of WGPu is shown in Fig. 4.15.

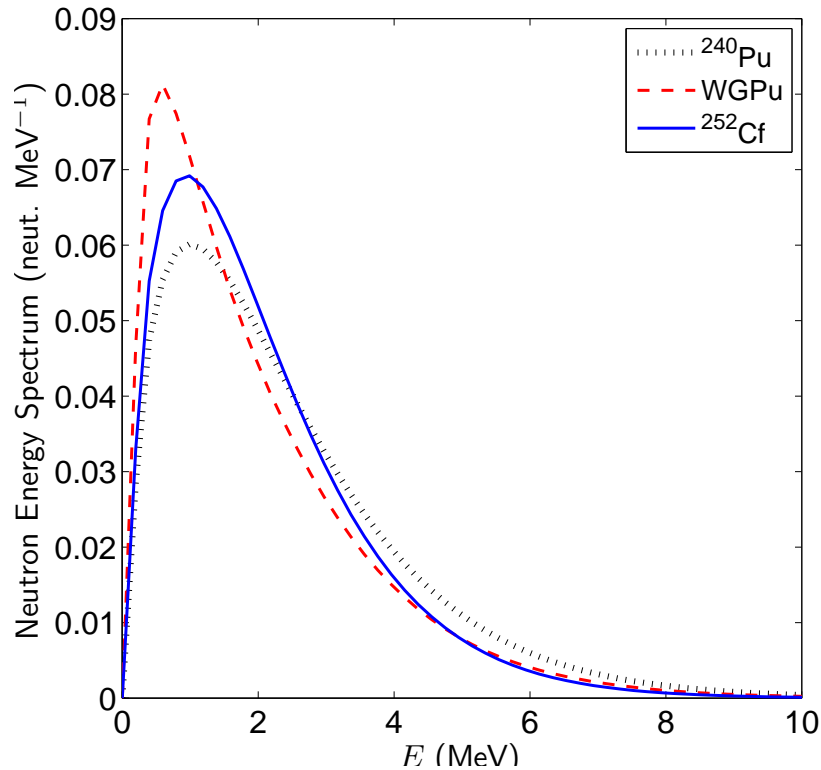


Fig. 4.15: Comparison of neutron source energy spectra for WGPu, ^{240}Pu , and ^{252}Cf .

The output energy spectrum from the sphere of WGPu described above is then taken to be the input in a spectrometer simulation for a beam of normal-incident neutrons, as described in Section 4.2.1. The resulting detector spectra (normalized to the second detector) is compared against that of pure ^{240}Pu and ^{252}Cf in Fig. 4.16. As demonstrated, the results are very similar to those of ^{240}Pu , so it would be very difficult to distinguish between pure ^{240}Pu and WGPu. This is because the induced fission energy spectrum of ^{239}Pu is very similar to the spontaneous spectrum of ^{240}Pu , as shown in Fig. 4.16. A positive result is

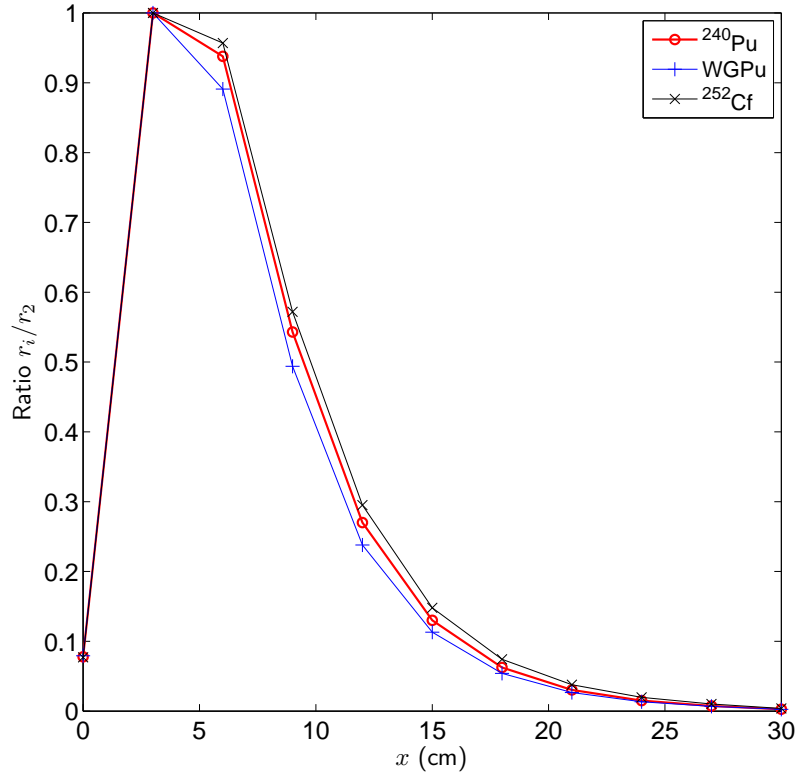


Fig. 4.16: Comparison of detector spectra from different fission neutron sources.

that WGPu detector spectrum is shifted away from the ^{252}Cf spectrum with respect to ^{240}Pu , indicating that WGPu is more distinguishable from ^{252}Cf than ^{240}Pu . Thus, the optimization results are conservative for this particular scenario, as they are based on how similar ^{252}Cf and ^{240}Pu spontaneous fission spectra are.

4.8 Shadow Shield Design and Optimization

4.8.1 Motivation

The shadow shield is a device to correct for neutrons scattered off of the environment (room scatter) that enter the spectrometer. The spectrometer methodology developed in the previous sections is effective at identifying neutron sources by comparing observed spectra to a library of reference spectra. However, when neutrons scatter off nearby material they lose energy, softening the energy spectrum of neutrons that enter the spectrometer. Also room-scattered neutrons enter the spectrometer at different locations and directions than those entering through the front of the device. The fraction of neutrons entering the spectrometer that have scattered off nearby material can be very high. This can result in the observed detector spectra being significantly different from the corresponding template spec-

tra (particularly in the first few detectors, which detect lower energy neutrons). For accurate identification of sources in application, room-scatter effects must be corrected.

One solution to correct room-scatter neutrons is to account for room scatter in the templates. However, it would be difficult to develop a manageable number of templates that covers the large variety of possible environments that could be encountered. Another approach would be to prevent room-scattered neutrons from entering the spectrometer. A layer of Cd around the cylindrical and back surface of the spectrometer, followed by a layer of several centimeters of HDPE would prevent the majority of neutrons from entering the side and back of the device. Although this would provide some correction, the overall weight would be significantly increased, and it would not account for room-scattered neutrons entering the front of the device, an issue discussed further in Section 4.8.6.

The shadow shield provides an alternative method that accounts for room-scattered neutrons by taking two separate measurements. For the first measurement, the shadow shield is placed between the source and the spectrometer. Ideally, the shield absorbs or deflects all neutrons traveling directly from the source to the front of the device, masking the spectrometer from the line-of-sight (LOS) response. In the second measurement, the shield is removed and the spectrometer measures the response from both the LOS and room-scattered neutrons. Fig. 4.17 illustrates the two measurements, as well as possible neutron paths. Because the second measurement is a superposition of LOS and room-scattered neutrons, the difference of the first measurement from the second results in the line of sight response (the shadow of the shield). This net response is much closer to that of a void and can be used to identify the source via comparison to templates from void simulations, eliminating dependence on the environment. It is noted the counting time of these two measurements is the same, with the neutron source and environment unchanged. Although taking two separate measurements is not ideal in practice, it is no different than background measurements required in the vast majority of radiation detection applications. Additionally, any non-directional background source that is constant in time (such as cosmic neutrons or a reactor) will be included in both measurements and thus eliminated from the net response. Although bursts of spallation neutrons in Fe produced by cosmic background (known as the “ship effect”) could be an issue, these can potentially be accounted for via temporal analysis of the measurements, as discussed in Kouzes et al. [2007].

Shadow shields (typically referred to as shadow cones) are commonly used for precise measurement of neutron energy spectra [ISO, 2000]. This section explores the utility of a shadow shield and optimizes the design and implementation of the shield via MCNP simulations. The procedure of identifying sources using *FOM* values is modified and demonstrated for a variety of sources for the optimal shield design and location. The impact of different

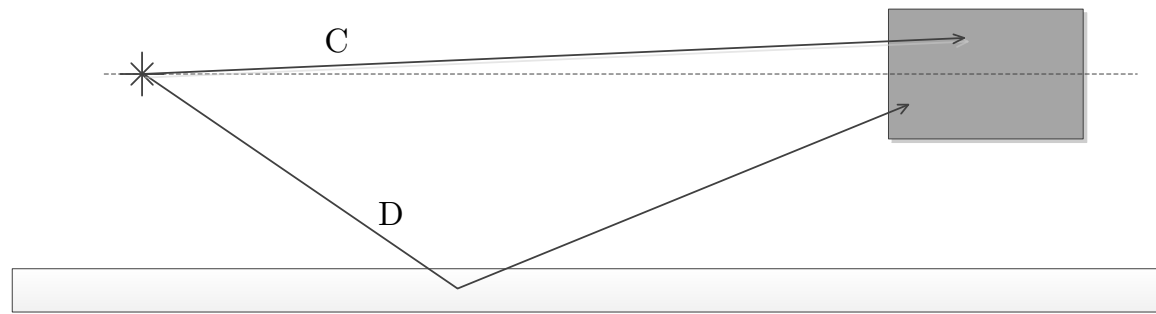
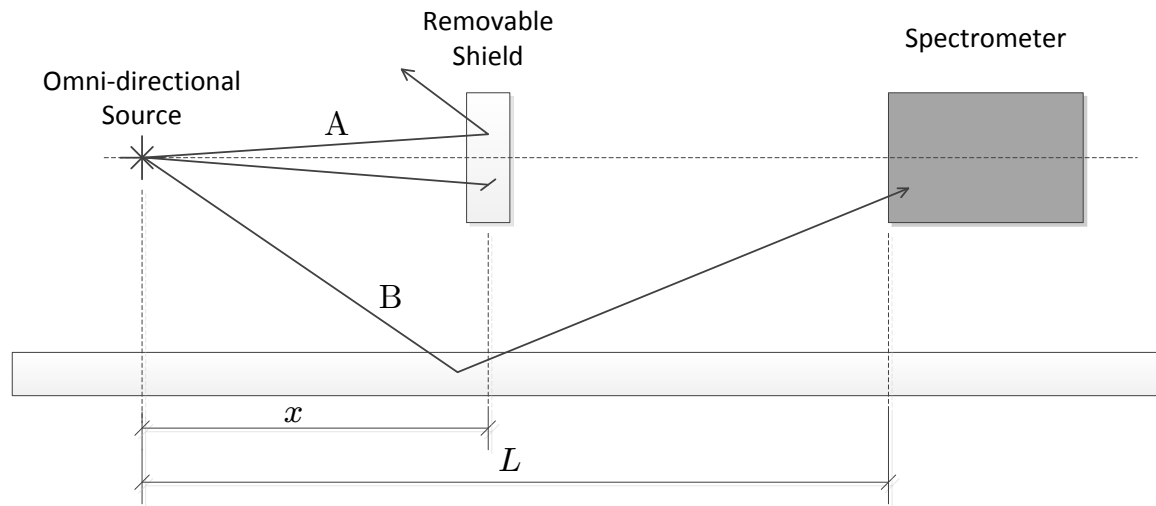


Fig. 4.17: Illustration of the two shadow shield measurements. Several possible neutron paths are illustrated: (**A**) neutrons deflected or absorbed in the shield, (**B**) neutrons scattered off of the environment entering the front of the spectrometer without interacting in the shield, (**C**) line-of-site neutrons, and (**D**) neutrons scattered off of the environment entering the front of the device.

types of rooms is briefly analyzed as well.

4.8.2 Source Identification with Shadow Shield Measurements

The difference in the detector spectra from the two shadow shield measurements described in the previous section (referred to herein as the net spectra) are used to identify observed sources by comparing the net spectra against templates created in a void using FOM values as before. The equation for the FOM value of the j -th source is

$$FOM^j = \sum_{i=1}^{N_{det}} \frac{(R_i - S_i^j)^2}{\sigma^2(R_i) + \sigma^2(S_i^j)}. \quad ((4.4))$$

The terms R_i and $\sigma^2(R_i)$ of the above equation are modified from the original definitions in Section 4.1.2 to account for the two different shadow shield measurements. The value R_i is the logarithm of the normalized difference in the two counting measurements, observed at the i -th detector position, i.e.,

$$R_i = \ln \left(\frac{C_i^{ns} - C_i^s}{C_{norm}^{ns} - C_{norm}^s} \right), \quad (4.29)$$

where the superscript ns indicates the observed counts with no shield present, the superscript s is the observed counts with the shield in place, and the subscript $norm$ indicates the chosen normalization detector position. The uncertainty term, $\sigma^2(R_i)$, is by definition

$$\sigma^2(R_i) = \sigma^2 \left[\ln \left(\frac{C_i^{ns} - C_i^s}{C_{norm}^{ns} - C_{norm}^s} \right) \right]. \quad (4.30)$$

Application of the error propagation formula (Eq. (2.27)) to the term in brackets reduces the above equation to

$$\sigma^2(R_i) = \frac{(C_i^{ns} + C_i^s)}{(C_i^{ns} - C_i^s)^2} + \frac{(C_{norm}^{ns} + C_{norm}^s)}{(C_{norm}^{ns} - C_{norm}^s)^2}. \quad (4.31)$$

There are no changes required to the template values $\{S_i\}$ to account for room scatter, except that the templates are generated using an isotropic point source; template simulations are still performed with the spectrometer and source present in a void. Tallies from void simulations are labeled with the superscript *void*. Values of FOM calculated using the modified definitions given above are referred to as FOM_{room} throughout this section for clarity.

4.8.3 Comparison of Shield Designs

The approximate χ^2 statistic is used to determine the relative effectiveness of a particular shield design (or location). For a particular shield design, the net detector spectra from the shadow shield measurements are compared against the template spectra from the same source in a void, effectively comparing the expected mean response of observed net spectra and the corresponding template spectra. This is much more efficient and simple than generating observed spectra and computing FOM_{room} values for many simulated observed responses. The approximate χ^2 statistic is computed using Eq. (2.31) and labeled as χ_{red}^2 ; the value of N is N_{det} , the degrees of freedom μ is N_{det} (there is no subtraction of one because the mean neither the data nor normalization are used to restrict the data), and the other variables are:

$$\begin{aligned} R_i &= r_i^{ns} - r^s, \\ S_i &= r_i^{void}, \\ \sigma^2(R_i) &= \sigma^2(r_i^{ns}) + \sigma^2(r_i^s), \\ \sigma^2(S_i) &= \sigma^2(r_i^{void}). \end{aligned} \tag{4.32}$$

Here, the values r_i represent the MCNP tally at the i -th detector position from the appropriate simulation indicated by superscripts described in the previous section. The uncertainties $\sigma^2(r_i)$ are the MCNP standard error for the appropriate tally, noting $\sigma^2(r_i)$ is an absolute error. It is also noted that the simulations are not normalized to a particular detector position in the above equation.

The statistic χ_{red}^2 defined above gives a measure of the deviation between detector responses from the net and void spectra, relative to the propagated uncertainties in the detector responses. The lower the value of χ_{red}^2 , the more closely the net spectra matches the void spectra. Therefore, the *lowest* value of χ_{red}^2 indicates the design for which the shadow shield net spectrum is most likely to be correctly identified by a corresponding template created in a void. Additionally, as χ_{red}^2 is a reduced chi-squared value, values less than one indicate that, relative to the propagated uncertainty of the $\{r_i\}$, the net and void spectra agree.

4.8.4 MCNP Model

The MCNP model described in Section 4.2.1 was modified to simulate shadow shield designs. All simulations in this section use the optimum spectrometer design determined in Section 4.6.4: 11 detectors, 2.5 cm thick HDPE sections, and a moderator radius of 6.8 cm. The model was modified to include a room with a floor and ceiling, as well as walls on three sides. Figure 4.18 depicts the geometry, with key dimensions given in Fig. 4.19. The room

was created with the intent of representing a worse case scenario (i.e., room scatter accounting for a large majority of the observed detection measurements), similar to a bunker. All surfaces in the room were 20 cm of concrete of the composition given in Table 4.11. The cylindrical shield was placed coaxially with the spectrometer and source. The source was 1.5 m from the front surface of the spectrometer, along the axis of the spectrometer, as shown in Fig. 4.19. All walls and the ceiling were tangentially 1.5 m away from the center of the front plane of the spectrometer. The source and spectrometer were placed a meter above the floor to represent the height that the spectrometer would be during a measurement as a hand held device.

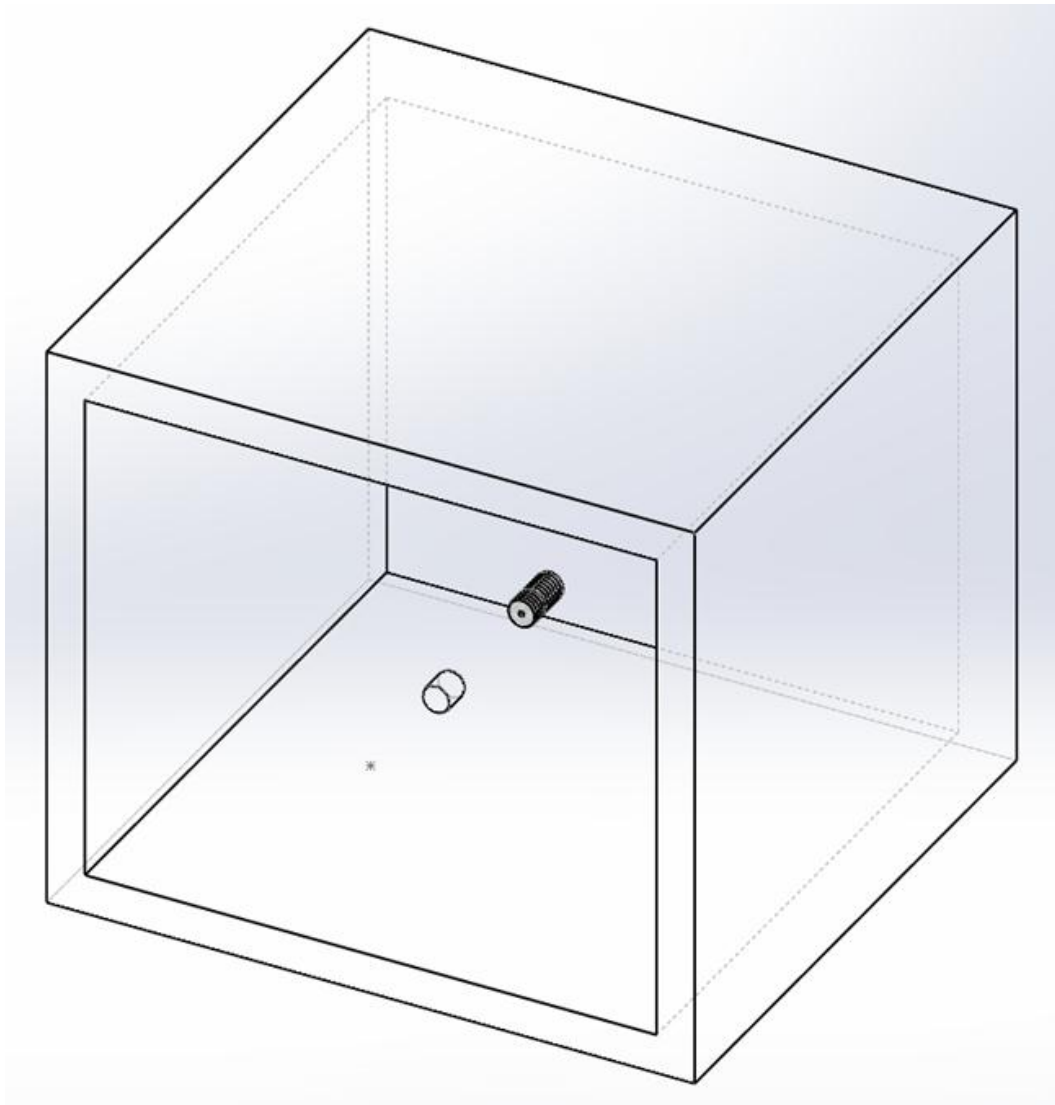


Fig. 4.18: Geometry for room shine scenario.

The neutron source was changed to an isotropic point source. An isotropic point source was used because the beam source does not introduce any room scatter directly from the

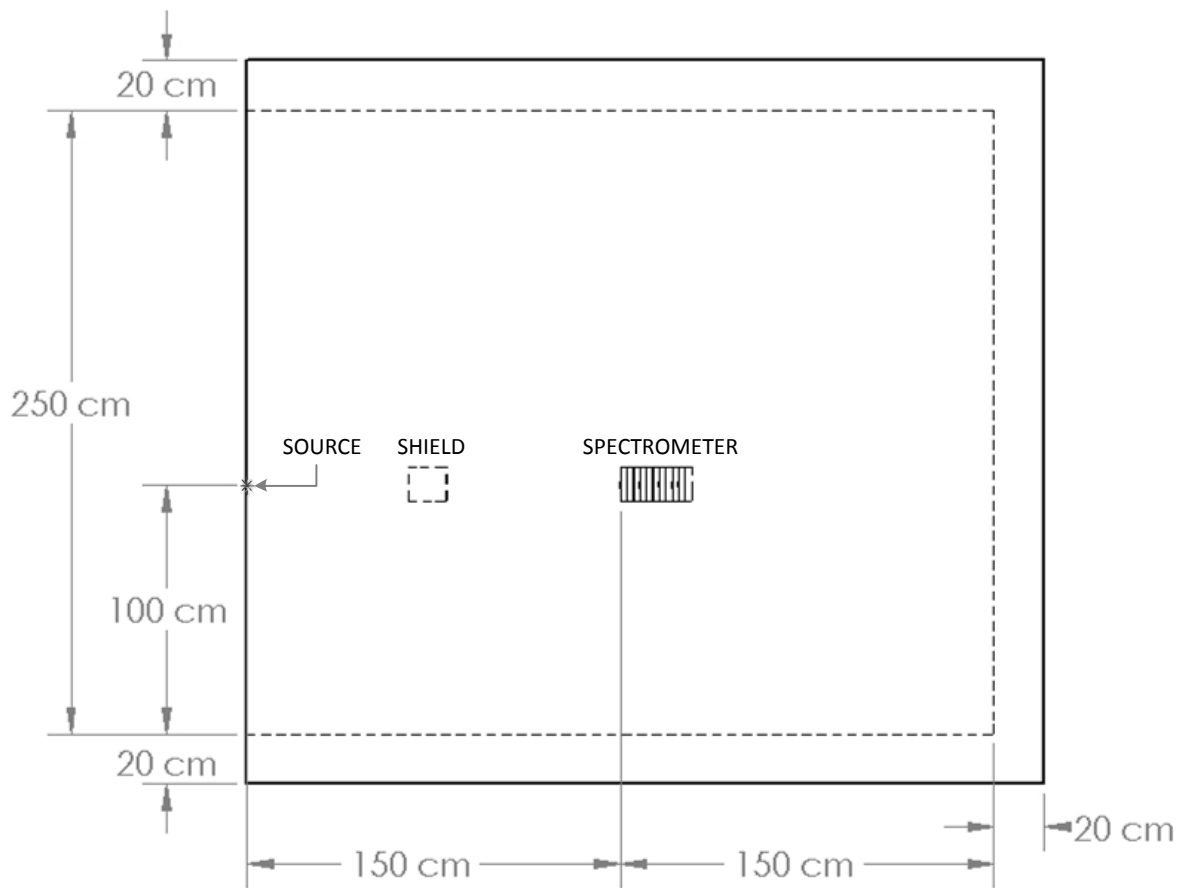


Fig. 4.19: Dimensions for room shine scenario.

Table 4.11: Concrete ($\rho = 2.70 \text{ g cm}^{-3}$) material composition for room scatter simulations.

MCNP5 Library	Mass Fraction
1001.70c	0.022100
6012.66c	0.002484
8016.70c	0.574930
11023.70c	0.015208
12000.66c	0.001266
13027.70c	0.019953
14000.66c	0.304627
19000.66c	0.010045
20000.66c	0.042951
26000.55c	0.006435

source. Also, fewer histories are required to reduce the variance for a point than a disk source. The reduced number of histories was of particular interest for the simulations with the shadow shield in place because the shield prevents the majority of neutron histories from reaching the tallies. The directional source biasing variance reduction method described in Section 2.3.2 was used. Particles were only created in direction cosines between 0 and 1, as measured from the central axis of the spectrometer and source. It is noted that here, because the source is a point, and room scatter is modeled, the tally per source particle is different than the tally per incident neutron on the device, unlike that in the previous beam source simulations.

To simulate the two shadow shield measurements, two simulations were performed. One with the shield in place, and another with the shield removed (the cells are replaced by a void in the model). The shield is of a cylindrical shape the same diameter as the spectrometer. The cylindrical shield's central axis is colinear with the axis of the spectrometer and source. It is noted that typically shadow shields are referred to as a shadow cone, because the shape is usually tapered towards the source [ISO, 2000]. The tapering is to prevent as little room scatter from the source from being shielded, while still blocking the entire LOS response. This geometry is not used here to help eliminate human error in lining up the shield in application.

The room scatter simulations are very inefficient computationally because many neutrons are terminated in the shield, and scattered neutrons have to go through multiple scatters in the room to reach the source; these effects lead to poor convergence. To limit the total number of simulations, a single neutron source was used for optimizing shield thickness and location. The 30-cm D₂O moderated ²⁵²Cf neutron source from Table 4.1 (²⁵²Cf - D₂O) was chosen. The ²⁵²Cf - D₂O source features a relatively strong epithermal energy neutron source, as well as covering the energy range of fast neutrons seen in the majority of neutron sources. The epithermal and lower energy neutrons are of particular interest when analyzing the room-scatter scenario because neutrons with low numbers of scatters in the room are the most likely to reach the first and last few detectors, where the biggest deviation from void templates is seen.

For optimization of shield thickness, an additional simulation was performed with the shadow shield and spectrometer in a void to determine the probability LOS neutrons escape the shield. A parallel uniform neutron beam of the same diameter as the shield was used. Parallel incident neutrons represent the highest probability of escaping the shield. An F1 tally, labeled as J_{shield} , was used on the front surface of the spectrometer to determine the probability, per source neutron, that a neutron escapes the shield and enters the spectrometer. An F1 tally determines the number of neutrons that cross a surface in any direction,

per source neutron. The neutron importance of the spectrometer region was set to zero (terminating all tallies that enter that region) so that neutrons backscattering out of the spectrometer are not tallied.

4.8.5 Shadow Shield Thickness

In application, a shadow shield is primarily made of a moderator (in this case HDPE) with a thermal neutron absorber between the shield and the spectrometer (Cd). The shadow shield needs to be light enough to be hand-held, but thick enough to deflect or absorb the majority of neutrons traveling from the source directly to the spectrometer. As the thickness of the shield design is increased, less neutrons will reach the spectrometer without interacting, but a minimal amount of moderator may be necessary to cause the majority of neutrons to interact and be deflected away from the spectrometer. The goal is to determine a minimal shield thickness for which enough of the LOS response is reduced that the net spectrum can be used to correctly identify a source by matching templates created in a void environment.

By modifying the room-scatter MCNP model described in the previous section, simulations were performed to determine the necessary thickness of the shadow shield to identify sources correctly. A total of 10^9 particle histories were simulated. The dimensions of the shield being considered can be seen in Fig. 4.21. The shield is placed with the center of the moderator half way between the source and the spectrometer, as recommended in [ISO, 2000]. The location of the shield is investigated further in Section 4.8.6. Figure 4.20 compares the detector spectrum for the void template and the room scatter simulation with a ^{252}Cf - D_2O source and no correction by the shadow shield method.

Figure 4.22 plots a comparison of the shadow shield corrected net detector spectra for various shield thicknesses, as well as the void templates; Figure 4.23 provides a larger view of the last few detector positions where the error bars are difficult to see and includes the spectrum for a 20-cm thick shield. The values and error bars in the figures were calculated using Eq. (4.32). Table 4.12 compares values of the weight of moderator and Cd, χ_{red}^2 , and J_{shield} for different shield thicknesses. Results are included for a simulation that calculated J_{shield} for an unmoderated ^{252}Cf source, which produces more high-energy neutrons than the ^{252}Cf - D_2O source, on average. Also, an entry is included in the table for a simulation with the ^{252}Cf - D_2O source in which the Cd sheet at the back of the shadow shield is removed. The relative uncertainty in the value of J_{shield} was less than 1% in all cases.

As demonstrated in Fig. 4.20, the deviation between the uncorrected and void spectra are significant, particularly in the first and last few detectors. These detectors are most affected by room-scatter neutrons because lower energy neutrons can reach them from the

front and back of the spectrometer. Beginning at a thickness of 15 cm, the net and void spectra agree within error, indicated by values of χ_{red}^2 less than 1.0. As the thickness of shield is increased beyond 20-cm, there is no statistically significant improvement in the values of χ_{red}^2 because J_{shield} is already well below 0.01. With some conservatism for higher energy sources, a 20-cm thick moderator shield was chosen to be the most effective while limiting weight. This shield's weight is less than 7 lbs. Table 4.12 demonstrates that for the higher energy ^{252}Cf unmoderated source, the shield still prevents 99% of neutrons from traveling directly from the source to the spectrometer. For the 20-cm shield, the Cd sheet at the back of the shield improved results minimally. The improvement was primarily from the responses in the first detector where thermal neutrons are measured. The removal of Cd may be of desire in environments where Cd is prohibited as a health risk.

As seen in Fig. 4.23, although χ_{red}^2 was less than one for $t_{shd} > 15$ cm, there is large uncertainty in the last few detectors, and the net spectra does not agree with the void spectra as well as in other detector positions. The cause of the disagreement and large uncertainty is that the majority of the response in the back detectors is from room-scattered neutrons; the LOS response only accounts for less than 5% of the total response in the last three detector positions. Even though the relative uncertainty in the shielded and unshielded measurements are $< 1\%$ for these detectors, the uncertainty in the differencing of the measurements scales with the magnitude of the two values added in quadrature, as shown in Eq. (4.32). Because the LOS response is on the order of the absolute error of each of the two measurements, the relative uncertainty in the final result is large. As Fig. 4.23 demonstrates, the value of R_i is higher than S_i in the last few detectors, and increasing the shield thickness does not correct this behavior. The overbias is likely due to neutrons would that enter the rear of the detector after scattering off the back wall being absorbed in the shield and thus not counted as room scatter, thereby increasing the net values. Because the 1.0-cm thick shield allows more of the signal in the last few detectors to be from the LOS response, these back scatter neutrons are not as significant (and are also less likely to be blocked by the thin shield), and the agreement in the last several detectors is better. However, overall the 1.0-cm response does worse than the 15- and 20-cm cases because of their ability to prevent the majority of LOS neutrons from entering the front of the detector. This issue in the last few detectors, and a possible correction, is discussed further in Section 4.8.7.

4.8.6 Optimal Shield Location

Simulations were performed to determine the effect of the location of the shadow shield, relative to the source and spectrometer. The base MCNP model with the ^{252}Cf - D_2O

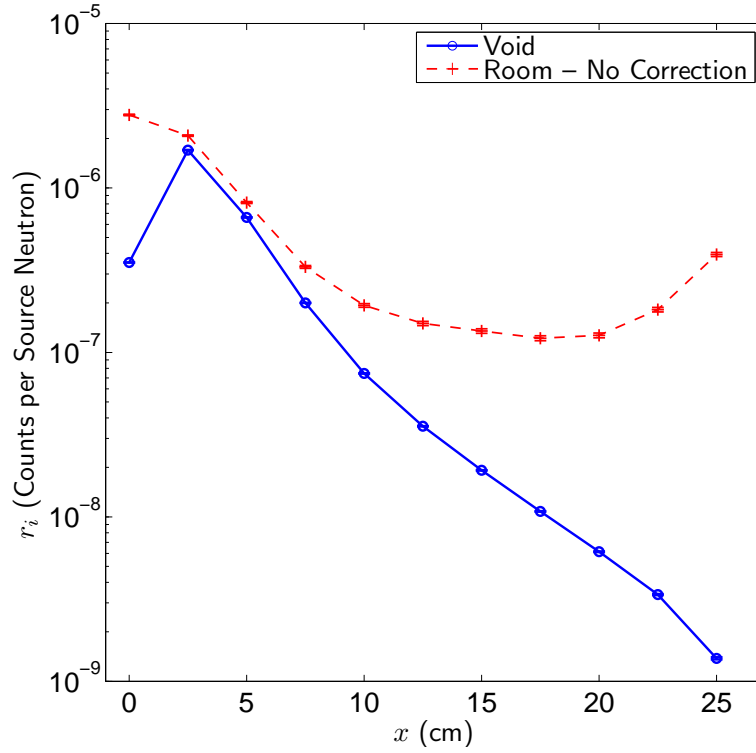


Fig. 4.20: Comparison of room-scatter spectra with no correction and void spectra.

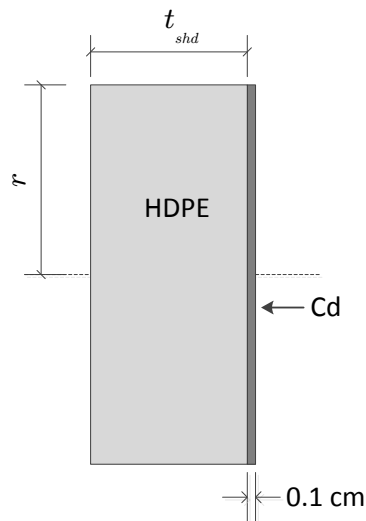


Fig. 4.21: Axial slice of shadow shield with dimension labels.

Table 4.12: Comparison of χ^2_{red} values for different shadow shield thicknesses.

t_{shd} (cm)	wgt. (lbs.)	χ^2_{red}	J_{shield}
1.0 (Cd)	0.58	74.23	2.92E-01
5.0 (Cd)	1.80	1.94	4.58E-02
10.0 (Cd)	3.32	0.36	1.29E-02
15.0 (Cd)	4.84	0.20	4.33E-03
20.0 (Cd)	6.36	0.21	1.62E-03
20.0 (<i>no</i> Cd)	6.08	0.24	1.66E-03
20.0 (Cd - ^{252}Cf)	—	—	6.40E-03
25.0 (Cd)	7.88	0.20	6.56E-04
30.0 (Cd)	9.40	0.24	2.82E-04
40.0 (Cd)	12.45	0.25	5.89E-05

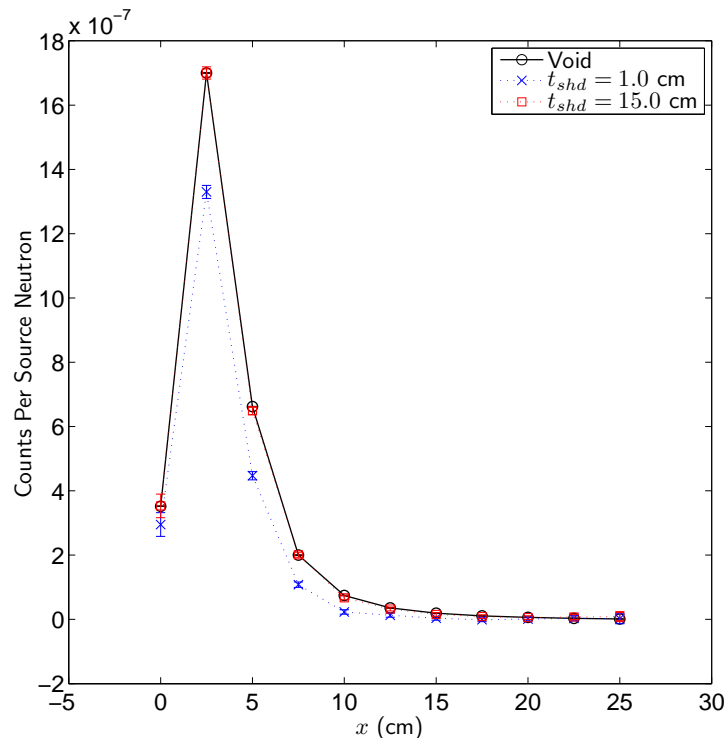


Fig. 4.22: Comparison of net detector spectra for various shadow shield thicknesses.

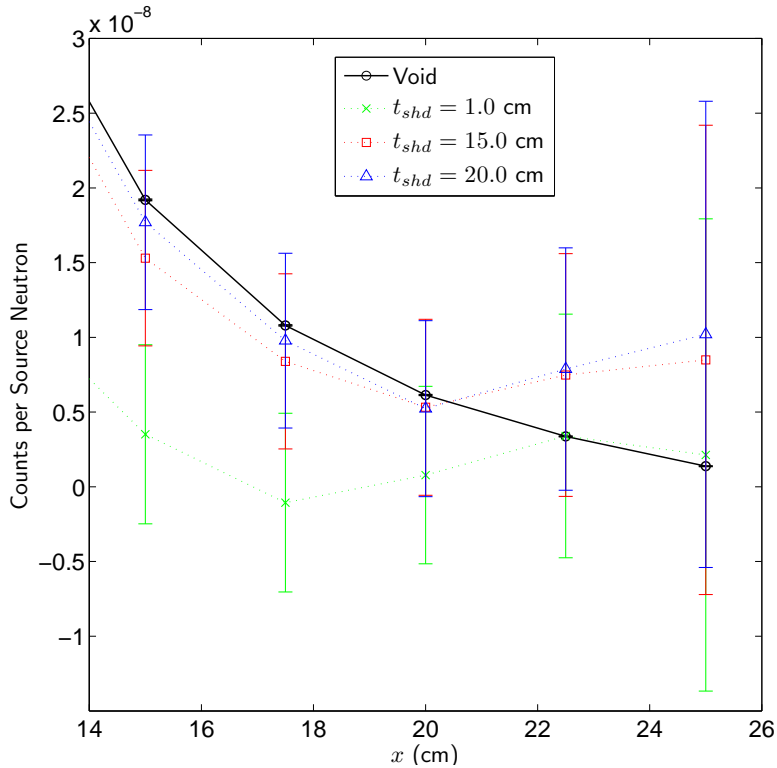


Fig. 4.23: Comparison of net detector spectra at last few detector positions.

source described in Section 4.8.4 was modified and simulations performed with a 20-cm thick shadow shield at different locations along the axis between the source and spectrometer. The dimensionless variable $z = x/L$, where x and L are depicted in Fig. 4.17 on page 76, is used to refer to shield locations; the value of x varies, and $L = 1.5$ m. Table 4.13 compares χ_{red}^2 for different values of z . Figure 4.24 gives a plot of detector spectra at $z = 0.5$, as compared to the void template. Figure 4.25 compares net spectra with void for various values of z . The value of $z = 0.0$ refers to the shield being placed 0.1 cm away from the source. The value $z = 1.0$ refers to the shield being 0.1 cm away from the spectrometer.

In general, spectrometer locations that are not too near to either the source or spectrometer produce net spectra that agree, within error, with the void template; in particular values of $z \in [0.4, 0.8]$. It is desirable that the performance is similar for a range of values because in application it would be easier to place the shadow shield some fixed value (a meter or so) in front of the spectrometer, rather than requiring the shield to be a specific distance in between.

The issue with placing the shield very near to the spectrometer is accounting for neutrons which scatter off the environment and enter the front of the spectrometer (path **B** in Fig. 4.17). These scattered neutrons are prevented from entering the front of the detector, so

they are views as being a portion of the LOS response (path **C** in Fig. 4.17). This causes a higher response in the front few detectors because the room-scattered neutrons are at lower energies because of scattering, as seen in Fig. 4.25. A similar problem occurs when the shield is placed too close to the source, inhibiting the ability of any neutrons that would exhibit room scatter to reach the walls and ultimately the spectrometer. and it does not stop the problem of neutrons entering through the front of the detector.

Although there is some statistical uncertainty in the values of χ_{red}^2 , $z = 0.8$ produced better results than $z = 0.5$, the ideal location suggested by [ISO, 2000]. The discrepancy is because in [ISO, 2000] the shield was of a cone shape, with the smaller end near the source. The shadow shield discussed here is of a cylindrical shape, so it stops some neutrons the cone would not from reaching the room. The neutrons would scatter back into the detector (particularly with the inclusion of the back wall in the model), being counted as room scatter. As the shield gets farther away from the source, the effect is lessened, until $z = 0.9$ where the problem discussed above occurs.

Table 4.13: Comparison of χ_{red}^2 for different locations of a 20-cm thick shadow shield.

$z = x/L$	χ_{red}^2
0.0	879.88
0.1	107.56
0.2	4.89
0.4	0.31
0.5	0.21
0.6	0.18
0.8	0.17
0.9	31.76
1.0	739.87

4.8.7 Results with Optimal Shield Design

To demonstrate the utility of the shadow shield method, various sources were simulated and FOM values computed to determine if the sources could be identified. The shadow shield was a 20-cm thick HPDE cylinder with a sheet of Cd at the back. The shield was placed at $z = 0.5$. MCNP simulations were performed for The list of sources listed in Table 4.1.

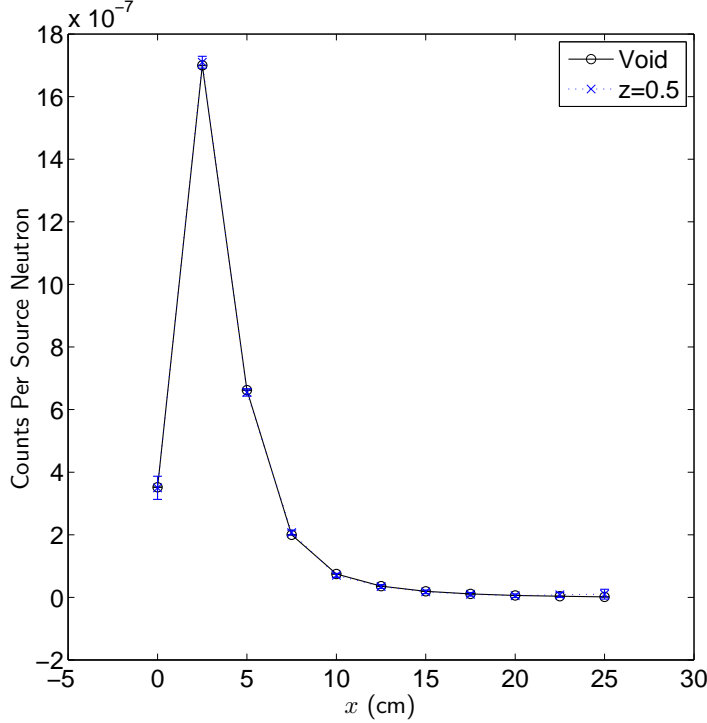


Fig. 4.24: Comparison of net detector spectra with void spectra for a 20-cm thick shadow shield at a location of $z = 0.5$.

For each source, MCNP simulations were performed for the void templates and the two room-scatter simulations described in Section 4.8.4, depicted in Fig. 4.17.

Similar to the procedures in Section 4.3, a total of $N_{trials} = 1000$ were performed, where each trial represents a sampling of data from all sources. For each source in each trial, detector measurements were sampled from the response functions for the two room-scatter simulations individually, based on counting statistics distributions (detailed in Section 4.3.3). Then, the difference of the spectra were taken and FOM_{room} values computed for each simulated spectra, as described in Section 4.8.2. For comparison, FOM values were computed between the uncorrected data sampled from the room-scatter simulation with no shield and the void templates. Also, FOM values are computed based on detector spectra sampled from the void templates. Several different source strengths were sampled. The percent of sources correctly identified out of all the simulated measured data, for all trials, was computed. It is noted that this is different than p_{succ} , as p_{succ} gives the percent of all trials that correctly identified all sources. The difference was made because the net spectra do not identify the sources as accurately, and more sources are being simulated, so there was often at least one source that was incorrectly identified in each trial.

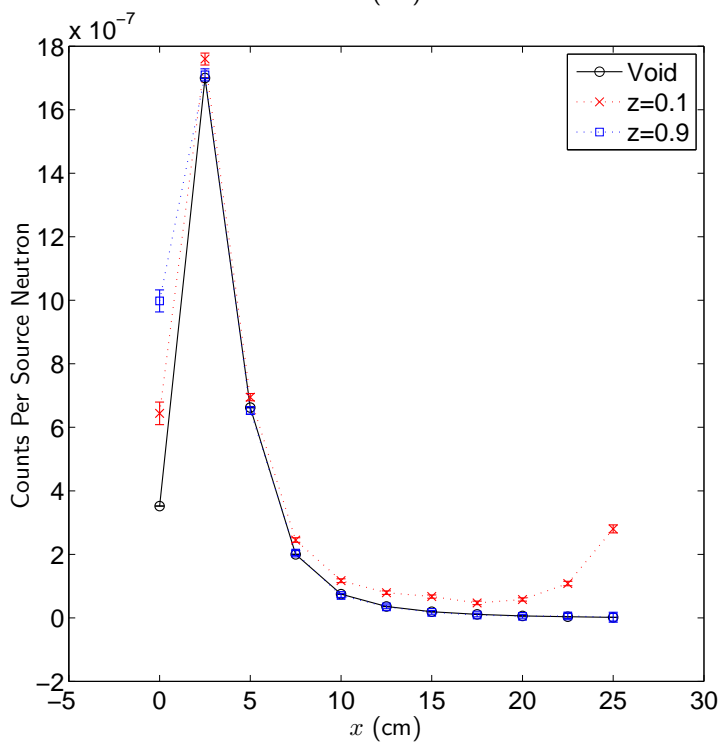
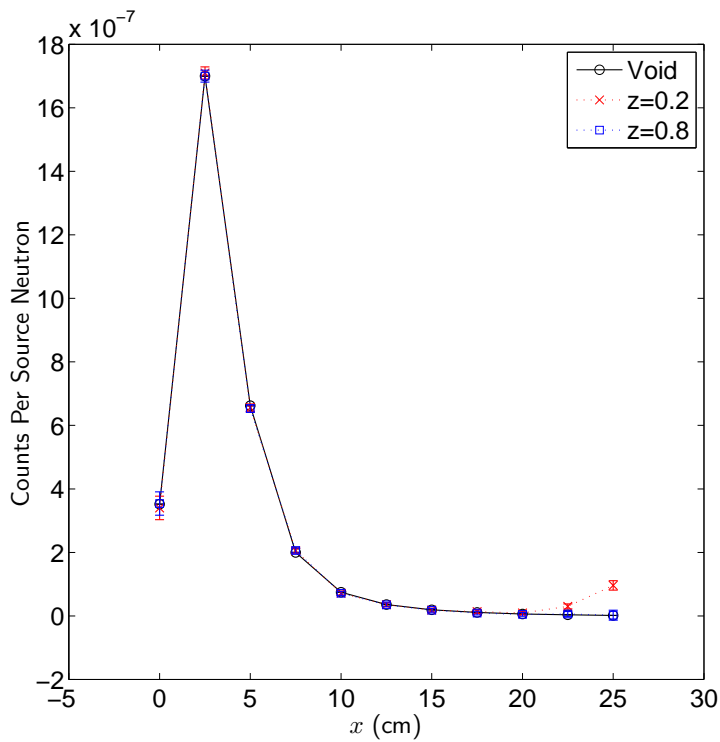


Fig. 4.25: Comparison of net spectra with room scatter included and void for various z , using a 20-cm thick shadow shield.

High Room-Scatter Environment: Confined Room

The procedure above was performed using the worse case scenario room, as depicted in Fig. 4.18. Table 4.14 compares the shadow shield method with no correction and purely

void templates. As demonstrated, although the shadow shield method is not as accurate as in a void, it identifies significantly more sources than for no correction. As discussed in Section 4.8.5, the main problem with identification is the LOS response is substantially smaller than the room-scattered response, particularly in the last few detectors in higher energy sources. Because the uncertainty in the shielding and non-shielding measurement are proportional to the square root of the number of counts, the uncertainty in the LOS response is large, relative to the net value, independent of the magnitude of the source strength. This could be corrected by implementing an algorithm that only includes detectors in the FOM calculation for which a high enough percentage ($\sim 10\%$) of the total response is LOS. The next section demonstrates the utility of the shadow shield in an environment where room-scattered neutrons are less prevalent.

Table 4.14: Source identification data with room scatter from an enclosed room.

S_0 (total neutrs.)	% Sources Correctly Identified		
	Void	Walls - Shield Correction	Walls - No Correction
10^{10}	100.0%	83.2%	15.5%
10^9	97.7%	77.3%	15.5%
10^8	89.2%	46.3%	15.0%

Moderate Room-Scatter Environment: Floor Only

For comparison, the above simulations were repeated with the room modified to only have a floor (all walls and ceiling were replaced with a void). The environment represents an outdoors, open space. All simulations and data sampling were the same as for the confined room. Fig. 4.26 compares the effect of the removal of the walls on detector spectra, with no shadow shield correction, for the ^{252}Cf - D_2O source. As demonstrated, the simulation with no walls has significantly less room scatter, but is still substantially different from the void template, particularly in the front detectors. Table 4.15 compares the results of the 1000 trials as before. An example set of simulated data and FOM values for several of the sources in one trial are given in Appendix D on page 193. With the walls removed, the simulation performance is improved significantly, however it is apparent that the shadow shield correction is still needed to account for room scatter. Because the majority of the signal in the detectors is not coming from the room-scattered neutrons, the room-scatter correction is able to predict the location of the source far more accurately than in the previous results given in Table 4.14.

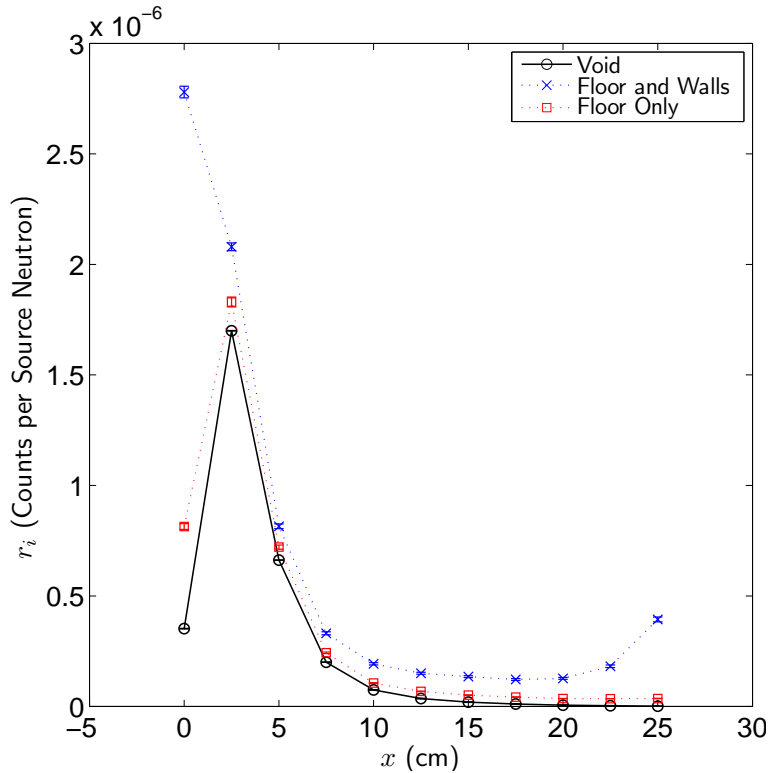


Fig. 4.26: Comparison of the effect of room type on detector spectra.

Table 4.15: Source identification data with room scatter from a concrete floor.

S_0 (total neut.)	% Sources Correctly Identified		
	Void	Floor - Shield Correction	Floor - No Correction
10^{10}	100.0%	96.4%	46.2%
10^9	97.7%	85.1%	46.0%
10^8	89.2%	59.3%	43.1%

4.9 Conclusions, Recommendations, and Future Work

The neutron source identification spectrometer was demonstrated to be effective at identifying sources using the FOM comparison method. The developed optimization methodology was able to improve the geometric design of the system and provide insight into the statistical behavior of the FOM equations. In general, the efficiency of the spectrometer needs to be improved to reduce the required source strength for identification. This can be easily and effectively implemented by adding more detectors at each position in the spectrometer, increasing the cross sectional area of the detection volume. The developed MCNP5 model is

in general accurate, but the fidelity can be improved by explicit modeling of the detectors in MCNP6. For actual detection of spontaneous fission sources, which have very similar energy spectra, templates should be generated from experimental data. For high energy neutron sources, which will register counts at deeper detector positions, the front response should not be included in FOM calculations. In general, the response of the first detector is not well modeled by the MCNP5 artificial detector model. Additionally, most thermal neutrons are actually from moderation through either room scatter or moderator surrounding the source, so the first position would not match well to experiments. However, the front detector is still very useful for identifying the presence of thermal neutron sources. The shadow shield method is an effective method, except for cases with extremely low LOS signal.

A simple simulation study still to be investigated would be adjusting the way that the algorithm accounts for detectors with low numbers of counts. The current algorithm contributes scores to the FOM from detector positions with non-zero counts. If this cutoff is raised from zero to a higher value, e.g., 20 then the FOM calculations would be improved, as the low count rates are mostly just contributing statistical noise to FOM calculations. Also, the effects on detector spectra from shielding and moderator placed around a neutron source should be investigated.

A more important and involved study would be to determine the confidence intervals for source identification. Although the relation of Θ and p_{succ} provided some insight, the actual distribution of the FOM values is unknown. Initial Monte Carlo studies demonstrate that for the template that matches the source, FOM has a $\chi^2(N_{det} - 1)$ distribution, and the error propagation estimate of $\sigma(FOM)$ is very accurate. However, the distribution of the FOM values for the incorrect templates are not χ^2 , and the estimate of $\sigma(FOM)$ is very poor, differing from the sample standard deviation by up to 150%. Additionally, in real application, the templates will not match measured spectra perfectly because of differences between reality and simulations. The differences would result in relatively large values of FOM^{min} , i.e., the FOM for the correct template. Thus, confidence of identification based on a χ^2 distribution is unlikely, even for the correct source¹. Future simulated data should add some form of a random term into the simulated responses to account for detector noise and modeling inaccuracies. Also, the inaccuracies in the estimated standard deviation can be improved by removing the logarithms from the FOM, as the error propagation estimate for logarithms is known to be very poor for large values [Taylor, 1997].

¹The majority of FOM^{min} values would be relatively large and located in the region of the domain that *should* be the low-probability tail of a $\chi^2(N_{det} - 1)$ distribution [Hogg et al., 2013]. Thus, FOM^{min} would not be distributed as $\chi^2(N_{det} - 1)$.

Chapter 5

Simulations of Neutron Multiplicity Measurements with Perturbations to Nuclear Data

5.1 Motivation

This chapter provides a summary of initial studies performed to analyze a known discrepancy between multiplicity distributions generated by MCNP modeling and experimental data. MCNP simulations have been known to demonstrate an overbias in multiplicity distributions from a sphere of WGPu [Miller et al., 2010; Sood et al., 2011], and the cause of the overbias is believed to be inaccuracies in the nuclear data, as demonstrated in Miller et al. [2010]. Perturbations were made to nuclear data for ^{239}Pu ENDF/B-VII.1 data in ACE format to attempt to correct the overbias.

Simulations of multiplicity and criticality experiments were performed to determine the correction of overbias caused by the individual perturbations. The sets of resulting data were compared using chi-squared analysis with the intent of reducing the bias in multiplicity distributions without sacrificing the accuracy of k_{eff} in criticality experiments. Energy-dependent perturbations to the mean of the *total* number of neutrons produced per fission, $\bar{\nu}$, of ^{239}Pu were analyzed. Also, energy-independent perturbations to microscopic neutron capture, elastic scattering, and fission cross sections were performed. Several methods were used to maintain realistic cross section relations from the original data. The main goal of the cross section alterations is to determine how effective the perturbations are, relative to $\bar{\nu}$ alterations; if the cross section alterations are ineffective, then simulations of the multiplicity experiments provide a useful tool for verifying tabulated $\bar{\nu}$ data.

5.2 Background

5.2.1 Neutron Multiplicity Distributions

A neutron multiplicity distribution depicts the probability of a particular number of neutrons created within a multiplying system being measured over some fixed, short amount of time (the coincident gate width). Multiplicity distributions provide information about the generation of neutrons from spontaneous fission, as well as other neutron sources. Neutron multiplicity distributions are created from correlated time-dependent measurements of a sub-critical system.

The procedure for constructing a multiplicity distribution provides intuitive understanding. Here, the multiplicity counting scenario is assumed to be perfect (i.e., there is no detector dead time and there are only spontaneous fission neutron sources). Detector dead time is the amount of time from the start of detecting one neutron before the measurement of another neutron can begin and be registered. A multiplicity counter measures neutrons leaving the system of interest. The counter consists of multiple thermal neutron detectors whose outputs are combined into one time-dependent output. The relation between the number of neutrons leaving the system and the number detected by all detectors can be determined based on a binomial distribution and absolute detection efficiency. The probability of detecting k neutrons given n neutrons have left the system over a time T is given by [Reilly et al., 1991]

$$P(k; n, T) = \frac{n!}{(n-k)!k!} \epsilon^k (1-\epsilon)^{n-k}, \quad k = 0, 1, \dots, n, \quad (5.1)$$

where ϵ is the absolute detection efficiency of the multiplicity counter. The time dependence the k neutron detection events is then used to construct a multiplicity distribution.

A time-dependent series of neutron detection events, referred to as a neutron pulse train, is recorded. A simple pulse train, depicted on the left side of Fig. 5.1, represents the time neutron detection events occurred. The total count time T is divided into coincident gates of a fixed width. Within the time of the first coincident gate, three detection events were recorded, representing a multiplicity of three; the second gate has a multiplicity of two, and so forth. No events were measured during the fifth gate. The *number of occurrences* of each multiplicity is then binned in a histogram, as seen in the right side of Fig. 5.1. This histogram is then *normalized* by dividing each bin by the total number of gates. Thus, each bin of the normalized multiplicity distribution represents the probability of a certain number of neutrons being detected during one gate width, forming a discrete PDF. The first moment of this distribution is the total count rate of the multiplicity counter. Normalized

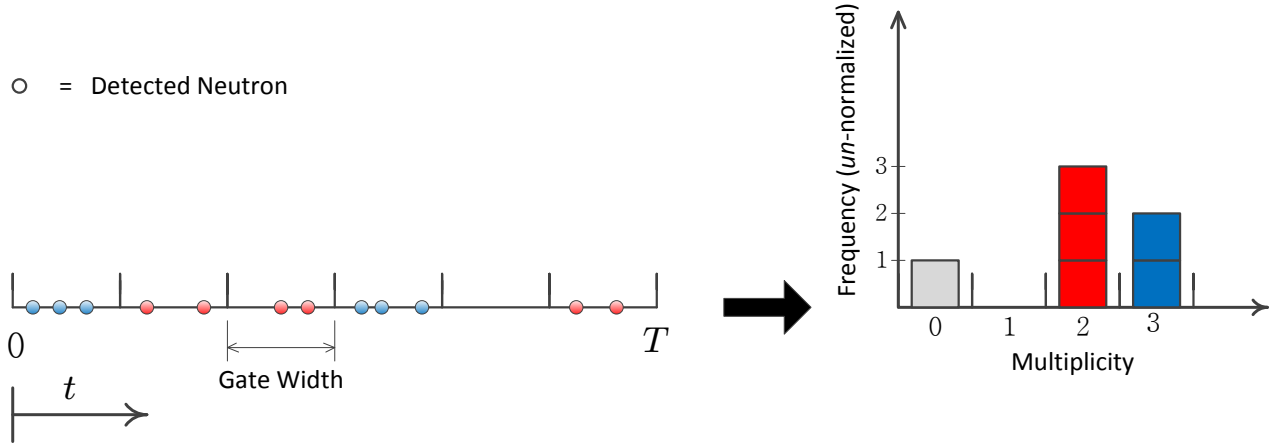


Fig. 5.1: Illustration of construction of a multiplicity distribution from a neutron pulse train. Multiplicity is the number of neutrons detected in one gate width; frequency is the number of gates with a certain multiplicity in counting time T .

multiplicity distributions can be seen in Fig. 5.7 on page 113. To correct for dead time, assuming non-paralyzable detectors, detection events that occur within the same detector less than the dead time apart would not be included in the pulse train. The total count time T is chosen such that the sample standard deviation of the probability for each bin is below some desired value.

5.2.2 Application of Multiplicity Distributions

Neutron multiplicity distributions are primarily applied for non-destructive assay of neutron systems containing fissionable isotopes. Neutrons produced from spontaneous and induced fission sources are created effectively instantaneously. These simultaneous neutrons can be measured by a multiplicity counter, and fission events identified. Because the number of neutrons emitted per fission are generally known values, relations can be developed to determine the amount of fissionable material in the system; the fissionable isotopes present can be discerned as well. Another benefit of the simultaneity of fission neutrons is background neutron sources (e.g. (α, n) reactions and room scattered neutrons) can be discriminated because they are emitted in non-coincidence [Reilly et al., 1991]. Multiplicity counters used for experiments typically consist of an array of 10–15 ^3He detectors. Often, the counter completely surrounds the fissionable material of interest. Coincidence and timing circuits are used to construct a distribution from the output pulse chains of the multiplicity counter, as discussed in Ensslin [1998]. For experimental measurements, the dead time of the individual detectors must be accounted for, as well as the neutron die-away time of the multiplicity

counter. The neutron die-away time is a time constant which describes the exponential decay of a neutron population in a multiplicity counter over time because of the finite thermalization and detection time of the device. Counter die-away and dead time are typically on the order of a few μs , compared to gate widths, which are on the order of 1000 μs .

The theory relating a measured distribution to the multiplication properties of a fissionable system has been applied since Feynman [1946], based on a simplified point model of the system. Typically multiplicity counting analysis does not use the entire multiplicity distribution. Instead, the first three factorial moments of the distribution are used. The n -th factorial moment of X is defined as $E[X(X-1)(X-2)\cdots(X-n+1)]$. In the case of multiplicity distributions, X is the discrete random variable defined as the number of measured events in one gate. The factorial moments of the measured multiplicity distribution are related to the moments of the spontaneous fission and induced fission rates of the system that is being studied [Reilly et al., 1991]. The first moment of a measured multiplicity distribution is the total neutron count rate. The second factorial moment ($E[\nu(\nu-1)]$) determines the “doubles” rate. The doubles rate is the expected number of true coincident events of two neutrons [Reilly et al., 1991], i.e., the rate that fission events releasing two neutrons occur and are measured. The triples rate is similarly defined. Multiplicity distributions can be misleading in that the measured multiplicities (the abscissa of the distribution) do *not* represent true coincidence. The true coincidence of 3 neutrons in a sample is rare [Reilly et al., 1991], even though multiplicities are much higher because there are many fission events happening randomly throughout the sample.

Other distribution parameters of interest in measurements are the divergence of the ratio of the variance to the mean from unity (unity is expected for a Poisson distribution), termed the Feynman-Y statistic. The Feynman-Y can be related to the subcritical multiplication of the system and used to verify the functionality of a multiplicity counter, as discussed in Croft et al. [2012]. The relations of factorial moments and other statistics to the fission rates of the system being measured are complex and beyond the scope and application of this work, but the relations are derived and explained in Ensslin [1998]. In this chapter, multiplicity distributions are used as a measure of subcritical multiplication, rather than to determine spontaneous fission rates, doubles rates, etc.

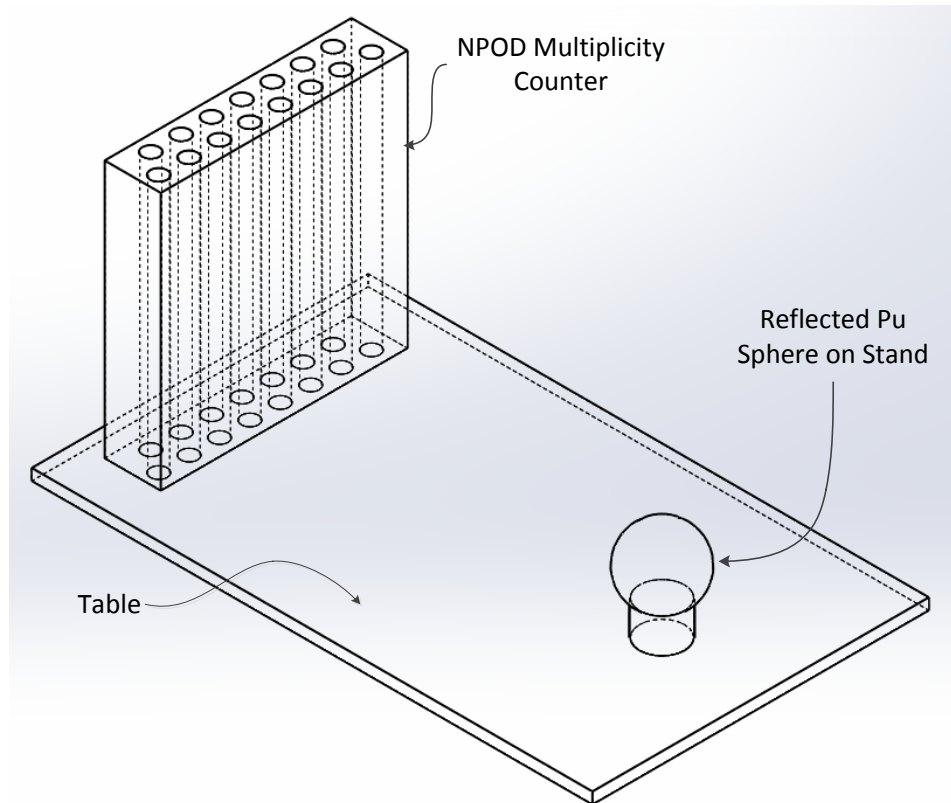


Fig. 5.2: Illustration of multiplicity experiments (not to scale).

5.3 Pu Experiments and Multiplicity Measurements

5.3.1 Overview of Experimental Setup

Previously, experiments were performed using a 4.5 kg sphere of 94% ^{239}Pu plutonium metal to generate multiplicity distributions with a multiplicity counter. Five different experiments were performed: one with the bare sphere and the remaining with various thicknesses of polyethylene reflectors surrounding the sphere. The reflectors were 0.5, 1.0, 1.5, and 3.0 inch spherical shells of polyethylene, which reflect and moderate fast neutrons. Multiplicity counting was performed using the nPod multiplicity counter. The nPod consists of a staggered array of 15 “15-inch-long, 1-inch-diameter, 10 atm, ^3He proportional counters embedded in an HDPE moderator block 16.6 inches tall and 4 inches deep” [Miller et al., 2010]. The individual detectors have a $4 \mu\text{s}$ dead time. The moderator casing is wrapped in Cd to minimize the effect of room scattered neutrons. The sphere of Pu and reflectors were placed on a steel stand on a table a meter above the ground. The experimental data in this work is from experiments performed through Los Alamos National Laboratory (LANL) discussed by Solomon [2011]. The specifics of the experiments are unpublished. However, a detailed

explanation of experiments very similar to the experiments used in this work can be found in [Mattingly, 2009]; the article discusses corrections to account for dead time and other factors, as well as the use of multiplicity factorial moments to validate the experiments. The primary difference between the experiments studied in this work (and by Solomon [2011]) and [Mattingly, 2009] is the reflector thicknesses. Another difference is the design of the stands that the Pu spheres are placed on. The experimental multiplicity distributions and their estimated statistical uncertainties are of high accuracy and validity in both cases, and separate modeling of the systems demonstrate similar results. A diagram from an MCNP model of the experiments in this work is given in Fig. 5.2. A SNAP-3 total neutron counter is modeled as well (not pictured). This detector was used to verify that the simulated source is accurate. Details on the SNAP-3 detector can be found in [Mattingly, 2009].

5.3.2 Previous Modeling Work

The LANL multiplicity experiments described above were previously modeled in a modified version of MCNP5 with a multiplication patch, **MCNP5_mult** [Sood et al., 2011; Solomon, 2011]. The patch allows sampling of spontaneous fission source events and produces list-mode tallies that provide time-dependent tally data. The detector geometry was modeled explicitly and the list-mode tallies can provide the number of absorptions that have occurred, as well as when each absorption occurred. The time-dependent tally data from the simulated multiplicity-counter detector array are used to reconstruct multiplicity distributions with the **mtool.pl** script. The **mtool.pl** script (used for work in Solomon [2011]) is a Perl script which takes the time-dependent tallies from the MCNP list-mode tallies and constructs a multiplicity distribution using a *non-paralyzable* dead-time correction. The non-paralyzable dead-time correction is such that if multiple events occur within the dead time interval, only one event is counted. This is alternative to a *paralyzable* dead-time correction where a second event occurring resets the dead time window, allowing the detector to become completely paralyzed. Previous studies using this MCNP5 model found that MCNP simulations predict the mean and variance of the multiplicity distributions to be significantly larger values than the multiplicity experiments [Miller et al., 2010; Solomon, 2011]. However, simulations were able to accurately predict multiplicity distributions for a ^{252}Cf source. The overbias was found to worsen as the amount of multiplication in the system was increased by surrounding the sphere with more polyethylene. A comparison of the experimental and **MCNP5_mult** generated multiplicity distributions¹ can be seen in Fig. 5.7 on page 113.

¹The measured and simulated multiplicity distributions throughout this work are normalized. The vertical axes are labeled as “Frequency”, referring to the probability of occurrence per multiplicity bin, i.e., the relative frequency, rather than the number of occurrences. Multiplicity bins are labeled as “Multiplets”.

Work has been done to determine the cause and magnitude of the overbias in MCNP using **MCNP_PoliMi** by [Miller et al., 2010], as well as from internal LANL analysis [Solomon, 2011; Sood et al., 2011]. Sensitivity studies on physical parameters were explored: diameter of device, dead time, ^{239}Pu mass density, etc. Previous results demonstrated that the bias can be reduced by modifying the value of $\bar{\nu}$ directly in the induced fission sampling routines by Miller et al. [2010]; this effectively changes the energy-averaged value of $\bar{\nu}$ by reducing all of the tabular $\bar{\nu}$ data by the same fraction. As a consequence, the computed values of k_{eff} for simulations using the shifted $\bar{\nu}$ data are very inaccurate. Because the MCNP bias over experimental data increases with the amount of surrounding moderator, an energy-dependent alteration of $\bar{\nu}$ should reduce the bias more effectively. Additionally, it is known that the $\bar{\nu}$ data tend to be artificially high below 1.5 MeV [Chadwick et al., 2006]. In order to match the JEZEBEL fast critical experiment [ICSBEP Handbook, 2004], $\bar{\nu}$ values were increased in the ENDF/B-VII.1 nuclear data. Below 1.5 MeV, $\bar{\nu}$ tends to lie around two standard deviations above the experimental data, as determined by covariance analysis by Chadwick et al. [2006].

5.4 Methodology

5.4.1 Modifying Nuclear Data Files

In this work, the nuclear data read by **MCNP5_mult** was modified. The United States Cross Section Evaluation Working Group is a collective group across many universities and national laboratories which maintains nuclear data. In particular, they manage the Evaluated Nuclear Data Files (ENDF) library. The current release of the ENDF library is ENDF/B-VII.1 [Chadwick et al., 2006], where VII.1 is the version and B indicates the release recommended for use (other versions contain non-verified data). The ENDF libraries contain all cross sections and other tabulated nuclear data needed to perform most Monte Carlo radiation transport simulations. The VII.1 release also contains experimentally-determined covariance matrices, in many arbitrary formats, for neutron cross section and $\bar{\nu}$ data.

The code MCNP5 reads data from “A Compact ENDF” (ACE) format files. The ACE format files contain large arrays of numbers, typically organized by energy data points and the value of the nuclear data of interest at that energy. Different portions of the nuclear data are indexed by chains of pointers and numerical flags, whose meanings are given in Vol. III of the MCNP manual [X-5 Monte Carlo Team, 2003]. Covariance data are only present in the ENDF format. The covariance data of interest in this work are, in general, organized as relative covariance terms, averaged over an energy group, divided into sub-matrices by

energy. However, the specific formats vary greatly.

The Nuclear Data Verification & Validation (NDVV) Python modules available at LANL were used and expanded for reading and modifying nuclear data, with the intent of being versatile enough to be applicable to other covariance data analyses. As the NDVV tools are large codes, only newly created modules that are specifically relevant to the results in this work are given. The modules added to NDVV for handling ENDF covariance matrices in this work are the `mf33.py` and `cov_matrices.py` modules. The ENDF format manual can be used to understand the behaviour of these files. All ACE data are handled using the `ace_sb.py` module written for this work. These Python modules can be found in Appendix E, with description on page 197.

5.4.2 Correlated Random Sampling of $\bar{\nu}$ in ACE Files

Unique sets of correlated random $\bar{\nu}$ data were used instead of employing a linear optimization or some subjective method. The methods discussed in Section 2.1.7 were used to sample correlated random values from covariance data. Both the Cholesky and eigenvalue decomposition methods, with optional correction for non-positive-semidefinite matrices were implemented. The decompositions were implemented using prebuilt Python linear algebra models with PyLab, a modified version of Python; open-source documentation is available at www.scipy.org/PyLab.

A small perturbation to $\bar{\nu}$ data can have a large effect on results because the many fission-based neutron multiplications that potentially take place throughout a single history. These multiplications result in a non-linear change in results with respect to $\bar{\nu}$ perturbations. A linear optimization problem would likely get stuck in a local minima. Additionally, because the problem was under-constrained (50 variables with only 6 sets of results), it is likely a standard step-descent method (e.g. as gradient descent [Press et al., 1992]) would find a minima that is not physically realistic. Using a covariance matrix to sample data adds statistical confinement to potential values of the data, but requires some form of random sampling of the space.

The covariance data used to correlate the randomly sampled numbers was read from the ^{239}Pu ENDF/B-VII.1 data library¹. The library that was used to compile the ACE libraries used in this work was ENDF/BVII.0. However, ENDF/B-VII.1 possesses the same values for $\bar{\nu}$ and all neutron cross sections as ENDF/B-VII.0 for ^{239}Pu . The $\bar{\nu}$ data for ^{239}Pu contain one row (and symmetric column) in the covariance matrix with all zeros. To handle this, the

¹For some nuclear data, the ENDF/B-VII.1 covariance data contain co-relation terms between different data types and isotopes, for different energy groups. Only co-relation terms between energy groups, for a particular type of nuclear data of ^{239}Pu , are considered in this work.

submatrix of the correlation matrix with the row and column of zeros absent was used for the decomposition and sampling process. Because there is no information on the variance for that row, that sampled value is taken as the original value. For $\bar{\nu}$ of ^{239}Pu , below thermal energies there is no covariance data.

The covariance matrix for $\bar{\nu}$ data of ^{239}Pu is positive definite and the Cholesky decomposition was used. The covariance data are given as averages over certain energy groups. The $\bar{\nu}$ data are evaluated at certain energies for which linear interpolation is applied in between to evaluate $\bar{\nu}$ during simulations [ENDF-6 Manual, 2011]. There are also more energies for which $\bar{\nu}$ is evaluated than corresponding covariance energy groups. To map the sampled covariance data to the $\bar{\nu}$ data points, $\bar{\nu}$ data was sampled as

$$\bar{\nu}'(E) = \sigma_{rel}(E_g)\nu(E)\tilde{\mathbf{R}}(E_g) + \bar{\nu}(E). \quad (5.2)$$

Here, $\bar{\nu}(E)$ is the original value of $\bar{\nu}$ at energy E , $\bar{\nu}'(E)$ is the perturbed $\bar{\nu}$ data, E_g is the covariance energy group that E lies in, $\sigma_{rel}(E_g)$ is the relative standard deviation in group E_g , and $\tilde{\mathbf{R}}(E_g)$ is the correlated standard normal random sample in group E_g as described in Eq. (2.21) on page 12. The standard-normal-distributed random numbers were generated using pre-built Python routines, which utilize the Mersenne Twister algorithm and allows for specification of the random number generator state through a numerical seed. Details on the sampling algorithms can be found in the open-source documentation at www.python.org/doc

Observation on Sampling Correlation Matrix

The sampling method described above was tested to determine if the method was sampling covariance matrices as intended. To verify the method, a unique vector of correlated values was generated 10,000 times for the covariance matrix data for $\bar{\nu}$ of ^{239}Pu . The samples were then used to generate a covariance matrix. It was found that the covariances were roughly two orders of magnitude higher in the generated correlation matrix than in the original correlation matrix for ^{239}Pu , or non-zero where zero was expected.

For another test the sampling routines were tested for an arbitrary matrix with cross-correlation values much higher ($O(10^{-1})$, rather than the $O(10^{-5})$ of ^{239}Pu). The correlation matrix was recreated accurately. These results demonstrate that the inability to recreate the correlation matrix has to do with the relatively small values in the covariance data and that, within statistics, the method is sampling accurately. As a comparison, a correlation matrix was generated from 10,000 vectors, each with 50 uncorrelated, normally-distributed random numbers. The numbers in these vectors should display no correlation. However, the

covariance values in the correlation matrix showed correlations on the same order as those of the regenerated correlation matrix for ^{239}Pu . The cross-correlations between energy groups are very small relative to the variances (the majority are $O(10^{-6})$). The effect of covariance between energy groups, thus, has very minimal constraint on the data for ^{239}Pu . However, the samples are still confined statistically by the variance terms.

5.4.3 Energy-Averaged Perturbations of Capture Cross Section

Here, σ_c is referring to the microscopic *capture* cross section related to the probability of a neutron absorption event that results in *no reemission* of one or more neutrons, sometimes referred to as the *removal* cross section¹. It is noted that in the case of ACE format ^{239}Pu data, the capture cross section only includes the (n, γ) radiative capture reaction. Alterations to σ_c of ^{239}Pu were made by increasing the energy-averaged value of σ_c , given analytically as $\bar{\sigma}_c = \int_0^{E_{max}} \sigma_c(E) dE / E_{max}$, where E_{max} is the maximum energy that σ_c is tabulated for. Multiple increases were investigated to determine their effect on the simulated multiplicity distributions. Alterations to the ACE data were performed by adjusting the tabular cross sections from the ESZ block, described in Vol. III of [X-5 Monte Carlo Team, 2003]. The ESZ block in an ACE file contains data for σ_c , σ_t , and σ_s , as functions of energy, separate from the typical MT reaction data in ENDF format [ENDF-6 Manual, 2011]. Although the only constituent of σ_c for ^{239}Pu is the (n, γ) cross section, the ACE data for (n, γ) cross section are not altered because only data in the ESZ block is used for determining the probability of capture reactions during transport of neutrons ((n, γ) and other MT reactions that do not emit neutrons are tabulated in ACE files for use with tallies). Each capture cross section data point (representing the microscopic cross section evaluated at some energy) was increased by a fixed percentage. This increases $\bar{\sigma}_c$ by the same percentage; all reference to increasing or decreasing nuclear data in this work is performed in this manner unless otherwise indicated. Because MCNP demonstrates an overbias in multiplicity distributions, an increase in the probability of capture in the system should decrease the probability of neutrons leaving the system and reaching the detectors, decreasing the discrepancy between MCNP and experiments.

Since σ_t is defined as the sum of all other individual cross sections, an adjustment of some form must be made to compensate for changes in σ_c . Different methods were explored for compensating for this change in either σ_t or σ_s . Also, the relation between σ_c and σ_s was adjusted in various ways to determine the effect on the system. One other case was

¹The nomenclature for a neutron absorption without reemission varies in nuclear data libraries. Absorption without reemission is described by the total absorption and disappearance cross sections in ACE and ENDF format data, respectively. Typically, the absorption cross section refers to $\sigma_a = \sigma_f + \sigma_c$.

considered in which σ_f was adjusted to compensate for the changes. It is useful to categorize the different methods by the change in σ_c and σ_t in each case. To describe the various cross section adjustments investigated, define the amount $\epsilon_i(E)$ that the i -th cross section $\sigma_i(E)$ was adjusted to become the perturbed value $\sigma'_i(E)$, at each energy, i.e.,

$$\sigma'_i(E) = \sigma_i(E) + \epsilon_i(E). \quad (5.3)$$

Then in all cases the changes in σ_c and σ_t are given by

$$\epsilon_c(E) = \alpha \sigma_c(E), \quad (5.4)$$

$$\epsilon_t(E) = \epsilon_c(E) + \epsilon_s(E), \quad (5.5)$$

where α is the signed fractional change in $\sigma_c(E)$, i.e., $\alpha = [\sigma'_c(E) - \sigma_c(E)]/\sigma_c(E)$. Dropping the energy notation, the value of ϵ_s for the various methods, at each energy for which cross sections are evaluated, is described and labeled as follows:

case 1. Only σ_t was adjusted to account for the increase in σ_c , therefore $\epsilon_s = 0$.

case 2. The scattering ratio $c = \sigma_s/\sigma_t$ remained constant, so that $\epsilon_s = \epsilon_c [c/(1 - c)]$.

case 3. The ratio of the scattering to capture cross sections remained constant, i.e., $\sigma'_s/\sigma'_c = \sigma_s/\sigma_c$, so that $\epsilon_s = \epsilon_c \sigma_s/\sigma_c$.

case 4. The sum of σ_c and σ_s remained constant ($\epsilon_t = 0$) for energies greater than 1 keV, i.e., $\epsilon_s = -\epsilon_c$, for $E > 1$ keV.

case 5. The sum of σ_c and σ_f remained constant ($\epsilon_t = 0$ and $\epsilon_s = 0$), i.e., $\epsilon_f = -\epsilon_c$.

Case 4 alters cross sections only for energies greater than 1 keV because at low energies capture is much more dominant than scattering. For any α greater than 0.25%, subtracting $\epsilon_c(E)$ from σ_s would yield an unrealistic negative value for $\sigma'_s(E)$. Additionally, the systems being studied are relatively fast with the majority of neutrons and fission interactions at energies above 1 keV, so changes made below 1 keV are expected to have minimal effect on results anyways. No alterations other than those described in the cases above were made to the ACE file. A unique ACE file was made for each set of altered cross sections. The XSn card was used in the MCNP input files to input the modified sets of data into simulations.

5.4.4 Energy-Averaged Perturbations of Fission Cross Section

The fission cross section modifications were made in the same manner as the capture cross section, with the exception of the location of the fission data within the ACE files. In ACE

format, the FIS block contains the energy-dependent total fission cross section data and was thus modified. All changes to other cross sections occur in the ESZ block, as described in Section 5.4.3. The methods in the previous section were performed with the exchange of σ_f and ϵ_f in place of σ_c and ϵ_c , respectively. Only case 1 and case 4 were explored for the fission cross section because of initial results, as discussed later in Section 5.7.1.

5.4.5 Quantifying Shifts in Cross Sections

In all cross section manipulations, a measure of how statistically realistic the alterations were was computed as how much a cross section had been shifted, relative to the variance of that cross section. The average number of standard deviations that the i -th cross section was shifted in the positive or negative direction, $\#s(\sigma_i)$, is thus calculated as

$$\#s(\sigma_i) = \frac{1}{N_{erg}} \sum_{j=1}^{N_{erg}} \frac{\epsilon_i(E_j)}{s(\sigma_i(E_j))}. \quad (5.6)$$

Here E_j is the j -th of N_{erg} energy at which $\sigma_i(E)$ was modified, and $s(\sigma_i(E_j))$ is the standard deviation for $\sigma_i(E_j)$. The values $s(\sigma_i(E_j))$ are taken from the energy group averaged covariance matrices from File 33 of ENDF/B-VII.1 library. Here the values for $s(\sigma_i(E_j))$ only consider variance within energy group, for the same material, for the i -th reaction. The sample standard deviation, $s(\#s(\sigma_i))$, of $\#s(\sigma_i)$ was also computed to demonstrate that the values of $\#s(\sigma_i)$ are not caused by to a very small variance in a particular energy regime.

5.5 Data Generation, Simulations, and Comparison to Experimental Data

Unique sets of nuclear data were generated and analyzed for many trials. Here, for clarity and brevity, a trial refers to a unique set of nuclear data. For each trial, the original nuclear data was read from the MCNP ACE format nuclear data files. The data was then perturbed via a method described earlier, depending on the nuclear data of interest, and written to a unique ACE format file.

For trials where $\bar{\nu}$ was sampled, correlated random samples of $\bar{\nu}$ were generated based on the procedure discussed in Section 5.4.2. The random number generator seeds used to generate the data were saved to regenerate ACE files at a later time and ensure each trial was unique. For cross sections, data points were shifted uniformly for multiple trials, based on the value of α (see Eq. (5.4)). Data was generated with the five different cases for the

capture cross section. The process was repeated with cases 1 and 4 for the fission cross section.

For each trial, the five different multiplicity simulations of the plutonium sphere surrounded by various thickness of reflectors, as described in Section 5.3.1, were performed. The simulations used the same MCNP input files as in Solomon [2011]. In the MCNP input files, the FISNU setting on the PHYS:N card was set to 1. This particular setting uses an evaluated Gaussian width to provide more accurate sampling of the number of neutrons per fission, which is better for sub-critical systems [X-5 Monte Carlo Team, 2003]. In addition to the multiplicity simulations, the JEZEBEL fast-critical bare Pu sphere experiment was simulated for each trial. The JEZEBEL benchmark consists of a critical, bare Pu sphere (primarily ^{239}Pu). This simulation measures how well MCNP5 would model a critical system using the perturbed sets of data, a critical feature in the simulation tools. The only modifications to the input files was an XS card used to specify the location of modified ACE file for each trial. All modified ACE file data libraries are labeled with the nomenclature 94239.99c to prevent the use of incorrect data. The simulations were performed using **MCNP5_mult**. Sample input files are available in Appendix F.

Multiplicity distributions were generated for each of the five multiplicity simulations in each trial using **mtool.pl**. The distributions were created with a coincident gate width of 2000 μs . To compare the simulation results to the experimental multiplicity distributions, a chi-squared goodness of fit statistic was computed. A reduced chi-squared value was computed for each of the five multiplicity experiments between the reference experimental data and the simulation as described in Eq. (2.29). Specifically, for the m -th multiplicity experiment

$$\chi_{mult,m}^2 = \frac{1}{N_B - 1} \sum_{i=1}^{N_B} \frac{(S_i - E_i)^2}{\sigma^2(S_i) + \sigma^2(E_i)}. \quad (5.7)$$

Here, S_i and E_i are the probabilities (i.e., the normalized frequencies) from the i -th bin of the multiplicity histograms of the j -th scenario for the simulation trial and experimental data, respectively; N_B is the number of bins that had a non-zero frequency in either the reference or simulated multiplicity distribution (different for each trial and experiment). For each bin, if either the reference or simulated value had a non-zero score it contributed to the total score, even if the other had a zero score. A chi-square statistic was also calculated for k_{eff} between the JEZEBEL criticality experiment and simulation labeled as $\chi_{k_{eff}}^2$.

Reduced chi-squared values were used to increase the importance of the constraint that a trial produce a critical system. An individual reduced chi-square test was calculated for each of the multiplicity scenarios and the criticality simulation. The degrees of freedom η in Eq. (2.31) for each multiplicity distribution is $N_B - 1$, where N_B is the number of bins that

had a non-zero score in either the reference or simulated multiplicity distribution. For the criticality simulation, η is unity.

The χ_{red}^2 values for all six simulations were then summed to form a FOM for each trial, i.e.,

$$FOM = \sum_{m=1}^5 \chi_{red,mult,m}^2 + \chi_{red,k_{eff}}^2. \quad (5.8)$$

Here, the subscripts $mult, m$ and k_{eff} indicate the χ_{red}^2 value for the m -th multiplicity experiment and the JEZEBEL experiment, respectively. The trial with the lowest FOM value represents the best match to the experimental multiplicity distributions and criticality benchmark. In the above equation, FOM is composed such that each simulation carries equal weight.

The summation of the multiplicity reduced χ^2 values $\chi_{red,mult,m}^2$ are also used to compare trials, i.e.,

$$\chi_{mult}^2 = \sum_{i=1}^5 \chi_{red,mult,m}^2. \quad (5.9)$$

The lower the value of χ_{mult}^2 , the better that particular set of nuclear data corrects the discrepancy in multiplicity distributions between simulation and experiment. The code that makes these comparisons is `mult_chi_sq.py`, a stand alone script, given on page 238.

5.6 Results for $\bar{\nu}$ Perturbations

The methodology described above was applied for 500 trials. The computed FOM value described in Eq. (5.8) and the χ^2 values for k_{eff} and χ_{mult}^2 are given in Table 5.1 below; entries are only included for the ten trials which produced the lowest FOM values. The numbering of the trials is arbitrary other than to refer to their random number generator seeds. Entries are also included in Table 5.1 for the original ENDF/B-VII.1 data, labeled as “Original”, and the best-case energy averaged $\bar{\nu}$ from Miller et al. [2010], labeled as “ $\bar{\nu}$ -1.14%”, throughout. The energy-averaged case shifts all values of $\bar{\nu}$ down by 1.14%. This is not necessarily the best-case shift for this set of experimental data; it is given for comparison of FOM and χ^2 results to demonstrate that energy-dependent perturbations to $\bar{\nu}$ has the potential to match multiplicity distributions while maintaining accuracy in k_{eff} .

As expected, Table 5.1 demonstrates that the original data matches k_{eff} within statistical error but has significant inaccuracy for the multiplicity distributions. Since $\bar{\nu}$ was shifted down at all points for the energy-averaged case, criticality is not preserved, and the $\chi_{k_{eff}}^2$ value was significantly higher than the best energy-dependent cases. The energy-dependent

perturbations were not able to match the multiplicity distributions as accurately as the energy-averaged case, but preserved k_{eff} more accurately.

Table 5.1: *FOM* and χ^2 values for ten trials with lowest *FOM* values, and original and shifted ENDF/B-VII.1 data.

Trial	<i>FOM</i>	χ^2_{mult}	$\chi^2_{k_{eff}}$
$\bar{\nu}$ -1.14%	164.24	130.58	33.66
303	197.07	192.89	4.18
243	264.3	261.33	2.97
55	267.9	267.9	0.01
471	271.34	268.34	3.00
396	273.42	272.1	1.32
335	273.62	273.55	0.07
99	276.88	276.4	0.49
473	284.21	282.54	1.67
127	285.87	284.82	1.05
90	333.93	333.91	0.66
Original	426.86	426.6	0.27

For the trial with the lowest FOM (trial 303), the MCNP expanded criticality validation suite was performed [X-5 Monte Carlo Team, 2003; ICSBEP Handbook, 2004]. Only the cases in the validation suite containing plutonium were analyzed. For each file in the suite, the original and trial 303 ACE data respective results are compared to reference experimental solutions. The notation is such that “*” indicates the mean was within one to two standard deviations of the experimental data, “**” is within two to three, “***” is within three or more, and no asterisk is within one standard deviation. Table 5.2 on page 108 compares the results of validation suite for trial 303 and original ENDF/B-VII.1 data as compared to the reference benchmark. The RMSD for the suite was calculated as:

$$RMSD = \sqrt{\frac{\sum_{i=1}^{N_{cases}} (k_{eff,i} - k_{eff,i}^{ref})^2}{N_{cases}}} \times 100\%. \quad (5.10)$$

Here, $k_{eff,i}^{ref}$ indicates the reference k_{eff} value for the i -th of N_{cases} benchmarks. The RMSD for trial 303 was found to be 0.51% as compared to the RMSD produced with the ENDF/B-VII.1 data of 0.49%. The energy-averaged shift of $\bar{\nu}$ down by 1.14% produced a RMSD of 1.23%.

A comparison of the multiplicity distributions generated from simulations with the orig-

Table 5.2: Comparison of k_{eff} for different data with the MCNP criticality validation benchmark suite.

Benchmark	Reference		ENDF/B-VII.1 $\bar{\nu}$ Data			Trial 303 $\bar{\nu}$ Data			
	k_{eff}	σ	k_{eff}	σ	# σ away	k_{eff}	σ	# σ away	
pu-met-fast-001	1.0000	0.0020	1.0000	0.0003		0.9967	0.0003	*	
pu-met-fast-002	1.0000	0.0020	1.0001	0.0003		0.9968	0.0003	*	
pu-met-fast-022-case-2	1.0000	0.0021	0.9983	0.0003		0.9950	0.0003	**	
mix-met-fast-001	1.0000	0.0016	0.9993	0.0003		0.9993	0.0003		
mix-met-fast-003	0.9993	0.0016	1.0008	0.0003		1.0008	0.0003		
pu-met-fast-006	1.0000	0.0030	0.9995	0.0003		0.9967	0.0003		
pu-met-fast-010	1.0000	0.0018	1.0001	0.0003		0.9963	0.0003	*	
pu-met-fast-020	0.9993	0.0017	0.9981	0.0003		0.9950	0.0003	**	
pu-met-fast-008-case-2	1.0000	0.0006	0.9977	0.0003	**	0.9942	0.0003	***	
pu-met-fast-005	1.0000	0.0013	1.0092	0.0003	***	1.0058	0.0003	***	
pu-met-fast-025-case-2	1.0000	0.0020	0.9988	0.0003		0.9954	0.0003	**	
pu-met-fast-026-case-2	1.0000	0.0024	0.9985	0.0003		0.9953	0.0003	*	
pu-met-fast-009	1.0000	0.0027	1.0053	0.0003	*	1.0022	0.0003		
pu-met-fast-023-case-2	1.0000	0.0020	0.9993	0.0003		0.9972	0.0003	*	
pu-met-fast-018	1.0000	0.0030	0.9964	0.0003	*	0.9932	0.0003	**	
pu-met-fast-019	0.9992	0.0015	0.9975	0.0003		0.9945	0.0003	**	
pu-met-fast-024-case-2	1.0000	0.0020	1.0019	0.0003		0.9983	0.0003		
pu-met-fast-011	1.0000	0.0010	1.0006	0.0003		0.9970	0.0003	**	
pu-met-fast-021-case-2	1.0000	0.0026	0.9931	0.0003	**	0.9897	0.0003	***	
pu-met-fast-021-case-1	1.0000	0.0026	1.0021	0.0003		1.0001	0.0003		
pu-met-fast-003-case-103	1.0000	0.0030	0.9981	0.0003		0.9958	0.0003	*	
pu-comp-inter-001	1.0000	0.0110	1.0121	0.0003	*	1.0099	0.0002		
mix-comp-therm-002-case-pnl30	1.0024	0.0060	1.0011	0.0003		0.9983	0.0003		
mix-comp-therm-002-case-pnl31	1.0009	0.0047	1.0025	0.0003		1.0004	0.0003		
mix-comp-therm-002-case-pnl32	1.0042	0.0031	1.0031	0.0003		1.0001	0.0003	*	
mix-comp-therm-002-case-pnl33	1.0024	0.0021	1.0079	0.0003	**	1.0046	0.0003		
mix-comp-therm-002-case-pnl34	1.0038	0.0025	1.0042	0.0003		1.0017	0.0003		
mix-comp-therm-002-case-pnl35	1.0029	0.0027	1.0066	0.0003	*	1.0036	0.0003		
pu-sol-therm-009-case-3a	1.0000	0.0033	1.0190	0.0002	***	1.0159	0.0002	***	
pu-sol-therm-011-case-16-5	1.0000	0.0052	1.0060	0.0004	*	1.0025	0.0004		
pu-sol-therm-011-case-18-1	1.0000	0.0052	0.9943	0.0004	*	0.9916	0.0003	*	
pu-sol-therm-011-case-18-6	1.0000	0.0052	0.9996	0.0004		0.9960	0.0004		
pu-sol-therm-021-case-1	1.0000	0.0032	1.0043	0.0004	*	1.0020	0.0004		
pu-sol-therm-021-case-3	1.0000	0.0065	1.0044	0.0005		1.0013	0.0004		
pu-sol-therm-018-case-9	1.0000	0.0034	1.0031	0.0003		1.0014	0.0003		
pu-sol-therm-034-case-1	1.0000	0.0062	0.9999	0.0004		0.9968	0.0004		
		RMSD		0.49%			0.51%		

inal ENDF/B-VII.1 $\bar{\nu}$ and from experimental data is given in Fig. 5.7 on page 113. The plot of multiplicity distributions for trial 303 as compared to experimental data is given in Fig. 5.8 on page 114. All multiplicity distributions are for a coincident gate width of 2000 μs . The generated set of $\bar{\nu}$ data in trial 303 corrects the overbias demonstrated using the original data, but is still inaccurate as compared to the experimental data.

For each multiplicity distribution, the first and second moments (*not* factorial moments) were computed using **mtool.pl**. Table 5.3 on page 109 compares the first and second moments of the multiplicity distributions for trial 303 and the original data, as compared to experimental data. The column “# σ away” indicates how many standard deviations away that moment is from the experimental moment. The σ is chosen as the biggest standard deviation of the experiment and simulated data for that row (in all cases the simulated data). As is shown, the best-case solution does not match the experimental data solution within statistics, but it is a significant improvement over the original data. The average deviation between the ENDF/B-VII.1 and trial 303 results over all multiplicity experiments was computed. Trial 303 reduced the average deviation in the mean of multiplicity distributions between simulation and experiment to 4.32% from 6.73% for the ENDF/B-VII.1 $\bar{\nu}$ data; the average deviation in the second moment was reduced from 13.87% to 8.74%.

Table 5.3: Comparison of first and second multiplicity moments for different thicknesses of polyethylene reflector.

Reflector	Moment	ENDF/B-VII.1 $\bar{\nu}$			Trial 303 $\bar{\nu}$			Experimental	
		Value	σ_{rel}	# σ away	Value	σ_{rel}	# σ away	Value	σ_{rel}
None	1	1.76E+001	2.68E-003	14.11	1.74E+001	2.68E-003	10.13	1.69E+001	1.38E-003
	2	3.31E+002	2.94E-003	24.43	3.24E+002	2.95E-003	17.59	3.08E+002	1.52E-003
0.5	1	2.40E+001	2.67E-003	16.72	2.37E+001	2.67E-003	11.75	2.29E+001	1.51E-003
	2	6.13E+002	2.90E-003	29.51	5.97E+002	2.90E-003	20.84	5.61E+002	1.65E-003
1.0	1	3.17E+001	2.66E-003	23.52	3.11E+001	2.66E-003	16.67	2.97E+001	1.77E-003
	2	1.07E+003	2.89E-003	41.52	1.03E+003	2.89E-003	29.59	9.38E+002	1.93E-003
1.5	1	3.80E+001	2.67E-003	28.61	3.70E+001	2.67E-003	19.27	3.51E+001	1.84E-003
	2	1.54E+003	2.92E-003	50.25	1.46E+003	2.91E-003	34.14	1.32E+003	2.01E-003
3.0	1	3.19E+001	2.70E-003	34.04	3.06E+001	2.70E-003	19.44	2.90E+001	1.75E-003
	2	1.11E+003	3.04E-003	58.05	1.02E+003	3.03E-003	33.72	9.17E+002	1.96E-003

Figure 5.3 on page 110 coplots the $\bar{\nu}$ data of trial 303 and the original ENDF/B-VII.1 data. As this plot is very difficult to read at low energies, Fig. 5.4 on page 111 depicts the modified and original $\bar{\nu}$ between 85 and 150 eV. Although $\bar{\nu}$ was shifted up or down randomly over each energy group, the smoothness of the data points has not been significantly reduced. Figure 5.5 on page 112 gives a plot of the correlated random numbers used for trial 303. The vertical axis represents the number of standard deviations that $\bar{\nu}$ was shifted with respect

to each energy in the horizontal axis. This plot qualitatively demonstrates that the values are being sampled from a Gaussian and that the correlation between groups is not visually significant. Figure 5.6 on page 112 plots the percent deviation of $\bar{\nu}$ from the ENDF/B-VII.1 data for trial 303; the average magnitude of deviation from the original data (averaged over all energy points where $\bar{\nu}$ was evaluated) was 0.38%. The maximum deviation was 1.61%.

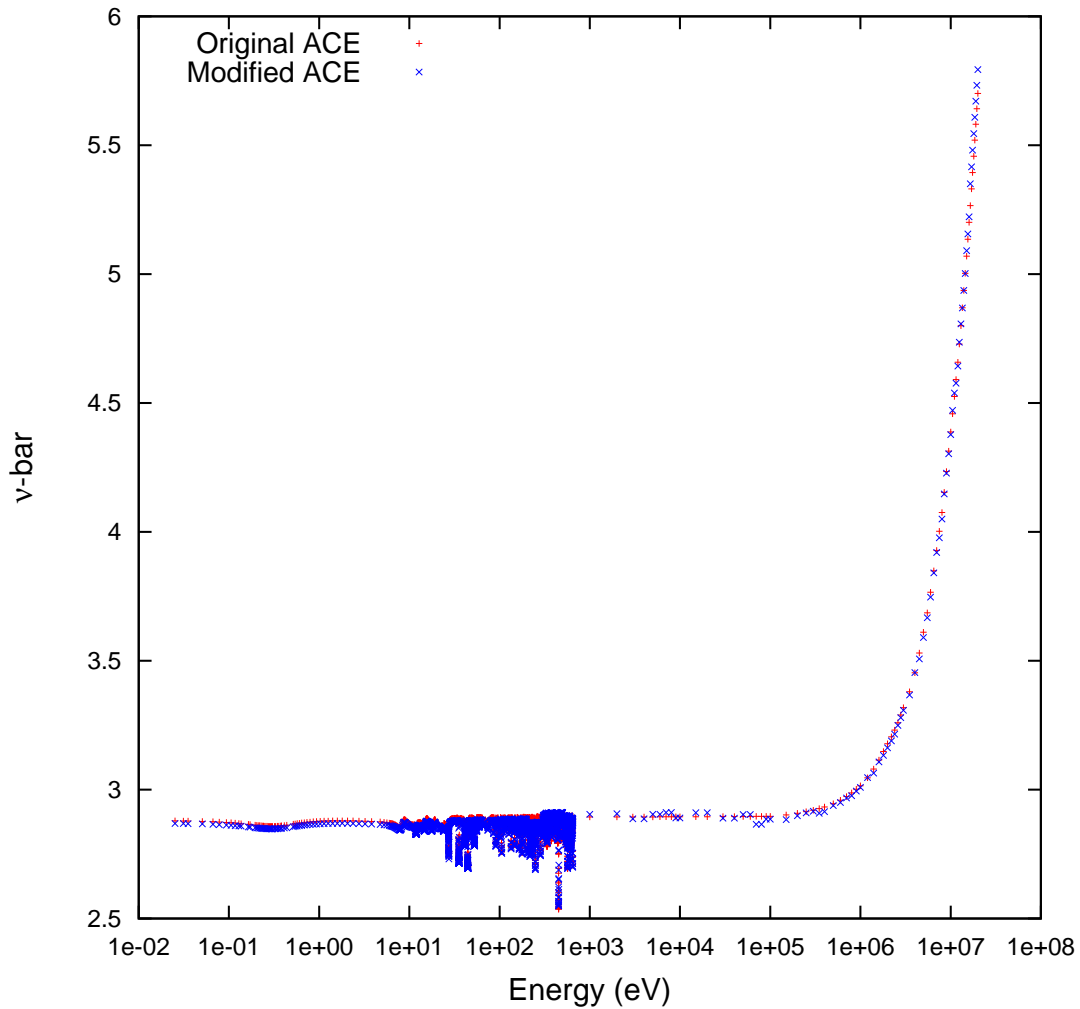


Fig. 5.3: Semi-log plot of $\bar{\nu}$ versus energy for trial 303 and ENDF/B-VII.1.

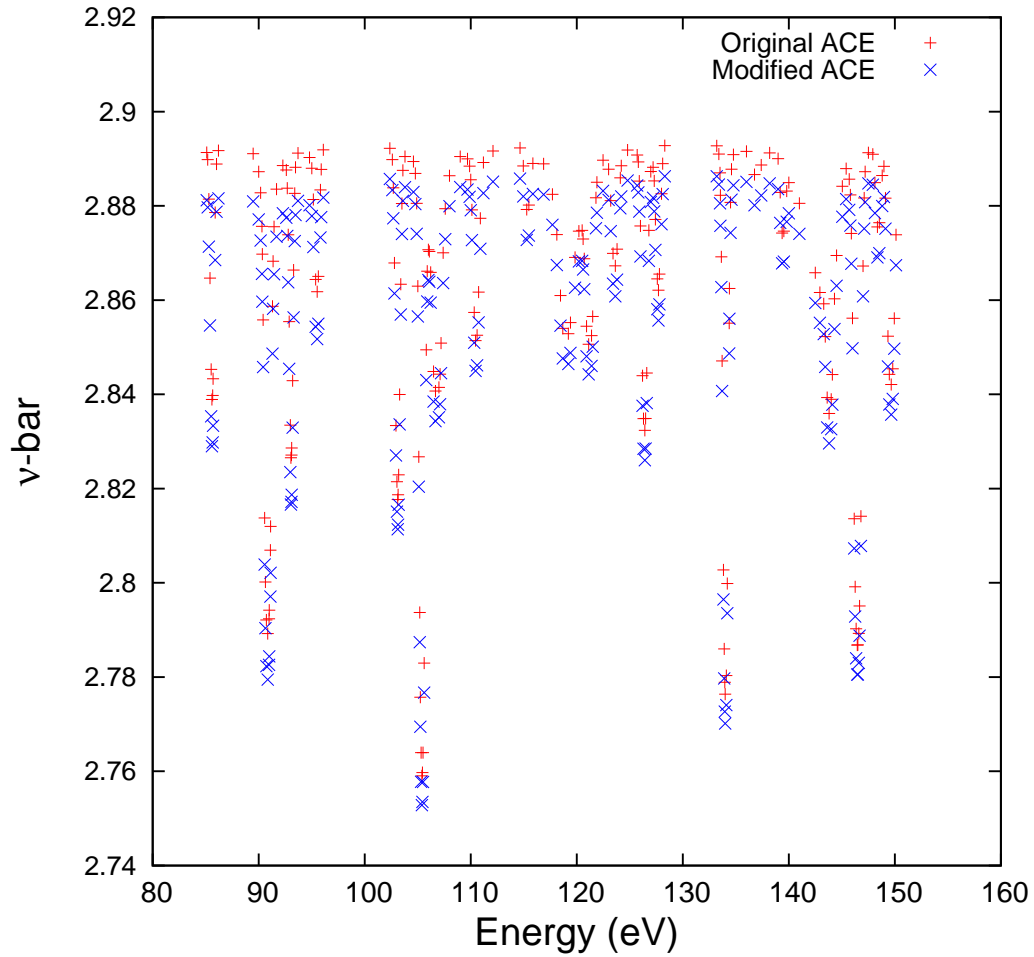


Fig. 5.4: Plot of $\bar{\nu}$ versus energy for trial 303 and ENDF/B-VII.1 for energies 85 to 150 eV.

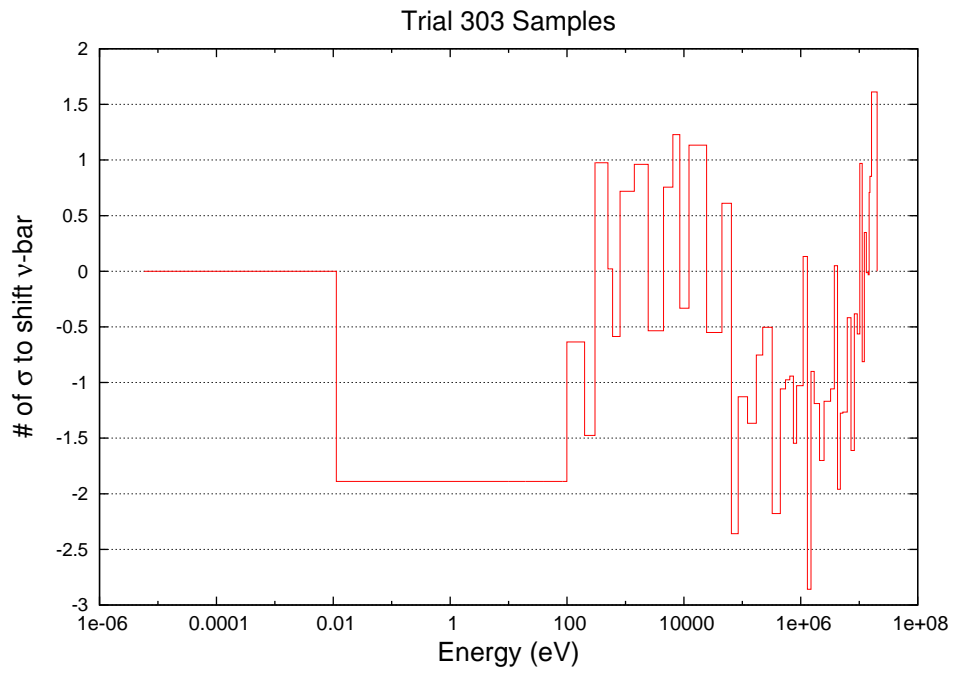


Fig. 5.5: Plot of number of standard deviations that trial 303 shifted $\bar{\nu}$ from original ENDF/B-VII.1 data by energy bin.

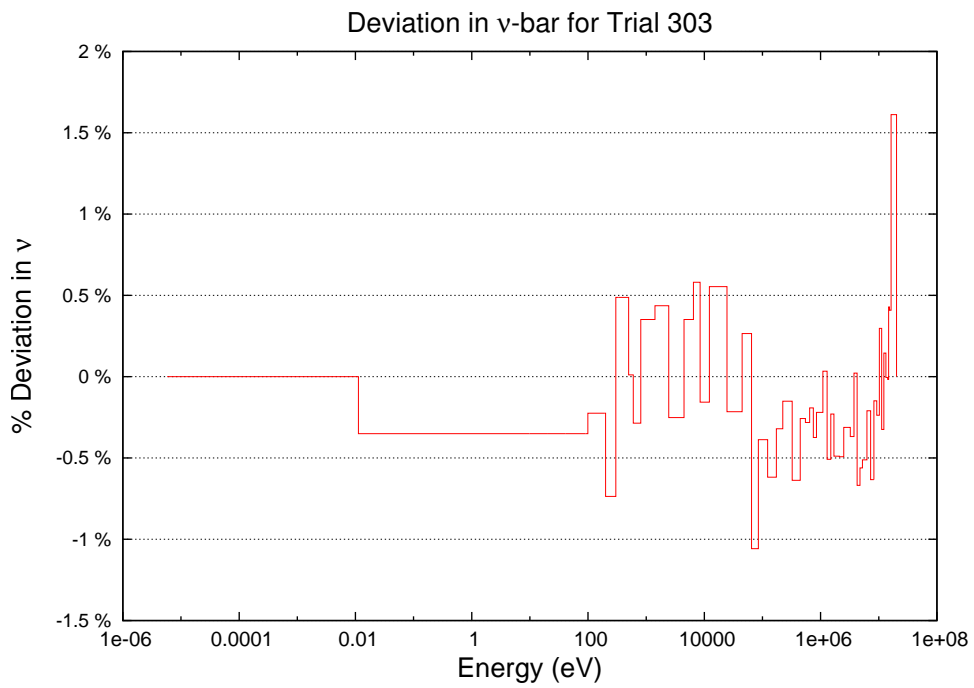


Fig. 5.6: Plot of percent deviation of $\bar{\nu}$ for trial 303 from the original ENDF/B-VII.1 data at each evaluated energy.

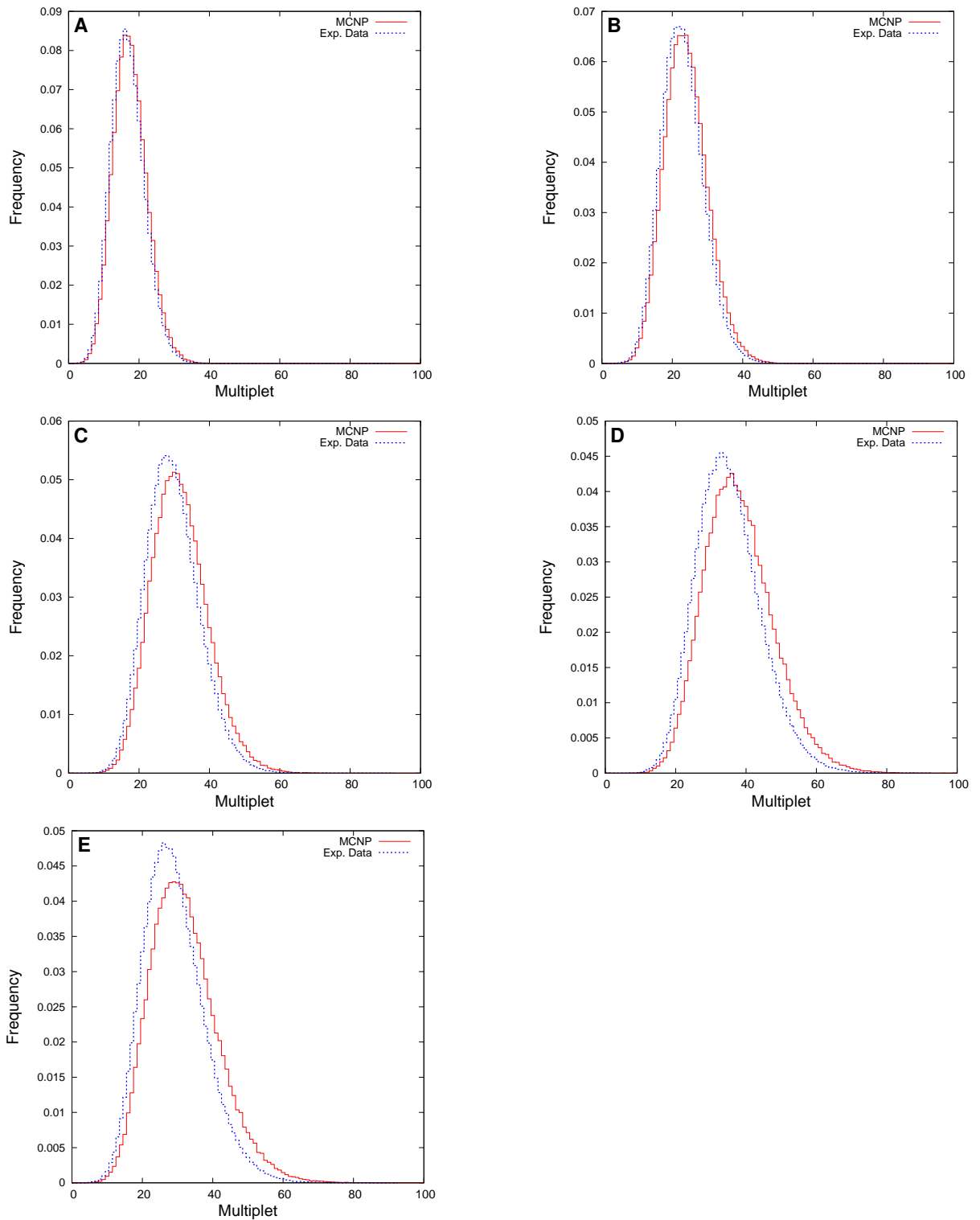


Fig. 5.7: Comparison of multiplicity distributions using original ENDF/B-VII.1 data and experimental multiplicity distributions. Distributions are for (A) bare Pu sphere, (B) 0.5-cm reflector, (C) 1.0-cm reflector, (D) 1.5-cm reflector, and (E) 3.0-cm reflector.

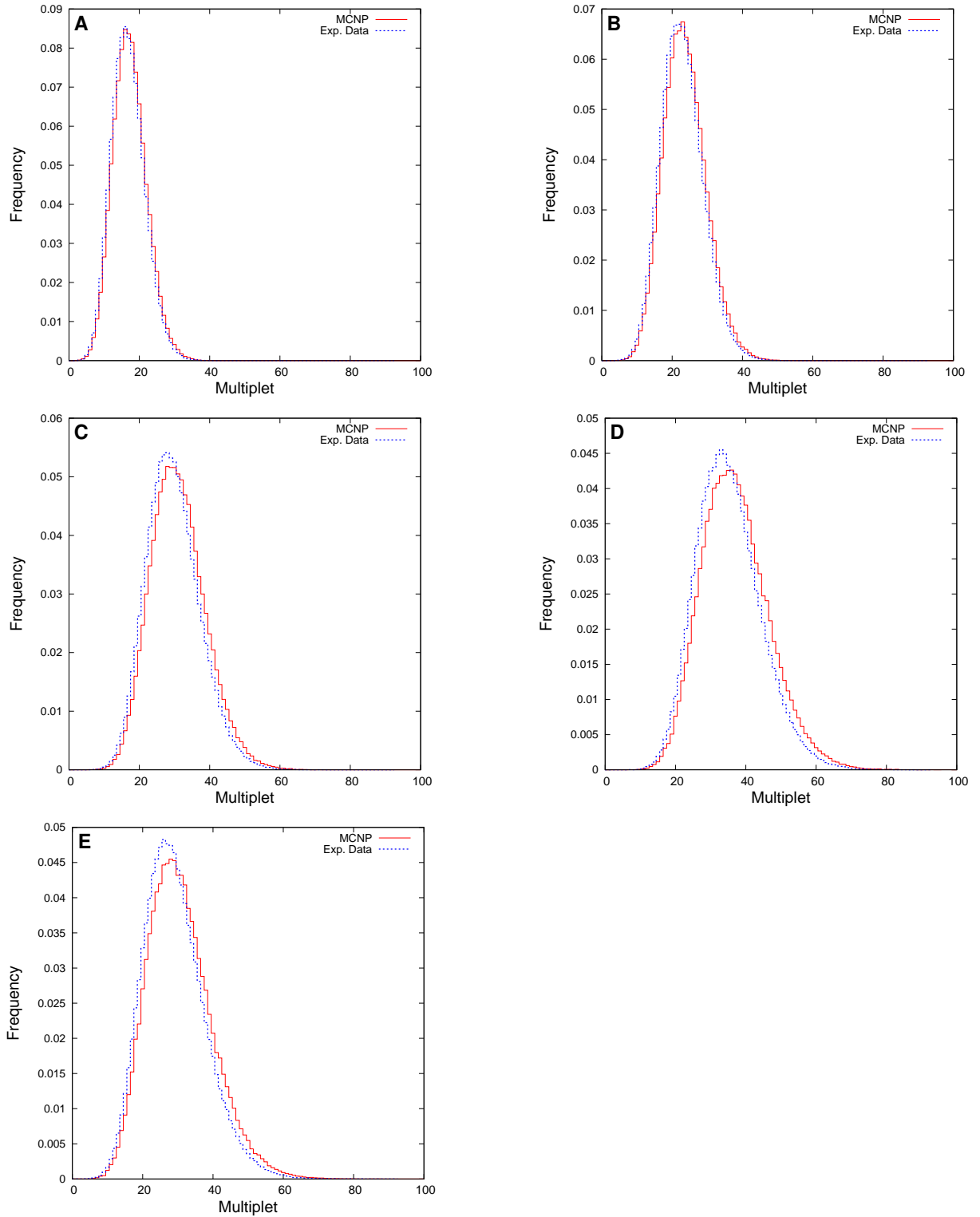


Fig. 5.8: Comparison of multiplicity distributions using trial 303 (modified ENDF/B-VII.1 $\bar{\nu}$ data) and experimental multiplicity distributions. Distributions are for (A) bare Pu sphere, (B) 0.5-cm reflector, (C) 1.0-cm reflector, (D) 1.5-cm reflector, and (E) 3.0-cm reflector.

5.7 Results of Cross Section Perturbations

The effect of the different cross section alteration schemes, discussed in Sections 5.4.3 and 5.4.4, are compared by the sum of the reduced chi-squared values for the multiplicity distributions χ_{mult}^2 given by Eq. (5.9). The first and second moments of multiplicity distributions are compared to experimental results to determine when cross section alterations produce high values of χ_{mult}^2 because of over-correcting the original overbias in the distributions. The average number of standard deviations that cross sections are shifted, as calculated with Eq. (5.6), are given as a measure of how realistic the cross section alterations are (where the variance data for that cross section were readily available); the sample standard deviation of the number of standard deviations data was shifted is also given. The chi-squared values for k_{eff} are also tabulated for comparison of the effect on the system to $\bar{\nu}$ alterations discussed in the previous section. Trials are labeled by the signed percent change in a cross section of interest (α in Eq. (5.4)). For reference, a comparison of the multiplicity distributions generated from simulations with the original ENDF/B-VII.1 cross sections and from experimental data is given in Fig. 5.7 on page 113; the distributions for the “ $\bar{\nu}$ -1.14%” trial are given in Fig. 5.10 on page 123.

5.7.1 Results of Capture Cross Section Perturbations

The results for case 1 of altering σ_c and σ_t discussed in Section 5.4.3 is given in Table 5.4 on page 117. The plot of multiplicity distributions produced with 16% increased σ_c from case 1 and the five experimental distributions is given in Fig. 5.11 on page 124. Based on the values of χ_{mult}^2 in Table 5.4, increasing the value of σ_c decreases the discrepancy between the MCNP and experimental multiplicity distributions. Significant alterations to the capture (and thus total) cross section had to be made to create a noticeable improvement in χ_{mult}^2 . As seen in Table 5.4, the 16% increase in σ_c corresponds to a 3.5 and 6.9 standard deviation increase in σ_f and σ_t , respectively. This set of data is well outside of statistical confidence, and the correction to the multiplicity distributions is still not as good as that of the $\bar{\nu}$ case. For comparison, in the “-1.14% $\bar{\nu}$ ” trial the value of $\bar{\nu}$ was decreased 3.9 standard deviations, on average, with $s(\#s(\bar{\nu})) = 1.82$ standard deviations. For most values of α , k_{eff} is not effected in any statistically significant manner.

As demonstrated in Fig. 5.11, a 16% increase in σ_c with compensation in σ_t corrects the overbias in multiplicity data produced by the original ENDF/B-VII.1 ^{239}Pu data, but in most cases is still inaccurate as compared to the experimental data. The 3.0-cm scenario is accurate to a high degree of precision. This indicates that χ_{mult}^2 improvements are dominated by corrections in the 3.0 cm scenario and energy-dependent alterations to σ_c may be able

to produce a more accurate match to all of the distributions. However, it would require a significant alteration based on the results of $\alpha = 16\%$.

The 3.0-cm simulation also has more moderation, so the effects of changes made to cross sections at lower energies are more prevalent. Figure 5.9 on page 117 compares multiplicity distributions for the 3.0 cm reflected scenario for various changes in σ_c , for case 1. The 2.0% and 8.0% increases in σ_c correspond to 0.86 and 3.45 for $\#s(\sigma_c)$, respectively; the latter value of $\#s(\sigma_c)$ is similar to $\#s(\bar{\nu})$ in the -1.14% $\bar{\nu}$ trial. The 2.0% increase (near one standard deviation) shows minimal correction to the distribution. It is of note that the 3.0-cm simulation shows the greatest correction in the distributions, but the 8.0% increase in σ_c , similar in magnitude to the $\bar{\nu}$ trial, does not fully correct this case. Also, for the 3.0-cm scenario, the $\bar{\nu}$ trial actually over-corrects the overbias in multiplicity, as seen in Fig. 5.10 on page 123. The over-correction is because the $\bar{\nu}$ data corrects all experimental distributions, and thus overcompensates in the case with the greatest change. This suggests that the system overall is not as sensitive to perturbations of σ_c as it is to $\bar{\nu}$.

The results for changing σ_c for case 2 and 3 are given in Tables 5.5 and 5.6 on page 118. Case 2 and 3 demonstrate that in general increasing scattering has a negative effect on χ_{mult}^2 , as compared to case 1. As a result, only case 1 and 4 were performed for the fission cross sections. The results for case 3 in Table 5.6 do not show a clear relation between α and χ_{mult}^2 . This is due to the stochastic spread of χ_{mult}^2 values (particular for relatively large values). In general, increasing scattering has a negative effect on the accuracy of simulated multiplicity distributions.

The results from case 4 for σ_c are depicted in Table 5.7 on page 119. The scattering cross section covariance matrix was in a format that is not yet implemented in the **ndvv** tools. Altering the cross sections was able to improve χ_{mult}^2 as compared to the original data by increasing capture and reducing the scattering cross section to compensate. For the same values of α , the improvements were not as great as in case 1. Changes were only made above 1 keV for case 4 because σ_c being orders of magnitude larger at times than σ_s at lower energies. To give some insight to the sensitivity of the systems to changes in σ_c at lower energies, Table 5.8 compares results of case 1 for changing data at all energies and for only above 1 keV. These results suggest, primarily because of correction in the 3.0-cm simulation, that the multiplicity experiments are sensitive to σ_c at lower energies.

Table 5.4: A comparison of results for case 1 where σ_c was increased and σ_t was increased to compensate for the change, at each energy.

Trial	χ^2_{mult}	χ^2_{keff}	$\#s(\sigma_t)$	$s(\#s(\sigma_t))$	$\#s(\sigma_c)$	$s(\#s(\sigma_c))$
$\bar{\nu}$ -1.14%	130.6	33.66	n/a	n/a	n/a	n/a
16.0%	142.6	1.86	3.47	3.05	6.90	2.47
14.0%	163.0	0.66	3.04	2.67	6.03	2.16
10.0%	209.0	0.11	2.17	1.90	4.31	1.55
8.0%	237.5	0.51	1.74	1.52	3.45	1.24
6.0%	277.8	0.08	1.30	1.14	2.59	0.93
4.0%	321.1	0.45	0.87	0.76	1.72	0.62
2.0%	371.2	0.02	0.43	0.38	0.86	0.31
1.5%	384.9	0.07	0.33	0.29	0.65	0.23
1.0%	396.4	0.16	0.22	0.19	0.43	0.15
0.5%	410.0	0.01	0.11	0.10	0.22	0.08
0.25%	423.6	1.06	0.05	0.05	0.11	0.04
Original	426.6	0.27	0	0	0	0

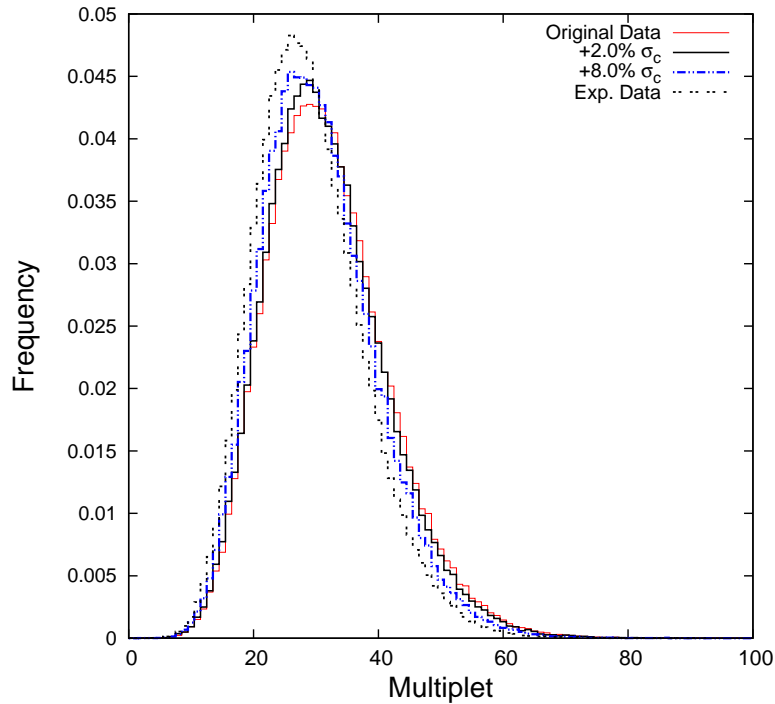


Fig. 5.9: Comparison of multiplicity distributions for the 3.0-cm polyethylene reflected sphere of Pu.

Table 5.5: A comparison of results for case 2 in which σ_c was increased and σ_s was increased to keep the ratio of scattering to σ_t the same as in the original data; σ_t was increased to compensate for the changes in σ_c and σ_s .

Trial	χ^2_{mult}	χ^2_{keff}	$\#s(\sigma_t)$	$s(\#s(\sigma_t))$	$\#s(\sigma_c)$	$s(\#s(\sigma_c))$
$\bar{\nu}$ -1.14%	130.58	33.7	n/a	n/a	n/a	n/a
10.0%	215.7	0.07	5.15	3.66	4.31	1.55
8.0%	249.0	1.08	4.12	2.93	3.45	1.24
6.0%	283.1	0.42	3.09	2.20	2.59	0.93
4.0%	326.1	1.09	2.06	1.47	1.72	0.62
2.0%	374.6	0.26	1.03	0.73	0.86	0.31
1.5%	389.8	0.26	0.77	0.55	0.65	0.23
1.0%	397.3	1.66	0.51	0.37	0.43	0.15
0.5%	409.7	0.48	0.26	0.18	0.22	0.08
0.25%	418.7	0.11	0.13	0.09	0.11	0.04
Original	426.6	0.27	0	0	0	0

Table 5.6: A comparison of results for case 3 in which σ_c was increased and σ_s was increased to keep the ratio of σ_c to σ_s the same as in the original data; σ_t was increased to compensate for the change in σ_c and σ_s .

Trial	χ^2_{mult}	χ^2_{keff}	$\#s(\sigma_t)$	$s(\#s(\sigma_t))$	$\#s(\sigma_c)$	$s(\#s(\sigma_c))$
$\bar{\nu}$ -1.14%	130.58	33.7	n/a	n/a	n/a	n/a
2.0%	394.4	0.05	1.03	0.73	0.86	0.31
1.5%	423.1	0.41	0.77	0.55	0.65	0.23
0.5%	423.6	0.04	0.26	0.18	0.22	0.08
1.0%	424.7	0.01	0.51	0.37	0.43	0.15
Original	426.6	0.27	0	0	0	0
0.25%	426.9	0.01	0.13	0.09	0.11	0.04
4.0%	434.5	2.32	2.06	1.47	1.72	0.62
6.0%	445.3	3.28	3.09	2.2	2.59	0.93
8.0%	454.2	2.91	4.12	2.93	3.45	1.24
10.0%	461.5	9.03	5.15	3.66	4.31	1.55

Table 5.7: A comparison of results for case 4 in which σ_c was increased and σ_s was decreased to keep σ_t the same as in the original data, for neutron energies greater than 1 keV.

Trial	χ^2_{mult}	χ^2_{keff}	$\#s(\sigma_c)$	$s(\#s(\sigma_c))$
$\bar{\nu}$ -1.14%	130.58	33.7	n/a	n/a
10.0%	345.1	0.22	4.04	1.21
8.0%	359.9	0.04	3.23	0.96
6.0%	372.7	1.11	2.42	0.72
4.0%	390.9	0.01	1.62	0.48
2.0%	408.8	0.13	0.81	0.24
1.5%	410.9	0.02	0.61	0.18
1.0%	417.9	0.01	0.40	0.12
0.5%	422.1	0.18	0.20	0.06
0.25%	425.4	0.04	0.10	0.03
Original	426.6	0.27	0	0

Table 5.8: A comparison of results for case 1 in which σ_c was increased and σ_s was decreased to keep σ_t the same. Changes were made to cross sections for neutron energies above E_{cut} .

α	χ^2_{mult}		$\#s(\sigma_c)$		$s(\#s(\sigma_c))$	
	$E_{cut} = 1$ keV	$E_{cut} = 0$	$E_{cut} = 1$ keV	$E_{cut} = 0$	$E_{cut} = 1$ keV	$E_{cut} = 0$
10.0%	349.9	209.03	4.04	4.31	1.21	1.55
4.0%	395.35	321.1	1.62	1.72	0.48	0.62
2.0%	410.0	371.15	0.81	0.86	0.24	0.31
1.0%	420.7	396.4	0.40	0.43	0.12	0.15
0.5%	421.2	410.02	0.20	0.22	0.06	0.08
0.25%	423.5	423.59	0.10	0.11	0.03	0.04

5.7.2 Results of Fission Cross Section Perturbations

Fission cross section perturbation results for case 1 and 4 are given in Tables 5.9 and 5.10, respectively. The trials are ordered by percent change in σ_f . The covariance data for σ_f was in a format not yet implemented in the NDVV tools, and thus $\#s(\sigma_f)$ was not computed. Overall, the changes in σ_f produced far better correction than the capture cases, using lower values of α . Additionally, σ_t was altered less than one standard deviation in the trials which produced the lowest values of χ_{mult}^2 . For σ_f reductions larger in magnitude than 2.0%, the value of χ_{mult}^2 begins to increase again due to over-correcting the overbias; the adjusted data produced multiplicity distributions which are shifted below the experimental distributions, based on the mean of the distributions, leading to a higher value of χ_{mult}^2 .

As Table 5.10 demonstrates, the fission decrease in case 4 was able to correct the problem by only changing σ_f and σ_s for energies above 1 keV. The multiplicity distributions generated from simulations with the -1.5% decrease in σ_f for case 4 are plotted against the experimental distributions in Fig. 5.12 on page 125. The corrected data are very accurate, and demonstrates a better correction for all reflector thicknesses than in the $\bar{\nu}$ results. The -1.14% $\bar{\nu}$ data are not optimized to this set of simulations (the results of Mattingly [2009] are from slightly different experimental setups). However, because the $\bar{\nu}$ results are over-correcting some distributions, while still under-correcting others, a set of data that produces a χ_{mult}^2 better than the -1.5% σ_f trial is unlikely. The values of $\chi_{k_{eff}}^2$ are increased significantly because the multiplication of the system has been reduced without any compensation. Energy-dependent alterations to σ_f would likely produce results which minimize both $\chi_{k_{eff}}^2$ and χ_{mult}^2 .

Table 5.9: A comparison of results for reduced σ_f with σ_t reduced to compensate for the changes, as described in case 1.

Trial	χ_{mult}^2	$\chi_{k_{eff}}^2$	$\#s(\sigma_t)$	$s(\#s(\sigma_t))$
-4.0%	1318.2	167.72	-1.16	0.82
-2.0%	101.0	48.31	-0.58	0.41
-1.6%	27.1	22.97	-0.47	0.33
-1.4%	17.4	22.79	-0.41	0.29
-1.2%	23.1	14.25	-0.35	0.25
-1.0%	47.7	9.37	-0.29	0.21
-0.5%	178.7	1.33	-0.14	0.10
$\bar{\nu}$ -1.14%	130.58	33.7	n/a	n/a
Original	426.6	0.27	0	0

Table 5.10: A comparison of results for σ_f alterations of case 4. Cross sections were altered for neutron energies greater than 1 keV.

Trial	χ_{mult}^2	χ_{keff}^2
-4.0%	1093.4	150.3
-2.0%	65.8	29.6
-1.5%	14.6	24.4
-1.2%	28.4	13.0
-1.0%	56.5	9.4
-0.8%	100.4	6.5
-0.5%	195.7	3.0
-0.25%	298.2	2.3
$\bar{\nu}$ -1.14%	130.58	33.7
Original%	426.6	0.0

Table 5.11: A comparison of the results for case 5 in which σ_c was increased and σ_f was decreased to keep σ_t the same as in the original data, for energies above E_{cut} .

Trial	χ_{mult}^2		$\#s(\sigma_c)$		$s(\#s(\sigma_c))$	
	$E_{cut} = 1 \text{ keV}$	$E_{cut} = 0$	$E_{cut} = 1 \text{ keV}$	$E_{cut} = 0$	$E_{cut} = 1 \text{ keV}$	$E_{cut} = 0$
10.0%	-	90.66	-	4.31	-	1.55
4.0%	328.05	222.47	1.62	1.72	0.48	0.62
2.0%	371.58	314.82	0.81	0.86	0.24	0.31
1.0%	399.77	367.18	0.40	0.43	0.12	0.15
0.5%	413.38	398.66	0.20	0.22	0.06	0.08
0.25%	421.05	413.23	0.10	0.11	0.03	0.04
$\bar{\nu}$ -1.14%	-	130.58	n/a	n/a	n/a	n/a
Original	-	426.6	0	0	0	0

5.7.3 Results of Altering both Fission and Capture

The results of case 5 from Section 5.4.3, where σ_c was increased and σ_f was decreased to account for the change, are depicted in Table 5.11 above. Results are given for changing cross sections at all energies and only at energies above 1 keV for comparison to case 4 results. The results were an improvement over cases 1-4 for σ_c , but not better than case 1 and 4 of σ_f . It is expected that increasing σ_c and decreasing σ_f together would produce a better result. Results are not improved because the percent changes were made with respect to the capture cross section. In this case, $\epsilon_f = -\epsilon_c$. Since σ_c is not as large as σ_f (particularly above 1 keV), the value of ϵ_f/σ_f is not as large in magnitude in case 5, compared to when

σ_f is altered directly. This result indicates that compensating for a change in σ_f with σ_c is not effective relative to the statistical uncertainty in σ_c ; compensating for σ_f in σ_t or σ_s produces a better result.

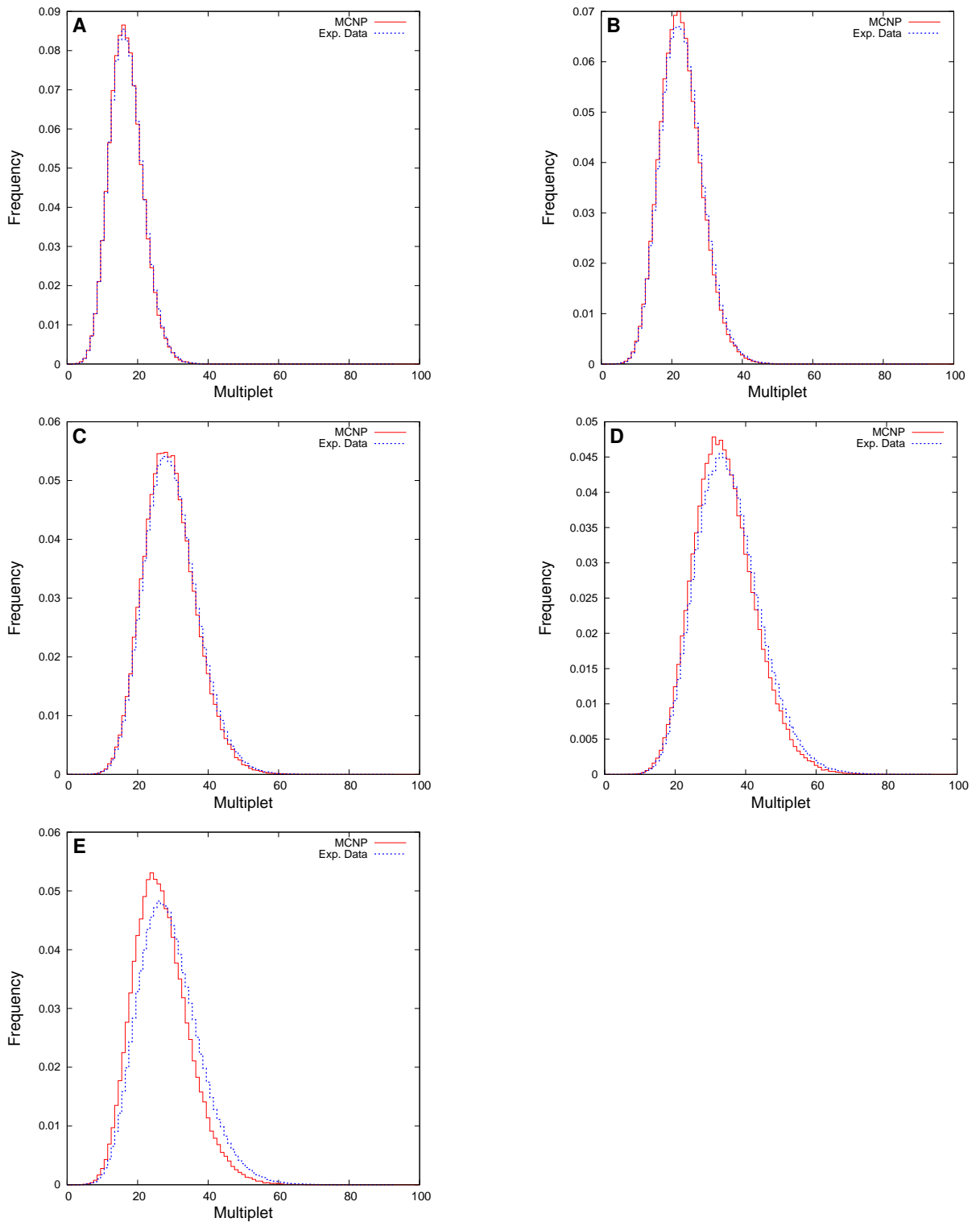


Fig. 5.10: Comparison of multiplicity distributions for -1.14% reduced energy averaged $\bar{\nu}$ and experimental multiplicity distributions. Distributions are for (A) bare Pu sphere, (B) 0.5-cm reflector, (C) 1.0-cm reflector, (D) 1.5-cm reflector, and (E) 3.0-cm reflector.

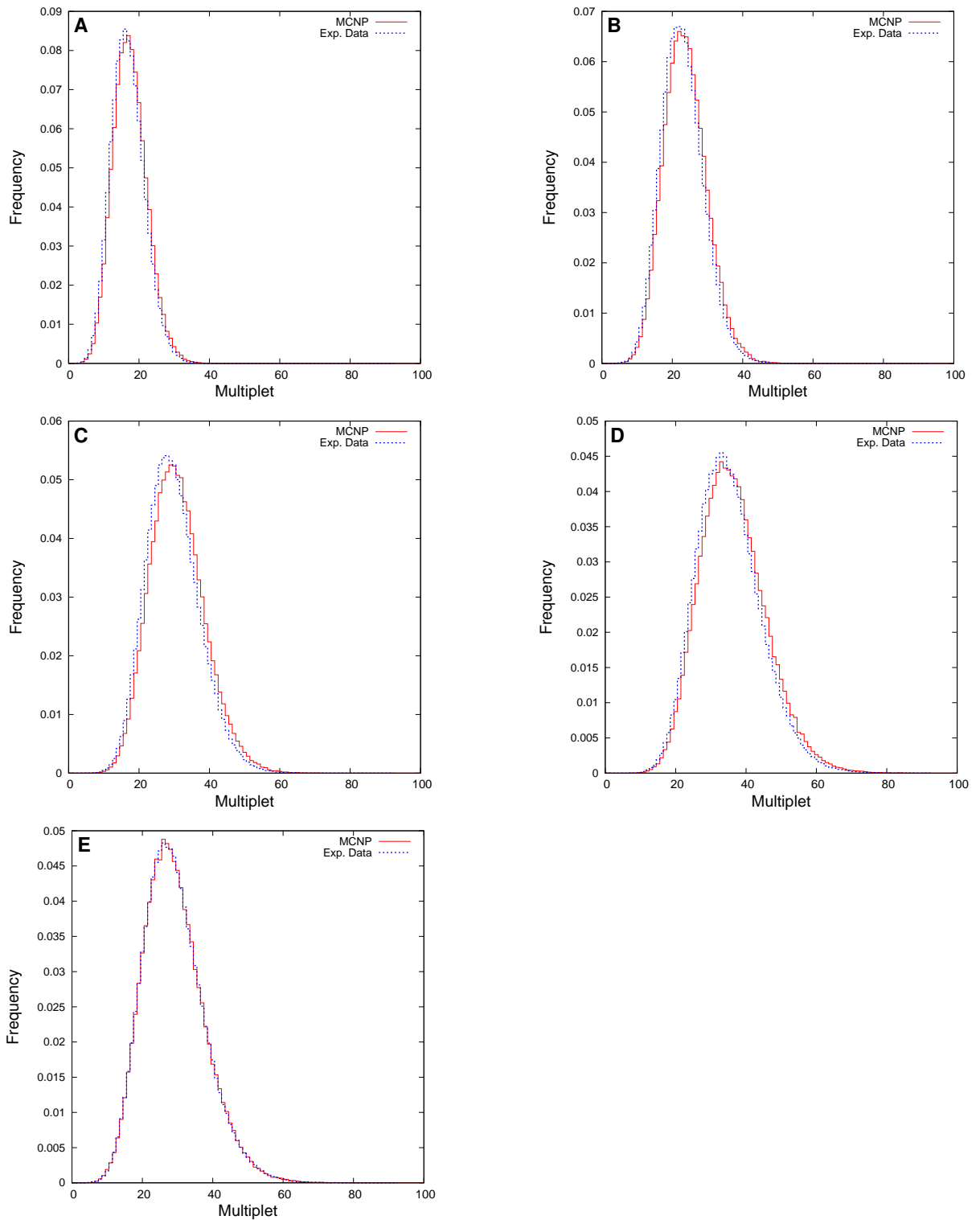


Fig. 5.11: Comparison of multiplicity distributions for 16% increased σ_c from case 1 and experimental multiplicity distributions. Distributions are for (A) bare Pu sphere, (B) 0.5-cm reflector, (C) 1.0-cm reflector, (D) 1.5-cm reflector, and (E) 3.0-cm reflector.

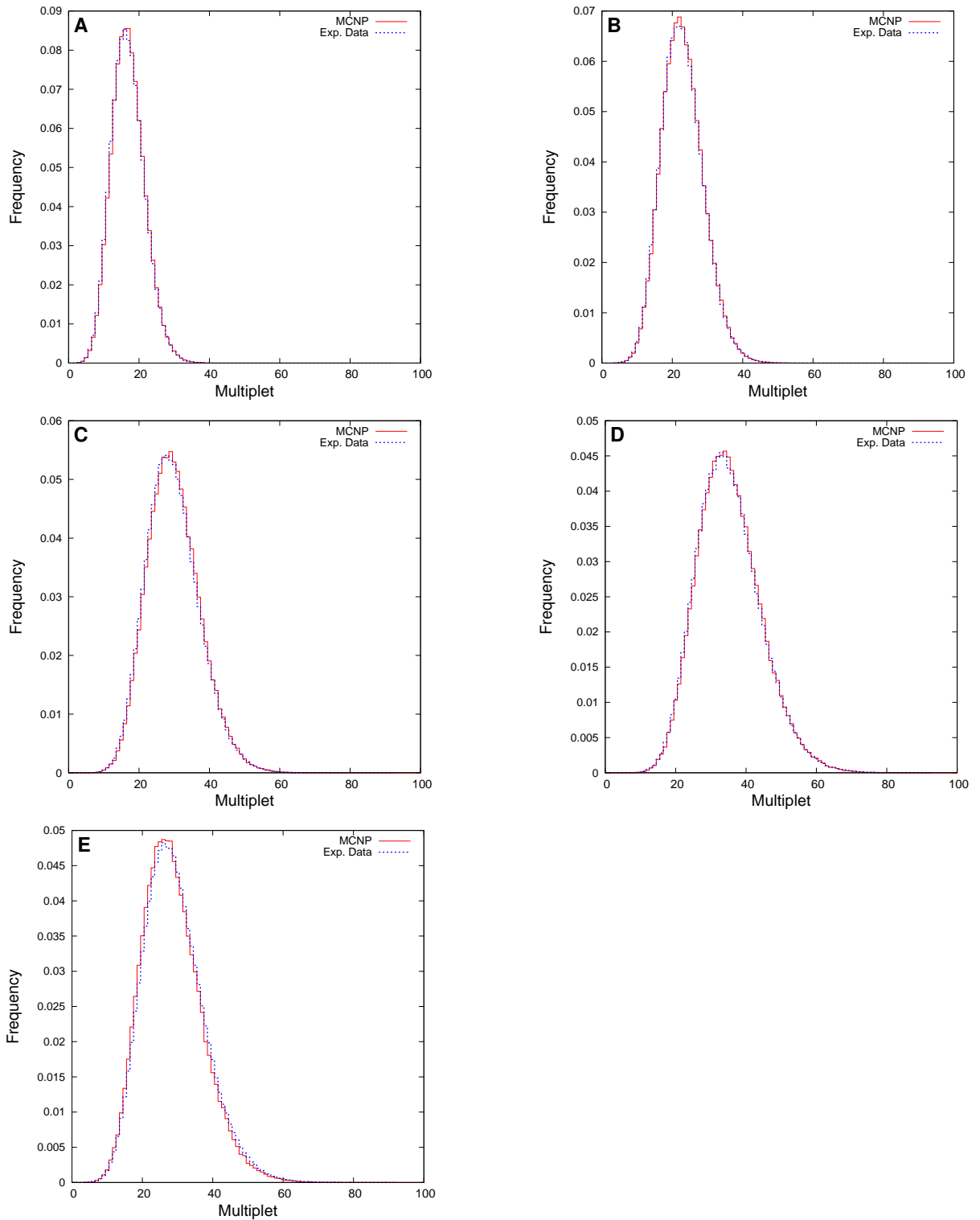


Fig. 5.12: A comparison of multiplicity distributions for σ_f reduced 1.5% and experimental multiplicity distributions; σ_s was increased to compensate for changes in σ_f , as described in case 4 of Section 5.4.3. Distributions are for (A) bare Pu sphere, (B) 0.5-cm reflector, (C) 1.0-cm reflector, (D) 1.5-cm reflector, and (E) 3.0-cm reflector.

5.8 Conclusions

The work presented in this chapter demonstrates that by exclusively changing $\bar{\nu}$ in an energy-dependent manner, multiplicity distributions can be recreated more accurately than with the original ENDF/B-VII.1 data, without changing criticality results significantly. Although energy-dependent perturbations were not as effective as shifting the entire spectrum of $\bar{\nu}$, the perturbations preserved k_{eff} and the statistical uncertainties. More trials would likely produce an energy-dependent modified set of data that would preserve k_{eff} while matching multiplicity distributions at least as accurately as an energy-averaged shift. The results also demonstrate that when $\bar{\nu}$ is calibrated during creation of nuclear data these multiplicity experiments should be considered. Although the accuracy of criticality problems was reduced somewhat for the new data, this is not entirely unexpected. If, on average, $\bar{\nu}$ has been shifted down to ensure multiplicity distributions match, it is likely some other area in the nuclear data needs adjustment to compensate.

Upon review of the cross section results, increasing the value of σ_c generally decreases the discrepancy between the MCNP and experimental multiplicity distributions. However, the multiplicity results are not sensitive to σ_c relative to the uncertainties in σ_c and σ_t . Decreasing σ_f was able to produce multiplicity distributions which match experimental results very well, particularly by increasing σ_s to compensate. This is to be expected because $\bar{\nu}$ alterations improved multiplicity results. If relatively small decreases in the mean number of fission neutrons released per fission improve results, then minor decreases in the probability of fission occurring should also be effective. The covariance data would be needed to ensure the alterations to σ_f were not statistically unreasonable. However, based on the best-case results from changing σ_t and σ_f , increasing σ_t by less than one standard deviation, it is likely that the σ_f perturbations are small relative to the statistical uncertainties in σ_f (σ_f is a significant portion of σ_t , particularly for energies above 1 keV).

The results of case 2 and 3 for σ_c suggest that increasing σ_s has a negative effect on multiplicity distributions, although case 4 decreased σ_f and was able to match multiplicity distributions very well by increasing σ_s . In case 4 for σ_c , σ_s is decreased, but the results were not able to produce a better improvement over changes in σ_t and σ_c . It is of note that when a cross section of interest is increased and σ_t is adjusted to compensate, the probability of all other events occurring is inherently decreased. Appendix A provides some insight into this phenomena. These results suggest that the effectiveness of case 1 for σ_c is partially because of the fact that the probability of fission occurring has been decreased. It is noted that the $\chi_{k_{eff}}^2$ value was not statistically increased in the majority of the σ_c alterations, unlike in the σ_f cases, even at the large value of 16%.

5.9 Summary and Suggestions for Future Work

Future work should include more correlated sampling trials of $\bar{\nu}$ data for ^{239}Pu . Energy-dependent sampling of σ_f , compensating with σ_s , should also be pursued in future work, as it has the potential to provide the best correction to multiplicity distributions, while preserving k_{eff} . For future samples, more criticality test cases should be included to introduce more energy-dependent restrictions on the data. For sampling of σ_f , a global optimization scheme may need to be applied. Cross sections have many covariance energy groups (400 for σ_t of ^{239}Pu), as compared to the 50 groups of $\bar{\nu}$, and will require far more trials and constraining problems if the purely random sampling approach is used. A global optimization approach should be used that takes random walks through the phase space (preventing the method from finding local minima) but is biased to pick results that produce better solutions. Additionally, the global optimization scheme should generate data that is statistically realistic, based on the covariance data.

In the ideal case, both $\bar{\nu}$ and sets of cross sections would be simultaneously sampled from covariance data. The ideal set of nuclear data would then be determined based on simulation results. This approach is inherently limited by the large degrees of freedom and heavy computational cost. The beginning of the necessary methods and programs to perturb energy-dependent nuclear data to match multiplicity distributions have been developed and tested. Additionally, by adjusting the Figure of Merit parameters, a better match to criticality problems as desired by the user can be found. Results have demonstrated that these simulations should be considered in validation and calibration of nuclear data, particularly $\bar{\nu}$. Initial findings are encouraging that this method will provide a tool for validating nuclear data, and generating data sets purposed for simulating specific problems in nuclear engineering

Bibliography

- Baum, E. M., Knox, H. D. and Miller, T. R. [2002], *Nuclides and Isotopes: Chart of the Nuclides*, 16th edn.
- Bellinger, S., Fronk, R., McNeil, W., Sobering, T. and McGregor, D. [2010], High Efficiency Dual-Integrated Stacked Microstructured Solid-State Neutron Detectors, in “IEEE NSS Conf”, Knoxville, TN, pp. 2008–2012.
- Biju, K., Tripathy, S., Sunil, C. and Sarkar, P. [2012], “FLUKA Simulations of a Moderated Reduced Weight High Energy Neutron Detection System”, *Nuclear Instruments and Methods in Physics Research Section A: Accelerators, Spectrometers, Detectors and Associated Equipment* **682**(0), 54 – 58.
- Brackenbush, L. W. [1983], “Spunit: A Computer Code for Multisphere Unfolding”.
- Bramblett, R. [1960], “A New Type of Neutron Spectrometer”, *Nuclear Instruments and Methods* **9**(1), 1–12.
- Brennan, J., Brubaker, E., Cooper, R., Gerling, M., Greenberg, C., Marleau, P., Mascarenhas, N. and Mrowka, S. [2011], “Measurement of the Fast Neutron Energy Spectrum of an ²⁴¹Am-Be Source Using a Neutron Scatter Camera”, *IEEE Transactions on Nuclear Science* **58**(5), 2426 –2430.
- Brooks, F. and Klein, H. [2002], “Neutron Spectrometry: a Historical Review and Present Status”, *Nuclear Instruments and Methods in Physics Research Section A: Accelerators, Spectrometers, Detectors and Associated Equipment* **476**(1-2), 1 – 11. Int. Workshop on Neutron Field Spectrometry in Science, Technology, and Radiation Protection.
- Caruso, A. N., Oakes, T., Miller, W. et al. [2011], High Intrinsic Efficiency Solid State Neutron Detector and Spectrometer, Presented at IEEE Nuclear Science Symposium: ³He Replacement, Valencia, Spain.

- Chadwick, M., Oblozinsky, P. et al. [2006], ENDF/B-VII.0: Next Generation Evaluated Nuclear Data Library for Nuclear Science and Technology, in “Nuclear Data Sheets”, 107th edn, pp. 2931–3060.
- Cooper, B., Bellinger, S., Caruso, A., Fronk, R., Miller, W., Oakes, T., Shultis, J., Sobering, T. and McGregor, D. [2011], Neutron Energy Spectrum with Microstructured Semiconductor Neutron Detectors, in “IEEE Nuclear Science Symposium”, Valencia, Spain.
- Croft, S., Favalli, A., Hauck, D. K., Henzlova, D. and Santi, P. A. [2012], “Feynman Variance-to-Mean in the Context of Passive Neutron Coincidence Counting”, *Nuclear Instruments and Methods in Physics Research Section A: Accelerators, Spectrometers, Detectors and Associated Equipment* **686**(0), 136–144.
- Dunn, P. F. [2005], *Measurement and Data Analysis for Engineering and Science*, McGraw Hill, 1221 Avenue of the Americas, New York, NY 10020.
- ENDF-6 Manual [2011], *ENDF-6 Formats Manual*, 2nd edn, Upton, NY.
- Ensslin, N. [1998], “Application Guide to Neutron Multiplicity Counting”. Los Alamos Report LA-13422-M.
- Fayegh, R. K. [1993], “Neural Network Unfolding of Photon and Neutron Spectra Using an NE-213 Scintillation Detector”, *Nuclear Instruments Methods in Physics Research: Section A, Accelerators, Spectrometers, Detectors and Associated Equipment* **329**(1-2), 269–276.
- Feynman, R. P. [1946], “Statistical Behavior of Neutron Chains”. Los Alamos Report LA-591-DEL.
- Flaska, M. and Pozzi, S. [2007a], “Identification of Shielded Neutron Sources with the Liquid Scintillator BC-501A Using a Digital Pulse Shape Discrimination Method”, *Nuclear Instruments and Methods in Physics Research Section A: Accelerators, Spectrometers, Detectors and Associated Equipment* **577**(3), 654 – 663.
- Flaska, M. and Pozzi, S. [2007b], Pulse-Shape Discrimination got Identification of Neutron Sources Using The BC-501A Liquid Scintillator, Oak ridge National Laboratory, Presented at M&C + SNA, Monterey, California.
- Grissom, J. T. and Koehler, D. R. [1971], “Data Smoothing”, *American Journal of Physics* **39**(11), 1314–1320.
- Hogg, R. V., McKean, J. W. and Craig, A. T. [2013], *Introduction to Mathematical Statistics*, 7th edn, Pearson Education, Inc., 501 Boylston Street, Suite 900, Boston, MA 02116.

- IAEA Report 403 [2001], “Compendium of Neutron Spectra and Detector Responses for Radiation Protection Purposes: Supplement to Technical Reports Series no. 318”, Technical Report Series no. 403.
- ICRU [2001], “Determination of Operational Dose Equivalent Quantities for Neutrons”, ICRU Report 66.
- ICSBEP Handbook [2004], “International Handbook of Evaluated Criticality Safety Benchmark Experiments”, Nuclear Energy Agency, NEA/NSC/DOC(95)03/I.
- ISO [2000], Reference Neutron Radiations – Part 2: Calibration Fundamentals of Radiation Protection Devices Related to the Basic Quantities Characterizing the Radiation Field, Technical Report ISO 8529-2, Geneva, Switzerland.
- Kouzes, R., Siciliano, E., Ely, J., Keller, P. and McConn, R. [2007], Passive Neutron Detection at Borders, *in* “Nuclear Science Symposium Conference Record, 2007. NSS '07. IEEE”, Vol. 2, pp. 1115 –1119.
- Mattingly, J. K. [2009], Polyethylene-Reflected Plutonium Metal Sphere: Subcritical Neutron and Gamma Measurements, Revision 2, Technical Report SAND2009-5804, Sandia National Laboratory.
- McLean, T. D. and Justus, A. L. [2012], “EAGLE Neutron Rem-Meter Dose Measurements at the Trident Laser Facility”, (LAUR-12-26418).
- Miller, E. C., Mattingly, J. K. et al. [2010], “Simulations of Neutron Multiplicity Measurements with MCNP-PoliMi”, (SAND2010-6830).
- Miller, S. C. [1993], AFITBUNKI: A Modified Iterative Code to Unfold Neutron Spectra from Bonner Sphere Detector Data, Master’s thesis, Air Force Inst. of Tech. Wright-Patterson.
- Mukherjee, B. [2002], “A High-Resolution Neutron Spectra Unfolding Method Using the Genetic Algorithm Technique”, *Nuclear Instruments and Methods in Physics Research Section A: Accelerators, Spectrometers, Detectors and Associated Equipment* **476**, 247 – 251. International Workshop on Neutron Field Spectrometry in Science, Technology and Radiation Protection.
- Olsher, R. [2004], “Prescila: A New, Lightweight Neutron Rem Meter”, *Health physics* **86**(6), 603–12.
- Olsher, R. H. [2000], “Wendi: An Improved Neutron Rem Meter”, *Health physics* **79**(2), 170–81.

- Press, W. H., Teukolsky, S. A., Vetterling, W. T. and Flannery, B. P. [1992], *Numerical Recipes in C: The Art of Scientific Computing*, 2nd edn.
- Reilly, D., Ensslin, N., Jr., H. S. and Kreiner, S., eds [1991], *Passive Nondestructive Assay of Nuclear Materials*, Los Alamos National Laboratory, P.O. Box 1663, MS E540, Los Alamos, NM 87545.
- Rousseuw, P. J. and Molenberghs, G. [1993], “Transformation of Non Positive Semidefinite Correlation Matrices”, *Communication in Statistics: Theory and Methods* **22**(4), 965–984.
- Ryan, B. C. [1998], *Analysis Methods for Bonner Sphere Spectrometry*, Master’s thesis, Kansas State University, Manhattan, KS.
- Shultis, J. and Faw, R. [2004], “An MCNP Primer”, Dept. of Mechanical and Nuclear Engineering, Kansas State University.
- Shultis, J. K. and Dunn, W. L. [2011], *Exploring Monte Carlo Methods*, 1st edn, Elsevier Science, San Diego, CA.
- Shultis, J. K. and Faw, R. E. [2000], *Radiation Shielding*, American Nuclear Society, Inc., 555 North Kensington Ave., La Grange Park, IL 60526.
- Shultis, J. K. and Faw, R. E. [2008], *Fundamentals of Nuclear Science and Engineering*, Taylor & Francis Group, 6000 Broken Sound Parkway NW, Suit 300, Boca raton, FL 33487.
- Shultis, J. and McGregor, D. [2009], Design and performance considerations of perforated semiconductor thermal-neutron detectors.
- Solomon, C. J. [2011], Polyethylene Reflected Pu Multiplication Inference Simulations, number LAUR-11-03933, Los Alamos National Laboratory, Presented at Nuclear Criticality Safety Program Subcritical Measurement Workshop, Los Alamos National Laboratory.
- Sood, A., Solomon, C. J. et al. [2011], Direct Calculation of Measured Observables in a Multiplying Sub-Critical System, number LAUR-11-02434, Los Alamos National Laboratory, Presented at INC, Edinburg, Scotland.
- Stacey, W. [2007], *Nuclear Reactor Physics*, John Wiley & Sons.
- Sweezy, J., Hertel, N. and Veinot, K. [2002], “BUMS: A Bonner Sphere Unfolding Made Simple: An HTML Based Multisphere Neutron Spectrometer Unfolding Package”, *Nuclear Instruments and Methods in Physics Research Section A: Accelerators, Spectrometers,*

- Detectors and Associated Equipment* **476**, 263 – 269. International Workshop on Neutron Field Spectrometry in Science, Technology and Radiation Protection.
- Taylor, J. R. [1997], *An Introduction to Error Analysis*, 2nd edn, University Science Books, Sausalito, California.
- Thomas, D. and Alevra, A. [2002], “Bonner Sphere Spectrometers: A Critical Review”, *Nuclear Instruments and Methods in Physics Research Section A: Accelerators, Spectrometers, Detectors and Associated Equipment* **476**(1–2), 12 – 20. Int. Workshop on Neutron Field Spectrometry in Science, Technology and Radiation Protection.
- Toraskar, J. and Melkonian, E. [1971], “Spontaneous Fission of ²⁴⁰Pu: Comparison with the Slow-Neutron-Induced Fission of ²³⁹Pu”, *Physical Review* .
- Toyokawa, H., Yohizawa, M., Uritani, A., Mori, C., Takeda, N. and Kudo, K. [1997], “Performance of a Spherical Neutron Counter for Spectroscopy and Dosimetry”, *IEEE Transactions on Nuclear Science* **44**(3), 788 –791.
- Tsoufanidis, N. [1995], *Measurement and Detection of Radiation*, 2nd edn, Taylor & Francis, Bristol, PA.
- Twomey, S. [1963], “On the Numerical Solution of Fredholm Integral Equations of the First Kind by the Inversion of the Linear System Produced by Quadrature”, *J. ACM* **10**(1), 97–101.
- Vega-Carrillo, H., Ortiz-Rodriguez, J. and Martinez-Blanco, M. [2012], “NSDUAZ Unfolding Package for Neutron Spectrometry and Dosimetry with Bonner Spheres”, *Applied Radiation and Isotopes* **71**, **Supplement**(0), 87 – 91. XII International Symposium on Solid State Dosimetry.
- X-5 Monte Carlo Team [2003], *MCNP - A General N-Particle Transport Code, Version 5, Volume I,II,III*, Los Alamos National Laboratory. LA-UR-03-1987.
- Yoshida, T., Tsujimura, N. and Yamano, T. [2011], “Development of a Hand-Held Fast Neutron Survey Meter”, *Radiation Protection Dosimetry* **146**(1-3), 72–75.

Appendix A

Changes in Probabilities of Interaction Events

This section develops an intuitive explanation of the behavior caused by altering the total interaction cross section, through a simplified example. Consider neutrons of a particular energy traveling through a homogeneous system. Consider only two reactions: a reaction of interest a and the occurrence of any other reaction, labeled as b . The total interaction cross section is $\sigma_t = \sigma_a + \sigma_b$. The cross section σ_a is to be perturbed, and σ_t must be adjusted to compensate. The probability of a neutron traveling a distance x to where it has an interaction of type i is

$$\begin{aligned} P(\text{Interaction } i, x) &= P(\text{Interaction}, x) * P(\text{Interaction } i \mid \text{Interaction}, x) \\ &= [1 - e^{-\sigma_t x}] \frac{\sigma_i}{\sigma_t}, \end{aligned} \tag{A.1}$$

where $P(\text{Interaction } i \mid \text{Interaction}, x)$ denotes the conditional probability that an interaction of type i occurs, given that an interaction at x has occurred. This conditional probability, given by σ_i/σ_t , is what was altered in Section 5.7 by adjusting the cross sections. However, the marginal probability of interaction (the term in squared brackets) is also implicitly adjusted. Consider the case in which σ_a is altered by ϵ_a , i.e., $\sigma'_a = \sigma_a + \epsilon_a$. The total cross section is then adjusted to compensate as $\sigma'_t = \sigma_t + \epsilon_a$. For the value of $P(\text{Interaction } a, x)$, both the conditional and marginal probability in Eq. (A.1) have increased from the original values to the perturbed values in a straightforward manner, so the probability of that interaction occurring has increased. Now, consider the change in probability for the unperturbed reaction b . The probability of a neutron undergoing interaction b at x in the perturbed system is given by

$$P'(\text{Interaction } b) = p'_b(x) = [1 - e^{-\sigma'_t x}] \frac{\sigma_b}{\sigma'_t}. \tag{A.2}$$

In this case, since σ'_t is greater than σ_t , the probability of an interaction occurring has

increased, but the conditional probability of interaction b occurring has decreased. To determine the net effect on $p_b(x)$ consider the Maclaurin series for $\exp(-\sigma'_t x)$:

$$p'_b(x) = \left[1 - (1 - \sigma'_t x + \frac{(\sigma'_t x)^2}{2} + \mathcal{O}(\sigma_t'^3 x^3)) \right] \frac{\sigma_b}{\sigma'_t}. \quad (\text{A.3})$$

Simplification yields

$$p'_b(x) = \sigma_b x - \frac{\sigma'_t x^2}{2} - \mathcal{O}(\sigma_t'^2 x^3). \quad (\text{A.4})$$

In the original, unperturbed system, the probability of interaction b at x is given by Eq. (A.4) with σ_t replacing σ'_t . The difference in $p_b(x)$ of the perturbed and original system is

$$\Delta p_b(x) = p'_b(x) - p_b(x) = -\frac{(\sigma'_t - \sigma_t)x^2}{2} + \mathcal{O}((\sigma_t'^2 - \sigma_t^2)x^3). \quad (\text{A.5})$$

Substituting for σ'_t in the first term yields:

$$\Delta p_b(x) = -\frac{\epsilon_a x^2}{2} + \mathcal{O}((\sigma_t'^2 - \sigma_t^2)x^3) \quad (\text{A.6})$$

The overall probability of interaction b occurring is $\propto -\epsilon_a$. Thus, altering a cross section and adjusting the total cross section to compensate for the change inherently alters the probability of all other reactions occurring in the opposite direction.

Appendix B

Spectrometer Scripts and Codes

File Name	Description	Page
spectrometer_maker.py	Python control script for creating MCNP5 inputs for all sources and geometries. Automatically calls modules to perform cell-splitting and parallel runs	136
input.i	Sample input for spectrometer_maker.py. This file contains MCNP5 cards that do not change between runs to be printed directly	142
source_printer.py	Python module that reads in source energy distributions based on key word entries	143
source_list.py	Input file for source_printer	144
importance_fn.py	Python module for automatic cell splitting	147
hydra_run.py	Python control module for running MCNP5 simulations in parallel. Includes auto-rerun if statistical checks are not passed	151
run_fom.py	Python control script for computing simulated responses and FOM values for many trials, before computing Θ	154
fom_comparison_format.py	Script with all_data class that parses and manipulates data from all trials to compute Θ , also has member functions for printing results	158
FOM_output.py	Reads tallies from MCNP outputs and compiles them by file name into master_file.fom	—
master_file.fom	Sample output from FOM_output.py	165
simul_resp.f90	Source code for simulating detector response; uses modules of code from [Press et al., 1992]	166
src_str.txt	Contains source strengths to be read in by simul_resp.exe. Format: number strengths, single column of strengths	—
fom.f90	Source code for calculating FOM values	170

spectrometer_maker.py: Generate and Run MCNP5 Files

```
import shutil # for copying files
import os # for directories and chmod etc.
import stat # for chmoding to user access
import subprocess # for running programs
import re # for regexps
import source_printer #reads sources from master file and prints them
import importance_fn #determines the "imp:n/p" in a file
import hydra_run #runs mcnp on hydra

# function for default file reading
def readinput(inputfilename):
    input = open(inputfilename)
    a = []
    for line in input:
        a.append(line)
    input.close()
    return a;

# directorymaker
def makedirectory(dir):
    if not os.path.exists(dir):
        os.makedirs(dir)
        os.chmod(dir, stat.S_IRWXU)
    else:
        os.chmod(dir, stat.S_IRWXU)

# prints a list of stuff with some justification to a file
def printer(file, stuff, justified):
    for item in stuff:
        temp = str(item)
        if(len(temp) < justified):
            file.write(temp.ljust(justified))
        else:
            file.write(temp.ljust(len(temp)+2))
    return

# prints stuff from the initial file
def initial_printer(ifile, initialfile, initialfile_counter):
    count = 0;
    for line in initialfile:
        if (count < initialfile_counter):
            count +=1
            continue
        else:
            # prints from initialfile until it finds a "c *" line
            temp = line.split()
            if (len(temp) > 1):
                if (temp[1] == '*'):
                    break
            ifile.write(line)
            count+=1
    return count+1

#moves file to a directory OVERWRITING any files in the way
def move_dir(file_name, dir):
    os.chdir(dir)
    if os.path.exists(file_name):
        print "IM IN YOUR DIRECTORY DELETING YOUR FILES!"
        os.remove(file_name)
    os.chdir("../")
    shutil.move(file_name, dir)
```

```

#makes a batch file for all mcnp files. A list of lists of names of files for each directory in directories.
def make_batch(mcnp_names, directories):
    print "Enter in the name of the batch file (no extension)"
    name = raw_input()
    print "How many nodes (separate files to run) do you want?"
    number = raw_input()
    batch = []
    for t in range(int(number)): #open a file for each node
        batch.append(open(name+str(t)+".bat", "w"))

    #determine number of files to be printed per batch
    files_per_batch = 0
    for i in mcnp_names:
        files_per_batch += len(i)
    files_per_batch = int(files_per_batch/float(number))
    filecount = 0 #keep track of how many files have been printed on each
    t=0 #which batch file are you in
    for direct in range(len(directories)): #loop through each directory
        batch[t].write("cd %s\n" % directories[direct]) #change from the main directory to the current one
        for name in mcnp_names[direct]: #writes
            if (filecount == files_per_batch and t != (int(number)-1)): #extra file because of odd numbers
                t+=1 #next file
                batch[t].write("cd %s\n" %directories[direct])
                filecount=0

            tempstring = name.replace(".i",".o")
            batch[t].write("mcnp5 i=%s o= %s\n" % (name, tempstring))
            filecount+=1 #increment nout of how many files printed per batch
            batch[t].write("erase runt*\n")
        batch[t].write("cd ..\n")

    for t in batch:
        t.close()

#searchs a line for a string, returns true if found, else false
def search_for(line, string):
    pattern = re.compile(str(string))
    if (pattern.search(line)):
        return True
    else:
        return False

# *****main *****

def main():
    #output info
    all_source_names = []

    # constants throughout
    mat_li = 2
    mat_hdpe = 1
    mat_board = 4
    mat_cd = 3
    source_erg_dist = 1

    #densities
    dens_li = -0.0835
    dens_hdpe = -0.9500
    dens_board = 0.00053
    dens_cd = -8.65

    #input data
    output_data = [] #output list to be printed
    names = [] #output file names

```

```

directories = [] #name of detector types that directories are made to store all the different stuff
detector_start = 100.0
cyl_radius = [10.0, 9.5, 9.0, 8.0, 7.5, 7.0, 6.5, 6.0, 5.5, 5.0, 4.5, 4.0] #outer radius of HDPE
#must be bigger than the size of the detectors and the board
number_detectors =[6,6,6,6,6,6,6,7,7,7,7,7,7,7,8,8,8,8,8,8]
poly_thick = [4.0, 4.5, 5.0, 5.5, 6.0, 6.5, 7.0, \
              3.5, 4.0, 4.5, 5.0, 5.5, 6.0, 6.5, \
              3.0, 3.5, 4.0, 4.5, 5.0, 5.5, 6.0 ]
cyl_radius = [6.0]*len(poly_thick)
if (len(poly_thick) != len(number_detectors)):
    print "your lengths don't match"
    exit()

cd_thick = 0.1
board_thick = 0.157
board_width = 1.1
li_thick = 0.1
normalization = 0.00333286*li_thick/0.1 # constant used for FMn tally card to account for efficiency

#cell numbers for the RPP that define the detector and the boards and CYL for boundary
det_box = 35
board_box = 40
outer_cyl = 30

source_list = readinput("source_names.txt")
for i in range(len(source_list)):
    source_list[i] =source_list[i].strip('\n')

#check to see if this is on hydra or a pc. Use hydra_check for particle balance function and mcnp runs
hydra_check = hydra_run.hydra_machine()
if hydra_check:
    num_nodes = raw_input("Enter the number of nodes: ")

for det in range(len(number_detectors)):
    initialfile = readinput('input.i') #stuff to print throughout
    directories.append("Det"+str(number_detectors[det])+"PE"+str(poly_thick[det])+"R"+str(cyl_radius[det]))
    makedirectory(directories[det])
    names = []
    for source in source_list:

        #open a file for each source
        names.append(source+".i")
        ifile = open(source+".i", "w")
        initialfile_counter = 0 # keeps track of where you are in the prebuilt input file
        initialfile_counter = initial_printer(ifile, initialfile, initialfile_counter) #returns
            #where you are at in the file, after the "*" break, see function for more details
        li_front = ([],[]) #[surface numbers], [locations in x plane], front is front of li cell
        li_back = ([],[]) #back of li cell
        cd_front = ([],[])
        li_cells = []
        poly_cells = []
        poly_cells_annulus=[]
        cd_cells = []
        cd_back = ([], [])
        board_cells = []

    #Create surfaces of the detector, front surfaces 100's, back 1100's, cd front 200's, cd back 1200's
    for i in range((number_detectors[det])):
        #front of detectors
        if (i==0):
            li_front[1].append(detector_start) #create the initial surface
        else:
            li_front[1].append(li_front[1][-1]+poly_thick[det]) #start of the current detector

        #other surfaces - each one is a thickness offset by the thickness of the last detector
        li_back[1].append(li_front[1][-1]+li_thick)
        cd_front[1].append(li_back[1][-1]+board_thick)
        cd_back[1].append(cd_front[1][-1]+cd_thick)

```

```

#create surface numbers and cell numbers for all surfaces
# --- cd cells: 500, polycells around detectors 11, 21, etc, licells: 10, 20, 30.., board_cells: 600's,
# poly behind cd: 400's---
for i in range((number_detectors[det])):
    li_front[0].append(100+i)
    li_back[0].append(1100+i)
    cd_front[0].append(200+i)
    cd_back[0].append(1200+i)
    cd_cells.append(500+i)

    #label detectors in increments of 10
    li_cells.append(10*(i+1))
    poly_cells_annulus.append(10*(i+1)+1) #annulus of HDPE around the lithium and board
    poly_cells.append(400+i)
    board_cells.append(600+i)

#add one more li_cell that is equal to the back of the detector
li_front[0].append(li_front[0][-1]+1)
li_front[1].append(li_front[1][-1]+poly_thick[det])

#print the cell cards:
# *****

#DEBUG: Different for if you want a poly sheet in back or not
poly_sheet = False
if(not poly_sheet):
    print poly_cells.pop(-1) #DEBUG is there a poly sheet in back or not
    li_front[1][-1] = li_front[1][-2]+cd_thick+board_thick+li_thick

#determine the array_width, the width of the RPP that holds all the poly
array_width = li_front[1][-1] - li_front[1][0]

#print the Li regions, board, and the poly around them
imp = 1.0
ifile.write("c ---- detector chunks, breadboards, and surrounding poly annuli ----\n")
for cell in range(number_detectors[det]):
    #print detector
    printer(ifile, [li_cells[cell], mat_li, str(dens_li), " "], 4)
    printer(ifile, [li_front[0][cell], -1*li_back[0][cell], -1*det_box], 6)
    ifile.write("    imp:n=%6.2f    $detector at %.0f cm \n" % (imp, li_front[1][cell]-100))

    #print bread board
    printer(ifile, [board_cells[cell], mat_board, str(dens_board), " "], 4)
    printer(ifile, [li_back[0][cell], -1*cd_front[0][cell], -1*board_box], 6)
    ifile.write("    imp:n=%6.2f    $breadboard at %.0f cm \n" % (imp, li_front[1][cell]-100))

    #print poly annuli outside of the lithium and breadboard
    if (cell == 0):
        printer(ifile, [poly_cells_annulus[cell], "0", " ", " "], 4)
        printer(ifile, [li_front[0][cell], -1*cd_front[0][cell], -1*outer_cyl, "("+str(det_box)+" "+
            str(-1*li_back[0][cell])+"):"+str(board_box)+""), 4)
        ifile.write("imp:n=%6.2f    $Voided annulus at %.0f cm \n" % (imp, li_front[1][cell]-100))
    else:
        printer(ifile, [poly_cells_annulus[cell], mat_hdpe, str(dens_hdpe)+"00", " "], 4)
        printer(ifile, [li_front[0][cell], -1*cd_front[0][cell], -1*outer_cyl, "("+str(det_box)+" "+
            str(-1*li_back[0][cell])+"):"+str(board_box)+""), 4)
        ifile.write("imp:n=%6.2f    $HDPE annulus at %.0f cm \n" % (imp, li_front[1][cell]-100))

#print the Cd behind the detectors
ifile.write("c ---- Cd slices behind detectors ----\n")
imp= 1.0
for cell in range(len(cd_cells)):
    printer(ifile, [cd_cells[cell], mat_cd, str(dens_cd)+"00", " "], 4)
    printer(ifile, [cd_front[0][cell], -1*cd_back[0][cell], -1*outer_cyl], 6)

```

```

        ifile.write("        imp:n=%6.2f    $cd slice behind detecor %d \n" % (imp, cell+1))

#print poly between cd and next detector
ifile.write("c ---- poly cylinders behind Cd ----\n")
imp = 1.0

for cell in range(len(poly_cells)):
    printer(ifile, [poly_cells[cell], mat_hdpe, str(dens_hdpe)+"00", "  "], 4)
    printer(ifile, [cd_back[0][cell], -1*li_front[0][cell+1], -1*outer_cyl], 6)
    ifile.write("        imp:n=%6.2f    $HDPE cylinder behind detecor %d \n" % (imp, cell+1))

#print the graveyards
ifile.write("c ---- graveyard and neutron beam ----\n")
printer(ifile, ["1", "0", "  ", 10, -1*li_front[0][0], -1*outer_cyl, "        imp:n=1",
    "$ void before spectrometer"], 4)
ifile.write("\n")
printer(ifile, ["999", "0", "  ", str(outer_cyl)+":"+str(-10)+":"+str(li_front[0][-1]),",",
    "        imp:n=0", "$ graveyard/problem boundary\n"], 4)

#print blank line at end of cells
ifile.write("\n")

#print the surface cards:
# *****

#print Some initial geometry that is fixed for each problem
initialfile_counter = initial_printer(ifile, initialfile, initialfile_counter)

printer(ifile, [outer_cyl, "CX", cyl_radius[det], "  "], 4)
ifile.write("        $ cylindrical surface of spectrometer\n")
printer(ifile, [det_box, "RPP", detector_start, array_width+li_front[1][0], "-1 1  -1 1"], 4) #
#box from start of detector, to end of last poly sheet, and 4cm^2 front centered along x-axis
ifile.write(" $ square box for detector edges (2x2square)\n")
#print the box for the breadbox of the array
printer(ifile, [board_box, "RPP", detector_start, array_width+li_front[1][0], -1*board_width,
    board_width, -1*board_width, board_width], 4)
ifile.write(" $ square box for PCB edges (%.1fx%.1square)\n" % (board_width, board_width))

#print front detector faces
ifile.write("c --- vertical slices thru the spectrometer I (front detector surfaces) ---\n")
for surf in range(len(li_front[0])):
    printer(ifile, [li_front[0][surf], "px", li_front[1][surf], "  "], 5)
    if (surf == len(li_front[0])-1):
        ifile.write("$back of last sheet of poly/spectr\n")
    else:
        ifile.write("$front of detector %d\n" % (surf))

#print back detector faces
ifile.write("c --- vertical slices thru the spectrometer II (back detector surfaces) ---\n")
for surf in range(len(li_back[0])):
    printer(ifile, [li_back[0][surf], "px", li_back[1][surf], "  "], 5)
    ifile.write("$back of detector %d\n" % (surf))

#print cadmium faces
ifile.write("c --- vertical slices thru the spectrometer III (Cd slices) ---\n")
for surf in range(len(cd_back[0])):
    printer(ifile, [cd_front[0][surf], "px", cd_front[1][surf], "  "], 5)
    ifile.write("$front cd of detector %d\n" % (surf))
    printer(ifile, [cd_back[0][surf], "px", cd_back[1][surf], "  "], 5)
    ifile.write("$back cd of detector %d\n" % (surf))

#print new line for end of block 2:
ifile.write("\n")

#print block 3
#*****

```

```

#print the source spatial definition
initialfile_counter = initial_printer(ifile, initialfile, initialfile_counter)
ifile.write("SI2 0 %.2f          $ radial sampling range: 0 to Rmax\n" % float(cyl_radius[det]))

#print the source energy distribution:
source_data = source_printer.get_source("source_list.txt", source)
source_printer.print_source(ifile, source_data, source_erg_dist)

#print some physics settings
initialfile_counter = initial_printer(ifile, initialfile, initialfile_counter)

#print detector:
ifile.write("F4:N ")
for cell in li_cells:
    ifile.write("%d " % cell) #print each of the detector cells
ifile.write("\nTF4 %d 7j\n" % len(li_cells)) #tells the tally fluctuation chart to optimize
#the last detector cell (the normalization cell), the 7j just means skip all the other
#entries, necessary for the card used

#print the rest of the detector and the material cards
initialfile_counter = initial_printer(ifile, initialfile, initialfile_counter)

ifile.close()

# RUN PARTICLE BALANCE ON EACH FILE TO GET THE CORRECT IMPORTANCE FUNCTION FOR EACH:
# *****
importance_fn.particle_balance(names[-1], cd_cells, [li_cells, poly_cells, poly_cells_annulus,
    board_cells], 300000, 'n', 1.00, hydra_check) #names[-1] is curent source file name, li_cells
    #is the ones being balance, particle type is , hydra_check is whether or not this is a hydra run
    #also case sensitive

#move the source files to the correct directory so you dont overwrite them
move_dir(source+".i", directories[det]) #store files

#append name
all_source_names.append(names)

#create an output list of all the directories
print directories
directories_file = open("directories.txt", "w")
for derp in directories:
    directories_file.write(derp+"\n")
directories_file.close()

if (hydra_check == True):
    count = 0
    for i in directories:
        for name in names:
            count +=1
            print "Running file: %s/%s, file %i of %i" % (i, name, count, len(directories)*len(names))
            hydra_run.hydra_mcnp_run(name, i, "same", num_nodes, auto_rerun = True, tallies = ["4"])
            #^^^i is directory of files, "same" for no output directory, auto rerun reruns if not
            # enough particles, tallies is which to make sure converged

else: #Local run with batch files on 4 processors
    break_check = True
    make_batch(all_source_names, directories)

if __name__ == "__main__":
    main()

```


input.i: Sample Input to spectrometer_maker.py

```
SPC8: Detectors every 3 cm in 30 cm x 20 cm-dia spectrometer
c A cylinder of polyethylene is used as neutron spectrometer.
c At various distances into cylinder square perforated neutron
c detectors (2x2 cm) are placed perpendicular to the axis. Behind
c each detector is a 1 mm disk of cadmium extending to the edge of
c the poly cylinder.
c
c ***** BLOCK 1: CELL CARDS *****
c GEOMETRY:
c * BREAK LINE FOR PYTHON
c ***** BLOCK 2: SURFACE CARDS *****
10 px -10          $ left problem boundary
c *
c ***** BLOCK 3: DATA CARDS *****
c
c ----- Source: disk source, different erg dist. for each file -----
SDEF   ERG=d1   PAR=1 VEC= 1 0 0 DIR=1 POS 0 0 0
      AXS=1 0 0 rad=d2 EXT=0
SP2 -21 1          $ weighting for radial sampling: her r^1
c * BREAK LINE FOR PYTHON
c ----- Problem parameters
mode n
nps 200000000
c
c ----- total thermal flux detector
c * BREAK LINE FOR PYTHON
c -----
c modify tallies to give no. (n,t) reactions per source neutron
c C=[(rho Na/A)x10^(-24) atom/(b-cm)] x Vol_detector
c for Li-6 to stop 50% of neutrons in .1 cm, density ~ 0.0835 g/cm^3
c Vol_det = 0.4 cm^3 ( 2 x 2 x .1 cm)
c find that C=0.0033286
c -----
FC4 tally modified to (n,t) reactions per source neutron
FM4 0.0033286 2 105
c
c ----- MATERIALS
c -----
c material: polyethylene d=0.95 g/cm^3
c -----
m1 1001 2
    6000 1
mt1 poly.01
c
c -----
c material: Li-6F nominal d=2.7 g/cm^3
c ignore F: Li-6 in LiF has a density of 0.6131 g/cm^3
c -----
m2 3006 1
c
c -----
c cadmium nominal density 8.65 g/cm^3
c -----
m3 48000 1
c
c -----
c Printed circuit board...still need this one
c
m4 5010 1
```

source_printer.py: Module for Source Distributions

```
import re
import os

# This is a function that will open a file of sources listed and find the
# source desired and print its distribution to a file with a particular
# distribution number. The sources should be found in the file by having: *
# source_name, including the *, as the line before the source distribution
# information. The source info is for the source energy distribution and the
# distribution number should be included, but will be disregarded when the info
# is read in. the name of the source file is also passed in.
#
# Note, could be easily modified to handle material properties

#find the source and read in its data to a list. NOTE: this data has the Dn and Pn # still in it,
#the calling function must get rid of these
def get_source(source_filename, source_name):

    source_file = open(source_filename, "r")
    source_flag = False
    source_data = []
    #search the file for the line containing the source name

    for line in source_file:
        if(not source_flag):
            if(search_for(line, source_name)):
                line_data = line.split()
                if(line_data[0] == "#"):
                    source_flag = True
            else: #in a source region
                if(search_for(line, "END")): #terminates each source
                    line_data = line.split()
                    if(line_data[0] == "#"):
                        source_file.close()
                        return source_data
                else:
                    source_data.append(line)
    source_file.close()

#print source_data to file output_file, with energy distribution given by distribution_number
def print_source(output_file, source_data, distribution_number):
    for line in source_data:
        if search_for(line, "[^s]+[iI]\d+"): #find lines that have SI in them and change the dist number
            m = re.search("[^s]+[iI]\d+", line)
            line = line[:m.start()] + line[m.end():]
            line = "SI" + str(distribution_number) + line
        elif search_for(line, "[^s]+[pP]\d+"):
            m = re.search("[^s]+[pP]\d+", line)
            line = line[:m.start()] + line[m.end():]
            line = "SP" + str(distribution_number) + line
        elif search_for(line, "[^s]+[bB]\d+"):
            m = re.search("[^s]+[bB]\d+", line)
            line = line[:m.start()] + line[m.end():]
            line = "SB" + str(distribution_number) + line
        output_file.write(line) #print each line to the file :D

#searchs a line for a string, returns true if found, else false
def search_for(line, string):
    pattern = re.compile(str(string))
    if (pattern.search(line)):
        return True
    else:
        return False
```

source_list.txt: Input for source_printer.py

```
# cfd2o
c UN PG 82 ISO SOURCE 8529 IS ORIGINAL REFERENCE
c ---- source is for a Cf-252 _D20 moderated (UN-403 p. 82)
SI1 H 0.0 0.2150E-06 0.4640E-06 0.1000E-05 0.2150E-05
      0.4640E-05 0.1000E-04 0.2150E-04 0.4640E-04 0.1000E-03
      0.2150E-03 0.4640E-03 0.1000E-02 0.2150E-02 0.4640E-02
      0.1000E-01 0.1260E-01 0.1580E-01 0.2000E-01 0.2510E-01
      0.3160E-01 0.3980E-01 0.5010E-01 0.6310E-01 0.7940E-01
      0.1000E+00 0.1260E+00 0.1580E+00 0.2000E+00 0.2510E+00
      0.3160E+00 0.3980E+00 0.5010E+00 0.6310E+00 0.7940E+00
      0.1000E+01 0.1260E+01 0.1580E+01 0.2000E+01 0.2510E+01
      0.3160E+01 0.3980E+01 0.5010E+01 0.6310E+01 0.7940E+01
      0.1000E+02 1.5807E+01
SP1 D 0.0 0.0 0.1838E-01 0.1850E-01 0.1883E-01 0.1969E-01
      0.2150E-01 0.2564E-01 0.3346E-01 0.3954E-01 0.4271E-01
      0.4907E-01 0.5275E-01 0.5970E-01 0.5330E-01 0.6534E-01
      0.2020E-01 0.2025E-01 0.2154E-01 0.1990E-01 0.1930E-01
      0.1919E-01 0.1926E-01 0.1912E-01 0.1833E-01 0.1739E-01
      0.1650E-01 0.1539E-01 0.1494E-01 0.1342E-01 0.1273E-01
      0.1052E-01 0.6375E-02 0.1255E-01 0.1360E-01 0.1135E-01
      0.1172E-01 0.1656E-01 0.2011E-01 0.2725E-01 0.2717E-01
      0.1774E-01 0.1784E-01 0.1195E-01 0.6157E-02 0.2445E-02
      0.7821E-03
# END

# pube
c Pu-238Be spectrum: Lehman (Ryan T-A.4)
SI1 H 0.250 0.500 0.750 1.250 1.500
      1.750 2.000 2.375 2.875 3.000
      3.500 4.250 4.500 5.000 5.250
      5.500 5.750 6.000 6.250 6.500
      7.125 7.625 8.000 8.375 8.750
      9.125 9.625 10.000 10.380
SP1 D 0.0 0.3421E-01 0.2955E-01 0.5288E-01 0.2384E-01
      0.1970E-01 0.2384E-01 0.4510E-01 0.5183E-01 0.1892E-01
      0.1068E+00 0.1151E+00 0.4250E-01 0.1099E+00 0.3836E-01
      0.3006E-01 0.2695E-01 0.1970E-01 0.1451E-01 0.1348E-01
      0.4277E-01 0.3732E-01 0.3266E-01 0.2100E-01 0.1244E-01
      0.6998E-02 0.1244E-01 0.1089E-01 0.6303E-02
# END

# ambe
c ---- source is for a AmBe (alpha,n) (UN-403 p. 82)
SI1 H 0.0 0.1000E+00 0.1260E+00 0.1580E+00 0.2000E+00
      0.2510E+00 0.3160E+00 0.3980E+00 0.5010E+00 0.6310E+00
      0.7940E+00 0.1000E+01 0.1260E+01 0.1580E+01 0.2000E+01
      0.2510E+01 0.3160E+01 0.3980E+01 0.5010E+01 0.6310E+01
      0.7940E+01 0.1000E+02 0.1580E+03
SP1 D 0.0 0.0 0.3838E-02 0.5003E-02 0.6767E-02
      0.8339E-02 0.1071E-01 0.1332E-01 0.1625E-01 0.1957E-01
      0.2209E-01 0.2446E-01 0.2728E-01 0.2875E-01 0.4268E-01
      0.5521E-01 0.9698E-01 0.1318E+00 0.1579E+00 0.1500E+00
      0.1329E+00 0.3830E-01 0.7870E-02
# END

# cf252mcpn
SP1 -3 1.025 2.926 $ Watt distn for f-252
# END

# pubers
c source is for a PuBe + room scat (UN-403 p 106)
SI1 H 0.0 0.1000E-07 0.2150E-07 0.4640E-07 0.1000E-06
      0.2150E-06 0.4640E-06 0.1000E-05 0.2150E-05 0.4640E-05
```

```

0.1000E-04 0.2150E-04 0.4640E-04 0.1000E-03 0.2150E-03
0.4640E-03 0.1000E-02 0.2150E-02 0.4640E-02 0.1000E-01
0.1260E-01 0.1580E-01 0.2000E-01 0.2510E-01 0.3160E-01
0.3980E-01 0.5010E-01 0.6310E-01 0.7940E-01 0.1000E+00
0.1260E+00 0.1580E+00 0.2000E+00 0.2510E+00 0.3160E+00
0.3980E+00 0.5010E+00 0.6310E+00 0.7940E+00 0.1000E+01
0.1260E+01 0.1580E+01 0.2000E+01 0.2510E+01 0.3160E+01
0.3980E+01 0.5010E+01 0.6310E+01 0.7940E+01 0.1000E+02
0.1580E+02
SP1 D 0.0 0.6186E-02 0.7848E-02 0.1006E-01 0.1118E-01
0.1062E-01 0.7626E-02 0.5842E-02 0.4809E-02 0.3740E-02
0.3131E-02 0.2039E-02 0.2028E-02 0.1577E-02 0.1308E-02
0.1060E-02 0.1011E-02 0.9771E-03 0.1021E-02 0.3352E-03
0.3690E-03 0.3867E-03 0.3907E-03 0.4330E-03 0.4938E-03
0.5340E-03 0.6115E-03 0.7768E-03 0.9575E-03 0.1181E-02
0.1453E-02 0.1898E-02 0.2317E-02 0.3432E-02 0.3692E-02
0.5824E-02 0.8122E-02 0.1142E-01 0.1816E-01 0.2774E-01
0.2761E-01 0.5635E-01 0.9223E-01 0.1053E+00 0.1576E+00
0.1372E+00 0.1308E+00 0.1066E+00 0.1200E-01 0.1546E-02
0.1565E-03

```

END

triga

c West and Larsen's TRIGA reflector spectrum (Ryan T-A.7)

```

SI1 H 0.1000E-07 0.2600E-07 0.6000E-07 0.1400E-06 0.2600E-06
0.4200E-06 0.6500E-06 0.1000E-05 0.3060E-05 0.2260E-04
0.1670E-03 0.1230E-02 0.9120E-02 0.2480E-01 0.6740E-01
0.1830E+00 0.4980E+00 0.8210E+00 0.1350E+01 0.2230E+01
0.3680E+01 0.4720E+01 0.6070E+01 0.7790E+01 0.1000E+02
SP1 D 0.0 0.2233E+00 0.2938E+00 0.2198E+00 0.1970E-01
0.3519E-02 0.2615E-02 0.2401E-02 0.1444E-01 0.4812E-01
0.4836E-01 0.4373E-01 0.3909E-01 0.7676E-02 0.7377E-02
0.7661E-02 0.9298E-02 0.2379E-02 0.2445E-02 0.2404E-02
0.1343E-02 0.1892E-03 0.2311E-03 0.7431E-04 0.6805E-05

```

END

puo2

c source is for a PuO2 (UN-403 p 106)

```

SI1 H 0.0 0.1000E-06 0.2150E-06 0.4640E-06 0.1000E-05
0.2150E-05 0.4640E-05 0.1000E-04 0.2150E-04 0.4640E-04
0.1000E-03 0.2150E-03 0.4640E-03 0.1000E-02 0.2150E-02
0.4640E-02 0.1000E-01 0.1260E-01 0.1580E-01 0.2000E-01
0.2510E-01 0.3160E-01 0.3980E-01 0.5010E-01 0.6310E-01
0.7940E-01 0.1000E+00 0.1260E+00 0.1580E+00 0.2000E+00
0.2510E+00 0.3160E+00 0.3980E+00 0.5010E+00 0.6310E+00
0.7940E+00 0.1000E+01 0.1260E+01 0.1580E+01 0.2000E+01
0.2510E+01 0.3160E+01 0.3980E+01 0.5010E+01 0.6310E+01
0.7940E+01 0.1000E+02 0.1580E+02 0.2510E+02
SP1 D 0.0 0.2328E+00 0.1123E+00 0.2135E-01 0.9035E-01
0.1423E-01 0.1068E-01 0.8039E-02 0.5817E-02 0.3994E-02
0.3568E-02 0.2778E-02 0.2166E-02 0.1715E-02 0.2139E-02
0.2850E-02 0.8854E-03 0.9530E-03 0.1191E-02 0.1343E-02
0.1587E-02 0.1848E-02 0.2169E-02 0.2677E-02 0.3402E-02
0.4499E-02 0.6034E-02 0.8149E-02 0.1193E-01 0.1631E-01
0.2350E-01 0.3323E-01 0.4328E-01 0.5031E-01 0.4574E-01
0.4453E-01 0.4022E-01 0.3712E-01 0.2546E-01 0.1254E-01
0.1776E-01 0.8123E-02 0.1278E-02 0.7384E-02 0.8090E-02
0.9691E-02 0.6772E-02 0.7130E-02 0.7839E-04

```

END

fusion

c ----- 14.1 MeV neutron source

SI1 L 14.1

SP1 D 1.0

END

```
# 50kev
c ----- 50 keV monoenergetic source
SI1 L 5.0E-02
SP1 D 1.0
# END
```

```
# 1mev
c ----- 1 MeV monoenergetic source
SI1 L 1.0
SP1 D 1.0
# END
```

```
# 100ev
c 100 ev monoenergetic
c ----- 100 eV monoenergetic source
SI1 L 1.0E-04
SP1 D 1.0
# END
```

importance_fn.py: Script for Automatic Cell Splitting

```
import shutil # for copying files
import os # for directories and chmod etc.
import stat # for chmoding to user access
import subprocess # for running programs
import re # for regexps
import hydra_run #for hydra runs

#searchs a line for a string, returns true if found, else false
def search_for(line, string):
    pattern = re.compile(str(string))
    if (pattern.search(line)):
        return True
    else:
        return False

#Runs MCNP for a given file and moves them to some output directory w/ same name as input file
#-MPI RUN
def mcnp_run_hydra(name):
    output_name_final = name #store file name
    output_name_final = output_name_final.replace(".i", ".o")
    output_name = "temp_pb.o"
    if os.path.exists(output_name):
        print "I DELETED A FILE!"
        os.remove(output_name)
    temp_string = "mpirun -n 16 /usr/local/bin/mcnp5.mpi"+" i=" + name + " o=" +
    output_name + " xsdir=/usr/local/data/MCNPDATA/xsdir"
    print temp_string
    #subprocess.check_call(temp_string) #run mcnp with output file name temp.o
    os.system(temp_string)
    if os.path.exists(output_name_final): #checks to make sure ouptut file name not already there
        print "I DELETED A FILE!"
        os.remove(output_name_final)
    os.rename(output_name, output_name_final) #change name to name of input with .o extension
    eraser_hydra()

#Deletes all teh mcnp worhtless files
def eraser_hydra():
    os.system("rm"+" runt*") #remove runtape files

#LOCAL RUN
def mcnp_run(name):
    output_name_final = name #store file name
    output_name_final = output_name_final.replace(".i", ".o")
    output_name = "temp_pb.o"
    if os.path.exists(output_name):
        print "I DELETED A FILE!"
        os.remove(output_name)
    temp_string = "mcnp5"+" i=" + name + " o=" + output_name
    subprocess.check_call(temp_string) #run mcnp with output file name temp.o
    if os.path.exists(output_name_final): #checks to make sure ouptut file name not already there
        print "I DELETED A FILE!"
        os.remove(output_name_final)
    os.rename(output_name, output_name_final) #change name to name of input with .o extension
    eraser()

#Deletes all teh mcnp shit files
def eraser():
    temp_file = open("eraser.bat","w")
    temp_file.write("erase runt*")
    temp_file.close()
    subprocess.check_call("eraser.bat") #remove runtape files
    os.remove("eraser.bat")
```

```

#performs the particle_balance to determine importance fn, also truncates if there is a jump of more than 4
#
# particle type is either "n", or "p" for neutron or photon, respectively double_cells is a list of lists
# of cells that will have same importance as there corresponding neighbor in the imp_cells list
# normalization is the number of the cell of least importance (most number of counts, therefore normalized
# to it), later in the function it is set to be the index of said cell.

def particle_balance(original_filename, imp_cells, double_cells, NPS, particle_type, initial_importance, hydra):

    #change particle type for search patterns
    #DEBUG DEBUG

    #open input file
    original_file = open(original_filename, "r")
    #name of particle balance file
    balance_name = "dragonfly.i"
    ifile = open(balance_name, "w")
    flag = False
    for line in original_file:
        if ((search_for(line, "^(NPS)|(nps)|(Nps)")) or (search_for(line, "^(ctme)|(CTME)"))):
            ifile.write("NPS " + str(NPS)+"\n")
            flag = True
        else:
            ifile.write(line)
    if (not flag):
        ifile.write("NPS" + str(NPS))
    ifile.close()

    #run mcnp for the quick file to get a rough particle balance
    if (hydra):
        mcnp_run_hydra(balance_name)
    elif (not hydra):
        mcnp_run(balance_name)
    os.remove(balance_name) #delete quick file

    #open output file and look for cell balance
    out_file = open(balance_name.replace(".i", ".o"), "r")
    flag = False
    cell_data = []
    for line in out_file:
        if (search_for(line, "population\s+collisions\s+")): #found start of particle balance stuff
            flag = True
        elif(search_for(line, "\s+total\s+")): # found end of particle balance stuff
            flag = False
        else:
            if(flag):
                if(search_for(line, "\s*\d+\s+")):
                    cell_data.append(line)

    #Loop through all the imp_cells, and if they match one of them, append the population to a list. Normalize
    #to the least important cell.
    imp_function = []
    maximum = 0
    print imp_cells
    for cell in imp_cells:
        for line in cell_data: #loop through all the data
            line_data = line.split()
            if(line_data[1] == str(cell)): #found a population of a correct cell
                imp_function.append(line_data[3]) # add population of that cell
                if (float(line_data[3]) > float(maximum)): #find the biggest one
                    maximum = line_data[3]
                normalization_index = len(imp_function) - 1

    #now normalize

```

```

temp_list = []
for value in range(len(imp_function)):
    try:
        check = float(initial_importance)*float(imp_function[normalization_index])/float(imp_function[value])
        #initial importance is what the cell was originally incase there is other cell splitting already done
    except ZeroDivisionError:
        if temp_list != []:
            check = temp_list[-1]
        else:
            check = 1.0

    if (value !=0):
        if (check/temp_list[-1] < 4):
            temp_list.append(check)
        elif(check > 9999):
            temp_list.append(9999)
        else:
            temp_list.append(4*temp_list[-1])
    else:
        temp_list.append(check)
imp_function = temp_list

#make less digits so it doesnt print a bunch of numbers:
temp_list = []
for i in imp_function:
    if(i < 10.0):
        i = '%.2f' % i
        temp_list.append(i)
    elif(i > 10.0 and i < 1000):
        i = '%.1f' %i
        temp_list.append(i)
    else:
        i = str(int(i))
        temp_list.append(i)
#overwrite:
imp_function = temp_list
print imp_function

#delete output file
out_file.close()
#open a temp input file that will eventually over write actual input file
temp_name = 'derpalerp.i'
ifile = open(temp_name, "w")

#read in all the lines of original_file and over write the old importances with the new ones
double_cells.append(imp_cells) #make a list of lists of cells so that you can check all at once
master_list = double_cells
imp_string = "imp:" + particle_type + "="

#make sure all the doubles_cells lists have the same name, if not you add a number tha tis fake.
#This is for the case that there is not poly behind the last detector so that the loops come out right:
for i in range(len(master_list)):
    for j in master_list:
        if (len(master_list[i]) < len(j)):
            master_list[i].append("999999999")
            print "i added a cell"
            print master_list[i], j
        else:
            continue

#repopen the original_file to start from beginning
original_file.close()
original_file = open(original_filename, "r")
for line in original_file:
    if( search_for(line, imp_string+"\s*\d+\.\d+")): #found a cell line
        printed_cell_flag = True

```



```

for cell_list in master_list: # loop through all the possible lists
    for i in range(len(cell_list)): # loop through all the possible cells in lists
        if (line.split()[0] == str(cell_list[i])): #one of the possible cells has been found,
            ifile.write(re.sub(imp_string+"\s*\d+\.\d+", imp_string+str(imp_function[i]), line))
            printed_cell_flag = False
    if printed_cell_flag:
        #If cell was just not one of the ones being balanced then you need to write it to the file
        ifile.write(line)

else:
    ifile.write(line)

#overwrite files
original_file.close()
ifile.close()
os.remove(original_filename)
os.rename(temp_name, original_filename)
os.remove(balance_name.replace(".i", ".o"))

```

hydra_run.py: Script for Running MCNP5 simulations

```
import os
import subprocess
import re
import shutil
import time
from FOM_output import Tally

#UPDATE: 01172013. The main has been updated to just run with autorerun activated, all the
#.i files in current directory. If you want use auto rerun you would need to change the tallies
#to list all tallies of interest, it is currently only set #for the tally 4, which was used for spectrometer.

#moves file to a directory OVERWRITING any files in the way
def move_dir(file_name, dir):
    os.chdir(dir)
    if os.path.exists(file_name):
        print "IM IN YOUR DIRECTORY DELETING YOUR FILES!"
        os.remove(file_name)
    os.chdir("../")
    shutil.move(file_name, dir)

#The following code checks an output to make sure a certain tally is converged or not
def check_statistics(output_name, tallies):

    #Get the errors if there are any from FOM_output module
    tally = Tally() #initialize a variable that will find all tallies in a file
    tally.clear_all() #
    tally.tally_file = output_name #name of the tally
    tally.get_tallies(output_name) #find all the tallies in a file with name of file and get data about them

    #check all errors to see if any missed
    for err in tally.errors:
        for line in err:
            for cell in tallies:

                # check for name in errors
                if re.match("^\\s+"+str(cell)+"\\s+missed", line):
                    return False

    #if not fails return True
    return True

#Runs MCNP for a given file and moves them to some output directory w/ same name as input file
def hydra_mcnp_run(name, input_direct, directory, num_nodes, auto_rerun = True, tallies = None):

    flag = False
    if os.path.exists(input_direct):
        os.chdir(input_direct)
        flag = True
    output_name_final = name #store file name
    output_name_final = output_name_final.replace(".i", ".o")
    output_name = "tempr.o" #Temp output name

    #Remove temp file if it exists
    if os.path.exists(output_name):
        print "I removed the temp file on first pass"
        os.remove(output_name)
    eraser()
```

```

if os.path.exists("runtpe"):
    os.remove("runtpe")

if os.path.exists(output_name):
    print "I DELETED A FILE!"
    os.remove(output_name)

#make python wait

time.sleep(2)

temp_string = "mpirun -n " + str(int(num_nodes)) + " /usr/local/bin/mcnp5.mpi "
temp_string += "i=" + name + " o=" + output_name + " xsdir=/usr/local/data/MCNPDATA/xsdir"
os.system(temp_string) #run mcnp in parallel with output file name temp.o

if (auto_rerun):
    if tallies == None:
        raise IOError("YOu need to include tallies if you are trying to check convergence")
    else:

        if not (check_statistics(output_name, tallies)):

            #Get the number of particles ran:
            temp_in = open(name, "r")
            nps_new = None

            #look through file till you find NPS card
            for line in temp_in:
                if re.search("^\s*(NPS|nps|Nps)\s+(\d+)", line):

                    m = re.search("\s*\w+\s+(\d+)", line)
                    nps_new = m.group(1)
                    print nps_new

            if nps_new == None:
                raise ValueError("IN hydra_run.py need to add a better catch line for nps or CTME")

#Need to rerun the problem, only try 5 times, each time run 20% more particles
for attempt in range(5):

    nps_new = int(float(nps_new) * 1.2)
    print nps_new

    #Create continuation run file
    cont_f = open("cont.i", "w")
    cont_f.write("CONTINUE\n")
    cont_f.write("NPS %i\n" % nps_new)
    cont_f.close()

    #clear out old output:
    print os.listdir(".")
    os.remove(output_name)
    if os.path.exists(output_name):
        os.system("rm %s" % output_name)

    #Make python wait
    print "waiting 2 seconds..."
    time.sleep(2)

    temp_string = "mpirun -n " + str(int(num_nodes)) + " /usr/local/bin/mcnp5.mpi "
    temp_string += "i=cont.i c o=" + output_name + " r=runtpe" +
        " xsdir=/usr/local/data/MCNPDATA/xsdir"
    print temp_string

```

```

        os.system(temp_string)
        os.remove("cont.i")

    if check_statistics(output_name, tallies):
        os.remove("runtpe")
        break

if os.path.exists(output_name_final): #checks to make sure ouput file name not already there
    print "I DELETED A FILE!"
    os.remove(output_name_final)
os.rename(output_name, output_name_final) #change name to name of input with .o extension
if os.path.exists(directory):
    move_dir(output_name_final, directory)
    move_dir(name, directory) #store files
eraser()
if flag:
    os.chdir("../")

#Deletes all teh mcnp shit files
def eraser():
    os.system("rm runt*")

#determine if hydra machine or not
def hydra_machine():
    print "Is this a hydra (0) or PC (1) run?: "
    hydra_flag = raw_input()
    if (hydra_flag == "0"):
        hydra_check = True
    else:
        hydra_check = False
    return hydra_check

def main():

    files = os.listdir(os.getcwd())
    derp = []

    for f in files:

        if re.search(".i$", f):

            derp.append(f)

    files = list(derp)

    num_nodes = raw_input("Input the number of nodes to use: ")

    for name in files:

        print "Running File "+name+", which is File %i of %i" % ((int(files.index(name))+1), len(files))

        hydra_mcnp_run(name, "nodirectorychange", "same", num_nodes, auto_rerun = True, tallies = ["4"])

if __name__ == "__main__":
    main()

```

run_fom.py: Control Script for Simulated Data and FOM calculations

```
# This module runs all the other codes to generate responses and fom results
# In the main it calls fom_comparison_format which calculates Theta

#UPDATE: 081412: Added the ability to run multiple trials and average results with statistical error

#UPDATE: 103012: Added ability to keep going if it fails. Also in fom_comparison_format changed
# a bug that was adding incorrect amounts to the average.

#Added ability to rerun file and only redo those that failed by default. Adding a -new
#to command line execution will initiate an overwrite of the old file

import shutil          # for copying files
import os              # for directories and chmod etc.
import stat            # for chmoding to user access
import subprocess     # for running programs
import re              # for regexps
import FOM_output     #gets outputs and prints htem as response functions
import time           # to tell program to wait
import fom_comparison_format
from sys import argv
import gc

#moves file to a directory OVERWRITING any files in the way
def move_dir(file_name, dir):
    os.chdir(dir)
    if os.path.exists(file_name):
        os.remove(file_name)
    os.chdir("..")
    shutil.move(file_name, dir)

def makedirectory(dir):
    if (not os.path.exists(dir)):
        os.mkdir(dir)
        os.chmod(dir, stat.S_IRWXU)
    else:
        os.chmod(dir, stat.S_IRWXU)

def main():

    # - - - - -
    #How many trials of results do you want to run and average?:
    num_trials = 1000
    nps = 2.E8      #number of histroies to scale to

    #changeable filenames:
    fom_name = "fom.exe"
    resp_name = "simul_resp.exe"
    src_str = "src_str.txt"
    fom_output = "FOM.out"

    #get the list of directories
    directories = []      #list of directories that contain output files
    completed_directories = [] #list of directories that have already been completed

    #If list of completed directories already exists, read in names from file
    if os.path.exists("completed_directories.txt"):

        if len(argv) > 1:
            if re.search("-n", argv[1]):
                #Will make new files later
                print "Creating new completed_directories file"
```

```

else:
    comp_dir_file = open("completed_directories.txt", "r")
    for line in comp_dir_file:
        if len(line) > 0:
            completed_directories.append(line.strip())

    comp_dir_file.close()
    comp_dir_file = open("completed_directories.txt", "a")

    print "The following directories are complete: "
    print completed_directories
    time.sleep(1.5)

else:

    comp_dir_file = open("completed_directories.txt", "w")

dir_list = os.listdir(os.getcwd())

for name in dir_list:
    if re.search("Det\d+PE", name.strip()):
        if os.path.isdir(name):
            directories.append(name.strip())

#rip the outputs from the files in each directory
#The main function will return a list of all the files in each one
file_list = []
print directories
for dir in directories:
    file_list.append(FOM_output.main(dir, scale=nps))

#create an initial 'irand' file which is used for the simulated response data as a random number seed
if os.path.exists('irand'):
    os.remove('irand')
irand = open('irand', "w")
irand.write("73907\n")
irand.close()

makedirs("FOM_outputs")

#open output file, if rerun (option "-n" not specified), then append to file, dont make new one,
#Else Make new one, also make new completed_directories file
if len(argv) > 1:
    if re.search("-n", argv[1]):
        outfile = open("FOM_outputs"+"-"+FOM_comparison.out", "w")
        comp_dir_file = open("completed_directories.txt", "w")
    else:
        outfile = open("FOM_outputs"+"-"+FOM_comparison.out", "a")

first_time = True
for dir in directories:

    #Skip directories that have already been completed
    if dir in completed_directories:
        continue

    #Initialize instance of class. Each Class recieves the same output file, and when called to print will
    #just print to the end of it
    all_data = fom_comparison_format.all_data(outfile, dir+".fomout")
    average_theta = []

    print "Comparing data for geometry: %s... " % dir

    for i in range(num_trials):

```

```

if i % int(0.1*num_trials) == 0:
    print "Completed %.0f%% of %i trials" % (100*float(i)/float(num_trials), num_trials)

if i == 0:

    shutil.copy(fom_name, dir)
    shutil.copy(resp_name, dir)
    shutil.copy(src_str, dir)
    move_dir('irand', dir)
    os.chdir(dir)

#run fom codes
if i % 900 == 0:
    time.sleep(2)
try:
    subprocess.check_call(resp_name)
    subprocess.check_call(fom_name)
except:
    print "HAD ONE FILE FAIL, DOES NOT AFFECT AVERAGE"
    time.sleep(1.0)
    continue

#change name of output and make copy in parent directory in folder "fom_results"
out_name_str = dir+".fomout"
if os.path.exists(out_name_str):
    try:
        os.remove(out_name_str)
    except:
        time.sleep(1.0)
        print "Waiting to delete file: ", out_name_str
        os.remove(out_name_str)

os.rename(fom_output, out_name_str)

#Get data
# - - - - -

all_data.parse()
average_theta.append(all_data.get_last_value(0))

if i == (num_trials - 1):

    #delete duplicate files
    os.remove(fom_name)
    os.remove(resp_name)
    os.remove(src_str)
    shutil.move('irand',"..") #move current random number seed back to parent directory
    shutil.copy(out_name_str, "../"+"FOM_outputs")

    #return to parent directory
    os.chdir("..")

else:

    #Need to remove all files that are not being kept, except on last trial
    try:
        #os.remove("FOM.plt")
        os.remove(out_name_str)
        os.remove("simul_resp.out")
    except:
        try:
            time.sleep(0.0001)
            os.remove("simul_resp.out")
            os.remove(out_name_str)
        except:
            continue

```

```

#averages output
averages_output = open("average.out","w")
for i in average_theta:
    averages_output.write("%f\n" % i)

all_data.average_results()

if first_time:
    first_time = False
    fp = None
else:
    fp = True

all_data.fprint(average=True, format=1, format_printed=fp)

#force so doesn't reuse same one, seems to be a wierd bug elsewhere
del all_data

gc.collect()

#Write out completed directories to a file, skip these directories if no errors
comp_dir_file.write(dir+"\n")

#when done get rid of 'irand' to not mess up the next time someone uses this code
os.remove('irand')
comp_dir_file.close()

if True:
    main()

```


fom_comparison_format.py: Data Utility Class

```
# Load local modules
# -----

import os
import re

# -----

#UPDATE: July 11 2012

#Added ability to generate many responses and average results

class all_data(object):
    """Each instance of this class contains all the data for all of the responses for one particular geometry.
    Averaging can be done more easily this way inside the class"""

    # - - - - -
    def __init__(self, outfile, infile_handle):

        #Get rid of the old data
        self.clear()

        self.outfile = outfile
        if self.outfile.closed:
            raise ValueError("Somehow you closed the file you passed in")

        self.file_name = infile_handle

        return None

    # - - - - -
    def clear(self):
        """Clears and initializes all data"""

        self.strength = []
        self.difference = []
        self.lowest_fom = []
        self.original_source = []
        self.closest_template = []
        self.smallest_template = []
        self.avg_eff = []
        self.not_matches = []
        self.outfile = None
        self.geometry = None
        self.diff_std_dev = None
        self.averaged = False
        self.format_printed = False

        self.functions_list = ["functions_list", "clear", "parse", "initialize_lists", "fprint",
                               "outfile", "file_name", "geometry", "average_results", "averaged",
                               "diff_std_dev", "format_printed"]

        self.file_name = None

        return None

    # - - - - -
    def initialize_lists(self, num_strengths):
        """makes all attributes be lists of the appropriate length so u can store data for each source strenght"""

        attributes = dir(self)

        #Get rid of the default functions
        temp_list = []
        for i in attributes:
```

```

        if not search_for(i, "__\S+__"):
            if i not in self.functions_list:
                temp_list.append(i)

        else:
            continue

    attributes = temp_list

    #Initialize each list
    for j in attributes:
        exec("self.%s = [ [] for i in range(num_strengths)] " % (j))

    return None

# - - - - -
def parse(self):
    """Reads in the data for a single geometry/configuration folder, and appends sorted data of it to each
    list. You can read in multiple sampling of the same geometry, but not different files

    The way it works is each item (e.g.) efficiency has a list for each source strength, then with in
    each source strength is a list for each trial. The last member is made the average eventually"""

    #open file passed in during init
    print "comparing data for:", self.file_name
    if self.file_name == None:
        raise ValueError("need to pass in a filename to be parsed")

    if (not search_for(self.file_name, ".fomout")):

        print self.file_name, "had no data"
        return None

    file_handle = open(self.file_name, "r")

    #Local variables.
    new_strength_flag = False
    temp_list = []
    counter_flag = 0
    first_time_flag = True
    efficiency = []
    strength = []
    difference = []
    lowest_fom = []
    closest_template = []
    smallest_template = []
    original_source = []
    avg_eff = []
    master_list = [] #Each member of list is for a specific energy

    for line in file_handle: #loop through all the lines in each file

        line_data = line.split()

        if search_for(line, 'c\*'):
            #Start of a new set of FOM data, figure out the actual source:

            source = line.split()[3]

            elif search_for(line, "total incident"):
                #Find and get the efficiency for this source strength

```

```

new_strength_flag = True
counter_flag = 0

#Reinitialize list for storing the first and second smallest FOM's:
temp_list = []
efficiency.append(line_data[14].rstrip('%'))
strength.append(line_data[10].strip())

elif search_for(line, 'c--+'):
    #All data has been read in for a particular source, now store it and reset lists

    if first_time_flag == True:
        #initialize the list of all results to have a slot for each source strength

        for i in strength:

            master_list.append([])
            avg_eff.append([])

        first_time_flag = False

    for each in range(len(strength)): #store each of the results, for each strength, then compare

        data_temp = [difference[each], strength[each], lowest_fom[each], original_source[each],
                    smallest_template[each], closest_template[each], efficiency[each]]
        master_list[each].append(data_temp)
        avg_eff[each].append(efficiency[each])

    # Organized by [difference[2], strength[2], smallest_template[2],
    #               closest_template[2], original_source[2], lowest_fom[2], efficiency[2]

    new_strength_flag = False
    temp_list = []
    counter_flag = 0
    efficiency = []
    strength = []
    difference = []
    lowest_fom = []
    closest_template = []
    smallest_template = []
    original_source = []

elif new_strength_flag:
    #Data for a new source strength

    #Counter flag is what line you are on in data for a particular source
    if (counter_flag <1):

        #Skip first line because it just contains the number of counts in each detector
        counter_flag +=1

    elif counter_flag < 3 :
        #Read in the top two lowest FOM scores

        if (search_for(line, "--ERROR:")): #when zero counts make sure it catches it by
            #setting diff to zero

            temp_list = [[0,0,0],[0,0,0]]
            temp_list[1][1] = 1.
            temp_list[0][1] = 1.
            temp_list[1][2] = 1.
            temp_list[0][0] = "ERROR: ZERO COUNTS"
            temp_list[1][0] = "ERROR: ZERO COUNTSNUMBER2"
            counter_flag = 80

        temp_list.append([line_data[0], line_data[2], line_data[4]])

```

```

        counter_flag += 1

    else:
        #have the data you need:
        #Templist[i] = [source type, FOM, std_dev]

        if (float(temp_list[1][1]) < 0.0001):
            #Make sure FOM not zero

            diff = 0.0
            source = "False Data, No counts in bins other than normaliz"

        else:

            diff = float(temp_list[1][1])-float(temp_list[0][1])
            diff = diff/float(temp_list[1][2])

        #Store data locally:

        difference.append(diff)
        original_source.append(source)
        lowest_fom.append(temp_list[0][1])
        smallest_template.append(temp_list[0][0])
        closest_template.append(temp_list[1][0])
        temp_list = []
        new_strength_flag = False

#Sort all the data for this file and append to the instance's lists
temp_master = []
for each in range(len(master_list)):

    temp_master.append(sorted(master_list[each], key = lambda diff: diff[0]))

#Compute the average efficiency
asum = 0.0
for num in avg_eff[each]:
    asum = asum + float(num)
avg_eff[each] = asum/float(len(avg_eff[each]))

master_list = list(temp_master)

#if necessary initialize lists to be same length as source strengths:
if self.strength == []:
    self.initialize_lists(len(master_list))

#determine the number of misses there are and store data:
for i in range(len(master_list)):

    if self.not_matches[i] == []:
        self.not_matches[i] = 0

    else:
        for data in master_list[i]:

            if not search_for(data[4], data[3].rstrip(".")) or data[0] < 0.000000001:

                master_list[i][master_list[i].index(data)][0] = 0.0
                #Not a match
                # print "adding to not matches"
                self.not_matches[i] +=1
                break #DEBUG TODO this break statement is for if you want to know that it failed
                    # in one "trial", somewhere, remove to know fails of all samples of all
                    # sources
            else:
                continue

```

```

#Store the worse case data:
for i in range(len(master_list)):

    self.avg_eff[i].append(avg_eff[i])
    self.difference[i].append(master_list[i][0][0])
    self.strength[i].append(master_list[i][0][1])
    self.lowest_fom[i].append(master_list[i][0][2])
    self.smallest_template[i].append(master_list[i][0][4])
    self.original_source[i].append(master_list[i][0][3])
    self.closest_template[i].append(master_list[i][0][5])

return None

# -----
def fprint(self, idx=None, average=None, format=None, format_printed=None):
    """Method that prints out to file nice and pretty. Only prints for case (geometry) specified by idx,
    but prints for all source strengths"""

    """format is used to print in special formats. Format == 1 prints it so that all of the data from
    the difference are printed for a single chi_sq value"""

    #Default to self.averaged:
    if average == None:
        average = self.averaged

    if format_printed != None:
        self.format_printed = format_printed

    #If not an averaged result
    if not average:

        self.outfile.write("\nc-----")
        self.outfile.write("\nc *** Geometry is: %s \n" % (self.file_name.strip()))

        #Default print the first one
        if idx == None:
            idx = 0

        self.outfile.write(" Source_Strength   Difference(in sigma's)   SmallestFOM"
            +" Source      Number Misses   Closest_Template   AvgEfficiency")

        for i in range(len(self.strength)):
            self.outfile.write("\n %13s %19.4f %19s %15s %11i %23s %18.4f%s" % (self.strength[i][idx],
                float(self.difference[i][idx]), self.lowest_fom[i][idx], self.original_source[i][idx],
                self.not_matches[i], self.closest_template[i][idx], (self.avg_eff[i][idx]),"%"))

    else:

        #If is an averaged result, just print the last one cause thats where the average is
        idx = -1

        if format == None or format == 0:

            self.outfile.write("\nc-----")
            self.outfile.write("\nc *** Geometry is: %s \n" % (self.file_name.strip()))
            self.outfile.write("Averaged Result:\n")
            self.outfile.write("Source_Strength   Difference(in sigma's)   Std Dev of Difference"
                +"SmallestFOM      Number Misses   AvgEfficiency")

            for i in range(len(self.strength)):
                self.outfile.write("\n %13s %19.4f %19.4f %18.3f %16.3f %18.4f%s" % (self.strength[i][idx],
                    float(self.difference[i][idx]), self.diff_std_dev[i], float(self.lowest_fom[i][idx]),
                    float(self.not_matches[i]), (self.avg_eff[i][idx]),"%"))

```

```

elif format == 1:
    #print the diference and the errors for each source strength in a column
    #for all thickness and such. Also print the thicknesses;

    if not self.format_printed:

        self.outfile.write("      GeometryName      Radius  No._Detectors  Thickness      ")

        #print the source strengths:
        for i in self.strength:
            self.outfile.write("Str:%8s_(n's) sig. number_miss " % i[0])

        self.outfile.write("\n")
        self.format_printed = True

    #get the number of detectors and thickness:
    m = re.search("Det(\d+)PE(\d+\.\d+)R(\d+\.\d+)\.fomout", self.file_name.strip())
    m_num_det = float(m.group(1))
    m_poly_thick = float(m.group(2))
    m_radius = float(m.group(3))

    #print name, geometry, etc.
    self.outfile.write("%21s%8.2f%9i%14.2f    " % (self.file_name.strip(), m_radius, m_num_det,
        m_poly_thick))

    for i in range(len(self.strength)):
        self.outfile.write("%13.4f%11.4f%12.4f" % (self.difference[i][idx], self.diff_std_dev[i],
            self.not_matches[i]))

    self.outfile.write("\n")

else:
    raise ValueError("Invalid format entry")

return None

# -----
def average_results(self):
    """Method that averages all results and stores the average to the results as the last in the list"""
    if self.averaged == True:
        raise ValueError("already averaged, wont work right")

    attributes = dir(self)

    #local average values
    avg_eff = [ 0. for i in range(len(self.strength))]
    diff = [ 0. for i in range(len(self.strength))]
    lowest_fom = [ 0. for i in range(len(self.strength))]
    diff_sq = [ 0. for i in range(len(self.strength))]

    not_matches = [ 0 for i in range(len(self.strength))]
    std_dev = []

    for i in range(len(self.not_matches)):
        self.not_matches[i] = float(self.not_matches[i])
        self.not_matches[i] /= float(len(self.strength[i]))

    #compute sum of values and square
    for idx in range(len(self.strength)):

        num_trials = len(self.avg_eff[idx])

```

```

        for i in range(len(self.avg_eff[idx])):

            avg_eff[idx] += self.avg_eff[idx][i]
            diff[idx] += self.difference[idx][i]
            diff_sq[idx] += self.difference[idx][i]*self.difference[idx][i]
            lowest_fom[idx] += float(self.lowest_fom[idx][i])

        #compute average
        avg_eff[idx] /= num_trials
        diff[idx] /= num_trials
        diff_sq[idx] /= num_trials

        if num_trials != 1:
            std_dev.append(1./(num_trials-1.)*(diff_sq[idx] - diff[idx]*diff[idx]))
        else:
            std_dev.append(1./(num_trials)*(diff_sq[idx] - diff[idx]*diff[idx]))

    #store all average results as last member of list
    self.diff_std_dev = std_dev

    for src in range(len(self.strength)):

        self.difference[src].append(diff[src])
        self.avg_eff[src].append(avg_eff[src])
        self.lowest_fom.append(lowest_fom[src])

    self.averaged=True

    return None

#searchs a line for a string, returns true if found, else false
def search_for(line, string):
    pattern = re.compile(string)
    if (pattern.search(line)):
        return True
    else:
        return False

if __name__ == "__main__":
    file = open("test.txt", "a")
    os.chdir("FOM_outputs")
    a = all_data(file, "Det6PE4.0R10.0.fomout")
    a.parse()
    os.chdir("..")
    a.fprint(idx=0)
    a.average_results()
    print a.averaged
    a.fprint(average=True)
    a.average_results()
    file.close()

# os.remove("test.txt")

```

master_file.fom: Sample Output from FOM_output.py

```
'100ev'  
11 6.8 ! number of detectors, radius of spectrometer  
4.07152E-07 0.0250 ! r_i, sigma(r_i)/r_i  
2.36026E-06 0.0235  
5.25792E-07 0.0304  
4.86122E-08 0.0637  
3.87641E-09 0.2023  
0.00000E+00 0.0000  
0.00000E+00 0.0000  
0.00000E+00 0.0000  
0.00000E+00 0.0000  
0.00000E+00 0.0000  
0.00000E+00 0.0000  
0.00000E+00 0.0000  
'ambe'  
11 6.8  
9.24320E-08 0.0572  
8.26495E-07 0.0429  
6.06992E-07 0.0408  
2.93210E-07 0.0454  
1.58648E-07 0.0501  
1.11427E-07 0.0475  
6.86984E-08 0.0474  
4.63191E-08 0.0436  
2.88369E-08 0.0405  
1.71930E-08 0.0412  
7.55912E-09 0.0573  
'cf252mcpn'  
11 6.8  
5.20806E-08 0.0964  
5.22608E-07 0.0511  
5.91422E-07 0.0430  
4.38491E-07 0.0409  
2.64141E-07 0.0409  
1.54190E-07 0.0420  
8.01043E-08 0.0448  
4.74482E-08 0.0437  
2.73162E-08 0.0449  
1.48358E-08 0.0440  
5.94480E-09 0.0523  
'cfd2oN'  
11 6.8  
3.36993E-07 0.0291  
1.81081E-06 0.0272  
6.92907E-07 0.0294  
1.91853E-07 0.0338  
6.97646E-08 0.0373  
3.21269E-08 0.0434  
1.85437E-08 0.0473  
1.10869E-08 0.0561  
5.49360E-09 0.0579  
3.42547E-09 0.0544  
1.39792E-09 0.0632  
'fusionN'  
11 6.8  
9.17220E-09 0.1917  
1.06044E-07 0.1095  
1.39183E-07 0.0868  
1.61640E-07 0.0848  
1.38673E-07 0.0805  
1.06838E-07 0.0808  
9.37919E-08 0.0864  
8.28473E-08 0.0817  
5.87632E-08 0.0745  
4.38710E-08 0.0836  
2.08117E-08 0.1000
```


simul_resp.f90: Source Code for Generating Simulated Responses

```
PROGRAM simul_resp
! Program to generate simulated count data from response functions
! Same as SIMUL but response functions are read from a file and not
! defined by DATA statements
IMPLICIT NONE
REAL, ALLOCATABLE, DIMENSION(:) :: resp, ecount, src
INTEGER, ALLOCATABLE, DIMENSION(:) :: ncount
CHARACTER(len=40) :: stype
REAL, PARAMETER :: PI = 3.14159265
COMMON/RANCOM/ISEED      !Random Num_seed

INTEGER :: open_error          !I/O STATUS
CHARACTER (len=20) :: output_name !output file name
INTEGER :: STATUS              !For dynamic memory status
INTEGER :: I, isrc, num_src, idet, iround, izeed!loop counters
REAL :: x, sig, cyl_rad, source
INTEGER :: n, num_det

! READ IN THE SOURCE INFORMATION FROM A FILE
OPEN(555,FILE='src_str.txt',STATUS='OLD',ACTION='READ', IOSTAT=open_error)
IF (open_error /= 0) THEN
  STOP "Can't find the src_str.txt file for source strengths"
END IF
READ (555,*) num_src

ALLOCATE(src(num_src), STAT=STATUS) !allocate memory for number of sources
IF (status /= 0) THEN
  STOP "Problem allocating memory"
END IF
DO I=1,num_src,1
  READ(555,*) src(I)
END DO

!Read izeed from a file so as not to use same random num every time
OPEN(UNIT=556,FILE='irand',STATUS='OLD',ACTION='READ', IOSTAT=open_error)
IF (open_error /= 0) THEN
  write(*,*) "No file found, use default seed of 73907"
  izeed = 73907
ELSE
  READ(556,*) izeed
  CLOSE(UNIT=556)
END IF

OPEN(11,FILE='simul_resp.out',STATUS='UNKNOWN')

!-- Begin loop to process all response functions
output_name = "master_file.fom"
OPEN (UNIT=10, FILE=output_name, STATUS='UNKNOWN', ACTION='READ', &
&IOSTAT=open_error)
IF (open_error /= 0) THEN
  STOP "No response function, (master_file.fomin), file"
END IF
98 READ(10,*,END=99) stype
READ(10,*) num_det, cyl_rad
ALLOCATE(resp(num_det), ncount(num_det), ecount(num_det), STAT=STATUS)
IF (status /= 0) THEN
  STOP "Problem allocating memory for detector arrays"
END IF
```

```

        DO 97 i=1,num_det
            READ(10,*) resp(i)
97    CONTINUE
! ** process both spectra
    stype= ' ' ' '//Source is '//stype
        WRITE(11,50) stype,' ' '
        WRITE(11,53) num_det, num_src, cyl_rad
53    FORMAT(1x, 2I5, 1F10.1)
50    FORMAT(A40,A3)

!-- loop over all source strengths
    DO 20 isrc=1,num_src
        !Normalize the responses to per area of 10cm^2. i.e., if you have
        !an area of 10cm^2, then the total source is what is read in
        source = src(isrc)*cyl_rad*cyl_rad/100.
!-- loop over all detector locations
    DO 30 idet=1,num_det
        ecount(idet)=resp(idet)*source
!-- sample from expected counts
        IF (ecount(idet).LE.0.01) THEN
            ncount(idet)=0
        ELSEIF (ecount(idet) .GT. 20.) THEN
            sig=SQRT(ecount(idet))
            CALL Normal(ecount(idet),sig,x)
!            -- round x to nearest integer
            n=INT(x)
            iround = INT(2*x-2*n)
            ncount(idet)=n+iround
        ELSE
            CALL Poiss(ecount(idet),n)
            ncount(idet)=n
        ENDIF
30    CONTINUE

        WRITE(11,52) source,(ncount(i),i=1,num_det)
52    FORMAT(1X, 1g14.4, 15I12)

20    CONTINUE
        DEALLOCATE(resp, ncount, ecount)
        GOTO 98

99    CLOSE(11)

DEALLOCATE(src)
!write the randomnumber seed to the directory
OPEN(UNIT=666,FILE='irand',STATUS='REPLACE', ACTION='WRITE', IOSTAT=open_error)
WRITE(666,*) iseed
CLOSE(UNIT=666)
END PROGRAM simul_resp

SUBROUTINE Normal(m,sig,x)
!-----
! Generates a random sample x from a normal N(m,sig) distribution
! using the Box-Muller method.
!
! INPUT:  m   = the mean of the Gaussian distribution
!         sig  = the standard deviation of the Gaussian distribution
!
! OUTPUT: x   = a random sample from the Gaussian distribution
!
! NOTE: Although, in general, m and sig can be independent, for
!       counting data m = sig^2
!-----
    REAL m
    rho1 = FLTRN()
    rho2 = FLTRN()

```

```

    y = SQRT(-2.*log(rho1))*COS(6.283185*rho2)
    x = sig*y + m
    RETURN
    END

    SUBROUTINE Poiss(m,n)
!-----
! Generates a random sample n from a Poisson distribution with mean m
!-----
    REAL m,lnm
!-- initialize
    rho = FLTRN()
    n=0
    em = EXP(-m)
    fn = em
    lnm = LOG(m)
    FFn = fn

!-- use inverse CDF method
    DO 10 i=1,45
    IF (rho .GT. FFn) THEN
        n=n+1
        fn = EXP(n*lnm - m - gammln(FLOAT(n+1)))
        FFn = FFn + fn
    ELSE
        RETURN
    ENDIF

10 CONTINUE
    WRITE(*,*) ' WARNING: Poisson sampling failed'
    END

    FUNCTION gammln(xx)
!-----
! Returns value of ln[Gamma(xx)]. From "Numerical Recipes"
!-----
    REAL gammln,xx
    INTEGER j
    DOUBLE PRECISION ser,stp,tmp,x,y,cof(6)
    SAVE cof,stp
    DATA cof,stp/76.18009172947146d0,-86.50532032941677d0, &
& 24.01409824083091d0,-1.231739572450155d0,.1208650973866179d-2, &
& -.5395239384953d-5,2.5066282746310005d0/
    x=xx
    y=x
    tmp=x+5.5d0
    tmp=(x+0.5d0)*log(tmp)-tmp
    ser=1.000000000190015d0
    DO 10 j=1,6
        y=y+1.d0
        ser=ser+cof(j)/y
10 CONTINUE
    gammln=tmp+log(stp*ser/x)
    RETURN
    END

    REAL FUNCTION FLTRN()
!-----
! PURPOSE: Returns a single precision floating point random
!          number in the open interval (0,1).
!          Works on any system for which the maximum value
!          of an integer variable is 2**31-1 or larger.
!
! ARGUMENTS: none (ISEED the seed number is kept in COMMON)
!

```

```
! METHOD: Minimal standard generator as specified in the article
!       S.K. Park and K.W. Miller, "Random Number Generators:
!       Good Ones are Hard to Find", Comm. ACM, vol. 31, no. 10,
!       October 1988.
```

```
!-----
```

```
INTEGER a,m,q,r,lo,hi,test,iseed
REAL minv
COMMON/RANCOM/ISEED
PARAMETER(a=16807,m=2147483647,q=127773,r=2836)
PARAMETER(minv=4.6566129E-10)
```

```
hi = iseed/q
lo = MOD(iseed,q)
test = a*lo-r*hi
```

```
IF(test .GT. 0) THEN
  iseed = test
ELSE
  iseed = test + m
ENDIF
```

```
FLTRN = minv*REAL(iseed)
RETURN
END
```

fom.f90: Source Code for Computing FOM Values

```
!***** Program for comparing a measured spectrometer response to templates
! The number 30 throughout is max number of different sources
! that are being simulated
```

```
!UPDATE 71112: Added ability to average results
```

```
PROGRAM fom_042412
```

```
IMPLICIT NONE
```

```
INTEGER, ALLOCATABLE, DIMENSION(:) :: ncount
```

```
REAL, ALLOCATABLE, DIMENSION(:) :: RR,sig2c
```

```
REAL, ALLOCATABLE, DIMENSION(:, :) :: rel
```

```
REAL, DIMENSION(30) :: fom,fom2,sigfom
```

```
REAL, DIMENSION(30,30) :: SS,sig2S, resp
```

```
CHARACTER(LEN=72) :: templ(30),templ2(30),label
```

```
INTEGER :: norm, nsrc, ndet,j,i,status,nresp
```

```
INTEGER :: nset, nsum, cnorm
```

```
REAL :: r2norm, Snorm, src, cyl_rad, eff
```

```
!** analysis parameters
```

```
norm = 2 !which detector to normalize to
!default is 10, radius of the spectrometer
!get number of source strengths
```

```
OPEN(UNIT=512,FILE='simul_resp.out',ACTION='READ',STATUS='OLD')
READ(512,*) label, ndet, nsrc !lable and ndet are just dummys here
CLOSE(UNIT=512)
```

```
!** open input/output files
```

```
OPEN(10,FILE='simul_resp.out',STATUS='OLD')
OPEN(11,FILE='master_file.fom',STATUS='OLD')
OPEN(12,FILE='FOM.out',STATUS='UNKNOWN')
OPEN(13,FILE='FOM.plt',STATUS='UNKNOWN')
```

```
!-- read in all templates and form ratios for the response functions
```

```
j=0
```

```
!-- loop to read response functions
```

```
40 j=j+1
```

```
READ(11,*,END=100) templ(j)
```

```
templ2(j)=templ(j)
```

```
READ(11,*) ndet, cyl_rad
```

```
ALLOCATE(RR(ndet), ncount(ndet), rel(30,ndet),&
&STAT=status)
```

```
IF (status /= 0) THEN
```

```
STOP "Problem allocating memory for detector arrays"
```

```
END IF
```

```
DO 15 i=1,ndet
```

```
READ(11,*) resp(j,i),rel(j,i)
```

```
15 CONTINUE
```

```
!-- calc ratios and variances
```

```
Snorm = resp(j,norm)
```

```
r2norm = rel(j,norm)**2
```

```
DO 16 i=1,ndet
```

```
SS(j,i) = LOG(resp(j,i)/Snorm)
```

```
sig2S(j,i) = (rel(j,i)**2 + r2norm)*100./(cyl_rad*cyl_rad)
```

```
16 CONTINUE
```

```
nresp=j
```

```
! DEALLOCATE MEMORY
```

```
DEALLOCATE(RR, ncount, rel,&
```

```
&)
```

```
GOTO 40
```

```
!-- big loop to read and process simulated count data
```

```
!** read in spectrometer count data
```

```

100  READ(10,*,END=300) label
      READ(10,*) ndet, nsrc, cyl_rad
      WRITE(12,31) label
      WRITE(13,31) label
31    FORMAT( // 'c***** ',(A)
      !Allocate memory
      ALLOCATE(ncount(ndet), RR(ndet), sig2c(ndet))
      nset=0
99    READ(10,306) src, (ncount(i),i=1,ndet)
306  FORMAT(1x, 1E14.4, 5000I12)
!-- find total number of counts
      nsum=0
      DO 35 i=1,ndet
          nsum=nsum + ncount(i)
35    CONTINUE

      eff = float(nsum)/(src)*100.
      WRITE(12,38) nsum,src,eff,(ncount(i),i=1,ndet)
      WRITE(13,34) label,nsum,(ncount(i),i=1,ndet)
34    FORMAT(/(A),/&
&      'Simulated count data: total counts = ',I10,/4000I8)
38    FORMAT('/Simulated count data: total counts = ',I10,' total incident&
& neutrons= ',ES10.1,' total efficiency = ',F7.4, '%'/4000I8)
      nset=nset+1
!-- check that normalization counts are not zero
      IF (ncount(norm).EQ.0) THEN
          WRITE(12,36)norm
          WRITE(12,333)
          WRITE(13,333)

          IF (nset.EQ.nsrc) THEN
              DEALLOCATE(ncount, RR, sig2c)
              WRITE(12,333)
              WRITE(13,333)
              GOTO 100

          ELSE
              GOTO 99
          ENDIF
      ENDIF
36    FORMAT('--ERROR: normalization detector',I2,' has zero counts')

!-- calculate log of ratios and stnd dev. for count data
      cnorm = ncount(norm)
      DO 11 i=1,ndet
          IF (ncount(i).GT.0) THEN
              sig2c(i) = 1./FLOAT(ncount(i)) + 1./FLOAT(cnorm) !Corrected
              RR(i) = LOG(1.*ncount(i)/FLOAT(cnorm))
          ELSE
              sig2c(i)=0.0
              RR(i) = LOG(1./cnorm)
          ENDIF
11    CONTINUE

!-- compare data to all response functions -- calc FOM and stnd dev.
      DO 10 j=1,nresp
!-- calc figure of merit (FOM)
          fom(j)=0.0
          DO 30 i=1,ndet
              IF((resp(j,i).GT.1E-15).AND.(ncount(i).GT.0)) THEN
                  fom(j)=fom(j)+(RR(i)-SS(j,i))**2/(sig2S(j,i) + sig2c(i))
              ENDIF
30    CONTINUE
          sigfom(j)=2*SQRT(fom(j))
          fom2(j)=fom(j)

```

```

10     CONTINUE

!-- sort the FOMs
      CALL mysort(nresp,fom,sigfom,templ)

!-- print out results
      DO 20 j=1,nresp
        WRITE(12,32) templ(j),fom(j),sigfom(j)
        WRITE(13,57) templ(j),j,fom(j),sigfom(j),sigfom(j)

!-- reset template names
      templ(j)=templ2(j)
32     FORMAT(A30,' FOM ',G12.4,' +- ',G12.4)
37     FORMAT((A))
57     FORMAT('c ',A30,/I4,G12.4,' ( ',G12.4,', ',G12.4,')')

20     CONTINUE
!-- process next set of simulated data
      IF (nset.EQ.nsrc) THEN !read all data for all src str's
        WRITE(12,333)
        WRITE(13,333)
333    FORMAT (/ 'c' ,72('-')//)
        DEALLOCATE(ncount, RR, sig2c)
        GOTO 100
      ELSE
        GOTO 99
      ENDIF

!-- terminate the program -- all data processed
300    CLOSE(10)
      CLOSE(11)
      CLOSE(12)
      CLOSE(13)

```

END PROGRAM fom_042412

```

!Fortran77 subroutine to sort a list from Numerical Recipes
SUBROUTINE mysort(n,arr,brr,crr)
  INTEGER n,M,NSTACK
  REAL arr(n),brr(n)
  CHARACTER*72 crr(n),c,ctemp
  PARAMETER (M=7,NSTACK=50)
  INTEGER i,ir,j,jstack,k,l,istack(NSTACK)
  REAL a,b,temp
  jstack=0
  l=1
  ir=n
1     if(ir-1.lt.M)then
      do 12 j=l+1,ir
        a=arr(j)
        b=brr(j)
        c=crr(j)
        do 11 i=j-1,1,-1
          if(arr(i).le.a)goto 2
          arr(i+1)=arr(i)
          brr(i+1)=brr(i)
          crr(i+1)=crr(i)
11     continue
        i=0
2     arr(i+1)=a
        brr(i+1)=b
        crr(i+1)=c
12    continue
      if(jstack.eq.0)return
      ir=istack(jstack)
      l=istack(jstack-1)

```

```

    jstack=jstack-2
else
    k=(l+ir)/2
    temp=arr(k)
    arr(k)=arr(l+1)
    arr(l+1)=temp
    temp=brr(k)
    brr(k)=brr(l+1)
    brr(l+1)=temp
    ctemp=crr(k)
    crr(k)=crr(l+1)
    crr(l+1)=ctemp
    if(arr(l+1).gt.arr(ir))then
        temp=arr(l+1)
        arr(l+1)=arr(ir)
        arr(ir)=temp
        temp=brr(l+1)
        brr(l+1)=brr(ir)
        brr(ir)=temp
        ctemp=crr(l+1)
        crr(l+1)=crr(ir)
        crr(ir)=ctemp
    endif
    if(arr(l).gt.arr(ir))then
        temp=arr(l)
        arr(l)=arr(ir)
        arr(ir)=temp
        temp=brr(l)
        brr(l)=brr(ir)
        brr(ir)=temp
        ctemp=crr(l)
        crr(l)=crr(ir)
        crr(ir)=ctemp
    endif
    if(arr(l+1).gt.arr(l))then
        temp=arr(l+1)
        arr(l+1)=arr(l)
        arr(l)=temp
        temp=brr(l+1)
        brr(l+1)=brr(l)
        brr(l)=temp
        ctemp=crr(l+1)
        crr(l+1)=crr(l)
        crr(l)=ctemp
    endif
    i=l+1
    j=ir
    a=arr(l)
    b=brr(l)
    c=crr(l)
3    continue
    i=i+1
    if(arr(i).lt.a)goto 3
4    continue
    j=j-1
    if(arr(j).gt.a)goto 4
    if(j.lt.i)goto 5
    temp=arr(i)
    arr(i)=arr(j)
    arr(j)=temp
    temp=brr(i)
    brr(i)=brr(j)
    brr(j)=temp
    ctemp=crr(i)
    crr(i)=crr(j)
    crr(j)=ctemp
    goto 3
5    arr(l)=arr(j)

```



```
arr(j)=a
brr(1)=brr(j)
brr(j)=b
crr(1)=crr(j)
crr(j)=c
jstack=jstack+2
if(jstack.gt.NSTACK) STOP 'NSTACK too small in sort2'
if(ir-i+1.ge.j-1)then
  istack(jstack)=ir
  istack(jstack-1)=i
  ir=j-1
else
  istack(jstack)=j-1
  istack(jstack-1)=1
  l=i
endif
endif
goto 1
END
```

Appendix C

Spectrometer MCNP Files

Description	Page
MCNP5 file for a uniform beam of ^{252}Cf irradiating a spectrometer in a void.	176
MCNP5 file for a point source of ^{252}Cf irradiating a spectrometer in an enclosed room with shadow shield included.	179
MCNP6 input file for verifying spectrometer response from ^{252}Cf	183

MCNP5 Input File for Void and Disk Source

```
SPC8: Detectors every 3 cm in 30 cm x 20 cm-dia spectrometer
c A cylinder of polyethylene is used as neutron spectrometer.
c At various distances into cylinder square perforated neutron
c detectors (2x2 cm) are placed perpendicular to the axis. Behind
c each detector is a 1 mm disk of cadmium extending to the edge of
c the poly cylinder.
c
c ***** BLOCK 1: CELL CARDS *****
c
c ---- detector chunks, breadboards, and surrounding poly annuli ----
10 2 -0.0835 100 -1100 -35 imp:n=1.00 $detector at 0 cm
600 4 0.00053 1100 -200 -40 imp:n=1.00 $breadboard at 0 cm
11 0 100 -200 -30 ((35 -1100):40) imp:n=1.00 $Voided annulus at 0 cm
20 2 -0.0835 101 -1101 -35 imp:n=1.31 $detector at 2 cm
601 4 0.00053 1101 -201 -40 imp:n=1.31 $breadboard at 2 cm
21 1 -0.9500 101 -201 -30 ((35 -1101):40) imp:n=1.31 $HDPE annulus at 2 cm
30 2 -0.0835 102 -1102 -35 imp:n=1.99 $detector at 5 cm
602 4 0.00053 1102 -202 -40 imp:n=1.99 $breadboard at 5 cm
31 1 -0.9500 102 -202 -30 ((35 -1102):40) imp:n=1.99 $HDPE annulus at 5 cm
40 2 -0.0835 103 -1103 -35 imp:n=3.26 $detector at 8 cm
603 4 0.00053 1103 -203 -40 imp:n=3.26 $breadboard at 8 cm
41 1 -0.9500 103 -203 -30 ((35 -1103):40) imp:n=3.26 $HDPE annulus at 8 cm
50 2 -0.0835 104 -1104 -35 imp:n=5.49 $detector at 10 cm
604 4 0.00053 1104 -204 -40 imp:n=5.49 $breadboard at 10 cm
51 1 -0.9500 104 -204 -30 ((35 -1104):40) imp:n=5.49 $HDPE annulus at 10 cm
60 2 -0.0835 105 -1105 -35 imp:n=9.30 $detector at 12 cm
605 4 0.00053 1105 -205 -40 imp:n=9.30 $breadboard at 12 cm
61 1 -0.9500 105 -205 -30 ((35 -1105):40) imp:n=9.30 $HDPE annulus at 12 cm
70 2 -0.0835 106 -1106 -35 imp:n=15.7 $detector at 15 cm
606 4 0.00053 1106 -206 -40 imp:n=15.7 $breadboard at 15 cm
71 1 -0.9500 106 -206 -30 ((35 -1106):40) imp:n=15.7 $HDPE annulus at 15 cm
80 2 -0.0835 107 -1107 -35 imp:n=26.3 $detector at 18 cm
607 4 0.00053 1107 -207 -40 imp:n=26.3 $breadboard at 18 cm
81 1 -0.9500 107 -207 -30 ((35 -1107):40) imp:n=26.3 $HDPE annulus at 18 cm
90 2 -0.0835 108 -1108 -35 imp:n=43.1 $detector at 20 cm
608 4 0.00053 1108 -208 -40 imp:n=43.1 $breadboard at 20 cm
91 1 -0.9500 108 -208 -30 ((35 -1108):40) imp:n=43.1 $HDPE annulus at 20 cm
100 2 -0.0835 109 -1109 -35 imp:n=69.9 $detector at 22 cm
609 4 0.00053 1109 -209 -40 imp:n=69.9 $breadboard at 22 cm
101 1 -0.9500 109 -209 -30 ((35 -1109):40) imp:n=69.9 $HDPE annulus at 22 cm
110 2 -0.0835 110 -1110 -35 imp:n=110.9 $detector at 25 cm
610 4 0.00053 1110 -210 -40 imp:n=110.9 $breadboard at 25 cm
111 1 -0.9500 110 -210 -30 ((35 -1110):40) imp:n=110.9 $HDPE annulus at 25 cm
c ---- Cd slices behind detectors ----
500 3 -8.6500 200 -1200 -30 imp:n=1.00 $cd slice behind detecor 1
501 3 -8.6500 201 -1201 -30 imp:n=1.31 $cd slice behind detecor 2
502 3 -8.6500 202 -1202 -30 imp:n=1.99 $cd slice behind detecor 3
503 3 -8.6500 203 -1203 -30 imp:n=3.26 $cd slice behind detecor 4
504 3 -8.6500 204 -1204 -30 imp:n=5.49 $cd slice behind detecor 5
505 3 -8.6500 205 -1205 -30 imp:n=9.30 $cd slice behind detecor 6
506 3 -8.6500 206 -1206 -30 imp:n=15.7 $cd slice behind detecor 7
507 3 -8.6500 207 -1207 -30 imp:n=26.3 $cd slice behind detecor 8
508 3 -8.6500 208 -1208 -30 imp:n=43.1 $cd slice behind detecor 9
509 3 -8.6500 209 -1209 -30 imp:n=69.9 $cd slice behind detecor 10
510 3 -8.6500 210 -1210 -30 imp:n=110.9 $cd slice behind detecor 11
c ---- poly cylinders behind Cd ----
400 1 -0.9500 1200 -101 -30 imp:n=1.00 $HDPE cylinder behind detecor 1
401 1 -0.9500 1201 -102 -30 imp:n=1.31 $HDPE cylinder behind detecor 2
402 1 -0.9500 1202 -103 -30 imp:n=1.99 $HDPE cylinder behind detecor 3
403 1 -0.9500 1203 -104 -30 imp:n=3.26 $HDPE cylinder behind detecor 4
404 1 -0.9500 1204 -105 -30 imp:n=5.49 $HDPE cylinder behind detecor 5
405 1 -0.9500 1205 -106 -30 imp:n=9.30 $HDPE cylinder behind detecor 6
406 1 -0.9500 1206 -107 -30 imp:n=15.7 $HDPE cylinder behind detecor 7
407 1 -0.9500 1207 -108 -30 imp:n=26.3 $HDPE cylinder behind detecor 8
408 1 -0.9500 1208 -109 -30 imp:n=43.1 $HDPE cylinder behind detecor 9
```

```

409 1  -0.9500      1209 -110 -30      imp:n=69.9  $HDPE cylinder behind detector 10
c ---- graveyard and neutron beam ----
1  0      10 -100 -30      imp:n=1  $ void before spectrometer
999 0      30:-10:111      imp:n=0  $ graveyard/problem boundary

c ***** BLOCK 2: SURFACE CARDS *****
10 px -10      $ left problem boundary
30 CX 6.803      $ cylindrical surface of spectrometer
35 RPP 100.0 125.357 -1 1 -1 1  $ square box for detector edges (2x2square)
40 RPP 100.0 125.357 -1.1 1.1 -1.1 1.1  $ square box for PCB edges (1.1x1.100000.1square)
c --- vertical slices thru the spectrometer I (front detector surfaces) ---
100 px 100.0      $front of detector 0
101 px 102.5      $front of detector 1
102 px 105.0      $front of detector 2
103 px 107.5      $front of detector 3
104 px 110.0      $front of detector 4
105 px 112.5      $front of detector 5
106 px 115.0      $front of detector 6
107 px 117.5      $front of detector 7
108 px 120.0      $front of detector 8
109 px 122.5      $front of detector 9
110 px 125.0      $front of detector 10
111 px 125.357      $back of last sheet of poly/spectr
c --- vertical slices thru the spectrometer II (back detector surfaces) ---
1100 px 100.1      $back of detector 0
1101 px 102.6      $back of detector 1
1102 px 105.1      $back of detector 2
1103 px 107.6      $back of detector 3
1104 px 110.1      $back of detector 4
1105 px 112.6      $back of detector 5
1106 px 115.1      $back of detector 6
1107 px 117.6      $back of detector 7
1108 px 120.1      $back of detector 8
1109 px 122.6      $back of detector 9
1110 px 125.1      $back of detector 10
c --- vertical slices thru the spectrometer III (Cd slices) ---
200 px 100.257      $front cd of detector 0
1200 px 100.357      $back cd of detector 0
201 px 102.757      $front cd of detector 1
1201 px 102.857      $back cd of detector 1
202 px 105.257      $front cd of detector 2
1202 px 105.357      $back cd of detector 2
203 px 107.757      $front cd of detector 3
1203 px 107.857      $back cd of detector 3
204 px 110.257      $front cd of detector 4
1204 px 110.357      $back cd of detector 4
205 px 112.757      $front cd of detector 5
1205 px 112.857      $back cd of detector 5
206 px 115.257      $front cd of detector 6
1206 px 115.357      $back cd of detector 6
207 px 117.757      $front cd of detector 7
1207 px 117.857      $back cd of detector 7
208 px 120.257      $front cd of detector 8
1208 px 120.357      $back cd of detector 8
209 px 122.757      $front cd of detector 9
1209 px 122.857      $back cd of detector 9
210 px 125.257      $front cd of detector 10
1210 px 125.357      $back cd of detector 10

c ***** BLOCK 3: DATA CARDS *****
c
c ----- Source: disk source, different erg dist. for each file -----
SDEF  ERG=d1  PAR=1  VEC= 1 0 0  DIR=1 POS 0 0 0
      AXS=1 0 0 rad=d2  EXT=0
SP2 -21 1      $ weighting for radial sampling: her r^1
SI2  0 6.8030      $ radial sampling range: 0 to Rmax
SP1 -3 1.025 2.926  $ Watt distn for f-252
c ----- Problem parameters

```

```

mode n
nps 200000000
c
c
c ----- total thermal flux detector
F4:N 10 20 30 40 50 60 70 80 90 100 110
TF4 11 7j
c -----
c modify tallies to give no. (n,t) reactions per source neutron
c C=[(rho Na/A)x10-24 atom/(b-cm)] x Vol_detector
c for Li-6 to stop 50% of neutrons in .1 cm, density ~ 0.0835 g/cm3
c Vol_det = 0.4 cm3 ( 2 x 2 x .1 cm)
c find that C=0.0033286
c -----
FC4 tally modified to (n,t) reactions per source neutron
FM4 0.0033286 2 105
c
c WEIGHT WINDOW GENERATOR
c MESH geom=cyl ref=10 0 0 origin -15 0 0 axs=1 0 0 vec=0 0 1
c imesh 1.5 15.1 iints=1 4
c jmesh 99 110 120 131 jints=1 11 10 8
c kmesh 1 kints=1
c WWG 4 0 0 4j
c WWGE:n 10
c
c ----- MATERIALS
c -----
c material: polyethylene d=0.95 g/cm3
c -----
m1 1001.50c 2
6000.50c 1
mt1 poly.01
c
c -----
c material: Li-6F nominal d=2.7 g/cm3
c ignore F: Li-6 in LiF has a density of 0.6131 g/cm3
c -----
m2 3006.66c 1
c
c -----
c cadmium nominal density 8.65 g/cm3
c -----
m3 48000.50c 1
c
c -----
c Printed circuit board...still need this one
c
m4 5010.50c 1

```

MCNP5 Input File for Enclosed Room with Shadow Shield

```

SPC8: Detectors every 3 cm in 30 cm x 20 cm-dia spectrometer
c A cylinder of polyethylene is used as neutron spectrometer.
c At various distances into cylinder square perforated neutron
c detectors (2x2 cm) are placed perpendicular to the axis. Behind
c each detector is a 1 mm disk of cadmium extending to the edge of
c the poly cyclinder.
c Added stuff:
c Added ability to handle point source and wall shine, moved source
c 1.5 m away instead of 1.0 m so more shine occurs
c
c ---- graveyard ----
999 0      50                                imp:n=0.0    $kill zone
c ---- detector chunks, breadboards, and surrounding poly annuli ----
10 2  -0.0835    100  -1100 -35          imp:n=1.10  $detector at 0.0 cm
600 4  0.00053   1100 -200  -40          imp:n=1.10  $breadboard at 0.0 cm
11 0
20 2  -0.0835    101  -1101 -35          imp:n=1.68  $detector at 2.5 cm
601 4  0.00053   1101 -201  -40          imp:n=1.68  $breadboard at 2.5 cm
21 1  -0.9500    101  -201  -30 ((35 -1101):40) imp:n=1.68  $HDPE annulus at 2.5 cm
30 2  -0.0835    102  -1102 -35          imp:n=2.24  $detector at 5.0 cm
602 4  0.00053   1102 -202  -40          imp:n=2.24  $breadboard at 5.0 cm
31 1  -0.9500    102  -202  -30 ((35 -1102):40) imp:n=2.24  $HDPE annulus at 5.0 cm
40 2  -0.0835    103  -1103 -35          imp:n=2.14  $detector at 7.5 cm
603 4  0.00053   1103 -203  -40          imp:n=2.14  $breadboard at 7.5 cm
41 1  -0.9500    103  -203  -30 ((35 -1103):40) imp:n=2.14  $HDPE annulus at 7.5 cm
50 2  -0.0835    104  -1104 -35          imp:n=2.16  $detector at 10.0 cm
604 4  0.00053   1104 -204  -40          imp:n=2.16  $breadboard at 10.0 cm
51 1  -0.9500    104  -204  -30 ((35 -1104):40) imp:n=2.16  $HDPE annulus at 10.0 cm
60 2  -0.0835    105  -1105 -35          imp:n=1.94  $detector at 12.5 cm
605 4  0.00053   1105 -205  -40          imp:n=1.94  $breadboard at 12.5 cm
61 1  -0.9500    105  -205  -30 ((35 -1105):40) imp:n=1.94  $HDPE annulus at 12.5 cm
70 2  -0.0835    106  -1106 -35          imp:n=1.96  $detector at 15.0 cm
606 4  0.00053   1106 -206  -40          imp:n=1.96  $breadboard at 15.0 cm
71 1  -0.9500    106  -206  -30 ((35 -1106):40) imp:n=1.96  $HDPE annulus at 15.0 cm
80 2  -0.0835    107  -1107 -35          imp:n=2.38  $detector at 17.5 cm
607 4  0.00053   1107 -207  -40          imp:n=2.38  $breadboard at 17.5 cm
81 1  -0.9500    107  -207  -30 ((35 -1107):40) imp:n=2.38  $HDPE annulus at 17.5 cm
90 2  -0.0835    108  -1108 -35          imp:n=2.09  $detector at 20.0 cm
608 4  0.00053   1108 -208  -40          imp:n=2.09  $breadboard at 20.0 cm
91 1  -0.9500    108  -208  -30 ((35 -1108):40) imp:n=2.09  $HDPE annulus at 20.0 cm
100 2  -0.0835   109  -1109 -35          imp:n=1.77  $detector at 22.5 cm
609 4  0.00053   1109 -209  -40          imp:n=1.77  $breadboard at 22.5 cm
101 1  -0.9500   109  -209  -30 ((35 -1109):40) imp:n=1.77  $HDPE annulus at 22.5 cm
110 2  -0.0835   110  -1110 -35          imp:n=1.00  $detector at 25.0 cm
610 4  0.00053   1110 -210  -40          imp:n=1.00  $breadboard at 25.0 cm
111 1  -0.9500   110  -210  -30 ((35 -1110):40) imp:n=1.00  $HDPE annulus at 25.0 cm
c ---- Cd slices behind detectors ----
500 3  -8.6500    200  -1200 -30          imp:n=1.10  $cd slice behind detector 1
501 3  -8.6500    201  -1201 -30          imp:n=1.68  $cd slice behind detector 2
502 3  -8.6500    202  -1202 -30          imp:n=2.24  $cd slice behind detector 3
503 3  -8.6500    203  -1203 -30          imp:n=2.14  $cd slice behind detector 4
504 3  -8.6500    204  -1204 -30          imp:n=2.16  $cd slice behind detector 5
505 3  -8.6500    205  -1205 -30          imp:n=1.94  $cd slice behind detector 6
506 3  -8.6500    206  -1206 -30          imp:n=1.96  $cd slice behind detector 7
507 3  -8.6500    207  -1207 -30          imp:n=2.38  $cd slice behind detector 8
508 3  -8.6500    208  -1208 -30          imp:n=2.09  $cd slice behind detector 9
509 3  -8.6500    209  -1209 -30          imp:n=1.77  $cd slice behind detector 10
510 3  -8.6500    210  -1210 -30          imp:n=1.00  $cd slice behind detector 11
c ---- poly cylinders behind Cd ----
400 1  -0.9500    1200 -101  -30          imp:n=1.10  $HDPE cylinder behind detecor 1
401 1  -0.9500    1201 -102  -30          imp:n=1.68  $HDPE cylinder behind detecor 2
402 1  -0.9500    1202 -103  -30          imp:n=2.24  $HDPE cylinder behind detecor 3
403 1  -0.9500    1203 -104  -30          imp:n=2.14  $HDPE cylinder behind detecor 4

```

```

404 1  -0.9500      1204  -105  -30      imp:n=2.16  $HDPE cylinder behind detecor 5
405 1  -0.9500      1205  -106  -30      imp:n=1.94  $HDPE cylinder behind detecor 6
406 1  -0.9500      1206  -107  -30      imp:n=1.96  $HDPE cylinder behind detecor 7
407 1  -0.9500      1207  -108  -30      imp:n=2.38  $HDPE cylinder behind detecor 8
408 1  -0.9500      1208  -109  -30      imp:n=2.09  $HDPE cylinder behind detecor 9
409 1  -0.9500      1209  -110  -30      imp:n=1.77  $HDPE cylinder behind detecor 10
c ---- graveyard and neutron beam ----
1  0      1300 -1301 1302 1304 -1305 -1306      imp:n=1      $ void before shadow shield
2  0      -100 1308 -30      imp:n=1      $ void behind shadow shield
301 1 -0.950000 -30 1306 -1307      imp:n=1.0    $ shadow shield
302 3 -8.650000 -30 1307 -1308      imp:n=1.0    $ Cd shield
3  0      1306 -111 30 1300 -1301 1304 -1305      imp:n=1      $ void around spectrometer
4  0      111 1300 -1301 -1303 1304 -1305      imp:n=1      $ void after spectrometer
c ---- Walls -----
5  11 -2.7 -1300 -50      imp:n=1.0    $ floor
6  11 -2.7 1301 -50      imp:n=1.0    $ ceiling
7  11 -2.7 1303 -50 -1301 1300 1304 -1305      imp:n=1.0    $ catcher wall
8  11 -2.7 -1304 -50 -1301 1300      imp:n=1.0    $ left wall
9  11 -2.7 1305 -50 -1301 1300      imp:n=1.0    $ right wall

c ***** BLOCK 2: SURFACE CARDS *****
c --- Planes for walls
1300 PZ -100.      $floor NU
1301 PZ 150.      $ceiling NU
1303 PX 250.      $Catcher NU
1304 PY -150.     $Left Wall
1305 PY 150.      $Right wall
c --- Plane for shadow shield
1306 PX 18.00     $Shadow Shield Front Plane
1307 PX 33.00     $Shadow Shield Back Plane
1308 PX 33.10     $Back Shield Cd
c --- Basic Geometry
50 RPP -60.0 270. -170. 170. -120. 170.      $outer boundary NU
1302 px -60.0     $left problem boundary
30 CX 6.8        $ cylindrical surface of spectrometer
35 RPP 100.0 125.357 -1 1 -1 1      $ square box for detector edges (2x2square)
40 RPP 100.0 125.357 -1.1 1.1 -1.1 1.1      $ square box for PCB edges (1.1x1.100000.1square)
c --- vertical slices thru the spectrometer I (front detector surfaces) ---
100 px 100.0     $front of detector 0
101 px 102.5     $front of detector 1
102 px 105.0     $front of detector 2
103 px 107.5     $front of detector 3
104 px 110.0     $front of detector 4
105 px 112.5     $front of detector 5
106 px 115.0     $front of detector 6
107 px 117.5     $front of detector 7
108 px 120.0     $front of detector 8
109 px 122.5     $front of detector 9
110 px 125.0     $front of detector 10
111 px 125.357   $back of last sheet of poly/spectr
c --- vertical slices thru the spectrometer II (back detector surfaces) ---
1100 px 100.1    $back of detector 0
1101 px 102.6    $back of detector 1
1102 px 105.1    $back of detector 2
1103 px 107.6    $back of detector 3
1104 px 110.1    $back of detector 4
1105 px 112.6    $back of detector 5
1106 px 115.1    $back of detector 6
1107 px 117.6    $back of detector 7
1108 px 120.1    $back of detector 8
1109 px 122.6    $back of detector 9
1110 px 125.1    $back of detector 10
c --- vertical slices thru the spectrometer III (Cd slices) ---
200 px 100.257   $front cd of detector 0
1200 px 100.357   $back cd of detector 0
201 px 102.757   $front cd of detector 1
1201 px 102.857   $back cd of detector 1
202 px 105.257   $front cd of detector 2

```

```

1202 px 105.357 $back cd of detector 2
1203 px 107.757 $front cd of detector 3
1203 px 107.857 $back cd of detector 3
1204 px 110.257 $front cd of detector 4
1204 px 110.357 $back cd of detector 4
1205 px 112.757 $front cd of detector 5
1205 px 112.857 $back cd of detector 5
1206 px 115.257 $front cd of detector 6
1206 px 115.357 $back cd of detector 6
1207 px 117.757 $front cd of detector 7
1207 px 117.857 $back cd of detector 7
1208 px 120.257 $front cd of detector 8
1208 px 120.357 $back cd of detector 8
1209 px 122.757 $front cd of detector 9
1209 px 122.857 $back cd of detector 9
1210 px 125.257 $front cd of detector 10
1210 px 125.357 $back cd of detector 10

c ***** BLOCK 3: DATA CARDS *****
c
c ----- Source: point source, biased, different erg dist. for each file -----
SDEF ERG=d1 PAR=1 VEC= 1 0 0 DIR=d2 POS -50.0 0. 0. $NU
SI2 -1. 0. 0.9990 1. $ histogram for cosine bin limits
SP2 0. 0. 0.4995 0.0005 $ fractional solid angle for each bin
SB2 0. 0. 1. 0.0 $Probability bias for each bin NU
SP1 -3 1.025 2.926 $ Watt distn for f-252
c ----- Problem parameters
mode n
nps 300000000
c
c
c ----- total thermal flux detector
F4:N 10 20 30 40 50 60 70 80 90 100 110
TF4 2 7j
c -----
c modify tallies to give no. (n,t) reactions per source neutron
c C=[(rho Na/A)x10-24 atom/(b-cm)] x Vol_detector
c for Li-6 to stop 50% of neutrons in .1 cm, density ~ 0.0835 g/cm3
c Vol_det = 0.4 cm3 ( 2 x 2 x .1 cm)
c find that C=0.0033286
c -----
FC4 tally modified to (n,t) reactions per source neutron
FM4 0.0033286 2 105
c
c WEIGHT WINDOW GENERATOR
c MESH geom=cyl ref=10 0 0 origin -15 0 0 axs=1 0 0 vec=0 0 1
c imesh 1.5 15.1 iints=1 4
c jmesh 99 110 120 131 jints=1 11 10 8
c kmesh 1 kints=1
c WWG 4 0 0 4j
c WWGE:n 10
c
c
c ----- MATERIALS
c -----
c material: polyethylene d=0.95 g/cm3
c -----
m1 1001.50c 2
6000.50c 1
mt1 poly.01
c
c -----
c material: Li-6F nominal d=2.7 g/cm3
c ignore F: Li-6 in LiF has a density of 0.6131 g/cm3
c -----
m2 3006.66c 1
c

```



```

c -----
c   cadmium nominal density 8.65 g/cm^3
c -----
m3   48000.50c  1
c
c -----
c   Printed circuit board...still need this one
c
m4   5010.50c  1
c -----
c   PNL CONCRETE:
c -----
c   Concrete, Ordinary, rho = 2.300
m11  1001.70c -0.022100
      6000.66c -0.002484
      8016.70c -0.574930
      11023.70c -0.015208
      12000.66c -0.001266
      13027.70c -0.019953
      14000.60c -0.304627
      19000.66c -0.010045
      20000.66c -0.042951
      26000.55c -0.006435

```

MCNP6 Input File for Spectrometer

```
MSND Device
C
C -----CELL CARDS-----
C
C Front Detector
  10 3 -2.329 -10 u=1          $ Sidewall
  11 1 -2.372 10 u=1          $ Trench, 90% PF
  12 3 -2.329 -11 lat=1 fill=1 u=2 $ Unit Cell
  13 0          -12 fill=2 u=3   $ Diode
  14 3 -2.329 -13          u=3   $ Bottom of Diode
  21 0          -21 fill=3       $ Entire top detector
  22 like 21 but trcl=(0.050 0 0.0025) $ Back detector
  15 4 -1.91 -14          $ Board
  30 6 -8.65 -15 -300 301     $ Cd
  23 5 -0.95 -15 (#15 #21 #22 #30) $ Moderator
c 2nd Detector
  110 3 -2.329 -10 u=4        $ Sidewall
  111 1 -2.372 10 u=4        $ Trench, 90% PF
  112 like 12 but fill=4 u=5  $ Unit Cell
  113 like 13 but fill=5 u=6  $ Diode
  114 3 -2.329 -13          u=6  $ Bottom of Diode
  121 0          -21 fill=6 trcl=1 $ Entire top detector
  122 like 121 but trcl=(-2.950 0 0.0025) $ Back detector
  115 like 15 but trcl =(-3.0 0. 0.) $ Board
  130 like 30 but trcl =(-3.0 0. 0.) $ Cd
  123 5 -0.95 -115 (#115 #121 #122 #130) $ Moderator
c 3rd Detector
  210 3 -2.329 -10 u=7        $ Sidewall
  211 1 -2.372 10 u=7        $ Trench, 90% PF
  212 like 12 but fill=7 u=8  $ Unit Cell
  213 like 13 but fill=8 u=9  $ Diode
  214 3 -2.329 -13          u=9  $ Bottom of Diode
  221 0          -21 fill=9 trcl=(-6 0. 0.) $ Entire top detector
  222 like 221 but trcl =(-5.950 0 0.0025)$ Back detector
  215 like 15 but trcl =(-6.0 0. 0.) $ Board
  230 like 30 but trcl =(-6.0 0. 0.) $ Cd
  223 5 -0.95 -215 (#215 #221 #222 #230) $ Moderator
c 4th Detector
  310 3 -2.329 -10 u=10       $ Sidewall
  311 1 -2.372 10 u=10       $ Trench, 90% PF
  312 like 12 but fill=10 u=11 $ Unit Cell
  313 like 13 but fill=11 u=12 $ Diode
  314 3 -2.329 -13          u=12  $ Bottom of Diode
  321 0          -21 fill=12 trcl=(-9. 0. 0.) $ Entire top detector
  322 like 321 but trcl =(-8.950 0 0.0025)$ Back detector
  315 like 15 but trcl =(-9.0 0. 0.) $ Board
  330 like 30 but trcl =(-9.0 0. 0.) $ Cd
  323 5 -0.95 -315 (#315 #321 #322 #330) $ Moderator
c 5th Detector
  410 3 -2.329 -10 u=13       $ Sidewall
  411 1 -2.372 10 u=13       $ Trench, 90% PF
  412 like 12 but fill=13 u=14 $ Unit Cell
  413 like 13 but fill=14 u=15 $ Diode
  414 3 -2.329 -13          u=15  $ Bottom of Diode
  421 0          -21 fill=15 trcl=(-12. 0. 0.) $ Entire top detector
  422 like 421 but trcl =(-11.950 0 0.0025)$ Back detector
  415 like 15 but trcl =(-12.0 0. 0.) $ Board
  430 like 30 but trcl =(-12.0 0. 0.) $ Cd
  423 5 -0.95 -415 (#415 #421 #422 #430) $ Moderator
C Region Outside of detector and kill zone
  100 0          -99 115 215 315 415 15 $ Gap around Moderator
  101 0 99          $ OUTSIDE WORLD

C -----SURFACE CARDS-----
C
```

```

C Front Device
 10 RPP 0.115 0.15 -1.0 1.0 -0.002 0 $ Sidewall
 11 RPP 0.115 0.15 -1.0 1.0 -0.005 0 $ Unit Cell
 12 RPP 0.115 0.15 -1.0 1.0 -1 1 $ Diode
 13 RPP 0.1 0.115 -1.0 1.0 -1 1 $ Back of Diode
 21 RPP 0.1 0.15 -1.0 1.0 -1 1 $Entire 1st detector
 14 RPP 0.0 0.1 -1.0 1.0 -1 1 $ Board
 15 RCC 0.2 0.0 0.0 -3.0 0. 0. 6.0 $ Moderator
 115 RCC -2.8 0. 0.0 -3.0 0. 0. 6.0 $ Moderator Det 2
 215 RCC -5.8 0. 0.0 -3.0 0. 0. 6.0 $ Moderator Det 3
 315 RCC -8.8 0. 0.0 -3.0 0. 0. 6.0 $ Moderator Det 4
 415 RCC -11.8 0. 0.0 -3.0 0. 0. 6.0 $ Moderator Det 5
 99 RCC 5.0 0.0 0.0 -30. 0. 0. 7.0 $ Prob Boundary
 300 PX 0.0 $Cd slice 1 front
 301 PX -0.1 $Cd slice 1 back

```

C

C -----DATA CARDS-----

C

C --- PHYSICS/CUT OFF -----

MODE N T A

```

IMP:N 1 9R 1 9R 1 9R 1 9R 1 0
IMP:T 1 6R 0 2R 1 6R 0 2R 1 6R 0 2R 1 6R 0 2R 1 6R 0 2R 0 0
IMP:A 1 6R 0 2R 1 6R 0 2R 1 6R 0 2R 1 6R 0 2R 1 6R 0 2R 0 0
PHYS:N 6J 3 $ NCIA, 3=ions are from neutron capture
CUT:N 2J 0 $ Analog capture
CUT:T J 0.001 0 $ Energy cut
CUT:A J 0.001 0 $ Energy cut

```

C

C MATERIALS

C

```

M1 $ 6-LITHIUM FLUORIDE, RHO = 2.635 (CRYSTALLINE)
 3006.70c -0.225502
 3007.70c -0.016789
 9019.70c -0.757709

```

C

C AIR, DRY, RHO = 0.001205

```

M2 6000.70c -0.000124
 7014.70c -0.755268
 8016.70c -0.231781
 18040.70c -0.012827

```

C

M3 \$ NATURAL SILICON, RHO = 2.3290

```

 14028.70c 9.22230000E-01
 14029.70c 4.68500000E-02
 14030.70c 3.09200000E-02

```

C

M4 \$ FR4 Electronics board material, rho = 1.91

```

 1001.70c -0.010 $ Epoxy
 5010.70c -0.0053 $ Fiberglass
 5011.70c -0.0147 $ Fiberglass
 6000.70c -0.040 $ Epoxy
 8016.70c -0.390 $ Fiberglass/Epoxy
 13027.70c -0.010 $ Fiberglass
 14028.70c -0.230 $ Fiberglass
 29063.70c -0.140 $ Copper
 29065.70c -0.060 $ Copper
 35079.70c -0.050 $ Epoxy
 35081.70c -0.050 $ Epoxy

```

C

C POLYETHYLENE (HIGH-DENSITY), RHO = 0.9500

```

M5 1001.70c -0.143716
 6000.70c -0.856284

```

MT5 POLY.10T

c

c cadmium nominal density 8.65 g/cm³

c

m6 48000.50c 1

```

SDEF pos= 1.5 0 0 PAR= 1 ERG= D2 VEC= 1 0 0 DIR= -1.
      rad=d1 ext=0 axs=1 0 0
SI1 0.0 6.0
SP1 -21 1
SP2 -3 1.025 2.926 $ Watt distn for f-252
c --- Cell Movements -----
TR1 -3.0 0.0 0.0
C --- TALLY -----
F6:A (10 14)
SD6 1
F16:T (10 14)
SD16 1
F8:A,T (10 14)
FT8 phl 2 6 1 16 1 0
E8 0 1E-5 1E-3 3E-1 5 $efficiency calc
c --- 2nd detector ---
F106:A (110 114)
SD106 1
F116:T (110 114)
SD116 1
F18:A,T (110 114)
FT18 phl 2 106 1 116 1 0
E18 0 1E-5 1E-3 3E-1 5 $efficiency calc
c -- 3rd detector ----
F206:A (210 214)
SD206 1
F216:T (210 214)
SD216 1
F28:A,T (210 214)
FT28 phl 2 206 1 216 1 0
E28 0 1E-5 1E-3 3E-1 5 $efficiency calc
c -- 4th detector ----
F306:A (310 314)
SD306 1
F316:T (310 314)
SD316 1
F38:A,T (310 314)
FT38 phl 2 306 1 316 1 0
E38 0 1E-5 1E-3 3E-1 5 $efficiency calc
c -- 5th detector ----
F406:A (410 414)
SD406 1
F416:T (410 414)
SD416 1
F48:A,T (410 414)
FT48 phl 2 406 1 416 1 0
E48 0 1E-5 1E-3 3E-1 5 $efficiency calc
c ---flux tallies ---
F54:n (21 22)
E54 0 0.0254E-6 10
F64:n (121 122)
E64 0 0.0254E-6 10
F74:n (221 222)
E74 0 0.0254E-6 10
C --- Problem Stuff -----
nps 1E8
dbcn 28j 1 $ Turns on MCNPX algorithms
FT138 CAP
print

```

Appendix D

Example Tabulated Data for Spectrometer Simulations

Description	Starting Page
Example of simulation data for a neutron beam uniformly irradiating a spectrometer in a void for various values of t .	187
Example of simulated counting measurements for room scatter and void template simulations for a point source with concrete floor. The optimal shadow shield and several sources were used. The spectrometer has the geometric parameters $N_{det} = 11$, $r = 6.8$ cm, $t = 2.5$ cm.	193

Fixed Radius Example Data

Table D.1: Simulation data for spectrometer with geometry parameters $N_{det} = 11$, $r = 10.00$ cm, and $t = 2.00$ cm.

Source is ^{252}Cf s.f.				
i	x (cm)	r_i	$\sigma_{rel}(r_i)$	C_i (counts)
1	0.00	5.18e-05	4.90e-03	52107
2	2.00	4.56e-04	3.60e-03	456575
3	4.00	6.03e-04	2.90e-03	603345
4	6.00	5.35e-04	2.70e-03	535444
5	8.00	4.08e-04	2.60e-03	406720
6	10.00	2.86e-04	2.50e-03	285371
7	12.00	1.92e-04	2.50e-03	191782
8	14.00	1.28e-04	2.60e-03	127731
9	16.00	8.27e-05	2.60e-03	82879
10	18.00	5.08e-05	2.80e-03	51005
11	20.00	2.31e-05	3.40e-03	22961
s_0 (n cm $^{-2}$)			Template	FOM
3.18e+06			^{252}Cf s.f.	2.30
			^{240}Pu s.f.	3632.00
Source is ^{240}Pu s.f.				
i	x (cm)	r_i	$\sigma_{rel}(r_i)$	C_i (counts)
1	0.00	5.55e-05	4.70e-03	55583
2	2.00	4.89e-04	3.50e-03	487576
3	4.00	6.30e-04	2.80e-03	630142
4	6.00	5.55e-04	2.60e-03	554393
5	8.00	4.14e-04	2.50e-03	413694
6	10.00	2.83e-04	2.40e-03	283514
7	12.00	1.85e-04	2.40e-03	184442
8	14.00	1.20e-04	2.40e-03	119510
9	16.00	7.56e-05	2.50e-03	75621
10	18.00	4.54e-05	2.60e-03	45187
11	20.00	2.04e-05	3.20e-03	20464
s_0 (n cm $^{-2}$)			Template	FOM
3.18e+06			^{240}Pu s.f.	2.42
			^{252}Cf s.f.	3287.00

Table D.2: Simulation data for spectrometer with geometry parameters $N_{det} = 11$, $r = 10.00$ cm, and $t = 3.00$ cm.

Source is ^{252}Cf s.f.				
i	x (cm)	r_i	$\sigma_{rel}(r_i)$	C_i (counts)
1	0.00	5.24e-05	4.90e-03	52292
2	3.00	7.48e-04	2.90e-03	748712
3	6.00	7.78e-04	2.40e-03	777503
4	9.00	5.07e-04	2.30e-03	507560
5	12.00	2.86e-04	2.30e-03	286121
6	15.00	1.55e-04	2.30e-03	154373
7	18.00	8.31e-05	2.30e-03	82917
8	21.00	4.48e-05	2.40e-03	44823
9	24.00	2.45e-05	2.40e-03	24939
10	27.00	1.31e-05	2.50e-03	13024
11	30.00	5.18e-06	3.10e-03	5137
s_0 (n cm $^{-2}$)		Template		FOM
3.18e+06		^{252}Cf s.f.		6.66
		^{240}Pu s.f.		7514.00
Source is ^{240}Pu s.f.				
i	x (cm)	r_i	$\sigma_{rel}(r_i)$	C_i (counts)
1	0.00	5.64e-05	4.70e-03	56720
2	3.00	7.97e-04	2.80e-03	796549
3	6.00	8.10e-04	2.30e-03	808712
4	9.00	5.10e-04	2.20e-03	508867
5	12.00	2.76e-04	2.20e-03	275981
6	15.00	1.43e-04	2.20e-03	142619
7	18.00	7.36e-05	2.20e-03	73704
8	21.00	3.79e-05	2.30e-03	37738
9	24.00	1.99e-05	2.30e-03	20095
10	27.00	1.02e-05	2.40e-03	10372
11	30.00	3.89e-06	2.90e-03	4029
s_0 (n cm $^{-2}$)		Template		FOM
3.18e+06		^{240}Pu s.f.		9.22
		^{252}Cf s.f.		6397.00

Table D.3: Simulation data for spectrometer with geometry parameters $N_{det} = 11$, $r = 10.00$ cm, and $t = 3.50$ cm.

Source is ^{252}Cf s.f.				
i	x (cm)	r_i	$\sigma_{rel}(r_i)$	C_i (counts)
1	0.00	5.29e-05	4.80e-03	52714
2	3.50	8.73e-04	2.60e-03	872715
3	7.00	7.88e-04	2.20e-03	787797
4	10.50	4.38e-04	2.20e-03	438737
5	14.00	2.18e-04	2.20e-03	217490
6	17.50	1.05e-04	2.20e-03	105040
7	21.00	5.15e-05	2.30e-03	51578
8	24.50	2.55e-05	2.40e-03	25315
9	28.00	1.29e-05	2.40e-03	12546
10	31.50	6.49e-06	2.50e-03	6508
11	35.00	2.43e-06	3.00e-03	2501
s_0 (n cm $^{-2}$)			Template	<i>FOM</i>
3.18e+06			^{252}Cf s.f.	12.61
			^{240}Pu s.f.	8599.00
Source is ^{240}Pu s.f.				
i	x (cm)	r_i	$\sigma_{rel}(r_i)$	C_i (counts)
1	0.00	5.66e-05	4.70e-03	56955
2	3.50	9.33e-04	2.50e-03	933247
3	7.00	8.09e-04	2.10e-03	808462
4	10.50	4.33e-04	2.10e-03	432803
5	14.00	2.05e-04	2.10e-03	204933
6	17.50	9.40e-05	2.20e-03	93966
7	21.00	4.37e-05	2.20e-03	43392
8	24.50	2.05e-05	2.20e-03	20476
9	28.00	9.85e-06	2.30e-03	9942
10	31.50	4.71e-06	2.40e-03	4724
11	35.00	1.70e-06	2.90e-03	1767
s_0 (n cm $^{-2}$)			Template	<i>FOM</i>
3.18e+06			^{240}Pu s.f.	5.52
			^{252}Cf s.f.	7613.00

Table D.4: Simulation data for spectrometer with geometry parameters $N_{det} = 11$, $r = 10.00$ cm, and $t = 4.00$ cm.

Source is ^{252}Cf s.f.				
i	x (cm)	r_i	$\sigma_{rel}(r_i)$	C_i (counts)
1	0.00	5.26e-05	4.80e-03	52415
2	4.00	9.73e-04	2.40e-03	974040
3	8.00	7.54e-04	2.10e-03	753923
4	12.00	3.64e-04	2.20e-03	364228
5	16.00	1.60e-04	2.20e-03	159829
6	20.00	7.04e-05	2.20e-03	70732
7	24.00	3.13e-05	2.30e-03	31155
8	28.00	1.44e-05	2.30e-03	14608
9	32.00	6.77e-06	2.40e-03	6678
10	36.00	3.23e-06	2.50e-03	3121
11	40.00	1.15e-06	3.10e-03	1116
s_0 (n cm $^{-2}$)			Template	FOM
3.18e+06			^{252}Cf s.f.	10.45
			^{240}Pu s.f.	8351.00
Source is ^{240}Pu s.f.				
i	x (cm)	r_i	$\sigma_{rel}(r_i)$	C_i (counts)
1	0.00	5.65e-05	4.70e-03	56561
2	4.00	1.03e-03	2.40e-03	1032070
3	8.00	7.71e-04	2.10e-03	771816
4	12.00	3.54e-04	2.10e-03	354063
5	16.00	1.47e-04	2.10e-03	145698
6	20.00	6.03e-05	2.20e-03	60317
7	24.00	2.55e-05	2.20e-03	25595
8	28.00	1.09e-05	2.30e-03	10857
9	32.00	4.89e-06	2.30e-03	4788
10	36.00	2.19e-06	2.40e-03	2243
11	40.00	7.51e-07	2.80e-03	765
s_0 (n cm $^{-2}$)			Template	FOM
3.18e+06			^{240}Pu s.f.	6.48
			^{252}Cf s.f.	7201.00

Table D.5: Simulation data for spectrometer with geometry parameters $N_{det} = 11$, $r = 10.00$ cm, and $t = 4.50$ cm.

Source is ^{252}Cf s.f.				
i	x (cm)	r_i	$\sigma_{rel}(r_i)$	C_i (counts)
1	0.00	5.29e-05	4.90e-03	53014
2	4.50	1.05e-03	2.30e-03	1048627
3	9.00	6.96e-04	2.10e-03	694879
4	13.50	2.93e-04	2.20e-03	292757
5	18.00	1.15e-04	2.20e-03	115449
6	22.50	4.62e-05	2.30e-03	46237
7	27.00	1.90e-05	2.30e-03	19134
8	31.50	8.14e-06	2.40e-03	8172
9	36.00	3.60e-06	2.50e-03	3510
10	40.50	1.63e-06	2.50e-03	1694
11	45.00	5.50e-07	3.00e-03	557
s_0 (n cm $^{-2}$)			Template	FOM
3.18e+06			^{252}Cf s.f.	6.13
			^{240}Pu s.f.	8259.00
Source is ^{240}Pu s.f.				
i	x (cm)	r_i	$\sigma_{rel}(r_i)$	C_i (counts)
1	0.00	5.68e-05	4.70e-03	56628
2	4.50	1.11e-03	2.20e-03	1107345
3	9.00	7.04e-04	2.10e-03	704396
4	13.50	2.79e-04	2.10e-03	280475
5	18.00	1.03e-04	2.20e-03	102770
6	22.50	3.83e-05	2.20e-03	38518
7	27.00	1.47e-05	2.30e-03	14645
8	31.50	5.87e-06	2.30e-03	5883
9	36.00	2.43e-06	2.40e-03	2403
10	40.50	1.03e-06	2.40e-03	1008
11	45.00	3.33e-07	3.00e-03	301
s_0 (n cm $^{-2}$)			Template	FOM
3.18e+06			^{240}Pu s.f.	6.61
			^{252}Cf s.f.	6601.00

Table D.6: Simulation data for spectrometer with geometry parameters $N_{det} = 11$, $r = 10.00$ cm, and $t = 5.00$ cm.

Source is ^{252}Cf s.f.				
i	x (cm)	r_i	$\sigma_{rel}(r_i)$	C_i (counts)
1	0.00	5.26e-05	4.90e-03	52098
2	5.00	1.10e-03	2.20e-03	1102268
3	10.00	6.25e-04	2.20e-03	624350
4	15.00	2.32e-04	2.20e-03	232509
5	20.00	8.19e-05	2.30e-03	81281
6	25.00	3.00e-05	2.30e-03	29727
7	30.00	1.15e-05	2.40e-03	11498
8	35.00	4.59e-06	2.40e-03	4670
9	40.00	1.92e-06	2.50e-03	1930
10	45.00	8.31e-07	2.60e-03	829
11	50.00	2.70e-07	3.10e-03	270
s_0 (n cm $^{-2}$)			Template	FOM
3.18e+06			^{252}Cf s.f.	8.75
			^{240}Pu s.f.	7494.00
Source is ^{240}Pu s.f.				
i	x (cm)	r_i	$\sigma_{rel}(r_i)$	C_i (counts)
1	0.00	5.67e-05	4.70e-03	56540
2	5.00	1.16e-03	2.10e-03	1162559
3	10.00	6.28e-04	2.10e-03	627665
4	15.00	2.16e-04	2.10e-03	217045
5	20.00	7.10e-05	2.20e-03	71238
6	25.00	2.40e-05	2.20e-03	23884
7	30.00	8.51e-06	2.30e-03	8516
8	35.00	3.15e-06	2.30e-03	3110
9	40.00	1.23e-06	2.40e-03	1224
10	45.00	4.98e-07	2.50e-03	485
11	50.00	1.54e-07	3.00e-03	135
s_0 (n cm $^{-2}$)			Template	FOM
3.18e+06			^{240}Pu s.f.	5.25
			^{252}Cf s.f.	6240.00

Room-Scatter, Floor Only Example Data

Table D.7: Simulated counting data from point sources of strength $s_0 = 10^9$ n cm⁻² above a concrete floor; FOM^{\min} and $FOM^{\min+}$ represent the lowest and second lowest FOM values, respectively, and C_i^{net} is the room shine net spectra, i.e., $C_i^{net} = C_i^{ns} - C_i^s$. Values in the table of “Correct” and “Inorrect” indicate whether the source was correctly identified.

Source is monoenergetic 100 keV neutrons					
i	C_i^{ns} (counts)	C_i^s (counts)	r_i^{void}	r_i^{void}/r_2^{void}	C_i^{net}/C_2^{net}
1	1069	563	3.94E-07	0.174	0.223
2	2411	145	2.26E-06	1.000	1.000
3	551	24	5.10E-07	0.226	0.233
4	66	17	4.91E-08	0.022	0.022
5	15	6	3.33E-09	0.001	0.004
6	16	8	2.39E-10	0.000	0.004
7	6	4	1.25E-11	0.000	0.001
8	9	8	0.00E+00	0.000	0.000
9	10	13	0.00E+00	0.000	-0.001
10	17	7	0.00E+00	0.000	0.004
11	23	16	0.00E+00	0.000	0.003
FOM_{room}^{\min} 2.37		$FOM_{room}^{\min+} = 1397.00$		Correct	
Source is monoenergetic 1 MeV neutrons					
i	C_i^{ns} (counts)	C_i^s (counts)	r_i^{void}	r_i^{void}/r_2^{void}	C_i^{net}/C_2^{net}
1	295	215	6.17E-08	0.090	0.114
2	887	188	6.85E-07	1.000	1.000
3	892	133	7.83E-07	1.143	1.086
4	637	127	5.37E-07	0.784	0.730
5	429	115	2.80E-07	0.409	0.449
6	220	92	1.29E-07	0.188	0.183
7	160	88	5.45E-08	0.080	0.103
8	126	106	2.16E-08	0.031	0.029
9	114	85	8.01E-09	0.012	0.041
10	78	94	3.02E-09	0.004	-0.023
11	73	72	9.51E-10	0.001	0.001
FOM_{room}^{\min} 7.50		$FOM_{room}^{\min+} = 11.28$		Incorrect	

Source is AmBe (α, n)					
i	C_i^{ns} (counts)	C_i^s (counts)	r_i^{void}	r_i^{void}/r_2^{void}	C_i^{net}/C_2^{net}
1	214	216	3.36E-08	0.088	-0.006
2	454	110	3.83E-07	1.000	1.000
3	538	86	4.47E-07	1.167	1.314
4	387	77	3.50E-07	0.916	0.901
5	325	64	2.45E-07	0.641	0.759
6	225	65	1.66E-07	0.434	0.465
7	134	77	1.04E-07	0.273	0.166
8	139	60	6.80E-08	0.178	0.230
9	97	49	4.23E-08	0.111	0.140
10	90	46	2.57E-08	0.067	0.128
11	53	42	1.16E-08	0.030	0.032
FOM_{room}^{\min} 11.33		$FOM_{room}^{\min+} = 15.70$		Incorrect	
Source is ^{252}Cf s.f.					
i	C_i^{ns} (counts)	C_i^s (counts)	r_i^{void}	r_i^{void}/r_2^{void}	C_i^{net}/C_2^{net}
1	264	234	4.75E-08	0.090	0.056
2	667	133	5.30E-07	0.235	1.000
3	728	98	6.03E-07	0.267	1.180
4	533	72	4.48E-07	0.198	0.863
5	346	78	2.60E-07	0.115	0.502
6	209	81	1.53E-07	0.068	0.240
7	137	53	8.28E-08	0.037	0.157
8	113	75	4.79E-08	0.021	0.071
9	92	67	2.66E-08	0.012	0.047
10	90	68	1.49E-08	0.007	0.041
11	43	37	5.94E-09	0.003	0.011
FOM_{room}^{\min} 3.28		$FOM_{room}^{\min+} = 9.66$		Correct	

Source is ^{252}Cf w/ 30-cm D_2O moderator					
i	C_i^{ns} (counts)	C_i^s (counts)	r_i^{void}	r_i^{void}/r_2^{void}	C_i^{net}/C_2^{net}
1	750	444	3.51E-07	0.209	0.182
2	1827	144	1.68E-06	1.000	1.000
3	723	57	6.67E-07	0.398	0.396
4	236	31	2.04E-07	0.122	0.122
5	84	22	7.44E-08	0.044	0.037
6	70	27	3.48E-08	0.021	0.026
7	54	43	1.90E-08	0.011	0.007
8	42	30	1.10E-08	0.007	0.007
9	25	26	5.89E-09	0.004	-0.001
10	37	25	3.38E-09	0.002	0.007
11	29	35	1.41E-09	0.001	-0.004
FOM_{room}^{\min} 7.54		$FOM_{room}^{\min+} = 240.60$		Correct	
Source is monenergetic 14.1 MeV neutrons					
i	C_i^{ns} (counts)	C_i^s (counts)	r_i^{void}	r_i^{void}/r_2^{void}	C_i^{net}/C_2^{net}
1	93	113	8.16E-09	0.085	-0.233
2	136	50	9.56E-08	1.000	1.000
3	196	42	1.41E-07	1.477	1.791
4	197	43	1.59E-07	1.662	1.791
5	193	52	1.37E-07	1.437	1.640
6	161	53	1.18E-07	1.239	1.256
7	164	42	9.87E-08	1.032	1.419
8	136	34	8.40E-08	0.878	1.186
9	104	48	6.30E-08	0.659	0.651
10	65	28	4.22E-08	0.442	0.430
11	33	20	2.06E-08	0.216	0.151
FOM_{room}^{\min} 6.43		$FOM_{room}^{\min+} = 265.80$		Correct	

Source is $^{238}\text{PuBe}$ (α, n)					
i	C_i^{ns} (counts)	C_i^s (counts)	r_i^{void}	r_i^{void}/r_2^{void}	C_i^{net}/C_2^{net}
1	217	198	2.77E-08	0.078	0.054
2	455	106	3.57E-07	1.000	1.000
3	497	74	4.26E-07	1.193	1.212
4	402	85	3.45E-07	0.967	0.908
5	302	75	2.54E-07	0.712	0.650
6	219	58	1.66E-07	0.464	0.461
7	169	74	1.08E-07	0.301	0.272
8	125	68	7.01E-08	0.196	0.163
9	101	63	4.39E-08	0.123	0.109
10	85	38	2.70E-08	0.076	0.135
11	48	43	1.21E-08	0.034	0.014
$FOM_{room}^{\min} = 7.70$		$FOM_{room}^{\min+} = 45.97$		Correct	

Appendix E

Multiplicity Scripts and Codes

File Name	Description	Page
mf33.py	Data utility class for MF33 and MF31 ENDF “files”. These MF files contain information for all covariance matrices for a particular isotope, and pointers to subsections that contain the actual covariance data. See [ENDF-6 Manual, 2011] for format details.	198
cov_matrices.py	Data utility class for entire covariance matrices from ENDF neutron data files. Contains all sub-routines for random samples of covariance matrices.	203
ace_sb.py	Data utility class for modifying and regenerating ACE format files. The sample_data member function is where actual data perturbations take place. This function was modified as needed to produce desired data for different cross sections and $\bar{\nu}$	217
mtool.pl	LANL internal script that computes multiplicity distributions using a non-paralyzable dead time correction.	—
mult_chi_sq.py	Procedural script that parses and manipulates data from all trials to compute FOM and χ_{mult}^2 values. The file directories and naming of trials are hard coded.	238

mf33.py: Utility Class for ENDF files

```
#!/usr/bin/env python
"Provides methods for working with ENDF102 MF33 Records."
#=====
__version__ = "$Id: mf33.py,v 1.9 2012/06/15 23:50:24 morgan Exp $"
#=====
# Load local python modules

from ndvv.endf.records.control import controlRecord
from ndvv.endf.records.list import listRecord
from ndvv.log import devnull
from ndvv.endf.records.peak import peak_at_controlRecord
from ndvv.endf.cov_matrices import endfCovMatrix
from math import sqrt

from numpy import zeros, array, diag

#=====
class mf33Record(object):
    """This class includes all of the combinations of mt's (mt1 and mt).

    33.2 Formats

    Section:

    [MAT, 33, MT/ ZA, AWR, 0, MTL, 0, NL] HEAD
        <subsection for n = 1>
        <subsection for n = 2>
        <subsection for n = NL>
    [MAT, 33, 0/ 0.0, 0.0, 0, 0, 0, 0] SEND

    Subsection:

    [MAT,33,MT/ XMF1, XLFS1, MAT1, MT1, NC, NI]CONT
        <sub-subsection for n =1>

    Sub-subsection:

        NI-type:

        LB=5: [MAT,33,MT/ 0.0, 0.0, LS, LB=5, NT, NE/ {Ek}-{Fk,k}] LIST.
            ariables : NT Total number of entries in the two arrays {Ek} and {Fk,k}.
                       NE Number of entries in the array {Ek} defining (NE-1) energy intervals.
                       LS Flag indicating whether the {F_(k,k')} matrix is symmetric or not.

    Definiton of Variables:

        AWR - Atomic mass of target ratio to neutron mass
        ZA - Atomic number Z*1000 plus atomic mass number A
        XMF1 - Floating point equivalent of the MF for the 2nd energy-dependent cross section
              of the pair, for which the correlation matrix is given. If MF1=MF,XMF1=0.0 or
              blank.
        XLFS1 - Floating point equivalent for the final excited state of the 2nd energy dependent
              cross section. For MF1=10, XLFS1 = 10; if MF16=10, XLFS1=0.0 or blank.
        MAT1 - MAT for the 2nd /energy-dependent cross section
        MT1 - MT for the 2nd energy-dependent cross section
        NC - Number of NC-type sub-subsections which follow the CONT record.
        NI - Number of NI-type sub-subsections which follow the NC-type subsubsections.
        MTL - Non-zero value of MTL is used as a flag to indicate that reaction MT is
              one component of the evaluator-defined lumped reaction MTL
        NL - Number of subsections within a section.
        LB - Flag whose numerical value determines the meanings of the numbers given
```

```

        in the arrays {Ek, Fk}{E1, F1}.
FOR LB=5:

NP      - Total number of pairs of numbers in the arrays {Ek, Fk}{E1, F1}.
NT      - Total number of numbers in the LIST record; NT=2*NP.
LT      - Number of pairs of numbers in the second array, {E1, F1}.
          If LT=0, the table contains a single array {Ek, Fk}.
          If LT not = 0, the table contains two arrays; the first array, {Ek, Fk}, has
          (NP - LT) pairs of numbers in it.

```

The first line read must contain a valid /MAT,MF,MT/. The loose variable may be used to ignore subsequent values.

A python logger may be used to capture messages about the data as it is parsed, checked, or manipulated.

```

"""
# -----
def __init__(self, f=None, loose=False, logger=None):
    "Initialize a MF33 covariance record possibly reading data from f[file object]."

    self.clear()

    if f is not None:
        self.parse(f=f,loose=loose,logger=logger)

    return None

# -----
def clear(self):
    "Clear the current record."
    self.__dict__['endfRecords'] = controlRecord()
    self.__dict__['endfCovMatrices'] = [endfCovMatrix()]
    return None

# -----
def __getattr__(self, name):
    "Override getattr to allow multiple ways of getting record values."

    cr = self.__dict__['endfRecords']
    endfCovMatrices = self.__dict__['endfCovMatrices']

    d = {
        'cr'           : 'cr',
        'matmfmt'     : 'cr.mat, cr.mf, cr.mt',
        'mfmt'        : 'cr.mf, cr.mt',
        'mat'         : 'cr.mat',
        'mf'          : 'cr.mf',
        'mt'          : 'cr.mt',
        'za'          : 'cr.c1',
        'awr'         : 'cr.c2',
        'mtl'         : 'cr.l2',
        'nl'          : 'cr.n2',
    }

    value = eval( d.get( name, 'None' ) )

    if value is not None:
        return value

    raise AttributeError("endf mf33 object has no attribute %s"%(name))

```

```

#-----
def __setattr__(self, name, value):
    "Override setattr to allow multiple ways of setting record values."

    cr = self.__dict__['endfRecords']
    endfCovMatrices = self.__dict__['endfCovMatrices']

    d = {
        'matmfmt'      : 'self.mat, self.mf, self.mt = value',
        'mfmt'         : 'self.mf, self.mt = value',
        'mat'          : 'cr.mat= value',
        'mf'           : 'cr.mf=value',
        'mt'           : 'cr.mt= value',
        'za'           : 'cr.c1 = value',
        'awr'          : 'cr.c2 = value',
        'mt1'          : 'cr.l2 = value',
        'nl'           : 'cr.n2= value'
    }

    exec( d.get( name, "self.__dict__[name] = value" ) )

    return None

# -----
def parse( self, f, loose=False, logger=None):
    "Read the MF33 data."

    if logger is None:
        logger = devnull
    logger.log(9,"entered routine ndvv.endf.mf33.parse")
    logger.log(8,"%s"%(__version__))

    "Read in the head record first:"
    cr = controlRecord(f=f, loose=loose, logger=logger)

    if (cr.l2 != 0):
        raise NotImplemented("There is a lumped reaction sum, not implemented in code yet, see section \
            33.2 of ENDF6 Manual for more info")
        #TODO

    #loop through all the subsections, storing their particular cov matrix data.
    covMatrixRecords = []
    for subSection in range(cr.n2):
        covMatrixRecords.append(endfCovMatrix(f=f, logger=logger, loose=loose))

    self.__dict__['endfCovMatrices'] = covMatrixRecords
    self.__dict__['endfRecords'] = cr

    return None

#-----
def get_endfCovMatrix(self, mf1=None, mt1=None, mat1=None):
    """"Returns the full covariance matrices for a particular mt1 & mf1 (certain subsection record
    in the form of cov_matrices class) and corresponding energies. Note
    that this is not all one cov matrix, but different pieces separated by
    energy""""

    "Look for same mf1 and mat1 and mt1 if there is none specified"
    if (mf1 == None):
        mf1 = 0.0
    if (mat1 == None):
        mat1 = 0
    if (mt1 == None):
        mt1 = self.mt

    "get the index of the covariance matrices you want by checking all subsections:"

```

```

counter = 0

for ss in self.endfCovMatrices:

    #put in temp check to make sure no mat1's different from mat TODO

    if (ss.mat1 != 0) or (ss.xmf1 != 0.0):
        raise NotImplementedError("There are mf1 and mat1 different from mf and mat")

    elif (ss.mt1 == mt1 and ss.mat1 == mat1 and ss.xmf1 == mf1):

        return self.endfCovMatrices[counter]

    else:
        counter += 1

return None

#-----
def get_full_matrix(self, mf1=None, mt1=None, mat1=None):
    """Returns a full covariance matrix (covers full energy range). If any entries are None,
    the program assumes mf1=mf, or mt1=mt, etc."""

    #find the write cov_matrices instance (sub section)
    ss = self.get_endfCovMatrix(mf1=mf1, mt1=mt1, mat1=mat1)

    #Generate full matrix
    return ss.get_full_matrix()

#-----
def get_corr_matrix(self, mf1=None, mt1=None, mat1=None):
    """Returns a full covariance matrix (covers full energy range). If any entries are None,
    the program assumes the same mat1mf1mt1 as section matmfmt"""

    #find the write cov_matrices instance (sub section)
    ss = self.get_endfCovMatrix(mf1=mf1, mt1=mt1, mat1=mat1)

    #Generate corr matrix
    return ss.get_corr_matrix()

#-----
def sample_cross_section(self, mf1=None, mt1=None, mat1=None, fi=None, cross_sections=None,
    interpolation=None):

    """Samples a vector of ne-1 normally distributed random numbers using Mersenne twister
    algorithm and then uses a specified correlation matrix to correlate the random numbers. If
    no mf1 or mt1 are specified it is assumed that you want mf1=mf & mt1=mt.

    This returns the modified cross sections as an array. WARNING: the fi in this class is not the fi that
    this class is associated with, so modifying it will not modify the original fi."""

    raise NotImplementedError("This function should work, but I have not explicitly tested it, so be wary."
    + "The alg. worked for ACE files so it should be k")

    #Generate the right cov_matrices instance (sub section)
    ss = self.get_endfCovMatrix(mf1=mf1, mt1=mt1, mat1=mat1)

    #Get the correct cross-sections out, noting that by default the mf is just mf - 30
    if fi==None:
        raise ValueError("Must pass in the file_index object you are working with")

    exec("section=fi.get_section(mf=%d, mt=%d)" % (ss.mf-30, ss.mt))

    #store cross sections in an array by finding the tab1 record:
    endfRecords = section.endfRecords

```

```

for rec in endfRecords:

    if getattr(rec, "line", False): #is it a TAB1 record?

        rec.line.y = array(rec.line.y)
        cross_sections = array(rec.line.y)
        energies = array(rec.line.x)
        endfRecord = rec
        break

    else:
        continue

#Sample cross sections using the cov_matrices class
return cov_matrix.sample_cross_section(cross_sections, energies, interpolation)

#=====
if __name__ == "main":

    #file name and directory of endf file
    endf_dir='/home/sbolding/ENDF_Stuff/CrossX061212/neutrons/'
    file_name='n-094_Pu_239.endf'

    # a = mf33Record(file_name)

```

cov_matrices.py: Utility Class for ENDF Covariance Matrices

```
#!/usr/bin/env python
"""Provides methods for handling the Covariances matrices specified in 31 and 33 series of files
    The subsections should really be read out into their own class so that each one will contain
    its own energy etc, currenly they are just lined up by index and two different members of this
    class.

    Need to be wary that if you were going to reprint these cov matrices to a file the NC
    type subsections MUST come first. You would need to not sort them by energy.

    WARNING: The current version creates the full matrix assuming that each sub_matrix is only for a
    particular energy range, if there is overlap it probably won't work. U235 nubar for example,
    this will not work on. I didn't add it simply because it wasnt in any of my cases.

    Need to add logger statements to most of this file"""

=====
__version__ = "$Id: cov_matrices.py,v 1.0 2012/06/15 23:50:24 sbolding $"
=====

# Load local python modules

from ndvv.endf.records.control import controlRecord
from ndvv.endf.records.list import listRecord

from numpy import zeros, matrix
from math import sqrt
from numpy.linalg import cholesky, eig, LinAlgError, norm
from numpy import random, array, diag, transpose, dot, matrix, interp
from scipy import interpolate

=====
class endfCovMatrix(object):
    """This class will hold the information for a subsection from a 30's series file that contains the
    covariance data for a set of cross sections, nubar data, etc. Each instance of this class
    contains the covariance matrix (stored as a bunch of submatrices) for a particular mf, mt1, mf1
    and mt (subsection). The unique submatrices of the covariance matrix for a particular combination
    of mt & mt1 (mostly by energy) are in a list for each instance called by self.covMatrices.

    The class mf33 includes all of the combinations of mt's (mt1 and mt).

    EndfFormat Section"""

    #-----
    def __init__(self, f=None, loose=False, logger=None, seed=None):
        "Initialize a Covariance Matrix record"

        self.clear()

        #Initialize random number generator to arbitrary value
        random.seed(self.seed)

        if f is not None:
            self.f = f
            self.parse(f=f, loose=loose, logger=logger)

        return None

    #-----
    def clear(self):
```

```

"Clear the current record."
self.__dict__['endfRecords'] = tuple([controlRecord(), listRecord()])
self.__dict__['covMatrices'] = [] #contains the portions of covariance matrices for each case
                                # each member of the list 'covRecords' is a full matrix
                                # that makes up some portion of a particular section. I
                                # think the portions have to do with energy, but i can't
                                # tell for sure.

self.__dict__['energies'] = [] #contains the energy bins for the corresponding covmatrix
self.__dict__['sorted'] = False #is the data sorted in order of increasing energy?
self.relative = False #Is the cov matrix relative (vs absolute)?
self.f = None #File object
self.modified_corr_matrix = None #If a fixup is applied, a new correlation matrix is stored
self.sampling_matrix = None #The matrix used for sampling is stored
self.full_matrix = None #2d array that is the original full matrix, ignoring modifications
self.fixup_applied = False #If a fixup has been applied or not, may not be used
self.seed = 17

return None

#-----
def __getattr__(self, name):
    "Override getattr to allow multiple ways of getting section values."

    cr = self.__dict__['endfRecords'][0]
    lrs = self.__dict__['endfRecords'][1:] #list of the list records

    d = {
        'cr' : 'cr',
        'matmfmt' : 'cr.mat, cr.mf, cr.mt',
        'mfmt' : 'cr.mf, cr.mt',
        'mat' : 'cr.mat',
        'mf' : 'cr.mf',
        'mt' : 'cr.mt',
        'nc' : 'cr.n1',
        'ni' : 'cr.n2',
        'mat1' : 'cr.l1',
        'mt1' : 'cr.l2',
        'xmf1' : 'cr.c1',
        'xlfs1' : 'cr.c2'
    }

    value = eval(d.get(name,'None'))

    if value is not None:
        return value

    raise AttributeError("endf covariance matrices object has no attribute %s"%(name))

#-----
def __setattr__(self, name, value):
    "Override setattr to allow multiple ways of setting record values."

    cr = self.__dict__['endfRecords'][0]
    lrs = self.__dict__['endfRecords'][1:] #list of the list records

    d = {
        'cr' : 'cr=value',
        'matmfmt' : 'cr.mat, cr.mf, cr.mt=value',
        'mfmt' : 'cr.mf=value',
        'mat' : 'cr.mat=value',
        'mf' : 'cr.mf=value',
        'mt' : 'cr.mt=value',
        'nc' : 'cr.n1=value',
        'ni' : 'cr.n2=value',
        'mat1' : 'cr.l1=value',
        'mt1' : 'cr.l2=value',
        'xmf1' : 'cr.c1=value',
        'xlfs1' : 'cr.c2=value'
    }

```

```

    }

    exec( d.get( name, "self.__dict__[name] = value" ) )

    return None

#-----
def parse(self, f, loose=False, logger=None):
    "Parses all sub and sub-sub section data and stores them into matrices and Records"

    if logger is None:
        logger=devNull
    logger.log(9,"entered routine ndvv.endf.cov_matrices.parse")
    logger.log(8,"%s"%(__version__))

    "Read in the header of the sub section"
    cr = controlRecord(f) #Control record for a single covariance matrix/single subsection
    endfRecords = [cr]

    #set subSection values
    ni = cr.n2
    nc = cr.n1
    xmf1 = cr.c1

    if (xmf1 != 0.0):
        raise ValueError("There is a dependence on another MF, this is not coded. See the"+ \
            "manual section 33.2.1")

    #Temp Variables for storing after iteration into tuples:
    covMatrices = []
    energies = []

    for nc in range(nc):
        if nc > 0:
            raise ValueError("Need to put in code to read in NC type sub-subsections")
            #TODO

    for ni in range(ni): #read in all of the NI sub-subsections

        lr = listRecord(f)
        lb = lr.l2 #type of cross section

        logger.log(9,"entering code that parses the subsubsection matrices")

        #-----
        "Parse the subsubsection matrices"
        #-----

        if (lb not in [5]):
            msg = "Need to put in code to read in LB=%d format NI sub-subsections" % lb
            raise NotImplementedError(msg)

        elif lb == 5:
            "Direct matrix data section"

            self.relative = True

            ls = lr.l1      #symmetric or not
            nt = lr.npl     #total number of entries in lr.b
            ne = lr.n2      #number of energies

            m = zeros([ne-1,ne-1])          #create matrix to store data
            erg = lr.b[0:ne]                #store list of energies

```



```

if ls == 1:
    "Read in an upper triangular (symmetric) format matrix:"

    "Store the matrix elements:"
    index=ne                    #start of b_n elements
    for i in range(ne-1):
        for j in range(i,ne-1):
            m[i][j] = lr.b[index]

            #Don't overwrite diagonal element
            if (j != i):
                m[j][i] = lr.b[index]

            index+=1            #increment location on data list

elif ls==0:
    "Read in a full (asymmetric) matrix"

    msg = "Warning, you have read in an asymmetric covariance matrix...whatever that " \
          +"means, for mt1=%d, subsection #%d. See ENDF manual chpt 33 for more" \
          % (cr.l2, len(covMatrices))+ "info. May not actually be asymmetric, use" \
          +" cov_matrices.symmetric to check\n"

    print msg
    logger.log(9,msg)          #NOT SURE IF THIS IS THE RIGHT FORMAT TODO"

    "Store the matrix elements:"
    index=ne                    #start of b_n elements
    for i in range(ne-1):
        for j in range(ne-1):
            m[i][j] = lr.b[index]
            index+=1            #increment locatioon in list

else:
    raise ValueError("Incorrect value for LS on an LB=5 card")

"Store the data after it is read in:"

energies.append(erg)
covMatrices.append(m)
endfRecords.append(lr)

"Store all data to instance:"

self.__dict__['covMatrices']=covMatrices
self.__dict__['energies']=energies
self.__dict__['endfRecords'] = tuple(endfRecords)

return None

#-----
def check(self):
    #TODO
    print """"Need to write checks to make sure mf1 mt1 mat1 all the same for a particular
instance""""

#-----
def get_full_matrix(self):
    """"Returns a full matrix for a particular subsection (one covMatrices class). This requires
making the matrix out of its various energy components. The correct MT1 and MF1/Mat1 are
specified in higher class mf33Record""""

    if self.full_matrix != None:
        return self.full_matrix

```

```

"If the measurement is relative warn user:"
if self.relative == True:

    print "WARNING: the covariance matrix you are using is for relative covariances"+ \
          ", the correlation matrix is correct and does not need to be changed"+ \
          ". See ENDF Chapter 33.2.2.2\n"

#Sort energies if not already done:
if not self.sorted:
    self.sort_by_energy()

#Determine the total number of energies:
energies = self.get_energies()
ne = len(energies)

#Create Matrix:
m = zeros([ne-1,ne-1])
xidx = 0
yidx = 0
counter=0
skip_cycles=0

for k in range(len(self.covMatrices)):

    yidx_initial = xidx

    for i in range(len(self.covMatrices[k])):

        #Set col location in m to start at the location of where rows being changed start
        yidx = yidx_initial

        for item in range(len(self.covMatrices[k][i])):

            if (k != 0):
                #for the first cov matrix you just print the whole thing

                if (item == 0) or (i == 0):
                    #for higher k you need to skip the first entry in row and column
                    continue

            m[xidx][yidx] = self.covMatrices[k][i][item]
            yidx += 1

        #Increment location in m after each row
        if (i == 0 and k != 0):
            continue
        else:
            xidx += 1

# CHECK MATRIX VALUES:

if not symmetric(m):
    raise ValueError("Non-symmetric cov matrix, need to add code to accounts for this")
"""
print m[55][45], self.covMatrices[0][55][45]
print m[len(self.covMatrices[0])-1][len(self.covMatrices[0][0])-1], self.covMatrices[0][-1][-1]
print m[-1][-1], self.covMatrices[1][-1][-1]
print m[-4][-3], self.covMatrices[1][-4][-3]
print m[len(self.covMatrices[0])][len(self.covMatrices[0])], self.covMatrices[1][1][1]
"""
self.full_matrix = m

return m

#-----

```

```

def get_energies(self):
    """Determine the total list of energies for this subsection. This data is in the endfRecords for a
    cross section, but this class doesn't have access to that data. I am not totally sure how
    it stores the different sections, so it may be better to not duplicate by brute force"""

    #Make sure in order of increasing energy:
    if not self.sorted:
        self.sort_by_energy()

    #append non duplicate energies to the list [0,1,2,...,m,m+1,...,p,p+1...q-1,q]:
    erg = []
    for eng in range(len(self.energies)):
        temp = self.energies[eng]

        #The lowest one covers the full range of its energies [0,1, 2,...,m]
        if eng == 0:
            erg.extend(self.energies[eng])

        #The Last one has a duplicate has two duplicates on its lower end [0,p,p+1,...q]:
        elif eng == (len(self.energies)-1):
            erg.extend(self.energies[eng][2:])

        #Middle ones lose two to their bottom as well as a top energy [0,m,m+1,...,p-1,p,q]:
        else:
            erg.extend(self.energies[eng][2:])

    return erg

#-----
def sort_by_energy(self):
    """Need to be wary that if you were going to reprint these cov matrices to a file the NC
    type subsections MUST come first. You would need to not sort them by energy"""

    #sort in order of ascending energy

    #put in debug error:
    if(len(self.energies) > 2):
        raise NotImplementedError("Has not been tested on data that has more than 2"
            +"subsubsections,make sure energies and matrix have values for all energies ")

    #create a list of data that can be sorted
    if (len(self.energies) != len(self.covMatrices)):
        raise ValueError("Somehow the number of energy arrays is different from the no. of matrices")

    matrix_data = []
    for erg in range(len(self.energies)):
        matrix_data.append(tuple([self.energies[erg], self.covMatrices[erg],
            self.endfRecords[erg+1]]))

    #put in order of increasing energy range
    matrix_data = sorted(matrix_data, key=lambda top_energy: top_energy[0][-1])

    #Store sorted data back to instance data
    self.energies = []
    self.endfRecords = [self.__dict__['endfRecords'][0]]
    self.covMatrices = []

    for erg in range(len(matrix_data)):

        self.energies.append(matrix_data[erg][0])
        self.endfRecords.append(matrix_data[erg][2])
        self.covMatrices.append(matrix_data[erg][1])

    self.sorted = True

    self.__dict__['endfRecords'] = tuple(self.__dict__['endfRecords'])

    return None

```

```

#-----
def get_corr_matrix(self):
    "Generates a correlation matrix for a particular subsection"

    #First generate the covariance matrix
    m = self.get_full_matrix()
    corr = zeros([len(m), len(m[0])])

    for i in range(len(m)):
        for j in range(len(m)):

            if (m[i][j] == 0.0):
                corr[i][j]=0.0

            else:
                corr[i][j] = m[i][j]/(sqrt(m[i][i]*m[j][j]))

    return corr

#-----
def gen_sampling_matrix(self, m=None):
    """Returns a sampling matrix for generating correlated random samples. m (cov matrix) can be
    specified. This is primarily for debugging and external use of this function"""

    #Get the correct correlation matrix and check for symmetry:
    if m==None:
        m = self.get_corr_matrix()

    #Check that none of the variances are zero, and if so store row and raise flag:
    zero_variances = []
    cov = self.full_matrix

    for i in range(len(self.full_matrix)):

        if cov[i][i] == 0.0:
            print "Zero variance in correlation matrix, setting row/column to zero in sampling matrix"
            zero_variances.append(cov[i][i])

            #Check that all columns and rows of this one are zero:
            for j in range(len(cov)):
                if cov[i][j] != 0.0 or cov[j][i] != 0.0:
                    raise ValueError("There is zero variance, but non zero covariance...not possible")

    #Remove the zero_variance rows and columns from the correlation matrix
    if zero_variances != []:
        temp_m = []

        for i in range(len(m)):

            if i in zero_variances:
                continue
            else:
                temp_list = []

                for j in range(len(m[i])):
                    if j in zero_variances:
                        continue
                    else:
                        temp_list.append(m[i][j])

                temp_m.append(temp_list)
        m = array(temp_m)

    try:

        #See if positive definite and cholesky decomposition will work (much more efficient)
        if not symmetric(m):

```

```

        raise LinAlgError("WARNING: non symmetric matrix")

    print "\nChecked if matrix was symmetric or not..."

    u = cholesky(m)    #Will raise LinAlgError if it fails

except LinAlgError:

    #Try eigenvalue decomposition
    print "Not positive definite, trying singular Eigenvalue decomposition..."

    evals, evecs = eig(m)

    #Check for negative eigenvalues, if so, then need to make a PSD correlation matrix:
    check = all(eval >= 0.0 for eval in evals)
    zero_check = all(eval != 0.0 for eval in evals)

    if not zero_check:
        raise LinAlgError("There is a zero eigenvalue, need to account for this")

    if not check:

        print "Negative eigenvalues, indefinite matrix, applying Eigenvalue Fixup Method..."

        m = self.eigenvalue_fixup(evals, evecs) #returns a new corr matrix that is PSD
        print "Fixup applied"
        evals, evecs = eig(m)

        #make sure nothing failed in fixup
        check = all(eval > 0 for eval in evals)

        if not eigenmatrix_check(evals,evecs):
            raise LinAlgError("Error in new eigenvector decomposition matrix")

        if not check:
            raise LinAlgError("Still have neg. eigenvalues, even after fixup method")

    if not eigenmatrix_check(evals,evecs):
        raise LinAlgError("Error in final eigenvector decompositon result")

#Generate u
sqrt_evals = []
for i in evals:
    sqrt_evals.append(sqrt(i))

    u = dot(evecs, sqrt_evals)

#If there were zero variances u need to set those values in sampling matrix to zero:

if zero_variances != []:
    temp_m = []
    x_idx = 0

    for i in range(len(cov)):

        temp_list = []
        y_idx= 0

        for j in range(len(cov[i])):

            if j in zero_variances or i in zero_variances:
                temp_list.append(0.0)
            else:
                temp_list.append(u[x_idx][y_idx])

            y_idx+=1

```

```

        if j in zero_variances:
            y_idx -= 1

        if i in zero_variances:
            x_idx -= 1

        temp_m.append(temp_list)
        x_idx += 1

    u = array(temp_m)

    self.sampling_matrix = u

    return None

#-----
def eigenvalue_fixup(self, evals, evecs):
    """Fixup applied to correlation matrices with negative eigenvalues that are not semi-positive
    definite. This method works by setting all the eigenvalues to positive and then generating
    a new correlation matrix with a fixed set of values

    This function returns the modified eigenvector matrix, but it stores the modified
    correlation matrix to self.modified_corr_matrix for access later"""

    #Check to make sure that the matrix is orthogonal etc. before applying fixup
    if not eigenmatrix_check(evals, evecs):
        raise LinAlgError("Need to apply Gramm-Schmidt method, not implemented")

    #Make a new array of positive evals
    pos_evals = []
    for i in evals:
        pos_evals.append(abs(i))

    pos_evals = array(pos_evals)

    #make diagonal matrix of pos eigenvalues:
    d = matrix(diag(pos_evals))

    #solve for new correlation matrix, use matrix module to simplify multiplication
    tr = matrix(evecs.transpose())
    emat = matrix(evecs)
    new_corr = emat*d*tr
    new_corr = array(new_corr)

    #Need to make sure diagonal elements are 1. In most cases they will not be:
    dd = diag(new_corr)

    for i in range(len(new_corr)):
        for j in range(len(new_corr)):

            new_corr[i][j] = new_corr[i][j]/(sqrt(dd[i]*dd[j]))

    self.modified_corr_matrix = new_corr

    #check that new correlation matrix is normalized
    for i in range(len(new_corr)):

        if abs(new_corr[i][i] - 1.0) > 0.000001:
            raise LinAlgError("Something has gone wrong in renormalizing the new corr matrix")

    #return the modified correlation_matrix
    return new_corr

#-----
def sample_corr_matrix(self, seed=None):
    """samples a set of normally distributed random numbers from a correlation matrix. Uses
    self.sampling_matrix if there is one, else reads it in using self.gen_sampling_matrix.

```

```

Returns correlated samples from a normal distribution with mean of zero and std deviation of one

The random seed can be specified here, or it uses the one stored. Self.seed is updated
BEFORE this function is ran. This is for storing the seed that generated each set of sampled
data external to this class"""

if self.sampling_matrix == None:
    self.gen_sampling_matrix()

#Generate a vector of random numbers, distributed normally: use specified seed if one is given
if seed != None:
    random.seed(seed)

self.seed = random.get_state()[1][0]

#Get the sampling matrix: sample_mat = self.sampling_matrix

#Generate normally distributed random numbers rand_array =
array(random.randn(len(sample_mat)))

#Sample 1000 numbers from the random number generator, this is so it
#jumps ahead in the period and the seed will be changed. The seed only
#changes every #623 samples because mersenne twister samples 623 numbers
#at each state. This is much easier than trying to store
#the whole state. 1000 is arbitrary, and numbers were checked to be random
random.randn(1000)

#multiplication by hand
temp_array = []
for i in range(len(sample_mat)):

    sum = 0.
    for j in range(len(sample_mat[i])):

        sum += sample_mat[i][j]*rand_array[j]

    temp_array.append(sum)

temp_array = array(temp_array)

return temp_array

#-----
def sample_cross_section(self, cross_sections, energies, seed=None, interpolation=None):
    """Samples a vector of ne-1 normally distributed random numbers using Mersenne twister
    algorithm and then uses a specified correlation matrix to correlate the random numbers.

    The energies in the input are those of the crossX, not those of the cov matrix.

    The energies of the crossx are typically different than those of the cov matrix, therefore
    the random numbers generated from the cov matrix have to be mapped onto the cross sections.
    The cov matrix values are group averaged.

    If any of the variances are zero, that cross section is not sampled and returned as the original
    value and there is no correlation to it."""

    #sample rand_array (generating sample matrix if one not already specified)
    rand_array = self.sample_corr_matrix(seed=seed)
    cov_energies = array(self.get_energies())

    #Get out the std_dev into an array
    cov = self.get_full_matrix()
    std_dev = array([ sqrt(cov[i][i]) for i in range(len(cov))])

    #If any of the variances are zero they will be canceled out by the way the corr_matrix is set up

```

```

#Map the variances on to the proper cross sections due to different numbers of energy pnts:
mapped_rand_array = []
mapped_std_dev= []
cov_idx = 0

#This next section makes a vector of correlated values that is same size as the number of cross sections
#by mapping values based on energies. The correlation matrix is for group averaged values, so if
#a cross section falls within that group, it is set to have the same relative variance/covariance
#that group corresponds to.
# - - - - -

if not self.relative:
    raise ValueError("The mapping of energies in this function only works for relative covariance data,"
        +" need to rewrite if not relative")

#raise error if different endpoint energies
if abs(cov_energies[-1] - energies[-1]) > 0.000001:
    print cov_energies[-1], energies[-1]
    raise ValueError("Different Upper Endpoint Energies b/w cov and CX data, handling this case not "
        +"implemented yet. Possible that energies of crossX not in eV, as they are in the cov data")

for i in range(len(energies)-1):
    while True:
        if (energies[i] - cov_energies[cov_idx]) >= -0.000000001:
            if (cov_energies[cov_idx+1] - energies[i]) > -0.000000001:
                #in the proper energy bin

                mapped_rand_array.append(rand_array[cov_idx])
                mapped_std_dev.append(std_dev[cov_idx])
                break

            else:
                cov_idx+=1

        else:
            if cov_idx == 0:
                #handle case where the cross sections have starting energies lower than the
                #covariance data by setting the sampling of all cross sections below that value to 0.0.
                #This effectively means no changes are made to those cross sections

                mapped_rand_array.append(0.0)
                mapped_std_dev.append(0.0)
                raise ValueError("You probably shouldnt need this, make sure it's actually how"
                    +"you want to handle this data. More details in source")
                break

            else:
                raise ValueError("Energies got out of order somehow")

#Store the last case which is always the last variance
mapped_rand_array.append(rand_array[-1])
mapped_std_dev.append(std_dev[-1])

mapped_rand_array = array(mapped_rand_array)
mapped_std_dev = array(mapped_std_dev)

if self.relative:

    mapped_std_dev = mapped_std_dev*cross_sections

#Generate modified cross section data
cx = mapped_rand_array*mapped_std_dev + cross_sections

#Use interpolation if desired

```



```

print interpolation
if interpolation != None:
    return self.inter_cross_section(cx, energies, interpolation=interpolation)

else:
    #DEBUG
    temp_file = open("/scratch/sbolding/nubar_plot.txt","w")
    for i in range(len(cx)):
        temp_file.write("%s %s %s\n" % (energies[i], mapped_rand_array[i], mapped_std_dev[i]))

    return cx

#-----
def inter_cross_section(self, cross_sections, energies, interpolation="linear"):
    """Function reads in a set of sampled cross sections and adjusts them such that the center of each
    cov energy group is the sampled value and in between some kind of interpolation method is used.

    By default linear interpolation is assumed."""

    #input check
    if len(cross_sections) != len(energies):
        raise ValueError("Length of cross sections and energies do not match")

    #intialize local variables
    cov_energies = self.get_energies()
    centered_cx = []
    centered_energies = []

    #find center point (or slightly lower energy) of each cov energy group and store cx and energy.

    avg_energies = []
    for i in range(len(cov_energies)-1):

        avg_energies.append((cov_energies[i] + cov_energies[i+1])/2.)

    #map centerpoints to energies and cross section values

    idx = 0
    for cx in range(len(cross_sections)):

        if energies[cx] < avg_energies[idx]:
            continue

        elif energies[cx] >= avg_energies[idx]:
            #Check to see if one above or below is closest

            check_hi = abs(energies[cx] - avg_energies[idx])
            check_low = abs(energies[cx-1] - avg_energies[idx])

            if check_hi < check_low:

                centered_cx.append(cross_sections[cx])
                centered_energies.append(energies[cx])

            else:

                centered_cx.append(cross_sections[cx-1])
                centered_energies.append(energies[cx-1])

            idx += 1
            if idx == len(avg_energies):
                break

    #add first and last value of cross_section and energy to make interpolation easier
    centered_cx.insert(0, cross_sections[0])
    centered_cx.append(cross_sections[-1])
    centered_energies.insert(0, energies[0])

```

```

centered_energies.append(energies[-1])

#perform interpolation
if interpolation == "linear":

    cx = interp(energies, centered_energies, centered_cx)
    for i in range(len(cx)):
        print energies[i], cross_sections[i], cx[i]

#    for j in range(len(centered_energies)):
#        print centered_energies[i], centered_cx[i]

    exit()

    return cx

elif interpolation == "cubic_spline":

    tck = interpolate.splrep(centered_energies, centered_cx)
    cx = interpolate.splev(energies, tck)

    for i in range(len(cx)):
        print cx[i]

    exit()

    return cx

else:
    raise ValueError("Invalid, or unimplimented, entry for interpolation scheme")

exit() #STILL DEBUGGING

return cross_sections

#-----
def eigenmatrix_check(evals, evecs):
    """Checks an eigenmatrix to ensure all columns are orthogonal and normalized to one
    and that there are no degenerate eigenvalues. Need to be careful, lots of potential issues with
    roundoff accumulation.

    Prints out any errors to the screen, and returns False if any tests failed"""

    TOL = 1.0e-05
    no_errors = True

    #Check for degenerate eigenvalues and zero eigenvalues
    for i in range(len(evals)):

        if evals[i] == 0.0:
            print "Zero valued eigenvalue"
            no_errors = False

        for j in range(i+1, len(evals)):
            if i != j:
                if evals[i] == evals[j]:
                    print "Degenerate Eigenvalues, matrix will not be orthogonal", evals[i], evals[j]
                    no_errors = False

```

```

#Check for normalization of eigenvectors
for i in range(len(evecs)):
    check = abs(norm(evecs[:,i]) - 1.0)
    if check > TOL:
        print "Not very-well normalized, most likely do to round off: norm = ",norm(evecs[:,i])
        raise ValueError("Not normalized, may just be round off")

#Check for orthogonality of eigenvectors:
for i in range(len(evals)):
    for j in range(len(evals)):
        if i != j:
            dp = dot(evecs[:,i],evecs[:,j])
            if abs(dp) > TOL:
                print "Not orthogonal for columns ", i, " and ", j, "dp = ", dp
                no_errors = False

return no_errors

#-----
def symmetric(m):
    """Check to see if a matrix is symmetric or not. Returns True if symmetric, else False"""
    return all(all(float(m[i,j]) == float(m[j,i]) for j in range(i,len(m[i])))for i in range(len(m)))

```

ace_sb.py: ACE Format Data Class

```
#!/usr/bin/env python

#!/home/sbolding/EPD/epd-7.3-1-rh5-x86_64/bin/python

# =====
#Local Modules
from numpy import array
from math import sqrt
import os
import linecache

#Module for reading in covariance data
from ndvv.endf.file_index import file_index
# =====

"""This module creates an ace file object from an ace file and contains
strategies for reading in a section from the file and reprinting a new ace file.

NOTE: If you change any of the cross sections stored in "self.data_arrays" in this file
it will be changed when you use fprint. To access the original data need to use
"self.orig_data_arrays".

NOTE: The indexing in this program typically starts from 0, but the ACE format
is based on starting from 1. At times this can be confusing, particularly with
line_cache.getline() and some of the get_array_element functions. In all cases the
values in this program are THE VALUE IN ACE FORMAT MANUAL - 1 so that they are indexed from 0

UPDATE 09/25/12: You can now change cross sections, not just nubar. All data is stored in
parrallel arrays and then accessed by an index. The indices are mapped using self.indices
dictionary and the names desired."""

# = = = = =
class ace_file_index:
    """This super class contains the files and such needed for parsing and to be used for printing etc.
    Also contains the ace sections that have been called and changed"""

    def __init__(self, section, xsdir_handle=None, output=None, dir=None):

        #get rid of the old data
        self.file_index_clear()

        if dir == None:
            #assume current directory
            self.dir = os.getcwd()
        else:
            self.dir=dir

        #open output file
        if output==None:
            print "must read in output file name later"
        else:
            self.output=output
            self.__dict__['outfile'] = open(self.output,"w")

        self.section = section

        #No XSDIR file:
        if xsdir_handle == None:
```

```

        raise IOError("need to specify a XSDIR file")

#XSDIR FILE READ
if xsdir_handle != None:

    self.xsdir = open(self.dir+xsdir_handle, "r")

    #Find line that has the file you need
    flag=False

    for line in self.xsdir:

        if search_for(section, line):

            flag=True #This is purely for reading the next line

            #store section_info and initiate input file
            self.sectionRecord = tuple(line.split())

            #Check to see if endf file is not in current directory
            if self.sectionRecord[4] == '1':

                self.f_handle = self.dir+self.sectionRecord[2]

            else:

                if not search_for(self.sectionRecord[4], "$(/\s*"):
                    self.f_handle = self.sectionRecord[4]+"/"+self.sectionRecord[2]
                else:
                    self.f_handle = self.sectionRecord[4]+self.sectionRecord[2]
                raise NotImplementedError("This has not been debugged")

            self.f = open(self.f_handle, "r")

            if self.sectionRecord[0] != self.section:
                raise IOError("Read in incorrect line in xsdir file")
        elif flag:

            #Get the stopping address from next line
            self.stop_address = int(line.split()[5])
            flag=False

    return None

# - - - - -
def file_index_clear(self):

    self.f = None                #input ACE file that is being read in and modified
    self.xsdir = None            #xsdir file
    self.xsdir_handle = None     #name of xsdir file
    self.output = None           #name of output file
    self.outfile = None          #output file
    self.of_idx = None           #Line in output file
    self.of_col = None           #col in output file
    self.dir = None              #directory location of xsdir (and possible f)
    self.section = None          #The name of the section being modified, e.g. "94239.70c"
    self.sectionRecord = None    #Contains information about the section, such as location in f
    self.f_handle = None         #name of f
    self.mod_secs = []           #list of classes containing all the info u need for new file
    self.stop_address = None     #The start of the next cross section data, when to stop printing
    self.fi_object = None        #File index object, has to do with getting covariance matrices

    return None

```

```

# -----
def lc_get_lines(self, fileName, start, nlines):
    "returns a list of lines gotten using the get_lines function"

    idx = start
    lines = []
    for i in range(nlines):
        lines.append(linecache.getline(fileName, idx))

    return lines

# =====
class ace_section(ace_file_index, object):
    """Contains the data for a particular section from an ace file"""

# -----
def __init__(self, section, section_type, xmdir_handle = None, output=None, dir=None):

    self.section_clear()
    ace_file_index.__init__(self, section, xmdir_handle=xmdir_handle, output=output, dir=dir)
    self.type = section_type

    if self.f != None:
        self.parse()
    else:
        raise ValueError("trouble opening input file from xmdir line")

    return None

# -----
def __getattr__(self, name):

    #Cr is just a local variable for quick reference
    cr = self.__dict__['controlData']

    d = {
        'nu_ne' : 'int(cr[3])',
        'lnu' : 'int(cr[1])',
        'knu' : 'int(cr[0])',
        'nr' : 'int(cr[2])',
        'totnu' : "self.__dict__['data_arrays'][1]",
        'promptnu': "self.__dict__['data_arrays'][0]"
    }

    value = eval( d.get( name, 'None' ) )

    if value is not None:
        return value

    raise AttributeError("ace_section object has no attribute %s"%(name))

# -----
def __setattr__(self, name, value):

    #Cr is just a local variable for quick reference
    cr = self.__dict__['controlData']

    d = {
        'nu_ne' : 'cr[3]=value',
        'lnu' : 'cr[1]=value',
        'knu' : 'cr[0]=value',
        'nr' : 'cr[2]=value'
    }

}

```

```

exec( d.get( name, "self.__dict__[name] = value" ) )

return None

# - - - - -
def parse(self, f=None):

#parse file from superClass
if f == None:
    f = self.f
    fileName = self.f_handle

print "Parsing section..."

#Store relevant line info:
sr = tuple(self.sectionRecord)
self.address =int(sr[5])
self.table_length = sr[6]
self.idx = int(self.address)          #index of where you are in the file

#++++++ Parse different types of data ++++++

if self.type == "totnu" or self.type == "promptnu":    #Need to parse both the totnu and promptnu data

    #Get the relative location of the nubar data and figure out how much offset:
    line_offset = self.get_jxs_value(1)          #no. of data entries to skip from end of information block

    if line_offset == "0":
        raise ValueError("No nuBar data")

    #there are 4 data entries per line and 12 lines of control information at the start:
    self.data_addresses.append(int(line_offset/4)+ self.address + 12)
    self.idx = int(self.data_addresses[-1])      #update the index
    self.data_offset_col= line_offset % 4       #column # @ for the beginning of data
    self.col = int(self.data_offset_col)
    self.data_offsets.append(self.col)

    #Read in the controlData:
    self.controlData = self.get_data_points(4,update=True)

    if self.knu < 0:
        #Parse the total and fast nubar stuff

        if self.lnu != 2:
            raise ValueError("Coefficient stuff, dont have code to handle this yet")

    #Read in the energies and the prompt nubar stuff efficiently
    energies = []
    for i in range(self.nu_ne):
        energies.append(float(self.get_line_data_point(update=True)))
    self.energies = array(energies)

    #Read in the prompt nubar data

    #Store the starting place of a modified section:
    self.start_changes.append(tuple([self.idx, self.col]))

    data_array = []
    for i in range(abs(self.knu) - len(self.controlData) - self.nu_ne + 1):
        data_array.append(float(self.get_line_data_point(update=True)))

    self.data_arrays.append(array(data_array))
    #Store the data_arrays as read in so u can access the original data when sampling
    self.orig_data_arrays.append(array(data_array))

    #Store the stopping place for data
    self.stop_changes.append(tuple([self.idx, self.col]))

```

```

#Read in the next control data temporarily and store data indexing locations
self.data_addresses.append(self.idx)
self.data_offsets.append(self.col)

cr = tuple(self.get_data_points(3, update=True))

#Checks:
if int(cr[2]) != self.nu_ne:
    raise ValueError("Different number of energies for prompt and total")
if int(cr[0]) != 2:
    raise ValueError("Coefficient stuff, dont have code to handle this yet")

#Read in energies just to check
energies = []
for i in range(self.nu_ne):

    energies.append(float(self.get_line_data_point(update=True)))

    #Make sure energies are teh same:
    if energies[-1] != self.energies[i]:
        raise ValueError("Energy arrays are not the same for total and prompt nubar")

del energies

#Store starting place of next set of data:
self.start_changes.append(tuple([self.idx, self.col]))

#Read in the total nubar data
data_array = []
for i in range(self.nu_ne):
    data_array.append(float(self.get_line_data_point(update=True)))

#store data and stopping point of data changes
self.data_arrays.append(array(data_array))
#Store the data_arrays as read in so u can access the original data when sampling
self.orig_data_arrays.append(array(data_array))
self.stop_changes.append(tuple([self.idx, self.col]))

#Store what the index is for total and prompt nubar:
self.data_indices["totnu"] = len(self.data_arrays) - 1
self.data_indices["promptnu"] = len(self.data_arrays) - 2

else:
    raise NotImplementedError("need to add stuff to get just total or just fast nubar data")

elif self.type == "capture" or self.type == "total" or self.type == "fission":
    #You have to read in the total to adjust capture or fission

    print "Warning: This function adjusts the total absorption or fission"+
        ", and elastic scattering cross section to compensate for the increase."
        +"This does not adjust the individual components of the absorption cross section"
        +" (such as radiative capture) or individual fission components""

    #Get energy table, which starts at JXS(1):
    self.go_to_xss(self.get_jxs_value(0))
    ne = self.get_nxs_value(2) #number of energies

    energies = []
    for erg in range(ne):
        energies.append(float(self.get_line_data_point(update=True)))

    self.energies = energies #energies for the total, capture, or elastic cxs

#Read in the total cross section
#Store the starting place of a modified section for total:
self.start_changes.append(tuple([self.idx, self.col]))

```



```

data_array = []
for i in range(ne):
    data_array.append(float(self.get_line_data_point(update=True)))

#store data and stopping point of data changes
self.data_arrays.append(array(data_array))
#Store the data_arrays as read in so u can access the original data when sampling
self.orig_data_arrays.append(array(data_array))
self.stop_changes.append(tuple([self.idx, self.col]))

#update data_index for total
self.data_indices["total"] = len(self.data_arrays)-1

#Read in the capture cross section
#Store the starting place of a modified section for total:
self.start_changes.append(tuple([self.idx, self.col]))

data_array = []
for i in range(ne):
    data_array.append(float(self.get_line_data_point(update=True)))

#store data and stopping point of data changes
self.data_arrays.append(array(data_array))
#Store the data_arrays as read in so u can access the original data when sampling
self.orig_data_arrays.append(array(data_array))
self.stop_changes.append(tuple([self.idx, self.col]))

#update data_index for capture
self.data_indices["capture"] = len(self.data_arrays)-1

#Read in the elastic cross sections
self.go_to_xss((self.get_jxs_value(0)+3*ne))
print self.idx, self.col

#Store the starting place of a modified section for total:
self.start_changes.append(tuple([self.idx, self.col]))

data_array = []
for i in range(ne):
    data_array.append(float(self.get_line_data_point(update=True)))

#store data and stopping point of data changes
self.data_arrays.append(array(data_array))
#Store the data_arrays as read in so u can access the original data when sampling
self.orig_data_arrays.append(array(data_array))
self.stop_changes.append(tuple([self.idx, self.col]))

#update data_index for total
self.data_indices["elastic"] = len(self.data_arrays)-1

#-----
#Read in the fission cross section
fis = self.get_jxs_value(20)

if int(fis) == 0:
    raise IOError("There is no FIS block for this file")

# go to start of fis block and check ne is same as ESZ grid
self.go_to_xss(fis)

ie = int(self.get_line_data_point(update=True))
if ie != 1:
    raise ValueError("The first value in the table is not that of the first energy point"
        +", you need to change the code to handle this case, see manual_volIII page F-33")

```

```

num_entries = int(self.get_line_data_point(update=True))
if num_entries != ne:
    raise ValueError("Have read in the wrong data block")

self.start_changes.append(tuple([self.idx, self.col]))

data_array = []
for i in range(ne):
    data_array.append(float(self.get_line_data_point(update=True)))

#store data and stopping point of data changes
self.data_arrays.append(array(data_array))
#Store the data_arrays as read in so u can access the original data when sampling
self.orig_data_arrays.append(array(data_array))
self.stop_changes.append(tuple([self.idx, self.col]))

#update data_index for capture
self.data_indices["fission"] = len(self.data_arrays)-1

"""
#The following code is stuff for getting out the n, gamma reaction
mt_table = self.get_mt_table()
lsig_table = self.get_lsig_table()
print self.get_jxs_value(7)
print mt_table.index("102"), len(mt_table), "index should be -3"
self.go_to_xss(self.get_jxs_value(6)+int(lsig_table[mt_table.index("102")]))
print self.idx, "start line"
num_entries = int(self.get_line_data_point(update=True))

data_array = []
for i in range(num_entries):
    data_array.append(float(self.get_line_data_point(update=True)))

data_array = array(data_array)
print data_array
print self.idx, "end line"
"""

else:
    raise NotImplementedError("Need to write stuff to parse other data")

return None

# - - - - -
def get_lsig_table(self):
    """Function returns lsig table, which is a bunch of pointers to all the cross section tables"""

    #store the old address to change it back after you leave this function
    original_idx = self.idx
    original_col = self.col

    #Need to get the MT_table first
    self.get_mt_table()

    #Go to the LSIG table. The 6th entry of the 8th line is the pointer to lsig table:
    lsig = self.get_jxs_value(5)
    self.go_to_xss(lsig)
    nmt = self.get_nxs_value(3)

    lsig_table = []
    for i in range(nmt):
        lsig_table.append(self.get_line_data_point(update=True))

    if lsig == "0":
        raise ValueError("No LSIG value to specify location for crossX tables")

```

```

    return lsig_table

# - - - - -
def get_mt_table(self):
    """generates self.mt_table which is a list of available mt values"""

    # keep old self.idx and col
    orig_idx = self.idx
    orig_col = self.col

    if self.mt_table != []:
        return

    #get the location of the mt_table
    lmt = self.get_jxs_value(2)

    #go to mtr table
    self.go_to_xss(lmt)

    #read in the values
    nmt = self.get_nxs_value(3) # of MT elements
    mt = []

    for val in range(nmt):

        mt.append(self.get_line_data_point(update=True))

    self.idx = int(orig_idx)
    self.col = int(orig_col)

    return mt

# - - - - -
def get_jxs_value(self, value):
    """This function returns a specified value from the jxs array. It uses
    self.address and lincache, so it doesnt actually have to change your
    self.idx or self.address or self.col. This function subtracts number
    by one automatically which is required for this program since indexing
    is always from 0

    NOTE: the values are offset from 0, so you should subtract 1 from the
    value in the ACE format manual, e.g. if you wanted to get nubar (which
    is JXS(2) in ACE manual), you would ask for get_jxs_value(1)."""

    #go to the first point in the jxs array
    idx = self.address + 8

    #increase the necessary number of lines
    idx += int(value/8)
    col = value % 8

    #get that data point
    line_data = (linecache.getline(self.f_handle, idx).split())

    return int(line_data[col])-1

# - - - - -
def get_nxs_value(self, value):
    """This function returns a specified value from the nxs array. It uses
    self.address and lincache, so it doesnt actually have to change your
    self.idx or self.address or self.col. This function DOES NOT subtract
    one from returned value automatically because in the NXS array, values
    have different means, rather than JXS where they were all just
    pointers.

```

```

NOTE: the values are offset from 0, so you should subtract 1 from the
value in the ACE format manual, e.g. if you wanted to get nubar (which
      is NXS(2) in ACE manual), you would ask for get_nxs_value(1).
Not real scenario"""

#go to the first point in the nxs array
idx = self.address + 6

#increase the necessary number of lines
idx += int(value/8)
col = value % 8

#get that data point
line_data = (linecache.getline(self.f_handle, idx).split())

return int(line_data[col])

# - - - - -
def go_to_xss(self, arr_index):
    """This function goes to the "value"-th member of the XSS array. This
    is useful for getting to the start of specific data arrays. The
    function updates self.idx and self.col to the appropriate value"""

    self.idx = int(arr_index/4)+ self.address + 12
    self.col = arr_index % 4

    return

# - - - - -
def sample_data(self, type=None, fi_handle=None, seed=None, scalar=None,
    interpolation=None, scattering_ratio=None, energy_cutoff=None,
    scat_fix_up=None):

    """Samples a set of data from a corresponding correlation matrix in an
    ENDF file. fi_handle is the file name with full path that contains the
    corresponding covariance matrix. This function returns the random
    number seed that was used to generate the data. Although there is many
    numbers that correspond to teh state of the generator, you can reseed
    the generator with the seed returned by this function to get back to
    the same state. Note that this function uses numpy's random number
    generator, not pythons default.

    If scalar is specified, then it simply multiplies original array by
    scalar for each value and returns the number of sigma the total cross
    section has been shifted by.

    Both index and type are not really needed, index is just left over from
    previous code, should probably be rewritten with just type and a
    dictionary for each data array, and all data arrays should be in their
    own class

    Scattering_ratio determines how the scattering is adjusted when fission
    and capture are adjusted. If it is set to be "total", then the ratio
    of elastic scatering to total is kept constant, if it is set to "cx"
    then the ratio of elastic scattering to the cross section of interest
    is kept the same. if it is "sum" then the sum of the cross section and
    the elastic scattering cross section is kept constant, so total is not
    effected, unless the scat_fix_up is set to "total" then any time
    elastic goes negative, the difference will be stored in the total to
    keep elastic non-negative. Energy_cutoff is the energy below which to
    not change cross sections; it is passed in in MeV.

    """

    if self.fi_handle == None:
        self.fi_handle = fi_handle

    #get data_index from the dictionary. The order is arbitrary

```

```

try:
    data_index = self.data_indices[type]
except:
    raise ValueError("Have not read in, or are not capable of reading in data you h"
        + "ave specified in sample_data call")

if energy_cutoff == None:
    #set to a negative value

    energy_cutoff = -1.0

self.energy_cutoff = energy_cutoff #update cutoff energy to whatever the current is

#If scalar multiply crossX by scalar and return None:
if scalar != None:

    temp_array = self.orig_data_arrays[data_index]*float(scalar)

    #change cx only for energies >= energy_cutoff:
    energies = list(self.energies)
    new_data = []

    for erg in range(0,len(self.energies)):

        if energies[erg] >= energy_cutoff:

            new_data.append(temp_array[erg])

        else:

            new_data.append(self.orig_data_arrays[data_index][erg])

self.data_arrays[data_index] = array(new_data)
self.store_modified_data(data_index)

if type == "capture" or type == "fission":
    #need to adjust the elastic scattering cross section and total cross section to compensate

    print "cross section before and after"
    print self.orig_data_arrays[data_index]
    print self.data_arrays[data_index]

    #function that adjusts elastic and ttoal cross sections
    self.balance_cross_sections(data_index, scalar, scattering_ratio, energy_cutoff=energy_cutoff)

    print "elastic before and after"
    print self.orig_data_arrays[self.data_indices["elastic"]]
    print self.data_arrays[self.data_indices["elastic"]]
    print "total before and after"
    print self.orig_data_arrays[self.data_indices["total"]]
    print self.data_arrays[self.data_indices["total"]]
    print "fission before and after"
    print self.orig_data_arrays[self.data_indices["fission"]]
    print self.data_arrays[self.data_indices["fission"]]

    #determine how many sigma cx and total have shifted
    tot_avg_shift, tot_shift_std = self.get_sig_shifted("total")
    avg_shift, shift_std = self.get_sig_shifted(type)

    if self.output != None:

        #create file with list of energies, old cross sections, and new cross sections
        nubar_outfile = open(self.output+"_cxplot", "w")
        nubar_outfile.write("#Energy      Original      New      Elastic_Orig      Elastic_New      "
            + "Total_Orig      Total_new      Tot_Sig_shifted      Tot_Rel_sig\n")
        energies = self.energies

```

```

        for erg in range(len(energies)):
            nubar_outfile.write("%s%s%s" % (str(energies[erg]*1000000).ljust(15),
                str(self.orig_data_arrays[data_index][erg]).ljust(15),
                str(self.data_arrays[data_index][erg]).ljust(15)))

            nubar_outfile.write("%s%s" % (str(
                self.orig_data_arrays[self.data_indices["elastic"]][erg]).ljust(15),
                str(self.data_arrays[self.data_indices["elastic"]][erg]).ljust(15)))
            nubar_outfile.write("%s%s\n" % (str(
                self.orig_data_arrays[self.data_indices["total"]][erg]).ljust(15),
                str(self.data_arrays[self.data_indices["total"]][erg]).ljust(15)))

        nubar_outfile.close()

        return tot_avg_shift, tot_shift_std, avg_shift, shift_std

    else:

        return None

else:
    if type == "capture" or type == "fission":
        raise NotImplementedError("Don't have stuff to handle covariance for capture")

# -----
#Sampling using covariance data
#-----

#Read in the covariance matrices if one has not been specified:
if not self.cov_class.has_key(type):

    if self.fi_object == None:

        if self.fi_handle == None:

            raise IOError("Need to input a path with name of endf file")

            print "Reading in covariance data from ENDF file_index object..."
            self.fi_object = file_index(self.fi_handle)

        #get the cov_matrices class and store it
        if type == 'totnu':
            section = self.fi_object.get_section(mf=31, mt=452)

        elif type == 'promptnu':
            section = self.fi_object.get_section(mf=31, mt=456)

        #store the cov_matrices class:
        self.cov_class[type] = section.get_endfCovMatrix()

        #store variance data
        cov = self.cov_class[type].get_full_matrix()

#Generate random sample from covariance matrix. If a seed is specified, then it will be used
#sample_cross_section returns the sampled cross section data from input of cross_section,
#energies in ACE file are in MEV, rather than the eV that the covariance matrices are in:

energies = self.energies*1000000
self.data_arrays[data_index] = self.cov_class[type].sample_cross_section(
    self.orig_data_arrays[data_index], energies, seed=seed, interpolation=interpolation)

#store data for printing
self.store_modified_data(data_index)

if self.output != None:

```

```

#create file with list of energies, old cross sections, and new cross sections
nubar_outfile = open(self.output+"_cxplot", "w")
nubar_outfile.write("Energy      Original      New\n")
for erg in range(len(energies)):
    nubar_outfile.write("%s%s%s\n" % (str(energies[erg]).ljust(15),
        str(self.orig_data_arrays[data_index][erg]).ljust(15),
        str(self.data_arrays[data_index][erg]).ljust(15)))

nubar_outfile.close()

#return random number seed that was used to generate this data
return self.cov_class[type].seed

# -----
def get_sig_shifted(self, type):
    #Determines how many sigma the section "type" has shifted, if it can get the covariance data, if
    #not, then it will return None and None.

    #Get the covariance data out if possible:
    if not self.var.has_key(type):

        try:

            self.init_covariance_data(type)

        except:

            print "Not able to get covariance data for %s data" % type

            #No variance, so return none

            return None, None

    #values for how much stuff has shifted
    sig_shifted = []
    sig_shifted_sq = []

    orig = (self.orig_data_arrays[self.data_indices[type]])
    new = self.data_arrays[self.data_indices[type]]
    mapped_var = self.var[type]
    energy_cutoff = self.energy_cutoff
    energies = self.energies

    for i in range(len(mapped_var)):

        if float(mapped_var[i]) != 0.0:
            temp_var = ((new[i] - orig[i])/sqrt(mapped_var[i]))

            if energies[i] < energy_cutoff:
                #not shifted at this energy

                continue

            sig_shifted.append(temp_var)
            sig_shifted_sq.append(temp_var*temp_var)

        else:
            continue

    #determine average number shifted
    avg_shift = sum(sig_shifted)/len(sig_shifted)
    avg_shift_sq = sum(sig_shifted_sq)/len(sig_shifted)
    shift_std = sqrt(avg_shift_sq - avg_shift*avg_shift)

    return avg_shift, shift_std

```

```

# -----
def init_covariance_data(self, type, fi_handle=None):
    """Stores the variance and covariance data for a particular reaction, or nuclide"""

    if not self.cov_class.has_key(type):

        if self.fi_object == None:

            if self.fi_handle == None:

                if fi_handle == None:

                    raise IOError("Need to input a path with name of endf file")

                else:

                    self.fi_handle = fi_handle

            print "Reading in covariance data from ENDF file_index object..."
            self.fi_object = file_index(self.fi_handle)

        #Determine section of ENDF file
        mt_map = {"fission":18, "capture":102, "total":1, "totnu":452, "promptnu":456}
        mt = mt_map[type]

        if type == "promptnu" or type == "totnu":
            mf = 31
        else:
            mf = 33

        section = self.fi_object.get_section(mf=mf, mt=mt)

        print "Getting out the %s cov matrix out..." % type

        #Store cov_class
        self.cov_class[type] = section.get_endfCovMatrix()

        cov = self.cov_class[type].get_full_matrix()
        if not self.cov_class[type].relative:
            raise IOError("This is set up for relative covariance")

        var = []
        for i in range(len(cov)):
            var.append(cov[i][i])

        var = array(var)

        #Get out the covariance energies
        self.cov_energies[type] = array(self.cov_class[type].get_energies())*0.000001
        cov_energies = self.cov_energies[type]
        energies = self.energies

        #Store variance
        rel_var = self.map_array_by_energy(energies, cov_energies, var)
        mapped_var = rel_var*self.orig_data_arrays[self.data_indices[type]]*
            self.orig_data_arrays[self.data_indices[type]]
        self.var[type] = array(mapped_var)

    return None

# -----
def map_array_by_energy(self, energies, cov_energies, cov_array):

    """This function takes the values of cov_array, and repeats them for any
    time that energies[i] is between cov_energies[i] and cov_energies[i+1], and
    returns it as an array that is len(energies) long. This assumes that

```



```

len(energies > cov_energies)"""

#raise error if different endpoint energies
if abs(cov_energies[-1] - energies[-1]) > 0.0000000001:
    print cov_energies[-1], energies[-1]
    raise ValueError("Different Upper Endpoint Energies b/w cov and crossX data")

if len(energies) < len(cov_energies):
    raise ValueError

new_arr = []
cov_idx = 0
for i in range(len(energies)-1):
    while True:

        if (energies[i] - cov_energies[cov_idx]) > -1.0E-12:
            if (cov_energies[cov_idx+1] - energies[i]) > -1.0E-12:
                #in the proper energy bin

                new_arr.append(cov_array[cov_idx])
                break

            else:
                cov_idx+=1

        else:

            if cov_idx == 0:

                break

            else:
                raise ValueError("Energies got out of order somehow")

#store last data point
new_arr.append(cov_array[-1])

return array(new_arr)

# - - - - -
def balance_cross_sections(self, data_index, scalar, scattering_ratio, energy_cutoff=None, scat_fix_up=None):
    """This function adjusts elastic scattering cross section and the total
    cross section based on the difference of shift in the cross section
    found at data_index, based on scalar shift. Note, it also shifts the
    total cross section based on difference, so you do not need to do that
    outside of this function if it is called. This function also stores
    the modified data for printing new ACE file for scattering and total
    cross section. If scattering ratio is "fission", then data_index must
    be capture. In this case it will adjust the fission cross section to
    compensate for changes in capture"""

    es_idx = int(self.data_indices["elastic"])
    tot_idx = int(self.data_indices["total"] )
    cap_idx = int(self.data_indices["capture"])

    #how much did cross section shift
    cx_diff = self.data_arrays[data_index] - self.orig_data_arrays[data_index]

    #determine how much to shift scattering cross section
    scat_diff = []
    fiss_diff = []

    if energy_cutoff == None:
        #change cx for all energies

        energy_cutoff = -1.

```

```

energies = list(self.energies)

for j in range(len(cx_diff)):

    if energies[j] < energy_cutoff:
        #store a zero and continue

        scat_diff.append(0.0)
        fiss_diff.append(0.0)
        continue

    if scattering_ratio == "total":
        # keep probability of scattering constant at each energy

        #determine probability of scattering
        prob_scatt = self.orig_data_arrays[es_idx][j]/self.orig_data_arrays[tot_idx][j]

        #det scattering shift
        scat_diff.append(prob_scatt/(1. - prob_scatt) * cx_diff[j])

    elif scattering_ratio == "None" or scattering_ratio == None:
        #Don't shift scattering cross section

        scat_diff.append(0.0)

    elif scattering_ratio == "cx":
        #keep probability of scattering ratio to cross section probability same

        #determine ratio
        ratio_to_cx = self.orig_data_arrays[es_idx][j]/self.orig_data_arrays[data_index][j]

        scat_diff.append(ratio_to_cx*cx_diff[j])

    elif scattering_ratio == "sum":
        #keep the sum of scattering and cx the same

        scat_diff.append(-1.*cx_diff[j])

    elif scattering_ratio == "fission":
        #keep the sum of capture and fission the same

        scat_diff.append(0.0)
        fiss_diff.append(-1.*cx_diff[j])
        cx_diff[j] = 0.0

    else:
        raise NotImplementedError("No method found for scattering ratio specified in call of sample_data")

#Shift total and scattering cross section
self.data_arrays[es_idx] = array(self.orig_data_arrays[es_idx] + scat_diff)
self.data_arrays[tot_idx] = array(self.orig_data_arrays[tot_idx] + scat_diff + cx_diff)

if scattering_ratio == "fission":

    self.data_arrays[self.data_indices["fission"]] = array(
        self.orig_data_arrays[self.data_indices["fission"]] + fiss_diff)
    self.store_modified_data(self.data_indices["fission"])

if not scat_fix_up == None:

    raise NotImplementedError("This is not meant to be used for fission and capture changes together")

#Go through scat data and make sure no negatives, if scat_fix_up is "total", then compensate for negative in
#the total cross section, else raise error

```

```

for j in range(len(self.data_arrays[es_idx])):
    if self.data_arrays[es_idx][j] < 0.0:
        if scat_fix_up == None:
            raise ValueError("Changed CX too much, change can not be compensated for in scattering cross"
                              + "section producing a negative value. Should apply scat_fix_up")

        elif scat_fix_up == "total":
            self.data_arrays[tot_idx][j] -= self.data_arrays[es_idx][j]
            self.data_arrays[es_idx][j] = 0.0

        else:
            raise IOError("You have passed in a scat_fix_up that is not recognized")

    else:
        continue

#store modified data for printing
self.store_modified_data(es_idx)
self.store_modified_data(tot_idx)

return None

# - - - - -
def store_modified_data(self, data_index):
    #This function is called if you have changed data and stores the relevent info needed
    #for printing that changed data later

    self.mod_secs.append(modified_section(data_tuple = tuple([self.start_changes[data_index],
                                                             self.stop_changes[data_index]]), data_index = data_index,
                                          data_array = self.data_arrays[data_index]))

    return None

# - - - - -
def clear_mod_secs(self):
    #All this does is clear out the modified sections. Useful if creating multiple files
    #from the same covariance matrix without
    #creating a new instance of ace_section

    self.mod_secs = []

    return None

# - - - - -
def section_clear(self):

    self.__dict__['controlData'] = None
    self.address = None
    self.data_addresses = []
    self.data_offsets = []
    self.table_length = None
    # self.ne = None
    self.idx = 0
    self.col = 0
    self.controlData = None
    self.energies = None
    self.data_arrays = []
    self.start_changes = []
    self.stop_changes = []
    self.data_offset_col = None
    # self.lnu = None
    # self.knu = None

    #Line in file where section starts
    #Location in file where data for a particular reaction starts
    #Offset column in a file where a particular data section starts
    #Length in words of the table of data for whole section
    #Number of energy points
    #Line in file you are at
    #column in line you are at
    #All the control data that you will need for printing
    #List of energies for cross section or nubar being changed.
    #List of the cross section/nubar data arrays
    #List of tuples of starting idx and column for each modified data
    #List of tuples of stopping idx and column for each modified data
    #The initial offset column
    #2 for table, 1 for coefficient type table
    #first point at data_address, kind of wierd, but has to do with

```

```

self.orig_data_arrays = []
self.cov_class = {}
self.cov_energies = {}
self.data_indices = {}
self.mt_table = []
self.lsig_table = {}
self.var = {}
self.energy_cutoff = None
self.fi_handle = None

#relative location of totnu data array of data
#The data arrays as originally read in
#This is the dict of endf covariance classes
#Energies of the cov matrices, may be different than cx
#Maps the different types of cross sections to the data index
#This is a list of all the possible MT values available
#Maps MT values to their location in the table, from JXS(7)
#Dict of the variance arrays
#Energy cutoff for sampling, by default is none
#Handle for file index

# - - - - -
def get_line_data_point(self, offset=None, update=False, line=False):
#Returns the data at a point in a row. Offset is how many data_points u
#want to offset from ur current idx and col in file. Only updates idx and
#column if update=True. IF update is true it sets the idx and col to be
#of the next point after the data_point you have gotten

#local var:
idx = int(self.idx)
col = int(self.col)

#Advance in file offset data points if requested
if offset != None:
    offset = int(offset)

    if (offset+col) > 3:
        #Need to increase line

        if (offset+col+1 > 8):
            #need to increase line index multiple times

            idx += int((offset+col+1)/4)
            col = ((offset+col) % 4)

        else:
            idx+=1
            col = ((offset+col) % 4)
    else:
        col += offset

if update == True:

#update location in file to location of next point after where you are at
if col == 3:
    self.col=0
    self.idx=idx+1
else:
    self.col = col+1
    self.idx = idx

if line == True:

    if update == True:
        self.idx += 1

#Return the full line
return tuple(linecache.getline(self.f_handle, idx).split())

else:

#Return a single data point
return str(linecache.getline(self.f_handle, idx).split()[col])

# - - - - -
def get_data_points(self, number, update=False):

```

```

#Returns several data points as a list and optionally updates
#the idx and col to be at the next location after the last data point

if float(number) < 2.:
    raise ValueError("Use get_line_data_point to get single data point")

#all but last case
temp_data = [self.get_line_data_point(offset=i) for i in range(number-1)]

#last case you can update
temp_data.append(self.get_line_data_point(update=update, offset=number-1))

return temp_data

# - - - - -
def fprint(self):
    #Prints a new outputfile with modified sections
    print "Writing output..."

    #Make sure outfile is open
    if self.outfile == None:
        self.outfile = open(self.output, "w")

    #The only way outfile will be closed is if you have already written
    #one outfile and are going to be writing a new one
    if self.outfile.closed:
        self.outfile = open(self.output, "w")
        print "Opening new output file..."

    #Make sure modified sections are in order if multiple
    if len(self.mod_secs) > 1:

        temp_list = self.mod_secs
        temp_list.sort(key=lambda mod_sec : mod_sec.start_idx )
        self.mod_secs = list(temp_list)

    #Make sure there are not multiple modifications to the same section
    for i in range(len(self.mod_secs)):
        for j in range(len(self.mod_secs)):

            sec = self.mod_secs[i]
            sec2 = self.mod_secs[j]

            if i != j:
                if str(sec.data_index) == str(sec2.data_index):
                    raise ValueError("You have changed the same cross section"
                                     +"twice without resetting the modsecs. fprint Does not know which one to print")

    # - - - - Begin Printing - - - - -
    #Loop over all modified sections
    of_idx = self.of_idx = int(self.address)          # What line r u at in the original file
    of_col = self.of_col = 0                          # What column r u at in the original and new file
    f_handle = self.f_handle

    for sec in self.mod_secs:

        #Print from original file until u reach modified line
        for line in range(sec.start_idx - of_idx):

            self.outfile.write(linecache.getline(f_handle, of_idx))
            of_idx += 1

        #Print first part of next line from input file if needed
        self.of_idx = of_idx      #Move to next line

    if self.mod_secs.index(sec) != 0:
        if sec.start_idx != self.mod_secs[self.mod_secs.index(sec)-1].stop_idx:

```

```

        #Else: This has been printed from a previous modified section

        for col in range(sec.start_col):

            line_data = linecache.getline(self.f_handle, self.of_idx)[20*col:(20*(col+1))]
            self.unformatted_write(line_data)

    else:

        for col in range(sec.start_col):

            line_data = linecache.getline(self.f_handle, self.of_idx)[20*col:(20*(col+1))]
            self.unformatted_write(line_data)

    #Print the modified section (which updates self.of_idx)
    print "Data modified from original file between lines ", sec.start_idx, " and ", sec.stop_idx

    for pnt in range(len(sec.data_array)):
        self.formatted_write(sec.data_array[pnt])

    #Print rest of current line if needed:
    if self.mod_secs.index(sec) != len(self.mod_secs)-1:
        if sec.stop_idx != self.mod_secs[self.mod_secs.index(sec)+1].start_idx:
            #ELSE: then the next modified section will print the portion of this line

            if self.of_col != 0:

                for col in range(4 - self.of_col):

                    line_data = linecache.getline(self.f_handle, self.of_idx).split()
                    self.unformatted_write(str(line_data[self.of_col]))

    of_idx = self.of_idx

    #Print the end of the file
    print "Writing end of file..."

    while True:

        #Check to see if end of file has been reached:
        if of_idx == self.stop_address:
            break

        self.outfile.write(linecache.getline(f_handle, of_idx))
        of_idx+=1

    print "..Output writing complete"

    self.outfile.close()

# - - - - -
def formatted_write(self, dbl):
    "Prints out a string formatted as data tables are in ACE format w/ 11 strings"

    temp_str = "%20.11e" % dbl

    if self.of_col == 3:

        temp_str += "\n"
        self.of_idx += 1
        self.of_col = -1

    self.outfile.write(temp_str)

```

```

        self.of_col +=1

        return None

#- - - - -
def unformatted_write(self, string):
    "Prints out a string to fit in 20 characters right justified, directly as passed in"

    string.strip()

    if self.of_col == 3:

        self.of_idx += 1
        self.of_col = -1
        self.outfile.write(string.rjust(20))
        self.outfile.write("\n")

    else:
        self.outfile.write(string.rjust(20))

    self.of_col+=1

# -----/-----
def search_for(object, string):
    import re
    """Reads in object, which is either a list of patterns or a single pattern
    and searches string for pattern(s). Returns true if all match"""

    "object is a list of patterns"
    if getattr(object, "pop", False):

        #loop through each pattern and search
        for i in object:

            if re.search(str(i), string, flags=re.IGNORECASE): #match
                continue
            else:
                return False

        return True #all matched

    elif getattr(str(object), "lstrip", False):

        #search for pattern in string

        if re.search(str(object), string, flags=re.IGNORECASE):
            return True
        else:
            return False

class modified_section(object):

    def __init__(self, data_tuple=None, data_array=None, data_index = None):
        #Gets passed in a data_tuple of all the info u need (optionally) in an order
        #for passing to printer and stores it in more usable format

        self.clear()

        if data_tuple != None:

            if len(data_tuple) == 2 and all(len(data_tuple[i]) == 2 for i in range(2)):

                self.start_idx, self.start_col = data_tuple[0]
                self.stop_idx, self.stop_col = data_tuple[1]

```

```

        else:
            raise ValueError("Did not pass proper data to modified_section.init")

    if data_array != None and data_index != None:

        self.data_array = data_array.copy()
        self.data_index = int(data_index)

    else:
        raise IOError("Need to pass in the data_array and/or corresponding data_index")
    return None

def clear(self):

    self.start_col = None
    self.stop_col = None
    self.start_idx = None
    self.stop_idx = None
    self.data_index = None
    self.data_array = None

    return None

# =====
def main():

    #Directories and other changable variables:

    dir = "/scratch/sbolding/ace_files/"
    ace_file_handle = dir+"endf70j"
    ace_file = open(ace_file_handle,"r")
    section = "94239.99c"
    output_dir = "/users/sbolding/src/sb_tools/"
    xsdir = "xsdir"
    section_type = "capture"
    # spec = "totnu"
    # section_type = "totnu"
    endf_dir=' /scratch/sbolding/ENDF_files/'
    file_name= 'n-094_Pu_239.endf'
    fi_handle = endf_dir+file_name
    fi=ace_section(section, section_type, output=output_dir+"test.out", dir = dir, xsdir_handle = xsdir)
    changes = fi.sample_data(type = section_type,scalar=1.005,
        scattering_ratio="None", fi_handle=fi_handle, energy_cutoff=None, scat_fix_up=None)
    fi.fprint()
    fi.clear_mod_secs()
    changes2 = fi.sample_data(type = section_type,scalar=1.01, scattering_ratio="None",
        fi_handle=fi_handle, energy_cutoff=None, scat_fix_up=None)
    print "0.5", changes[0], changes[1], changes[2], changes[3]
    print "1.0", changes2[0], changes2[1], changes2[2], changes2[3]

if __name__ == '__main__':
    main()

```


mult_chi_sq.py: Multiplicity Distribution Data Analysis Script

```
"""Tool that reads in outputs from mtool and mparser scripts and computes chi-sq, which is then written to a file, along with keff results. Meant to be ran in directory containing different trials"""
```

```
#####
#Local Modules

import os
import math
import re
import subprocess
import sys

#####

#UPDATES:
#on 08/24/12 added abilited to skip directories that are bad

#-----
def main():

    #-----
    #ADJUSTABLE VARIABLES

    gate_widths = [1000,2000]
    gate_widths = [str(i) for i in gate_widths]
    det = ".lm14"
    crits = 'CASE_1'
    count_time_original = '300.00'
    dead_time = '4'
    mparser_path = "/users/sbolding/log_files"
    chi_out_path = "/scratch/sbolding/"
    chi_sq_output = "chi_squared.out"
    all_data_list = [[] for i in gate_widths]
    m1_list = [[] for i in gate_widths]
    m2_list = [[] for i in gate_widths]
    sort_data = True
    bad_dir = ['trial-713-16', 'debug-trial']

    #Get path from command line optionally
    if len(sys.argv) > 1:
        os.chdir(sys.argv[1])
        chi_out_path = sys.argv[1]

    #-----
    """Read in the experimental data using mparser"""

    exp_data = []

    for i in gate_widths:

        out_name = "mparse_"+i+".mpout"
        os.system("mparser -f %s/*.log -b %s -o %s -t" % (mparser_path, i, out_name) )

        data_f = open(out_name, "r")
        data_flag = False
        names = []
        multiplets = []
        gate_times = []
        list_of_mult = []
```

```

exp_m1 = []
exp_m2 = []

for line in data_f:
    line_data = line.split()

    if line_data[1] == "m1":
        exp_m1.append(tuple([line_data[3], line_data[4]]))

    elif line_data[1] == "m2":
        exp_m2.append(tuple([line_data[3], line_data[4]]))

    elif line_data[1] == "multiplet":
        #read in file names, found data:

        data_flag = True
        line_of_names = line_data[2:]

        for i in range(len(line_of_names)):

            word = line_of_names.pop(0)

            if i % 2 == 0:
                names.append(word.rstrip(","))

            else:
                gate_times.append(word)

        #Make an instance of multiplicity_data for each name
        for i in range(len(names)):

            list_of_mult.append(multiplicity_data(name=names[i], gate_width = gate_times[i]))

        #store m1 and m2
        for i in range(len(exp_m1)):
            list_of_mult[i].m1 = exp_m1[i]
            list_of_mult[i].m2 = exp_m2[i]

    elif data_flag:
        #store multi. distribution data

        multiplets.append(line_data[0])

        idx=1
        for i in range(len(names)):

            list_of_mult[i].mult_dist.append(float(line_data[idx]))
            list_of_mult[i].abs_error.append(float(line_data[idx+1])*float(line_data[idx]))

            idx += 2

        #Store multiplet numbers to classes
        for i in range(len(list_of_mult)):
            list_of_mult[i].multiplets = multiplets

        #Store to master list
        exp_data.append(list_of_mult)
        data_f.close()

#-----
"""GETTING OUT MCNP DATA"""

#Get all the directories with mtoolout files:
base_dir = os.path.abspath(os.getcwd())

```

```

#open chi sq file for each gatewidth:
chi_out = []
for gw in gate_widths:
    chi_out.append(open(chi_out_path+"chi_squared_gw"+gw+".out", "w"))

directories = []
for d in os.listdir(os.getcwd()):

    if search_for("trial", d):
        bad_dir_flag = False

        for bad in bad_dir:
            if search_for(bad, d):
                print "\nSkipping directory %s \n" % d
                bad_dir_flag = True

        if not bad_dir_flag:
            directories.append(d)

    else:
        continue

#Sort directories by date:
directories.sort(reverse=False)

#Print file header
for ff in chi_out:

    ff.write("Data for list_mode tally: %s, reference keff value: 1.0000 +/- 0.0020\n\n" % det)
    ff.write("%s%s%s%s%s%s\n" % ("Trial".center(27), "Chi-sq".center(21),
        "Sigma Chi-sq".center(17), "Red. Chi-sq".center(21),
        "Red. Sigma Chi-sq".center(17), "keff Chi-sq".center(15), "keff".center(13),
        "Sigma-keff".center(15)))

#Get out mtool files for each directory
for d in directories:
    os.chdir(d)

    print "In directory %s\n" % d
    sub_dir = os.listdir(os.curdir)

    for dd in sub_dir:

        if search_for("trial", dd):
            os.chdir(dd)

            print "Looking in subdirectory %s" % dd

            #Look for the mtool.out files
            files = os.listdir(os.curdir)
            berp_files = []
            mtool_files = []

            for f_handle in files:

                if search_for('o\Z', f_handle):
                    #Found an MCNP output file that should be appended

                    if search_for(crits, f_handle):

                        #-----
                        """Get out the keff and error for each trial"""

                        kfile = open(f_handle, "r")

                        for line in kfile:

```

```

        if search_for("the final estimated combined", line):

            keff = float(line.split()[8])
            keff_err = float(line.split()[15])*keff

            kfile.close()
            break

        else:
            continue

    continue

else:
    berp_files.append(re.search('(\S+)o\Z', f_handle).group(1))

elif search_for('\.mtoolout', f_handle):
    mtool_files.append(f_handle)

else:
    continue

#-----
"""Generate mtool.out files if there is not one for each case:"""

berp_files.sort()

for f in berp_files:

    #Make sure that mtool files do not already exist:
    if search_for(f, mtool_files, flags="any"):

        #make sure a file exists for each gatewidth
        for gw in gate_widths:

            temp_list = []
            for mf in mtool_files:

                if f in mf:
                    temp_list.append(mf)

            if search_for(gw, temp_list, flags="any"): #TODO
            #if search_for("falsenamenfeauonflaef", temp_list, flags="any"): #DEBUG
                for temp_f in temp_list:
                    if search_for(gw, temp_f):
                        temp_file = open(temp_f, "r")
                        line = temp_file.readline()
                        check = abs(float(line.split()[3]) -
                                float(count_time_original))
                        if check < 0.001:
                            temp_file.close()
                            continue
                        else:
                            print "failed", line.split()[3], count_time_original, check, line
                            print d+dd
                            os.system("mtool -f %s.lm14 %s.lm34 -c %s -d %s -b %s -o %s.mtoolout"
                                    % (f, f, count_time_original, dead_time, gw, (f+"_"+gw)))
                            temp_file.close()
                            #####END TEMP STUFF

                    continue

            else:
                os.system("mtool -f %s.lm14 %s.lm34 -c %s -d %s -b %s -o %s.mtoolout" %
                        (f, f, count_time_original, dead_time, gw, (f+"_"+gw)))

        else:
            #no mtool file for this berp ball, generate using mtool:

```

```

        for gw in gate_widths:
            os.system("mtool -f %s.lm14 %s.lm34 -c %s -d %s -b %s -o %s.mtoolout" %
                      (f, f, count_time_original, dead_time, gw, (f+"_"+gw)))

#-----
"""Parse the mcnp data"""

#Get new list of mtool files:
mtool_files = []
for file in os.listdir(os.getcwd()):

    if search_for(".mtooloutZ", file):
        mtool_files.append(file)

#Read in data:
mcnp_data = []
for gw in gate_widths:

    #this list will contain data for all berp files and all detectors:
    mcnp_temp_list = []

    for file in mtool_files:

        if not gw in file:
            continue

        data_f = open(file, "r")

        data_flag = False
        names = []
        multiplets = []
        gate_times = []
        list_of_mult = []
        mcnp_m1 = []
        mcnp_m2 = []
        first_line = True

        for line in data_f:
            line_data = line.split()

            if first_line:

                count_time = line_data[3]
                dead_time = line_data[7]
                gate_time = line_data[11]

                first_line = False

            elif line_data[1] == "m1":

                mcnp_m1.append(tuple([line_data[3], line_data[4]]))

            elif line_data[1] == "m2":

                mcnp_m2.append(tuple([line_data[3], line_data[4]]))

            elif search_for("#multiplet", line):
                #read in file names (different detectors) found data:

                data_flag = True
                line_of_names = line_data[1:]

                for i in line_of_names:

                    names.append(i)

```

```

#Make an instance of multiplicity_data for each name
for i in range(len(names)):

    list_of_mult.append(multiplicity_data(name=names[i], gate_width = gate_time))

#Store m1 and m2
for i in range(len(names)):

    list_of_mult[i].m1 = mcnp_m1[i]
    list_of_mult[i].m2 = mcnp_m2[i]

elif data_flag:
    #store multi. distribution data

    multiplets.append(line_data[0])

    idx=1
    for i in range(len(names)):

        list_of_mult[i].mult_dist.append(float(line_data[idx]))
        list_of_mult[i].abs_error.append(float(line_data[idx+1])*float(line_data[idx]))

        idx += 2

#Store multiplet numbers to classes
for i in range(len(list_of_mult)):
    list_of_mult[i].multiplets = multiplets

#Store to master list
mcnp_temp_list += list_of_mult

data_f.close()

mcnp_data.append(mcnp_temp_list)

#-----
"""Compute chi_sq of all the data for each trial, for each gatewidth"""

for gw in range(len(gate_widths)):
    #Loop through all gate_widths

    chi_sq = 0.0
    red_chi_sq = 0.0
    m1_mcnp_data = []
    m2_mcnp_data = []
    m1_exp_data = []
    m2_exp_data = []

    if berp_files == []:
        error_flag = True
        msg = "NO MCNP_OUTPUT FILES, MAJOR ERROR MADE"
        print msg

    for berp in berp_files:
        #Loop through all berp_files

        #Get out mcnp data and matching exp data:
        mcnp = None
        for data in mcnp_data[gw]:

            if search_for(berp, data.name):
                if search_for(gate_widths[gw], data.gate_width):
                    if search_for(det, data.name):

```

```

        #Found the right one
        m1_mcnp_data.append(data.m1)
        m2_mcnp_data.append(data.m2)
        mcnp = data
        break
error_flag = False
#Should not be missing anything:
if mcnp == None:
    msg = "\nWARNING: MCNP output no good in %s for %s, ignoring in FOM calc" %
        ((d+dd), berp)

    print msg
    error_flag = True
    continue

#Get corresponding exp_data:
for data in exp_data[gw]:

    if search_for(berp, data.name):
        if search_for(gate_widths[gw], data.gate_width):
            #Found the right one
            m1_exp_data.append(data.m1)
            m2_exp_data.append(data.m2)

            exp = data
            break

# -----
"""Compute the chi_sq value for each berp_file.  The exp data usually has
less points, so loop over those only"""

if len(exp.mult_dist) > len(mcnp.mult_dist):
    raise ValueError("Need to check this")

#Determine how many non zero bins are being compared each time
sum = 0
num_bins = 0
for i in range(len(exp.mult_dist)):

    if (exp.mult_dist[i] == 0.0 and mcnp.mult_dist[i] == 0.0):
        #zero_score, ignore
        continue

    else:

        num_bins += 1

        temp_val = exp.mult_dist[i] - mcnp.mult_dist[i]
        temp_val = temp_val*temp_val
        temp_val = temp_val/(math.pow(exp.abs_error[i],2)+math.pow(mcnp.abs_error[i], 2))

        sum += temp_val

#Compute reduced chi-sq:
red_chi_sq += sum/(float(num_bins))
chi_sq += sum/(float(num_bins))

#Store m1 and m2 for mcnp
m1_list[gw].append(m1_mcnp_data)
m2_list[gw].append(m2_mcnp_data)

#Add in term for keff:
temp_val = (1.0 - keff)*(1.0 - keff)/(keff_err*keff_err+0.002*0.002)
k_chi = temp_val
red_chi_sq += temp_val

#Compute chi_sq standard error based on error propogation

```

```

        chi_err = 2.*math.sqrt(chi_sq)
        red_chi_err = 2.*math.sqrt(red_chi_sq)*1/math.sqrt(6)
        all_data_list[gw].append([d+"/" + dd, chi_sq, chi_err, red_chi_sq, red_chi_err,
                                   k_chi, keff, keff_err, m1_mcnp_data, m2_mcnp_data])

        #print to output file for each gate_width
        if error_flag:
            all_data_list[gw][-1][0] = all_data_list[gw][-1][0]+msg
            # chi_err, red_chi_sq, red_chi_err, k_chi, keff, keff_err))

        os.chdir(base_dir)
        os.chdir(d)

    os.chdir(base_dir)

#Sort data or not?
if sort_data:
    temp_all_data = []
    for gw in all_data_list:

        temp_sort = gw
        gw.sort(key=lambda trial : trial[3])
        temp_all_data.append(gw)

    all_data_list = temp_all_data

#print to output file
for gw in range(len(gate_widths)):
    for i in range(len(all_data_list[0])):
        chi_out[gw].write("%27s %14.2f %17.2f %17.2f %17.2f %15.4f %14.4f +/-%10.4f" %
                          (all_data_list[gw][i][0], all_data_list[gw][i][1], all_data_list[gw][i][2],
                           all_data_list[gw][i][3], all_data_list[gw][i][4], all_data_list[gw][i][5],
                           float(all_data_list[gw][i][6]), float(all_data_list[gw][i][7])))

        #Print out m1
        chi_out[gw].write(" m1:")
        for t in range(len(all_data_list[gw][i][8])):
            chi_out[gw].write("%s %s " % (all_data_list[gw][i][8][t][0],
                                           all_data_list[gw][i][8][t][1]))

        chi_out[gw].write(" m2:")
        for t in range(len(all_data_list[gw][i][8])):
            chi_out[gw].write("%s %s " % (all_data_list[gw][i][9][t][0],
                                           all_data_list[gw][i][9][t][1]))

        chi_out[gw].write("\n")

        #Print out m1
        chi_out[gw].write("Exp Data: \n m1:")
        for t in range(len(m1_exp_data)):
            chi_out[gw].write("%s %s " % (m1_exp_data[t][0],m1_exp_data[t][1]))

        chi_out[gw].write(" \n m2:")
        for t in range(len(m2_exp_data)):
            chi_out[gw].write("%s %s " % (m2_exp_data[t][0],m2_exp_data[t][1]))

for file in chi_out:
    file.close()

return None

# -----/-----
class multiplicity_data(object):
    """Container for the data for a set of experimental data for a berpfile (multiplicity distr etc)"""

    def __init__(self, name=None, gate_width=None):

```



```

    self.clear()
    self.gate_width = gate_width
    self.name = name

    return None

def clear(self):

    self.name = None
    self.multiplets = []
    self.mult_dist = []
    self.abs_error = []
    self.gate_width = None
    self.count_time = None
    self.m1 = None
    self.m2 = None

    return None

# -----/-----
def search_for(pattern, strings, flags=None):
    import re
    """Reads in strings, which is either a list of strings or a single string and searches string
    for pattern. Returns true if all match by default."""

    "strings is a list of strings"
    if getattr(strings, "pop", False):

        #loop through each pattern and search
        for i in strings:

            if re.search(pattern, str(i), flags=re.IGNORECASE): #matca

                if flags == "any":
                    return True
                else:
                    continue

            else:
                if flags == "all":
                    return False
                else:
                    continue

        if flags == "all":
            return True #all matched
        else:
            return False

    elif getattr(str(strings), "lstrip", False):

        #search for pattern in string

        if re.search(pattern, str(strings), flags=re.IGNORECASE):
            return True
        else:
            return False

#CALL MAIN BY DEFAULT
if __name__ == '__main__':
    main()

```

Appendix F

Multiplicity and Criticality MCNP Input Files

Description	Page
MCNP5_mult input file for JEZEBEL fast critical benchmark.	248
MCNP5_mult file for a 3.0-cm reflected Pu sphere multiplicity experiment.	249

MCNP5_mult Input File for JEZEBEL Criticality Experiment

```
Bare Pu-239 Jezebel, ref. PU-MET-FAST-001
1 1 0.04029014 -1 imp:n=1
2 0 1 imp:n=0

1 so 6.3849

m1 94239.55c 0.037047
   94240.50c 0.0017512
   94241.50c 0.00011674
   31000.50c 0.0013752
kcode 2500 1.0 10 110
ksrc 0 0 0
print
c m0303 is the ACE file for trial 303
XS1 94239.99c 236.998600 m0303 0 1 1 808738 0 0 2.5301E-08 ptable
```

MCNP5_mult Input File for 3.0-cm Reflected Multiplicity Experiment

```

LANL BERP BALL MEASUREMENTS
c Configuration: BERP ball w/ 3" poly reflector
c Diagnostics: 1 NPODS, 1 SNAP (no poly), 1 HPGe
c =====
c                               CELL CARDS
c =====
c ++++++
c                               begin non-detector cells
c ++++++
c -----
c BeRP ball
c -----
1001  1 -19.604   -101                $ (19.604 w/ rho,M,V; 19.655
      imp:n=1
1002  0          101 -102              $ void between ball and ss304
      imp:n=1
1003  2  -7.92    102 -103              $ ss304
      imp:n=1
1004  9  -0.962  110 -160 116 -119      $ poly sleeve
      imp:n=1
1005  9  -0.962  (161 162 -163):           $ 4 in diameter poly reflector
      (-161 162 -163 119)
      imp:n=1
1006  9  -0.962  (161 163 -164):           $ 5 in diameter poly reflector
      (-161 163 -164 119)
      imp:n=1
1007  9  -0.962  (161 164 -165):           $ 6 in diameter poly reflector
      (-161 164 -165 119)
      imp:n=1
1008  9  -0.962  (161 165 -166):           $ 9 in diameter poly reflector
      (-161 165 -166 119 110)
      imp:n=1
1009  21 -0.0012 (161 166 -167):           $ 15 in diameter poly reflector
      (-161 166 -167 (110:111:-112:113:-114) 141)
      imp:n=1
c -----
c BeRP ball stand
c -----
1101  3 -2.70    -110 141 -111 112 -113 114  $ Base
      imp:n=1
1102  3 -2.70    110 115 -116 -117           $ Stand neck
      imp:n=1
1103  3 -2.70    117 -119 -121 (118:-120)    $ Stand
      imp:n=1
c -----
c tables
c -----
1201  8 -7.874   140 -142 143 -146 147 -150  $ Table 1
      (-141:-144:145:-148:149)
      imp:n=1
1202  8 -7.874   140 -142 151 -143 147 -150  $ Table 2
      (-141:-152:153:-148:149)
      imp:n=1
c -----
c room
c -----
1800  21 -0.0012 122 -999                $ inside room
      103                                $ outside BeRP ball
      #1101 #1102 #1103                    $ not the BeRP ball stand
      #1004                                $ not the poly sleeve
      #1005 #1006 #1007 #1008 #1009        $ not the poly reflectors
      #1201                                $ not the tables
      #1202

```

```

#3000          $ not the NPOD3
#5000          $ not the SNAP3
imp:n=1

c -----
c floor
c -----
1901 23 -2.3    -122 123 -999          $ concrete floor
                                imp:n=1
1902 21 -0.0012 -123 -999          $ "basement"
                                imp:n=1
9999 0          999                $ outside world
                                imp:n=0

c -----
c detectors
c -----
3000 0          131 -132 133 -134 135 -136 $ NPOD3 container cell
                                imp:n=1 fill= 3 (3)
5000 0          -178 179 -180 -199        $ SNAP3 container cell
                                imp:n=1 fill= 5 (5)

c ++++++
c                               end non-detector cells
c ++++++
c ++++++
c                               begin NPOD version 3 cells
c ++++++
c -----
c Detector body
c -----
3001 3001 -0.962 3001 -3002 3003 -3004 3005 -3006 (3020:-3005:3006) $ poly body
                                (3023:-3005:3006) (3026:-3005:3006) (3029:-3005:3006)
                                (3032:-3005:3006) (3035:-3005:3006) (3038:-3005:3006)
                                (3041:-3005:3006) (3044:-3005:3006) (3047:-3005:3006)
                                (3050:-3005:3006) (3053:-3005:3006) (3056:-3005:3006)
                                (3059:-3005:3006) (3062:-3005:3006)
                                imp:n=1 u=3

c -----
c Holes in poly body for tubes
c -----
3002 0          -3020 3005 -3006 (3019:-3005:3006) $ hole 1 $ front row
                                imp:n=1 u=3
3003 0          -3023 3005 -3006 (3022:-3005:3006) $ hole 2
                                imp:n=1 u=3
3004 0          -3026 3005 -3006 (3025:-3005:3006) $ hole 3
                                imp:n=1 u=3
3005 0          -3029 3005 -3006 (3028:-3005:3006) $ hole 4
                                imp:n=1 u=3
3006 0          -3032 3005 -3006 (3031:-3005:3006) $ hole 5
                                imp:n=1 u=3
3007 0          -3035 3005 -3006 (3034:-3005:3006) $ hole 6
                                imp:n=1 u=3
3008 0          -3038 3005 -3006 (3037:-3005:3006) $ hole 7
                                imp:n=1 u=3
3009 0          -3041 3005 -3006 (3040:-3005:3006) $ hole 8
                                imp:n=1 u=3
3010 0          -3044 3005 -3006 (3043:-3005:3006) $ hole 9 $ back row
                                imp:n=1 u=3
3011 0          -3047 3005 -3006 (3046:-3005:3006) $ hole 10
                                imp:n=1 u=3
3012 0          -3050 3005 -3006 (3049:-3005:3006) $ hole 11
                                imp:n=1 u=3
3013 0          -3053 3005 -3006 (3052:-3005:3006) $ hole 12
                                imp:n=1 u=3
3014 0          -3056 3005 -3006 (3055:-3005:3006) $ hole 13
                                imp:n=1 u=3
3015 0          -3059 3005 -3006 (3058:-3005:3006) $ hole 14
                                imp:n=1 u=3
3016 0          -3062 3005 -3006 (3061:-3005:3006) $ hole 15
                                imp:n=1 u=3

```

```

c -----
c Al wall for He3 tubes
c -----
3017 3002 -2.70 -3019 3005 -3006 (3018:-3013:3014) $ Al wall tube 1
(3018:-3014:3015) (3018:-3015:3006)
imp:n=1 u=3
3018 3002 -2.70 -3022 3005 -3006 (3021:-3013:3014) $ Al wall tube 2
(3021:-3014:3015) (3021:-3015:3006)
imp:n=1 u=3
3019 3002 -2.70 -3025 3005 -3006 (3024:-3013:3014) $ Al wall tube 3
(3024:-3014:3015) (3024:-3015:3006)
imp:n=1 u=3
3020 3002 -2.70 -3028 3005 -3006 (3027:-3013:3014) $ Al wall tube 4
(3027:-3014:3015) (3027:-3015:3006)
imp:n=1 u=3
3021 3002 -2.70 -3031 3005 -3006 (3030:-3013:3014) $ Al wall tube 5
(3030:-3014:3015) (3030:-3015:3006)
imp:n=1 u=3
3022 3002 -2.70 -3034 3005 -3006 (3033:-3013:3014) $ Al wall tube 6
(3033:-3014:3015) (3033:-3015:3006)
imp:n=1 u=3
3023 3002 -2.70 -3037 3005 -3006 (3036:-3013:3014) $ Al wall tube 7
(3036:-3014:3015) (3036:-3015:3006)
imp:n=1 u=3
3024 3002 -2.70 -3040 3005 -3006 (3039:-3013:3014) $ Al wall tube 8
(3039:-3014:3015) (3039:-3015:3006)
imp:n=1 u=3
3025 3002 -2.70 -3043 3005 -3006 (3042:-3013:3014) $ Al wall tube 9
(3042:-3014:3015) (3042:-3015:3006)
imp:n=1 u=3
3026 3002 -2.70 -3046 3005 -3006 (3045:-3013:3014) $ Al wall tube 10
(3045:-3014:3015) (3045:-3015:3006)
imp:n=1 u=3
3027 3002 -2.70 -3049 3005 -3006 (3048:-3013:3014) $ Al wall tube 11
(3048:-3014:3015) (3048:-3015:3006)
imp:n=1 u=3
3028 3002 -2.70 -3052 3005 -3006 (3051:-3013:3014) $ Al wall tube 12
(3051:-3014:3015) (3051:-3015:3006)
imp:n=1 u=3
3029 3002 -2.70 -3055 3005 -3006 (3054:-3013:3014) $ Al wall tube 13
(3054:-3014:3015) (3054:-3015:3006)
imp:n=1 u=3
3030 3002 -2.70 -3058 3005 -3006 (3057:-3013:3014) $ Al wall tube 14
(3057:-3014:3015) (3057:-3015:3006)
imp:n=1 u=3
3031 3002 -2.70 -3061 3005 -3006 (3060:-3013:3014) $ Al wall tube 15
(3060:-3014:3015) (3060:-3015:3006)
imp:n=1 u=3
c -----
c He-3 regions; note the tube numbering scheme. Eight tubes in front
c seven in back. Tubes are numbered in clockwise direction starting at "347"
c -----
3032 3003 -0.001434 -3018 3013 -3014 $ 3He+C+0, 10.2 atm, tube 1 ldr
imp:n=1 u=3
3033 3003 -0.001434 -3021 3013 -3014 $ 3He+C+0, 10.2 atm, tube 2 ldr
imp:n=1 u=3
3034 3003 -0.001434 -3024 3013 -3014 $ 3He+C+0, 10.2 atm, tube 3 ldr
imp:n=1 u=3
3035 3003 -0.001434 -3027 3013 -3014 $ 3He+C+0, 10.2 atm, tube 4 ldr
imp:n=1 u=3
3036 3003 -0.001434 -3030 3013 -3014 $ 3He+C+0, 10.2 atm, tube 5 ldr
imp:n=1 u=3
3037 3003 -0.001434 -3033 3013 -3014 $ 3He+C+0, 10.2 atm, tube 6 ldr
imp:n=1 u=3
3038 3003 -0.001434 -3036 3013 -3014 $ 3He+C+0, 10.2 atm, tube 7 ldr
imp:n=1 u=3
3039 3003 -0.001434 -3039 3013 -3014 $ 3He+C+0, 10.2 atm, tube 8 ldr
imp:n=1 u=3

```

3040 3003 -0.001434 -3042 3013 -3014 \$ 3He+C+O, 10.2 atm, tube 9 ldr
 imp:n=1 u=3
 3041 3003 -0.001434 -3045 3013 -3014 \$ 3He+C+O, 10.2 atm, tube 10 ldr
 imp:n=1 u=3
 3042 3003 -0.001434 -3048 3013 -3014 \$ 3He+C+O, 10.2 atm, tube 11 ldr
 imp:n=1 u=3
 3043 3003 -0.001434 -3051 3013 -3014 \$ 3He+C+O, 10.2 atm, tube 12 ldr
 imp:n=1 u=3
 3044 3003 -0.001434 -3054 3013 -3014 \$ 3He+C+O, 10.2 atm, tube 13 ldr
 imp:n=1 u=3
 3045 3003 -0.001434 -3057 3013 -3014 \$ 3He+C+O, 10.2 atm, tube 14 ldr
 imp:n=1 u=3
 3046 3003 -0.001434 -3060 3013 -3014 \$ 3He+C+O, 10.2 atm, tube 15 ldr
 imp:n=1 u=3

c

3047 3003 -0.001434 -3018 3014 -3015 \$ 3He+C+O, 10.2 atm, tube 1 ar
 imp:n=1 u=3
 3048 3003 -0.001434 -3021 3014 -3015 \$ 3He+C+O, 10.2 atm, tube 2 ar
 imp:n=1 u=3
 3049 3003 -0.001434 -3024 3014 -3015 \$ 3He+C+O, 10.2 atm, tube 3 ar
 imp:n=1 u=3
 3050 3003 -0.001434 -3027 3014 -3015 \$ 3He+C+O, 10.2 atm, tube 4 ar
 imp:n=1 u=3
 3051 3003 -0.001434 -3030 3014 -3015 \$ 3He+C+O, 10.2 atm, tube 5 ar
 imp:n=1 u=3
 3052 3003 -0.001434 -3033 3014 -3015 \$ 3He+C+O, 10.2 atm, tube 6 ar
 imp:n=1 u=3
 3053 3003 -0.001434 -3036 3014 -3015 \$ 3He+C+O, 10.2 atm, tube 7 ar
 imp:n=1 u=3
 3054 3003 -0.001434 -3039 3014 -3015 \$ 3He+C+O, 10.2 atm, tube 8 ar
 imp:n=1 u=3
 3055 3003 -0.001434 -3042 3014 -3015 \$ 3He+C+O, 10.2 atm, tube 9 ar
 imp:n=1 u=3
 3056 3003 -0.001434 -3045 3014 -3015 \$ 3He+C+O, 10.2 atm, tube 10 ar
 imp:n=1 u=3
 3057 3003 -0.001434 -3048 3014 -3015 \$ 3He+C+O, 10.2 atm, tube 11 ar
 imp:n=1 u=3
 3058 3003 -0.001434 -3051 3014 -3015 \$ 3He+C+O, 10.2 atm, tube 12 ar
 imp:n=1 u=3
 3059 3003 -0.001434 -3054 3014 -3015 \$ 3He+C+O, 10.2 atm, tube 13 ar
 imp:n=1 u=3
 3060 3003 -0.001434 -3057 3014 -3015 \$ 3He+C+O, 10.2 atm, tube 14 ar
 imp:n=1 u=3
 3061 3003 -0.001434 -3060 3014 -3015 \$ 3He+C+O, 10.2 atm, tube 15 ar
 imp:n=1 u=3

c

3062 3003 -0.001434 -3018 3015 -3006 \$ 3He+C+O, 10.2 atm, tube 1 udr
 imp:n=1 u=3
 3063 3003 -0.001434 -3021 3015 -3006 \$ 3He+C+O, 10.2 atm, tube 2 udr
 imp:n=1 u=3
 3064 3003 -0.001434 -3024 3015 -3006 \$ 3He+C+O, 10.2 atm, tube 3 udr
 imp:n=1 u=3
 3065 3003 -0.001434 -3027 3015 -3006 \$ 3He+C+O, 10.2 atm, tube 4 udr
 imp:n=1 u=3
 3066 3003 -0.001434 -3030 3015 -3006 \$ 3He+C+O, 10.2 atm, tube 5 udr
 imp:n=1 u=3
 3067 3003 -0.001434 -3033 3015 -3006 \$ 3He+C+O, 10.2 atm, tube 6 udr
 imp:n=1 u=3
 3068 3003 -0.001434 -3036 3015 -3006 \$ 3He+C+O, 10.2 atm, tube 7 udr
 imp:n=1 u=3
 3069 3003 -0.001434 -3039 3015 -3006 \$ 3He+C+O, 10.2 atm, tube 8 udr
 imp:n=1 u=3
 3070 3003 -0.001434 -3042 3015 -3006 \$ 3He+C+O, 10.2 atm, tube 9 udr
 imp:n=1 u=3
 3071 3003 -0.001434 -3045 3015 -3006 \$ 3He+C+O, 10.2 atm, tube 10 udr
 imp:n=1 u=3
 3072 3003 -0.001434 -3048 3015 -3006 \$ 3He+C+O, 10.2 atm, tube 11 udr
 imp:n=1 u=3

```

3073 3003 -0.001434 -3051 3015 -3006 $ 3He+C+0, 10.2 atm, tube 12 udr
imp:n=1 u=3
3074 3003 -0.001434 -3054 3015 -3006 $ 3He+C+0, 10.2 atm, tube 13 udr
imp:n=1 u=3
3075 3003 -0.001434 -3057 3015 -3006 $ 3He+C+0, 10.2 atm, tube 14 udr
imp:n=1 u=3
3076 3003 -0.001434 -3060 3015 -3006 $ 3He+C+0, 10.2 atm, tube 15 udr
imp:n=1 u=3
c -----
c Cadmium Wrap
c -----
3077 3004 -8.65 3007 -3008 3009 -3010 3011 -3005 $ bottom Cd
imp:n=1 u=3
3078 3004 -8.65 3007 -3001 3009 -3010 3005 -3006 $ Cd -x
imp:n=1 u=3
3079 3004 -8.65 3002 -3008 3009 -3010 3005 -3006 $ Cd +x
imp:n=1 u=3
3080 3004 -8.65 3001 -3002 3009 -3003 3005 -3006 $ Cd -y
imp:n=1 u=3
3081 3004 -8.65 3001 -3002 3004 -3010 3005 -3006 $ Cd +y
imp:n=1 u=3
c -----
c Cadmium shield
c -----
3082 3004 -8.65 3007 -3008 3009 -3010 3006 -3012 $ Cd top
imp:n=1 u=3
c -----
c Pre-amp housing
c -----
3083 3002 -2.7 3063 -3064 3065 -3066 3012 -3067
imp:n=1 u=3
3084 0 3069 -3070 3071 -3072 3067 -3068 $ inside housing
(-3073:3074:-3075:3076:-3077:3078)
(-3073:3074:-3075:3076:-3079:3080)
imp:n=1 u=3
3085 3002 -2.7 3063 -3064 3065 -3066 3067 -3068
(-3069:3070:-3071:3072:-3067:3068)
imp:n=1 u=3
3086 3004 -8.65 3073 -3074 3075 -3076 3077 -3078 $ rf shield
imp:n=1 u=3
3087 3006 -2.33 3073 -3074 3075 -3076 3079 -3080 $ dielectric circuit board
imp:n=1 u=3
c -----
c Display Housing
c -----
3088 0 3001 -3002 3009 -3081 3068 -3082
(-3001:3083:-3009:3081:-3068:3082)
(-3083:3084:-3009:3085:-3068:3082)
(-3084:3002:-3009:3081:-3068:3082)
(-3083:3084:-3086:3081:-3068:3082)
(-3083:3084:-3085:3086:-3087:3082)
(-3083:3084:-3085:3086:-3088:3089)
imp:n=1 u=3
3089 3002 -2.7 3001 -3083 3009 -3081 3068 -3082 $ Al wall, -x
imp:n=1 u=3
3090 3002 -2.7 3083 -3084 3009 -3085 3068 -3082 $ Al wall, -y
imp:n=1 u=3
3091 3002 -2.7 3084 -3002 3009 -3081 3068 -3082 $ Al wall, +x
imp:n=1 u=3
3092 3002 -2.7 3083 -3084 3086 -3081 3068 -3082 $ Al wall, +y
imp:n=1 u=3
3093 3002 -2.7 3083 -3084 3085 -3086 3087 -3082 $ Al top
imp:n=1 u=3
3094 3006 -2.33 3083 -3084 3085 -3086 3088 -3089 $ dielectric circuit board
imp:n=1 u=3
c
3999 0 (-3001:3002:-3003:3004:-3005:3006) $ outside detector
(-3007:3008:-3009:3010:-3011:3005) $ for use in universes

```



```

(-3007:3001:-3009:3010:-3005:3006)
(-3002:3008:-3009:3010:-3005:3006)
(-3001:3002:-3009:3003:-3005:3006)
(-3001:3002:-3004:3010:-3005:3006)
(-3007:3008:-3009:3010:-3006:3012)
(-3063:3064:-3065:3066:-3012:3067)
(-3063:3064:-3065:3066:-3067:3068)
(-3001:3002:-3009:3081:-3068:3082)
imp:n=1 u=3
c ++++++
c                               end NPOD version 3 cells
c ++++++
c ++++++
c                               begin SNAP3 cells
c ++++++
c -----
c Tripod plate
c -----
5001 5001 -2.7      5002 -5003 -5004 -5005      $ Aluminum
                        imp:n=1 u=5
c
c -----
c Bottom cover
c -----
5002 5002 -0.962   5003 -5006 -5007 -5008      $ High Density poly
                        imp:n=1 u=5
c
c He3 Tube
c -----
5003 5003 -0.001284 -5009 5011 -5012      $ lower dead region
                        imp:n=1 u=5
5004 5003 -0.001284 -5009 5012 -5013      $ active region l = 10.1
                        imp:n=1 u=5
5005 5003 -0.001284 -5009 5013 -5014      $ upper dead region
                        imp:n=1 u=5
5006 5001 -2.7      5010 -5015 -5016 (5009:-5011:5014) $ SST wall of he3 tube
                        imp:n=1 u=5
c -----
c HN Connector
c -----
5007 0              -5018 5015 -5027
                        imp:n=1 u=5
5008 5004 -7.89     -5017 5015 -5027 5018
                        imp:n=1 u=5
5009 5004 -7.89     5027 -5039 5018 -5017
                        imp:n=1 u=5
5010 5002 -0.962    5026 -5021 5019 -5020      $ poly sleeve
                        imp:n=1 u=5
5011 5005 -8.65     5021 -5022 5019 -5020      $ Cd top
                        imp:n=1 u=5
5012 5002 -0.962    5022 -5027 5019 -5020      $ top spacer - pol
                        imp:n=1 u=5
5013 5005 -8.65     5006 -5023 5024 -5025      $ Cd shield
                        imp:n=1 u=5
c -----
c Detector body
c -----
5014 5002 -0.962    5006 -5027 5028 -5007 -5008
                        (-5046:-5033: 5034)
                        (-5029: 5030)
                        5048
                        imp:n=1 u=5
5015 5002 -0.962    5006 -5027 5028 -5007 -5048
                        imp:n=1 u=5
c -----
c Protective cover
c -----
5016 5001 -2.7      5003 -5039 5007 -5032 -5008

```

```

                                imp:n=1 u=5
c -----
c Inner front protective cover
c -----
5017 5001 -2.7      5006 -5027 5033 -5034 5046 -5008
                                imp:n=1 u=5
c -----
c Removable CH2 Shield
c -----
5018 0              5008 -5047 5035 -5036 5003 -5039      $ NO CH2 in front of S
c 5018 5002 -0.962  5008 -5047 5035 -5036 5003 -5039      $ CH2 in front of SN
                                imp:n=1 u=5
c -----
c Top cover
c -----
5019 5002 -0.962  -5007 -5008 5027 -5039 (5019 (-5038:5037))  $ top plate
                                imp:n=1 u=5
c -----
c MC PCB Housing
c -----
5020 0              -5043 -5008 5039 -5044 (5043:5008:-5039:5041)
                                (5043:5008:-5041:5044) (5042:5040:-5041:5044)
                                imp:n=1 u=5
5021 5001 -2.7      -5043 -5008 5039 -5041
                                imp:n=1 u=5
5022 5001 -2.7      -5043 -5008 5041 -5044 (5042:5040:-5041:5044)
                                imp:n=1 u=5
5023 0              -5042 -5040 5041 -5044
                                imp:n=1 u=5
c -----
c Display housing
c -----
5024 5001 -2.7      -5043 -5008 5044 -5045
                                imp:n=1 u=5
c -----
c Cd bottom shield
c -----
5025 5005 -8.65    5006 -5026 -5024
                                imp:n=1 u=5
c -----
c voids in detector
c -----
5026 0              5010 -5015 5016 -5019
                                imp:n=1 u=5
5027 0              5015 -5027 5017 -5019
                                imp:n=1 u=5
5028 0              5023 -5027 5020 -5028
                                imp:n=1 u=5
5029 0              5026 -5023 5020 -5024
                                imp:n=1 u=5
5030 0              5006 -5023 5025 -5028
                                imp:n=1 u=5
5031 0              5026 -5010 -5019
                                imp:n=1 u=5
5032 0              5006 -5027 5029 -5030 5028 -5046 5048
                                imp:n=1 u=5
5033 0              5027 -5039 -5037 (5038:-5019) 5017
                                imp:n=1 u=5
5034 0              5027 -5039 -5018
                                imp:n=1 u=5
c -----
c voids outside detector
c -----
5035 0              5001 -5002 -5031
                                imp:n=1 u=5
5036 0              5002 -5003 5004 -5031
                                imp:n=1 u=5
5037 0              5002 -5003 5005 -5031 -5004

```

```

                    imp:n=1 u=5
5038 0              5003 -5039 5008 -5031
                    (5036:5047:-5035)
                    imp:n=1 u=5
5039 0              5003 -5039 -5008 5032 -5031
                    imp:n=1 u=5
5040 0              5039 -5041 5008 -5031
                    imp:n=1 u=5
5041 0              5039 -5041 -5008 5043 -5031
                    imp:n=1 u=5
5042 0              5041 -5044 5008 -5031
                    imp:n=1 u=5
5043 0              5041 -5044 -5008 5043 -5031
                    imp:n=1 u=5
5044 0              5044 -5045 5008 -5031
                    imp:n=1 u=5
5045 0              5044 -5045 -5008 5043 -5031
                    imp:n=1 u=5
c -----
c Outside detector (for including in universe)
c -----
5999 0              5031:-5001:5045
                    imp:n=1 u=5
c ++++++
c                                     end SNAP3 cells
c ++++++

c =====
c                                     SURFACE CARDS
c =====
c ++++++
c                                     begin non-detector surfaces
c ++++++
c -----
c BeRP ball minus the Be (i.e. a Pu Sphere)
c see Eldon Brandon, "Assembly of 239Pu Ball for Criticality Experiment"
c   CMB-11-FAB-80-65 (Oct 23, 1980)
c -----
101 sz  97.425  3.7938  $ mean diameter 75.876 mm of pu ball
102 sz  97.425  3.827   $ IR ss304 clad
103 sz  97.425  3.8558  $ OR ss304 clad; see Atwater memo Q2-85-5045A (22 Apr 85)
c -----
c stand for BeRP ball
c -----
110 pz  86.487                                     $ top of base
c use surf of table, surface 141, as bottom
111 px   7.62                                     $ sides of base
112 px  -7.62                                     $ sides of base
113 py   7.62                                     $ sides of base
114 py  -7.62                                     $ sides of base
115 cz   0.3937                                    $ lower cylinder inside
116 cz   0.9535                                    $ lower cylinder outside
117 pz  92.04325                                   $ lower cylinder top
118 cz   1.87579                                   $ upper cylinder inside
119 cz   2.21615                                   $ upper cylinder outside
120 pz  92.78239                                   $ upper cylinder mid
121 pz  94.05239                                   $ upper cylinder mid
c -----
c concrete floor
c -----
122 pz   0.0
123 pz  -91.44   $ 3 ft of concrete
c -----
c NPOD container surfaces
c -----
131 3 px -21.668699
132 3 px  21.668699
133 3 py   0.000001

```

```

134 3 py 10.317439
135 3 pz 0.000001
136 3 pz 49.428399
c -----
c tables
c -----
c ~~~ table 1: BeRP & NPOD3 ~~~
140 pz 84.951316 $ bottom
141 pz 85.217 $ surface
142 pz 89.027 $ top of edges
143 px -61.2775 $ -x outer edge
144 px -61.011816 $ -x inner edge
145 px 61.011816 $ +x inner edge
146 px 61.2775 $ +x outer edge
147 py -30.7975 $ -y outer edge
148 py -30.531816 $ -y inner edge
149 py 30.531816 $ +y inner edge
150 py 30.7975 $ +y outer edge
c ~~~ table 2: SNAP3 ~~~
c use same bottom, surface 140
c use same surface, surface 141
c use same top of edges, surface 142
151 px -183.83250 $ -x outer edge
152 px -183.566816 $ -x inner edge
153 px -61.543184 $ +x inner edge
c use table 1 -x outer edge for table 2 +x outer edge, surface 143
c use table 1's -y outer and inner edges and +y outer and inner edges
c -----
c polyethylene reflector surfaces
c -----
160 pz 91.567 $ poly sleeve
161 pz 97.425
c
162 sz 97.425 3.90271
163 sz 97.425 5.12572
164 sz 97.425 6.39572
165 sz 97.425 7.66572
166 sz 97.425 11.47572
167 sz 97.425 19.09572
c -----
c SNAP container surfaces
c -----
178 5 cz 10.4
199 5 px 7.3659999
179 5 pz 0.000001
180 5 pz 36.525199
c -----
c problem boundary
c -----
999 sph 0 0 0 500 $ outside world
c ++++++
c begin non-detector surfaces
c ++++++
c begin NPOD version 3 surfaces
c ++++++
3001 px -21.59
3002 px 21.59
3003 py 0.07874
3004 py 10.2387
3005 pz 0.07874
3006 pz 42.2427
3007 px -21.6687
3008 px 21.6687
3009 py 0.0
3010 py 10.31744
3011 pz 0.0
3012 pz 42.3214

```

```

3013 pz    0.15748                $ bottom of ldr
3014 pz    2.49174                $ top of ldr - bottom of ar
3015 pz   40.59174                $ top of ar - bottom of udr
c 3016 pz   43.688                $ top of udr
c 3017 pz   43.7667              $ top of al wall
3018 c/z -17.85874 8.255 1.19126 $ tube 1
3019 c/z -17.85874 8.255 1.27
3020 c/z -17.85874 8.255 1.3462
3021 c/z -12.77874 8.255 1.19126 $ tube 2
3022 c/z -12.77874 8.255 1.27
3023 c/z -12.77874 8.255 1.3462
3024 c/z  -7.69874 8.255 1.19126 $ tube 3
3025 c/z  -7.69874 8.255 1.27
3026 c/z  -7.69874 8.255 1.3462
3027 c/z  -2.61874 8.255 1.19126 $ tube 4
3028 c/z  -2.61874 8.255 1.27
3029 c/z  -2.61874 8.255 1.346
3030 c/z   2.46126 8.255 1.19126 $ tube 5
3031 c/z   2.46126 8.255 1.27
3032 c/z   2.46126 8.255 1.3462
3033 c/z   7.54126 8.255 1.19126 $ tube 6
3034 c/z   7.54126 8.255 1.27
3035 c/z   7.54126 8.255 1.3462
3036 c/z  12.62126 8.255 1.19126 $ tube 7
3037 c/z  12.62126 8.255 1.27
3038 c/z  12.62126 8.255 1.3462
3039 c/z  17.70126 8.255 1.19126 $ tube 8
3040 c/z  17.70126 8.255 1.27
3041 c/z  17.70126 8.255 1.3462
3042 c/z  15.3187  4.064 1.19126 $ tube 9
3043 c/z  15.3187  4.064 1.27
3044 c/z  15.3187  4.064 1.3462
3045 c/z  10.2387  4.064 1.19126 $ tube 10
3046 c/z  10.2387  4.064 1.27
3047 c/z  10.2387  4.064 1.3462
3048 c/z   5.15874 4.064 1.19126 $ tube 11
3049 c/z   5.15874 4.064 1.27
3050 c/z   5.15874 4.064 1.3462
3051 c/z  -0.07874 4.064 1.19126 $ tube 12
3052 c/z  -0.07874 4.064 1.27
3053 c/z  -0.07874 4.064 1.3462
3054 c/z  -5.00126 4.064 1.19126 $ tube 13
3055 c/z  -5.00126 4.064 1.27
3056 c/z  -5.00126 4.064 1.3462
3057 c/z -10.08126 4.064 1.19126 $ tube 14
3058 c/z -10.08126 4.064 1.27
3059 c/z -10.08126 4.064 1.3462
3060 c/z -15.16126 4.064 1.19126 $ tube 15
3061 c/z -15.16126 4.064 1.27
3062 c/z -15.16126 4.064 1.3462
c -----
c  pre-amp housing
c -----
3063 px -21.4071
3064 px  21.4071
3065 py   0.18288
3066 py  10.1295
3067 pz  42.7786
3068 pz  44.8614
3069 px -21.0566
3070 px  21.0566
3071 py   0.5334
3072 py   9.77898
c -----
c  rf shield
c -----
3073 px -20.9423
3074 px  20.9423

```

```

3075 py 0.64769
3076 py 9.66469
3077 pz 43.0
3078 pz 43.15748
3079 pz 42.8
3080 pz 42.8787
c -----
c display housing
c -----
3081 py 10.3124
3082 pz 49.4284
3083 px -20.3955
3084 px 20.3955
3085 py 0.6355
3086 py 9.6774
3087 pz 48.7934
3088 pz 45.0
3089 pz 45.07874
c ++++++
c end NPOD version 3 surfaces
c ++++++
c ++++++
c begin SNAP3 surfaces
c ++++++
c -----
c vibration pads
c -----
5001 pz 0
5002 pz 3.81
c -----
c tripod plate
c -----
5003 pz 4.445
5004 px 7.366
5005 cz 10.34796
c -----
c Bottom plate
c -----
5006 pz 9.3726
5007 cz 10.16
5008 px 4.7752
c -----
c He3 gas cavity & sst wall
c -----
5009 cz 1.1938
5010 pz 10.399375 $ a guess at the tube height above bottom detector poly
5011 pz 10.475575
5012 pz 12.786975
5013 pz 22.946975
5014 pz 26.045775
5015 pz 26.121975
5016 cz 1.27
c -----
c HN Connector
c -----
5017 cz 1.016
5018 cz 0.9398
c -----
c Poly sleeve
c -----
5019 cz 1.35001
5020 cz 3.81
5021 pz 26.27884
c -----
c Cd Shield top
c -----
5022 pz 26.35504
c -----

```

```

c Cd shield
c -----
5023 pz 27.1526 $ top of shield
5024 cz 3.8354
5025 cz 3.91414
c -----
c bottom Cd shield
c -----
5026 pz 9.45134
c -----
c Detector Body
c -----
5027 pz 28.1051
5028 cz 3.9624
5029 py -3.622
5030 py 3.622
5031 cz 10.3505
5032 cz 10.2108
c -----
c inner front protective cover
c -----
5033 py -6.35
5034 py 6.35
c -----
c front protective cover
c -----
5035 py -7.3152
5036 py 7.3152
c -----
c top cover
c -----
5037 cz 2.3495
5038 pz 31.0007
5039 pz 33.0327
5040 px 4.5212
c -----
c MC PCB Housing
c -----
5041 pz 33.2613
5042 cz 9.9568
5043 cz 10.2362
5044 pz 34.9377
5045 pz 36.5252
5046 px 4.69668
5047 px 7.3152
c -----
c detector body ambiguity surface
c -----
5048 px 0.0
c ++++++
c end SNAP3 surfaces
c ++++++

c =====
c DATA CARDS
c =====
c -----
c translation cards
c -----
tr3 60.31744 0 85.217 0 1 0 -1 0 0 0 0 1 $ NPOD3
tr5 -100 0 85.217 1 0 0 0 1 0 0 0 1 $ SNAP3
c -----
c source definition
c -----
rdum 1001 94240 39290034 3 9 1 0 0 97.425 2
      1001 99999 130898 3 9 1 0 0 97.425 2
nps 39420932
c

```

```

si2  0  3.7938
sp2  -21  2
c
sp3  -3  0.799  4.903
c
si9  0  300.0e8
sp9  0  1
c
c -----
c tally cards
c -----
c leakage tallies
f01:n  101
c01  0  1
fm01  39420932
fq01  c m
f11:n  103
c11  0  1
fm11  39420932
fq11  c m
c Detector Incident Spectra
f21:n  131 132 133 134 135 136
e21  1e-10 49ilog 1e1
c21  0  1
fm21  39420932
f31:n  178 179 180 199
e31  1e-10 49ilog 1e1
c31  0  1
fm31  39420932
c NPOD Tubes 2 ways
f04:n  3047 3048 3049 3050 3051 3052 3053 3054
      3055 3056 3057 3058 3059 3060 3061      T
sd04  300 15r
e04  1e-10 49ilog 1e1
fm04 -39420932 3003 -2
t04  300e8 1e33
cf04  1901
fq04  f m
tf04  16 6j 1
c
f14:n  3047 3048 3049 3050 3051 3052 3053 3054
      3055 3056 3057 3058 3059 3060 3061      T
sd14  300 15r
e14  1e-10 49ilog 1e1
fm14  39420932
fu14  2003      $ <- list-mode tally
t14  300e8 1e33
cf14  1901
fq14  f u
tf14  16 6j 1
c SNAP
f24:n  5004
sd24  300
e24  1e-10 49ilog 1e1
t24  300e8 1e33
fm24 -39420932 5003 -2
cf24  1901
fq24  f m
tf24  7j 1
c
f34:n  5004
sd34  300
e34  1e-10 49ilog 1e1
t34  300e8 1e33
fu34  2003
fm34  39420932
cf34  1901
fq34  u t

```


tf34 7j 1

c

c -----

c material cards

c -----

m1 6000.70c -230.e-6
26000.50c -10.e-6
31000.50c -335.0e-6
92234.70c -41.1e-6
92235.70c -786.6e-6
92236.70c -183.2e-6
92238.70c -1.5e-8
94238.70c -0.0002
94239.99c -0.93735
94240.70c -0.0595
94241.70c -0.002685
94242.70c -0.00028
95241.70c -2506.0e-6

\$ alpha pu BeRP ball decay

c

m2 14028.70c -0.009223 \$ Stainless Steel
14029.70c -0.000468
14030.70c -0.000309
24050.70c -0.008690
24052.70c -0.167578
24053.70c -0.019002
24054.70c -0.004730
25055.70c -0.02
26054.70c -0.037992
26056.70c -0.596401
26057.70c -0.013774
26058.70c -0.001833
28058.70c -0.081692
28060.70c -0.031468
28061.70c -0.001368
28062.70c -0.004361
28064.70c -0.001111

c

m3 13027.70c -0.96530 \$ aluminum 6061
12024.70c -0.00790
12025.70c -0.00100
12026.70c -0.00110
14028.70c -0.00551
14029.70c -0.00029
14030.70c -0.00020
22046.70c -0.00012
22047.70c -0.00011
22048.70c -0.00111
22049.70c -0.00008
22050.70c -0.00008
24050.70c -0.00008
24052.70c -0.00167
24053.70c -0.00019
24054.70c -0.00005
25055.70c -0.00150
26054.70c -0.00040
26056.70c -0.00643
26057.70c -0.00015
26058.70c -0.00002
29063.70c -0.00192
29065.70c -0.00088
30000.70c -0.00250

c

m8 26054.70c 0.05845 \$ natural iron
26056.70c 0.91754
26057.70c 0.02119
26058.70c 0.00282

m9 1001.70c 0.666667
6000.70c 0.333333

```

mt9  poly.60t
c
m21  8016.70c  0.2
      7014.70c  0.8
c
m23  1001.70c -0.010      $ schaeffer portland concrete (page 451)
      8016.70c -0.529
      11023.51c -0.016
      12000.51c -0.002
      13027.70c -0.034
      14000.51c -0.337
      19000.51c -0.013
      20000.51c -0.044
      26000.50c -0.014
      6000.70c -0.001      $ see ne handbook(7-113) for another portland comp
c
c ++++++
c                                     begin NPOD version 3 materials
c ++++++
c -----
c ENDF/B-VI Evaluations
c -----
c m3001  1001.66c  0.666667      $ High Density poly (dens=.95 g/cc)
c        6000.66c  0.333333
c mt3001  poly.60t
c m3002  13027.66c  1.000000      $ al 6061
c m3003  2003.66c  0.9423      $ He-3 With Quench Gas
c        6000.66c  0.0192
c        8016.66c  0.0385
c m3004  48106.66c  0.0125      $ Natural Cd
c        48108.66c  0.0089
c        48110.66c  0.1249
c        48111.66c  0.1280
c        48112.66c  0.2413
c        48113.66c  0.1222
c        48114.66c  0.2873
c        48116.66c  0.0749
c m3006  14028.66c  0.922297      $ Natural Si
c        14029.66c  0.046832
c        14030.66c  0.030871
c -----
c ENDF/B-VII Evaluations
c -----
m3001  1001.70c  0.666667      $ High Density poly (dens=.95 g/cc)
      6000.70c  0.333333
mt3001  poly.60t
m3002  13027.70c  1.000000      $ al 6061
m3003  2003.70c  0.9423      $ He-3 With Quench Gas
      6000.70c  0.0192
      8016.70c  0.0385
m3004  48106.70c  0.0125      $ Natural Cd
      48108.70c  0.0089
      48110.70c  0.1249
      48111.70c  0.1280
      48112.70c  0.2413
      48113.70c  0.1222
      48114.70c  0.2873
      48116.70c  0.0749
m3006  14028.70c  0.922297      $ Natural Si
      14029.70c  0.046832
      14030.70c  0.030871
c ++++++
c                                     end NPOD version 3 materials
c ++++++
c ++++++
c                                     begin SNAP3 materials
c ++++++
c -----

```

```

c ENDF/B-VI evaluations
c -----
c m5001 13027.66c 1.000000 $ Aluminum 6061
c m5002 1001.66c 0.666667 $ High Density poly (rho=.95 g/cc)
c 6000.66c 0.333333
c mt5002 poly.60t
c m5003 2003.66c 0.9423 $ He-3 With Quench Gas
c 6000.66c 0.0192
c 8016.66c 0.0385
c m5004 14028.66c -0.009223 $ Stainless Steel
c 14029.66c -0.000468
c 14030.66c -0.000309
c 24050.66c -0.008690
c 24052.66c -0.167578
c 24053.66c -0.019002
c 24054.66c -0.004730
c 25055.66c -0.02
c 26054.66c -0.037992
c 26056.66c -0.596401
c 26057.66c -0.013774
c 26058.66c -0.001833
c 28058.66c -0.081692
c 28060.66c -0.031468
c 28061.66c -0.001368
c 28062.66c -0.004361
c 28064.66c -0.001111
c m5005 48106.66c 0.0125 $ Natural Cd
c 48108.66c 0.0089
c 48110.66c 0.1249
c 48111.66c 0.1280
c 48112.66c 0.2413
c 48113.66c 0.1222
c 48114.66c 0.2873
c 48116.66c 0.0749
c -----
c ENDF/B-VII evaluations
c -----
m5001 13027.70c 1.000000 $ Aluminum 6061
m5002 1001.70c 0.666667 $ High Density poly (rho=.95 g/cc)
6000.70c 0.333333
mt5002 poly.60t
m5003 2003.70c 0.9423 $ He-3 With Quench Gas
6000.70c 0.0192
8016.70c 0.0385
m5004 14028.70c -0.009223 $ Stainless Steel
14029.70c -0.000468
14030.70c -0.000309
24050.70c -0.008690
24052.70c -0.167578
24053.70c -0.019002
24054.70c -0.004730
25055.70c -0.02
26054.70c -0.037992
26056.70c -0.596401
26057.70c -0.013774
26058.70c -0.001833
28058.70c -0.081692
28060.70c -0.031468
28061.70c -0.001368
28062.70c -0.004361
28064.70c -0.001111
m5005 48106.70c 0.0125 $ Natural Cd
48108.70c 0.0089
48110.70c 0.1249
48111.70c 0.1280
48112.70c 0.2413
48113.70c 0.1222
48114.70c 0.2873

```

```
48116.70c 0.0749
c ++++++
c                                     end SNAP3 materials
c ++++++
c -----
c problem specifications
c -----
mode n
phys:n 4j 1 $ analog
cut:n 2j 0 $ analog
totnu
print
prdmp 2j 1
c m0303 is the ACE file for trial 303
XS1 94239.99c 236.998600 m0303 0 1 1      808738 0 0 2.5301E-08 ptable
```